

**Contributions to the Chemistry of Arene Ruthenium Half Sandwich
Complexes: Complexes Bearing Labile Chalcogen Ligands and
Alkynol Coupling Reactions**

JADRANKA ČUBRILO

**Universität Stuttgart, Institut für Anorganische Chemie
Stuttgart**

Contributions to the Chemistry of Arene Ruthenium Half Sandwich Complexes: Complexes Bearing Labile Chalcogen Ligands and Alkynol Coupling Reactions

Von der Fakultät Chemie der Universität Stuttgart zur Erlangung der Würde eines Doktors der Naturwissenschaften (Dr. rer. nat.) genehmigte Abhandlung

vorgelegt von

JADRANKA ČUBRILO

aus Sombor (Serbien)

Stuttgart, 2008

- | | |
|------------------------------------|---------------------------------|
| 1. Hauptberichter: | Prof. Dr. Rainer Winter |
| 2. Mitberichter: | Prof. Dr. Thomas Schleid |
| 3. Mitberichter: | Prof. Dr. Stephen Hashmi |
| Tag der Einreichung: | 19.12.2006 |
| Tag der mündlichen Prüfung: | 22.02.2007 |

**Universität Stuttgart, Institut für Anorganische Chemie
Stuttgart**

...to my dearest parents

Acknowledgements

I am most grateful to Prof. Dr. Rainer Winter for his guidance through all these years starting from my Diplomarbeit, continued with my dissertational work in Stuttgart, as well as in this past year when the group moved to Regensburg. I am also thankful for opportunity to work on various research topics where I learned a lot both synthetic preparations and different measurement techniques. I sincerely appreciate his patience and great ability for communicating the knowledge. It was always pleasant to work in a such atmosphere.

I would like to acknowledge:

Dr. Falk Lissner and Dr. Ingo Hartenbach for performing single crystal structure analysis and structure determinations, Dr. Reiner Ruf for additional calculations, providing me with necessary data very quickly especially in the final phase of my work.

Prof. Dr. Dietrich Gudat for professional recording of 1D and 2D NMR spectra, making possible assignment of to us important compounds.

Ms. Katarina Török for recording routine NMR and teaching me how to operate NMR spectrometer.

Finally, all people from the Prof. Kaim's group for all the help, working atmosphere and talks.

My special thank to Jörg Maurer for his great help always when needed, Sebastian Burck for assisting me with first Birch reduction done in the lab, Samir Chikkali, Andrea Hokky for being good company in late hours in the lab.

I am truly grateful to my great colleagues from Regensburg, Markus Pichlmaier, Johannes Schnödt and Florian Pevny for nice atmosphere while setting up the laboratories, positive attitude and making getting used to the new city more easy.

I am deeply grateful to my parents, my sister Maja and brother Nikola whom I missed the most past years for supporting me, giving me strength and believing in me.

I also address my special acknowledgements to Lars Bonnekamp for his understanding, being so much helpful and nice times throughout these years. To family Bonnekamp who was always interested in my work and were encouraging me I am also thankful.

I would also like to show my appreciation to all of my friends who left a sign on this past 4 years: Eva Zurek, Sandra Prohaska, Aleksandar Tucić, Zoran Vujić, Thorsten Schnabel, Jelena Radulović, Jasna Romić, Alejandro Meleg and Vitomir Marić.

Contents

1	Introduction	8
1.1	Ruthenium half sandwich complexes $[(\eta^6\text{-arene})\text{RuCl}_2]_2$ and $[(\eta^6\text{-arene})\text{RuCl}_2(\text{L})]$ ($\text{L} = \text{PR}_3$, alkene, N-heterocyclic carbene) in catalysis	8
1.2	Activation of alkynols by half sandwich ruthenium complexes: ruthenium allenylidene complexes.....	12
1.3	Half sandwich complexes of ruthenium with tethered arene ligands	14
1.4	Coupling reactions of alkynes and alkynols on ruthenium templates.....	16
2	p-Cymene Ruthenium Thioether Complexes	21
2.1	Known arene thioether ruthenium complexes.....	21
2.2	Synthesis of half sandwich complexes $[(\eta^6\text{-arene})\text{RuCl}_2(\text{SRR}')]$	23
2.3	X-ray structure determinations of $[(\eta^6\text{-p-cymene})\text{RuCl}_2(\text{SRR}')]$ (5), (6), $[(\eta^6\text{-p-cymene})\text{RuCl}(\text{SMe}_2)_2]^+ \text{SbF}_6^-$ (7), and $[(\eta^6\text{-p-cymene})\text{Ru}]_2(\mu\text{-Cl})_3]^+ \text{SbF}_6^-$ (8)	27
2.4	Complexes $[(\eta^6\text{-p-cymene})\text{RuCl}_2\text{L}]$ where $\text{L} =$ substituted pyridine	34
2.5	X-ray structure determination of $[(\eta^6\text{-p-cymene})\text{RuCl}_2(4\text{-methylpyridine})]$ (11)...	38
2.6	Attempted synthesis of $[(\eta^6:\eta^1\text{-arene-L})\text{RuCl}_2]$ where $\text{L} =$ thioether or pyridine pendant functionalities	40
2.7	Attempts toward the synthesis of novel pyridine and thioether analogs of Dixneuf's metathesis catalysts $[(\eta^6\text{-p-cymene})\text{Cl}(\text{L})\text{RuC}=\text{C}=\text{CPh}_2]^+ \text{X}^-$	42
2.7.1	Attempted synthesis by chloride substitution from $[(\eta^6\text{-p-cymene})\text{Ru}(\text{L})\text{Cl}_2]^+ \text{X}^-$	42
2.7.2	Attempted phosphine ligand substitution in $[(\eta^6\text{-p-cymene})\text{Cl}(\text{PCy}_3)\text{Ru}=\text{C}=\text{C}=\text{CPh}_2]^+$	44
2.8	Electrochemical investigations on the thioether ruthenium complexes	46
2.9	Electronic spectra	50
3	Half sandwich complexes bearing alcohol or ether functionalities on the arene	52
3.1	Introduction.....	52
3.2	Synthesis of half sandwich complexes $[(\eta^6:\eta^1\text{-C}_6\text{H}_5(\text{CH}_2)_m\text{OR})\text{RuCl}_2]_n$	

(n = 1, 2; m = 2 or 3)	53
3.3 X-ray structure determinations of $[(\eta^6:\eta^1\text{-C}_6\text{H}_5(\text{CH}_2)_3\text{OH})\text{RuCl}_2]$ (13) and $[(\eta^6\text{-C}_6\text{H}_5(\text{CH}_2)_3\text{OMe})\text{RuCl}_2]$ (14)	55
3.4 Phosphine derivatives of complexes 13-15	62
3.5 Electrochemistry	64
3.6 Synthesis of $[(\eta^6\text{-C}_6\text{H}_5(\text{CH}_2)_n\text{OR})(\text{PR}'_3)\text{ClRu}=\text{C}=\text{C}=\text{CPh}_2]^+$	70
3.7 Assessment of the biological activity of complexes $[(\eta^6\text{-C}_6\text{H}_5(\text{CH}_2)_n\text{OR})\text{RuCl}(\text{PR}_3)]$	74
4 The coupling of alkynols on arene ruthenium platforms	76
4.1 Cyclotrimerization of 2-methylbut-3-yn-1-ol	76
4.2 Crystal structure of $[(\eta^6\text{-p-cymene})\{\eta^6\text{-C}_6\text{H}_3(\text{CMe}_2\text{OH})_{3-1,3,5}\}\text{Ru}]^{2+}(\text{Cl})_2 \times 2 \text{H}_2\text{O}$ (16)	81
4.3 NMR studies on the activity of $[(\eta^6\text{-p-cymene})\text{RuCl}_2]_2$ in the cyclotrimerization of alkynols	84
4.4 Cocyclization of 2-methylbut-3-yn-1-ol and of a phenylate group from tetraphenylborate	86
4.5 Mechanistic aspects and investigation of the proposed mechanism by DFT calculations	90
4.6 Labeling studies as a mechanistic support to origin of the phenyl ring of the naphthalenide skeleton	92
4.7 Cocyclization reactions involving different propargylic alcohols	95
4.8 Electrochemical investigations on the dihydronaphthalenide complexes	99
5 Experimental Part	103
5.1 General methods and procedures	103
5.1.1 Solvents	103
5.1.2 Commercially available starting compounds were purchased in the specifications given from the following suppliers:	103
5.2 Analytical and spectroscopic instruments	104
5.2.1 NMR-spectroscopy	104
5.2.2 IR-spectroscopy	104
5.2.3 CHN analysis	104
5.2.4 Biological activity assessment	104
5.2.5 X-ray analysis	105
5.2.6 Cyclic voltammetry	106
5.3 Synthesis of the starting materials	107
5.3.1 Synthesis of $[(\eta^6\text{-p-cymene})\text{RuCl}_2]_2$ (1)	107
5.3.2 Synthesis of $[(\eta^6\text{-C}_6(\text{CH}_3)_6)\text{RuCl}_2]_2$	107

5.3.3	Synthesis of $[(\eta^6\text{-p-cymene})(\eta^6\text{-C}_{10}\text{H}_8)\text{RuCl}_2]^{2+} (\text{BF}_4^-)_2$	107
5.3.4	Synthesis of $[(\eta^6\text{-C}_6\text{H}_6)\text{RuCl}_2]_2$	108
5.3.5	Synthesis of $\text{NaB}(\text{C}_6\text{H}_5)_4\text{-d}_{20}$	108
5.3.6	Synthesis of 3-phenyl-1-propylmethylether, $\text{C}_6\text{H}_5(\text{CH}_2)_3\text{OCH}_3$	108
5.3.7	Synthesis of 3-(1,4-cyclohexadiene)-1-propyl methyl ether	109
5.3.8	Synthesis of 3-(1,4-cyclohexadiene)-1-propanol.....	110
5.3.9	Synthesis of 2-(1,4-cyclohexadiene)ethanol	110
5.3.10	Synthesis of (2-phenylpropyl)isopropyl sulfide	111
5.3.11	Synthesis of methyl(2-phenylethyl)sulfide.....	111
5.4	Synthesis of compounds.....	112
5.4.1	Synthesis of $[(\eta^6\text{-p-cymene})\text{RuCl}_2(\text{PhC}_3\text{H}_6\text{S}^i\text{Pr})]$ (4).....	112
5.4.2	Synthesis of $[(\eta^6\text{-p-cymene})\text{RuCl}_2(\text{PhC}_2\text{H}_4\text{SMe})]$ (5)	113
5.4.3	Synthesis of $[(\eta^6\text{-p-cymene})\text{RuCl}_2(\text{SMeC}_3\text{H}_5)]$ (6)	113
5.4.4	Synthesis of $[(\eta^6\text{-p-cymene})\text{RuCl}(\text{SMe}_2)_2]^+ \text{SbF}_6^-$ (7) and $[(\eta^6\text{-p-cymene})\text{Ru}]_2(\mu\text{-Cl})_3]^+ \text{SbF}_6^-$ (8)	114
5.4.5	Synthesis of $[(\eta^6\text{-p-cymene})\text{RuCl}_2(\text{PhC}_3\text{H}_6\text{Py})]$ (9)	115
5.4.6	Synthesis of $[(\eta^6\text{-p-cymene})\text{RuCl}_2(2\text{-benzylaminopyridine})]$ (10)	115
5.4.7	Synthesis of $[(\eta^6\text{-p-cymene})\text{RuCl}_2(4\text{-methylpyridine})]$ (11)	116
5.4.8	Synthesis of $[(\eta^6\text{-p-cymene})\text{RuCl-bis}(4\text{-methylpyridine})]^+ \text{PF}_6^-$ (12)	117
5.4.9	Synthesis of $[(\eta^6\text{-C}_6\text{H}_5(\text{CH}_2)_3\text{OH})\text{RuCl}_2]_2$ (13)	118
5.4.10	Synthesis of $[(\eta^6\text{-C}_6\text{H}_5(\text{CH}_2)_3\text{OH})\text{Ru}(\text{P}^i\text{Pr}_3)\text{Cl}_2]$ (13a).....	118
5.4.11	$[(\eta^6\text{-C}_6\text{H}_5(\text{CH}_2)_3\text{OH})\text{Ru}(\text{PCy}_3)\text{Cl}_2]$ (13b).....	119
5.4.12	$[(\eta^6\text{-C}_6\text{H}_5(\text{CH}_2)_3\text{OH})\text{RuCl}_2\{\text{P}(\text{CH}_2\text{OH})_3\}]_3$ (13c)	119
5.4.13	$[(\eta^6\text{-C}_6\text{H}_5(\text{CH}_2)_3\text{OH})\text{RuCl}(\text{P}(\text{CH}_2\text{OH})_3)_2]^+ \text{Cl}^-$ (13d).....	120
5.4.14	$[(\eta^6\text{-C}_6\text{H}_5(\text{CH}_2)_3\text{OMe})\text{RuCl}_2]_2$ (14).....	120
5.4.15	Synthesis of $[(\eta^6\text{-C}_6\text{H}_5(\text{CH}_2)_3\text{OCH}_3)\text{Ru}(\text{P}^i\text{Pr}_3)\text{Cl}_2]$ (14a)	121
5.4.16	$[(\eta^6\text{-C}_6\text{H}_5(\text{CH}_2)_3\text{OCH}_3)\text{Ru}(\text{PCy}_3)\text{Cl}_2]$ (14b).....	121
5.4.17	$[(\eta^6\text{-C}_6\text{H}_5(\text{CH}_2)_2\text{OH})\text{RuCl}_2]$ (15).....	122
5.4.18	$[(\eta^6\text{-C}_6\text{H}_5(\text{CH}_2)_2\text{OH})\text{Ru}(\text{P}^i\text{Pr}_3)\text{Cl}_2]$ (15a).....	122
5.4.19	Synthesis of $[(\eta^6\text{-C}_6\text{H}_5(\text{CH}_2)_3\text{OCH}_3)\text{Ru}(\text{P}^i\text{Pr}_3)\text{ClRu}=\text{C}=\text{C}=\text{CPh}_2]^+ \text{BF}_4^-$..	123
5.4.20	Synthesis of $[(\eta^6\text{-p-cymene})\text{Ru}(1\text{-methylene-1,2-dihydro-naphthalenide})]^+ \text{BPh}_4^-$ (17)	124
5.4.21	Synthesis of complex 18	124
5.4.22	Synthesis of complex 19	125
5.4.23	Synthesis of complex 17d₄/d₅	126

6 Summary 127

7 Zusammenfassung 135

8	Appendix	143
8.1	Crystal data for $[(\eta^6\text{-p-cymene})\text{RuCl}_2(\text{MeSC}_2\text{H}_4\text{Ph})]$ (5)	143
8.2	Crystal data for $[(\eta^6\text{-p-cymene})\text{RuCl}_2(\text{MeSC}_3\text{H}_5)]$ (6)	149
8.3	Crystal data for $[(\eta^6\text{-p-cymene})\text{RuCl}(\text{SMe}_2)_2]^+ \text{SbF}_6^-$ (7)	155
8.4	Crystal data for $[(\eta^6\text{-p-cymene})\text{Ru}]_2(\mu\text{-Cl})_3]^+ \text{SbF}_6^-$ (8)	161
8.5	Crystal data for $[(\eta^6\text{-p-cymene})\text{RuCl}_2(4\text{-methylpyridine})]$ (11)	168
8.6	Crystal data for $[(\eta^6:\eta^1\text{-C}_6\text{H}_5(\text{CH}_2)_3\text{OH})\text{RuCl}_2]$ (13)	174
8.7	Crystal data for $[(\eta^6\text{-C}_6\text{H}_5(\text{CH}_2)_3\text{OMe})\text{RuCl}_2]_2$ (14)	179
8.8	Crystal data for $[(\eta^6\text{-p-cymene})((\eta^6\text{-C}_6\text{H}_3(\text{CMe}_2\text{OH})_3)_{1,3,5})\text{Ru}]^{2+}$ $(\text{Cl}^-)_2 \times 2 \text{H}_2\text{O}$ (16)	185
9	List of Abbreviations	194
10	References	197
11	Curriculum Vitae for Jadranka Čubrilo	205

1 Introduction

1.1 Ruthenium half sandwich complexes $[(\eta^6\text{-arene})\text{RuCl}_2]_2$ and $[(\eta^6\text{-arene})\text{RuCl}_2(\text{L})]$ ($\text{L} = \text{PR}_3$, alkene, N-heterocyclic carbene) in catalysis

The chemistry of organoruthenium compounds is dominated by the +2 oxidation state. Since the first reports on chloro-bridged arene complexes of ruthenium in the oxidation state +2 more than 30 years ago,^{1, 2} compounds of this kind had a tremendous impact on organometallic synthesis and catalysis. Dimeric complexes $[(\eta^6\text{-arene})\text{RuCl}_2]_2$ constitute the most important entry point to (arene)Ru chemistry. This field has continuously gained in importance since various (arene)Ru complexes turned out to be highly active catalysts or precatalysts, performing a large number of organic transformations in many different areas.

Considering the vast number of catalytically active (arene)Ru complexes, this introductory overview focuses just on recent developments with special emphasis on complexes that are crucial for this work as a lead in our search for new (arene)RuL_n derivatives with potential utility in catalysis. These include allenylidene (propadienyldiene, =C=C=RR') complexes $[(\eta^6\text{-arene})\text{Cl}(\text{PR}_3)\text{Ru}=\text{C}=\text{C}=\text{RR}']^+$, similar derivatives bearing hemilabile thioether and ether functionalities, and simple thioether and pyridine adducts $[(\text{arene})\text{RuCl}_2(\text{L})]$ and $[(\text{arene})\text{RuCl}(\text{L})_2]^+$ ($\text{L} =$ substituted pyridine, thioether). Studies on transformations of alkynols widened our spectrum of interests from ruthenium allenylidene complexes to coupling reactions of alkynols and of a phenyl group on ruthenium templates. These give rise to the highly selective assembly of dihydronaphthalenide ligands.³

Amongst other transformations, $[(\eta^6\text{-arene})\text{RuCl}_2]_2$ complexes have been employed as catalysts for the conversion of aldoximes to nitriles,⁴ for the 1,4-addition of alkynes to conjugated enones,⁵ for the hydrolytic oxidation of organosilanes,⁶ for hydrosilylations,⁷ for arene hydrogenation,⁸ and for the oxidation of alcohols.⁹ They serve as starting materials for the synthesis of a large variety of mononuclear catalysts such as $[(\eta^6\text{-arene})\text{Ru}(\text{L-L}')\text{Cl}]$ ($\text{L-L}' =$ anionic bidentate ligand) which are important for H-transfer hydrogenation of ketones¹⁰ or olefin cyclopropanation.¹¹ Complexes $[(\text{arene})\text{Ru}(\text{L-L}')\text{Cl}]^+$ ($\text{L-L}' =$ neutral

bidentate chiral ligand) catalyze asymmetric Diels-Alder reactions¹² and arene hydrogenations.¹³

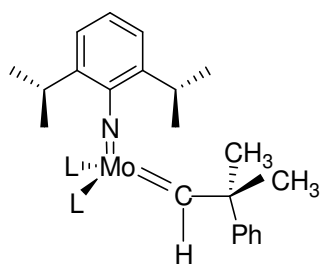
Olefin metathesis is arguably the most powerful carbon-carbon bond breaking and making reaction in chemical synthesis and therefore a highly valuable and versatile method for the modern synthetic chemist.¹⁴ Depending on the nature of the reaction partners, olefin metathesis can be used for ring opening polymerization (ROMP)¹⁵ to create advanced polymer materials,¹⁶ transformations of acyclic diene substrates into complex cyclic molecules in ring-closing metathesis (RCM)^{17, 18} or into polymers in acyclic diene metathesis (ADMET),¹⁹ or to generate unsymmetrical olefins in cross metathesis (CM)^{20, 21}. It is generally acknowledged that transition metal carbene species $[L_nM=CRR']$ are required for olefin metathesis. Because each olefin step during metathesis is fully reversible, RCM, ADMET, and CM rely on the elimination of ethylene, the simplest olefin, as a thermodynamic driving force.^{22, 23}

Metal carbenes are generally classified as being nucleophilic (electron rich) or electrophilic (electron poor) in character at the carbene carbon atom, but an effective metathesis catalyst is of an electronic character in between these two extremes. The rapidly increasing demand for efficient and highly tolerant pre-catalysts for all kinds of metathesis reactions is a drawback from nucleophilic metal-carbene complexes of molybdenum and tungsten (see Figure 1) as developed by *Schrock*.²⁴⁻²⁶ These alkylidene based catalysts display high activities and stabilities but are sensitive to moisture and ambient air and possess highly limited compatibility with polar functional groups. These problems were partially solved with the advent of 16 valence electron ruthenium carbenes that were pioneered by *Grubbs*.^{27, 28} The Grubbs catalyst portfolio consists of a variety of ruthenium-based systems of the general formula $[Cl_2(L)(L')Ru=C(H)R]$ (compounds **1b**, **1c**) which are significantly more tolerant toward functional groups, but do not exhibit the same levels of activity or longevity as Schrock catalysts.

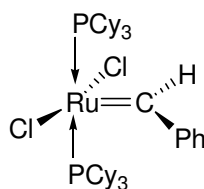
The root of the lower activities of the Grubbs systems lies in their mode of initiation and the accessibility of the reactive species, which has been shown experimentally²⁹ and computationally³⁰ to be the 14-electron alkylidenes $[Cl_2(L)Ru=C(H)R]$ formed upon reversible dissociation of L' from $[Cl_2(L)(L')Ru=C(H)R]$. The reaction temperatures required to overcome this initiation step can lead to decreased catalyst lifetimes. Successful improvements to the "Grubbs first generation" catalyst $[Cl_2(PCy_3)_2Ru=C(H)R]$ are modifications that either encourage the loss of L' ³¹ or reduce the tendency of

1. Introduction

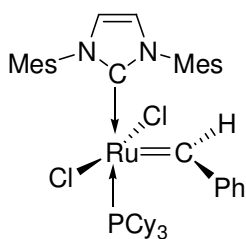
$[\text{Cl}_2(\text{L})\text{Ru}=\text{C}(\text{H})\text{R}]$ to re-capture the liberated ligand L^{32} which competes with the olefin substrate for the coordinatively unsaturated metal center in $[\text{Cl}_2(\text{L})\text{Ru}=\text{C}(\text{H})\text{R}]$.



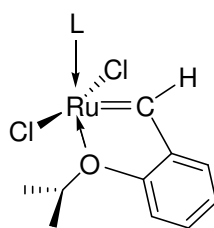
Schrock **1a**



Grubbs 1st Generation **1b**



Grubbs 2nd Generation **1c**



Grubbs-Hoveyda **1d**

Figure 1: Commercially available olefin metathesis catalysts (Cy = cyclohexyl, Mes = 2,4,6-trimethylphenyl).

As a potential way to overcome such problems, *Hoveyda and co-workers* have developed catalysts **1d** (Figure 1) in which a substitutionally labile ether moiety is attached as a loosely chelating group to the carbene ligand that is removed upon the first metathesis event.^{33, 34}

Still, the introduction of the carbene ligand remained rather cumbersome and even the most active of these catalysts displayed only poor activities in the processing of sterically crowded tri- or tetrasubstituted olefins or of alkynes. Other researchers have shown that coordinatively saturated 18 valence electron complexes of the general formula

$[(\eta^6\text{-arene})\text{RuCl}_2(\text{PR}_3)]$ are also active in the processing of olefins. The complex $[(\eta^6\text{-p-cymene})\text{RuCl}_2(\text{PPh}_3)]$ catalyzes the addition of carboxylic acids to alkenes for the synthesis of vinyl esters, such as vinyl acetate and vinyl haloacetates, which are important substrates for polymerization reactions.³⁵ Complexes of the type $[(\eta^6\text{-arene})\text{Ru}(\text{PR}_3)\text{Cl}_2]$ were successfully applied in ring-opening^{36, 37} and ring closing metathesis³⁸ reactions and atom transfer radical polymerizations.³⁹

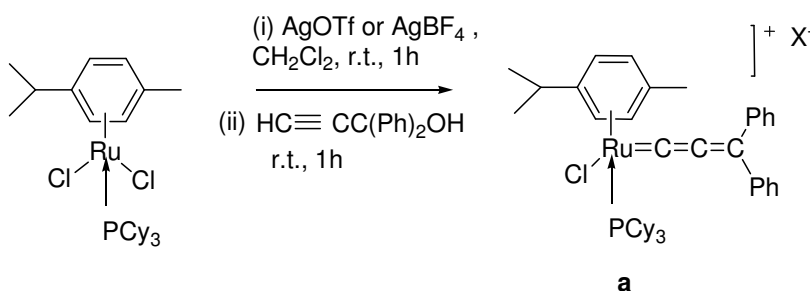
An attractive feature of these catalysts is the fact that they are easily available in high yields from the respective $(\eta^6\text{-arene})$ ruthenium chloro-bridged dimers by simple addition of a phosphine.⁴⁰ The increased stability of these phosphine adducts against oxygen and moisture represents an important advantage for their use in organic synthesis and polymerization reactions.⁴¹ Formation of the most active catalysts was observed when basic and sterically rather demanding phosphines were added. The electron richness on ruthenium is evaluated by its oxidation potential as measured e.g. by cyclic voltammetry. Apparently, the ruthenium(II) centers have to be electron rich in order to efficiently catalyze olefin metathesis.⁴²

The complex $[(\eta^6\text{-p-cymene})\text{RuCl}_2(\text{PCy}_3)]$ has emerged as a precursor for highly efficient alkene metathesis catalysts for ROMP upon photochemical irradiation.^{37, 43} Irradiation likely induces decomplexation of p-cymene from the saturated complex thus generating vacant coordination sites. The catalytically active species also exhibits activity for RCM,⁴⁴ ATRP,⁴⁵ and atom transfer radical additions (ATRA).⁴⁶ Activation of $[(\eta^6\text{-p-cymene})\text{RuCl}_2(\text{PCy}_3)]$ can be accomplished either upon addition of diazoalkanes⁴⁷ or by *in situ* irradiation with UV light.⁴⁸

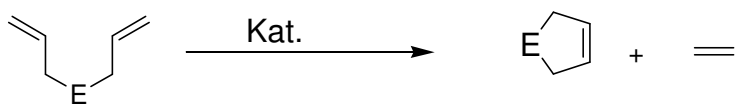
Besides acting as efficient catalysts in the synthesis of complex molecules, ruthenium(II) arene complexes are potential anticancer agents since they bind to DNA bases and have similar ligand exchange kinetics as the successful and widely used cis-Platinum compounds $[\text{Pt}(\text{NH}_3)_2\text{Cl}_2]^+$, and $[\text{Pt}(\text{NH}_3)_2\text{Cl}(\text{H}_2\text{O})]^+$.⁴⁹ Moreover, ruthenium compounds possess low general toxicity.⁵⁰ As an example, the ruthenium complex $[(\eta^6\text{-arene})\text{Ru}(\text{en})\text{Cl}]^+$ exhibits reproducible cytotoxicities against A2780 human ovarian cancer cells.⁵¹ In addition, it has been shown that a number of water soluble $(\eta^6\text{-p-cymene})$ ruthenium(II) complexes exhibit specific antiviral and antimicrobial activities.⁵²

1.2 Activation of alkynols by half sandwich ruthenium complexes: ruthenium allenylidene complexes

In the search for alternative to Grubbs carbene catalysts $[\text{Cl}_2(\text{PR}_3)_2\text{Ru}=\text{CRR}']$, efficient single component, cationic 18 valence electron allenylidene ruthenium complexes $[(\eta^6\text{-arene})(\text{L})\text{ClRu}=\text{C}=\text{C}=\text{CR}_2]^+$ ($\text{L} = \text{PCy}_3, \text{P}^i\text{Pr}_3, \text{PPh}_3$) were designed by *Dixneuf* and *Fürstner*. The discovery of a general method for the preparation of allenylidene complexes based on the direct activation of propargylic alcohols has allowed for detailed studies on these highly unsaturated compounds. Since the first catalytic application in alkene metathesis of $[(\eta^6\text{-p-cymene})\text{Cl}(\text{PCy}_3)\text{Ru}=\text{C}=\text{C}=\text{CPh}_2]^+ [\text{PF}_6]^-$ (**a**) was presented,³⁸ numerous accounts highlight their utility for such processes.⁵³⁻⁵⁸ The complexes of type of **a** are easily prepared from $[(\eta^6\text{-p-cymene})\text{RuCl}_2(\text{L})]$ and prop-2-yn-1-ols such as 1,1-diphenylprop-2-yn-1-ol in the presence of NaPF_6 and in MeOH at room temperature or by treatment of the isolable 16 valence electron complex $[(\eta^6\text{-p-cymene})(\text{PCy}_3)\text{ClRu}]^+$ with an excess of the disubstituted propargylic alcohol (see Scheme 1). These reactions were reported to cleanly lead to the formation of the respective cationic allenylidene complexes, which turned out to successfully rival Grubbs catalysts. As it is case for Grubbs catalysts, these ruthenium based allenylidenes complexes show great tolerance towards a broad array of functional groups and participate in enyne metathesis or ROMP (see Scheme 2).



Scheme 1: Preparation of $[(\eta^6\text{-p-cymene})(\text{L})\text{ClRu}=\text{C}=\text{C}=\text{CPh}_2]^+$ (**a**).



Scheme 2: Ring closing metathesis (RCM) of bisallyl substrates.

It is important to emphasize that the performance of these complexes in ring closing metathesis revealed a strong correlation with the nature the phosphine coordinated to the metal center, the substituents at the phenyl group, the escorting counter anion, and the reaction temperature.⁵⁴ Thus, the catalytic activity of ruthenium-based initiators decreases in the order $\text{PCy}_3 > \text{P}^i\text{Pr}_3 \gg \text{PPh}_3$.³⁸

Investigations into the process of activation of these allenylidene precatalysts revealed two different possible pathways. Irradiation or thermal activation induces the loss of the arene ligand, thus transforming the precatalyst into the active species.^{38, 54, 59-61} Alternatively, phosphine dissociation would also provide a coordinatively unsaturated metal center and an active catalyst. This is thought to be the case in the Lewis or Brønsted acid promoted activation. Considering the counter ion effect,⁵⁴ it was suggested that the high activity of the TfO^- salt arises from its weakly coordinating ability which should favor the dissociation of the p-cymene ligand. The complex containing the bulky BPh_4^- counter ion is thus comparable to the congener containing the PF_6^- anion. The anion BF_4^- may release F^- and BF_3 in its decomposition. It was observed that the F^- anion strongly coordinates to the ruthenium atom and dramatically inhibits the catalytic activity towards RCM,³⁸ thus explaining the poor performance of the BF_4^- salts.

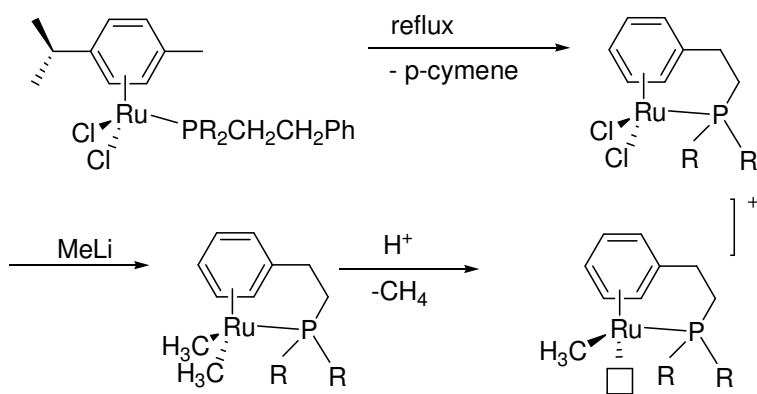
Interestingly, there are only few examples of allenylidene complexes of the type $[(\eta^6\text{-arene})(\text{L})\text{ClRu}=\text{C}=\text{C}=\text{CRR}']^+$ or $[\text{Cl}_2(\text{L})\text{Ru}=\text{C}=\text{C}=\text{CRR}']$ with L other than PR_3 or carbene such as an ether, thioether, or selenoether. Recently, *Hidai's* and *Uemura's* groups have used thiolate-bridged diruthenium complexes of the type $[\text{Cp}^*\text{RuCl}(\mu\text{-SR})_2\text{RuCp}^*\text{Cl}]$ as catalyst precursors for hydroxy substitution reactions of propargyl alcohols. This so-called Nicholas reaction, was proposed to take place via allenylidene intermediates.⁶²⁻⁶⁴ We thus anticipated that thioether-tethered arene complexes $[(\eta^6:\eta^1\text{-C}_6\text{H}_5(\text{CH}_2)_n\text{SR})\text{Cl}(\text{L})\text{Ru}]^+$ may serve as protected forms of $[(\text{arene})\text{Cl}(\text{L})\text{Ru}]^+$ platforms with possible applications in various (arene)Ru-catalyzed reactions.

1.3 Half sandwich complexes of ruthenium with tethered arene ligands

Transition metal half-sandwich complexes with potentially coordinating groups appended to the cyclic perimeter are receiving increasing attention as a special class of complexes bearing hemilabile ligands. These so-called tethered ligands are a class of mixed donor ligands that involve an arene or cyclopentadienyl (Cp) ring to which a pendant donor atom is linked. The dangling coordinating functionality may serve to stabilize otherwise elusive and coordinatively unsaturated species by forming an additional coordinate bond to the metal, thus rendering the respective arene a tetradentate chelate ligand. Examples of tethered $\eta^6:\eta^1$ -arene ruthenium(II) complexes have been reported with nitrogen, oxygen⁶⁵,⁶⁶ phosphorus⁶⁶⁻⁷⁴ and arsenic⁷¹ donors.

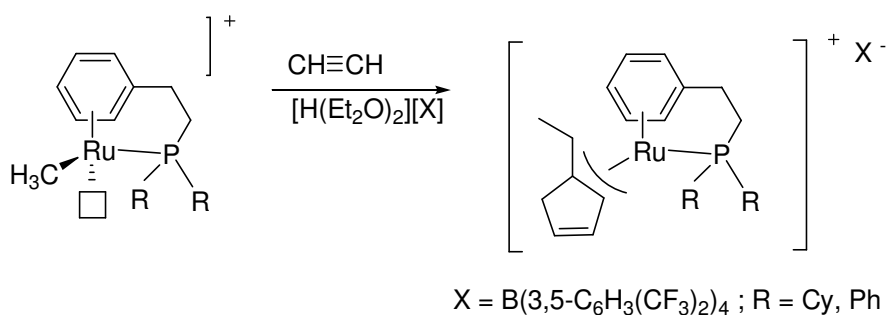
Almost all of those examples center around arene phosphine derivatives with the phosphine donor linked to the arene via a flexible hydrocarbyl spacer. Such an appended phosphine group may even serve as a “Trojan horse” by anchoring the functionalized arene to the metal prior to π -coordination. Arene displacement of complexes $[(\eta^6\text{-arene})\text{RuCl}_2\{\text{PR}_2(\text{CH}_2)_n\text{aryl}\}]$ is then achieved in an either thermally^{61, 67, 69, 73} or oxidatively⁶⁷ induced substitution step. These studies have also disclosed, that such tethers may endow the complexes with reactivities that differ significantly from their non-tethered analogues.^{75, 76} They can considerably contribute to the stability of a complex or a performing catalyst by making use of the chelate effect or enrich them with other favorable properties such as enhanced solubilities in polar or protic media and thermal stabilities.

As an example, *Lee and others* presented a family of ruthenium(II) complexes containing arene-phosphine ligands $\text{C}_6\text{H}_5\text{CH}_2\text{CH}_2\text{PR}_2$ where R = Cy, Ph, Et. Their synthesis follows the sequence shown in Scheme 3. Abstraction of a single methyl group from $[(\eta^6:\eta^1\text{-C}_6\text{H}_5\text{CH}_2\text{CH}_2\text{PR}_2)\text{Ru}(\text{CH}_3)_2]$ affords a vacant site *cis* to the residual methyl group.⁷³



Scheme 3: Strategy in the synthesis of $[(\eta^6:\eta^1\text{-C}_6\text{H}_5\text{CH}_2\text{CH}_2\text{PR}_2)\text{Ru}(\text{CH}_3)]^+$.

A significant characteristic of the coordinatively unsaturated monomethyl complex is that it allows the easy insertion of unsaturated organic species such as alkenes, conjugated dienes, and of CO into the metal-carbon bond. This is the most critical step in oligomerization or polymerization reactions due to its intrinsically high energy barrier.⁷⁵ Scheme 4 displays the product that arises from a sequence of addition, insertion and elimination steps of acetylene into the ruthenium- CH_3 bond.⁷⁷



Scheme 4: Formation of a coordinated unsaturated carbocyclic ligand from the multiple insertion of acetylene into a Ru-CH_3 bond in a tethered (arene)Ru complex.

Severin and co-workers have demonstrated that functional groups, besides tethering, may also serve to immobilize active homogeneous catalysts by grafting them onto solid supports.⁷⁸ It was also shown that those immobilized systems catalyzed the H-transfer hydrogenation of ketones with *i*propanol as efficiently as their discrete mononuclear counterparts.

1. Introduction

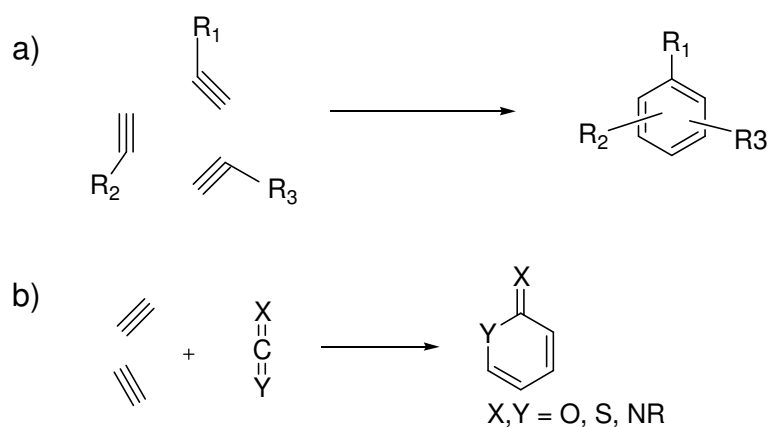
Whereas there exists a considerable number of arene ruthenium half-sandwich complexes with tethered phosphine donors, much less work has been done on complexes of arenes with oxygen containing groups such as ethers or alcohols⁷⁹ or on the alkylthio function. Synthesis of alkylthio arene Ru complexes has been achieved through inconvenient multistep procedures affording only low overall yields. This may be due to the lower strength of the Ru-element bonds compared to that to the phosphine ligand. In fact, there is a likewise limited number of examples of non-tethered thioether adducts $[(\eta^6\text{-arene})\text{Cl}_2\text{Ru}(\text{SR}_2)]$. These have been reported to be labile in solution and to be in equilibrium with their dinuclear, chloro-bridged precursors.^{80, 81} *Kurosawa and co-workers* have briefly reported on $[(\eta^6\text{-C}_6\text{H}_5(\text{CH}_2)_n\text{OH})\text{RuCl}_2]$ ($n = 2, 3$) and assumed them to be chloro bridged dimers with dangling hydroxy groups.^{66, 82} The hydroxy group, however, readily coordinates to the metal center upon removal of a chloride ligand and in cationic derivatives such as $[(\eta^6:\eta^1\text{-C}_6\text{H}_5(\text{CH}_2)_3\text{OH})\text{Ru}(\text{PR}_3)\text{Cl}]^+$ ($\text{PR}_3 = \text{PPh}_3, \text{PEt}_3$) and $[(\eta^6:\eta^1\text{-C}_6\text{H}_5(\text{CH}_2)_3\text{OH})\text{RuL}_2]^{2+}$, where L_2 is a chelating diimine donor such as 2,2'-bipyridine, 1,10-phenanthroline or a bisoxazolonyl ligand. The utility of such complexes for cycloisomerization and ring closing metathesis of diolefins has recently been demonstrated.⁸³

1.4 Coupling reactions of alkynes and alkynols on ruthenium templates

Transition metal catalyzed oligomerization reactions, and coupling reactions in general, are probably the oldest and most extensively studied classes of reactions of organometallic chemistry. They date back to 1950 when *Reppé* published his pioneering work on the cyclotetramerization of acetylene to cyclooctatetraene.⁸⁴ Typical examples of carbon-carbon and carbon-heteroatom bond forming reactions involve the cyclotrimerization of alkynes to substituted benzenes (Scheme 5a), and linear oligomerization and polymerization to butenyne, butatriene, hexadienyne or octatetraenes. In the metal mediated $[2+2+2]$ cyclotrimerization of alkynes for the synthesis of substituted benzenes three C-C bonds are sequentially formed⁸⁴ and this process is exothermic.⁸⁵ Cyclocotrimerization of two alkynes with unsaturated organic compounds containing C=X bonds ($X = \text{C}, \text{O}, \text{S}, \text{N}, \text{etc.}$) gives rise to carbocycle and heterocycle structures as exemplarily shown in Scheme 5b. The nitrile group, as a triply bonded species, does not self-trimerize under the conditions of alkyne cyclotrimerization,

but can be co-trimerized with alkynes to give pyridines. In spite of detailed documentation of those reactions, the development of new cyclisation methods is still attracting great attention because of the biological activity of the synthesized carbocycles (arenes) and heterocycles in Scheme 5b.

A wide array of transition metal complexes were found to catalyze cyclization reactions. Cobalt and ruthenium proved to be particularly efficient and to tolerate the presence of different functionalities on the alkynes. Lying in the heart of the periodic table, ruthenium combines valuable properties of both its early- and late transition-metal neighbors. Thus, the high reactivity of elements to its left, and the less oxophilic and Lewis acidic nature of those to its right, results in a special array of desirable properties.⁸⁶



Scheme 5: Metal catalyzed cyclotrimerization of alkynes for synthesis of substituted benzenes and heterocycles.

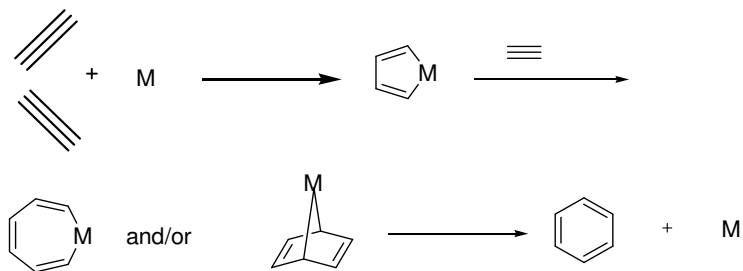
Transition metal catalyzed alkyne cyclotrimerization can be broadly divided into three categories depending on their mechanism. The most widely accepted mechanism is so-called “common mechanism” in which a metallacyclopentadiene intermediate is first formed by oxidative cyclization of two alkyne molecules on a low-valent metal center and reacts further with another alkyne to afford the aromatic product (Scheme 6a).⁸⁷ A myriad of metallacyclopentadiene complexes relevant to cyclotrimerization have been isolated to date and shown to yield the corresponding aromatic products upon treatment with alkynes. On the other hand, a sequential carbometalation mechanism operates when starting from transition-metal hydrides or halides M-X (Scheme 6b).^{88, 89, 90} In addition to these well-known precedents, a metathesis cascade using Grubbs’ ruthenium carbene complexes

1. Introduction

quite recently proved to be very effective in producing arenes upon reaction with an alkyne (Scheme 6c).⁹¹

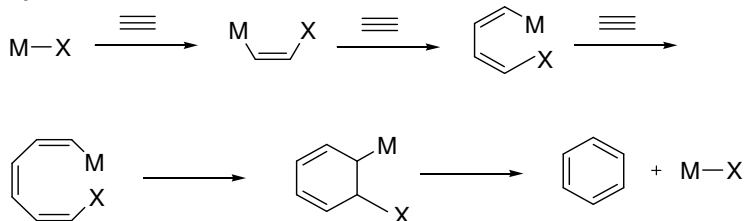
Metallacycle Route (Common Mechanism)

a)



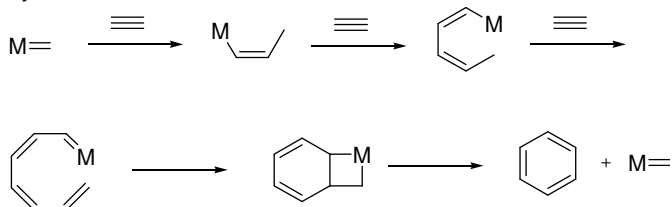
Sequential Insertion Route

b)



Metathesis Cascade Route

c)

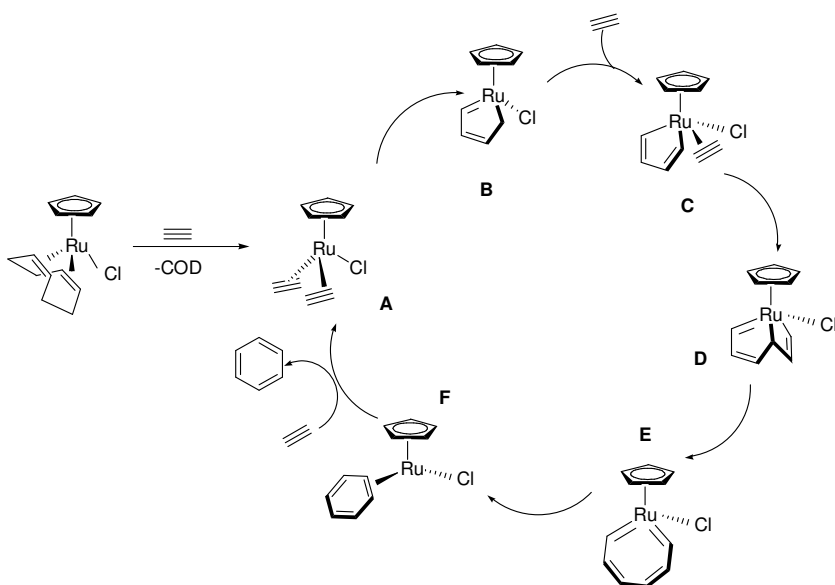


Scheme 6: Possible mechanisms for the cyclotrimerization of alkynes.

Enormous progress in computational and theoretical chemistry during the past several years has allowed to study the thermodynamics and mechanisms of such

cyclotrimerization reactions. These studies have revealed that this process is extremely exothermic and that completely different intermediates are involved when comparing $\text{CpCo}(\text{L})_2$ ⁹² and 14 valence electron species $\text{Cp}^{\text{R}}\text{RuCl}$ derived from $\text{Cp}^{\text{R}}\text{Ru}(\text{COD})\text{Cl}$ precursors by olefin dissociation (Cp^{R} = substituted cyclopentadienyl ligand).^{93, 94}

The accepted mechanism of alkyne cyclotrimerization promoted by $\text{Cp}^{\text{R}}\text{Ru}(\text{COD})\text{Cl}$ complexes is shown in Scheme 7. The initial step of the reaction is replacement of the labile COD ligand by two molecules of acetylene. Metallacycle **B** forms easily and can be studied *in situ* by NMR spectroscopy; it has even been structurally characterized.⁹⁵ The reaction of **B** with another alkyne gives complex **C**. The next step is a facile C-C coupling between the coordinated acetylene and metallacyclopentadiene to afford an unusual bicyclic 1-ruthenabicyclo[3.2.0]hepta-1,3,6-triene **D**, featuring anellated five and four membered rings. Then, the bicycle opens to yield **E**, which in turn undergoes facile reductive elimination to give **F** containing a η^2 -coordinated benzene ligand.⁹³



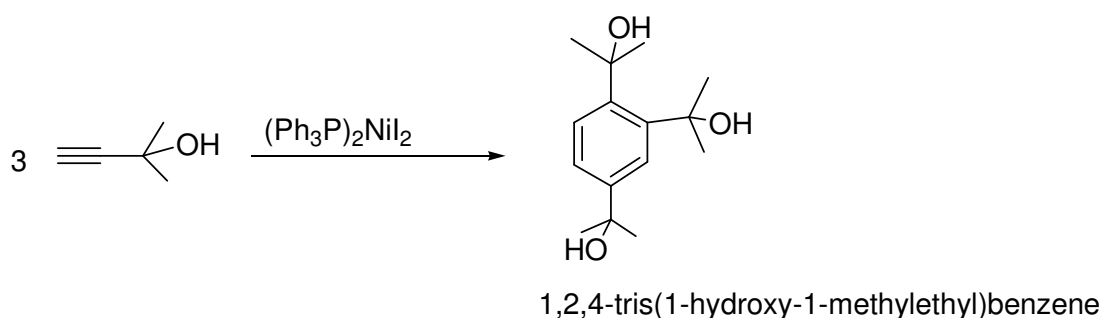
Scheme 7: Catalytic cycle of “CpRu” catalyzed cyclotrimerization of acetylene.

CpRu and $(\text{arene})\text{Ru}^+$ entities are isoelectronic. This isoelectronic relationship was not utilized in cyclotrimerization so far. Our goal was to investigate the reactivity of various $(\text{arene})\text{Ru}$ complexes with alkynes and see whether they would induce similar reactions.

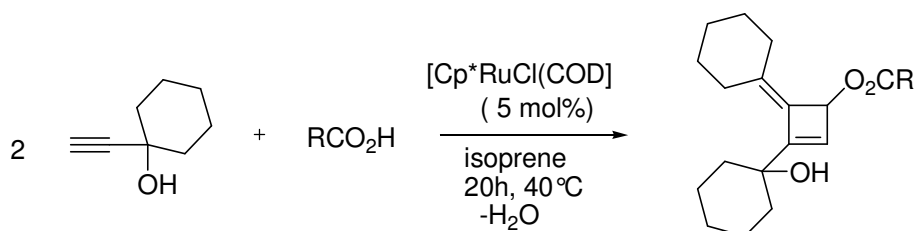
Despite the wealth of such alkyne coupling reactions, efficient transformations of alkynols are extremely rare. This is because the free hydroxy group strongly interacts with many of

1. Introduction

the cyclisation catalysts employed to date, thus preventing efficient transformations. The few reported examples include their linear tail-to-tail dimerization to give hydroxy substituted butadienones,⁹⁶ their cyclodimerization to alkylidene cyclobutenes (Scheme 9) in the presence of carboxylic acids,⁹⁷ and the insertion of alkynols into a ruthenacyclopentatriene to give vinylbutatrienyl ligands.⁹⁸ The nickel catalyzed cyclotrimerization of 2-methylbut-3-yn-2-ol to either 1,2,4- or 1,3,5- $C_6H_3(CH_2OH)_3$ (Scheme 8),^{99, 100} and the cyclotrimerization under mild conditions in water of but-2-yne-1,4-diol to the corresponding benzene have also been observed.¹⁰¹



Scheme 8: Selective catalytic activity of $(PPh_3)_2NiI_2$ in the cyclotrimerization of 2-methylbut-3-yn-2-ol.

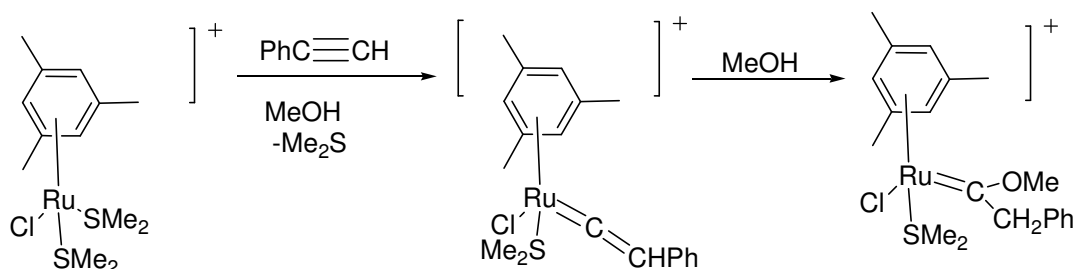


Scheme 9: Ruthenium-catalyzed one step transformations of propargylic alcohols into alkylidene cyclobutenes.

2 p-Cymene Ruthenium Thioether Complexes

2.1 Known arene thioether ruthenium complexes

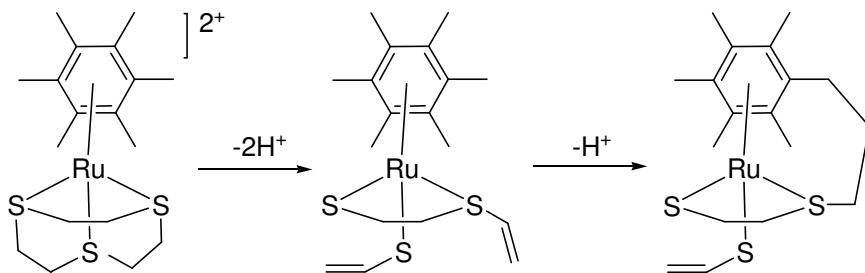
Half-sandwich arene complexes of ruthenium with heteroatom donor ligands such as phosphines and amines are intensively being explored and used in catalysis as it has been described in the Introduction. $(\eta^6\text{-arene})\text{Ru(II)}$ complexes bearing sulfur based ligands are of special interest because of their relevance to biological and industrial processes.¹⁰² In particular, $(\eta^6\text{-arene})\text{Ru(II)}$ complexes containing chelating bi- or tridentate thiolate ligands are well established. On the other hand, complexes of monodentate thioethers R_2S , e.g. dimethyl sulfide and tetrahydrothiophene such as $[(\eta^6\text{-arene})\text{RuCl}_2(\text{SR}_2)]$ and $[(\eta^6\text{-arene})\text{RuCl}(\text{SR}_2)_2]^+$ (arene = p-cymene, 1,3,5- $\text{C}_6\text{H}_3\text{Me}_3$ or C_6Me_6), are generally unstable toward thioether dissociation or displacement presumably because of the inherently weak Ru-SR_2 bond and hence are rather uncommon. Studies by *Dixneuf* revealed that complexes $[(\eta^6\text{-arene})\text{RuCl}_2(\text{SR}_2)]$ are labile and exist in equilibrium with their dimeric halide bridged precursors $[(\eta^6\text{-arene})\text{RuCl}_2]_2$. They may easily exchange the thioether ligand by better donors such as phosphines. Cationic bisadducts $[(\eta^6\text{-arene})\text{RuCl}(\text{SR}_2)_2]^+$ are more stable but, in methanolic solution, still react readily with terminal alkynes by replacement one of thioether ligand, giving rise to methoxycarbene complexes via vinylidene intermediates (Scheme 10).⁸⁰ The use of thiacrown or mixed thioether/thiolate chelates also aids to stabilize thioether coordination.



Scheme 10: Substitution of a labile SMe_2 ligand with phenylacetylene.

2. p-Cymene Ruthenium Thioether Complexes

However, *Bennett and Goh* have isolated stable complexes of the $[(\eta^6\text{-HMB})\text{Ru}(\text{II})]$ entity (HMB = $(\eta^6\text{-C}_6\text{Me}_6)$) containing a (1,4,7-trithiacyclononane) and acyclic thioether/thiolate ligands by base-induced fragmentation of the macrocyclic precursors (see Scheme 11).¹⁰³ Several examples for centered reactivity and thioether/thiolate interconversions within the coordination sphere of various (Cp/Cp*)Ru(II) and (HMB)Ru(II) complexes are known in the literature.¹⁰⁴



Scheme 11: Successive deprotonation of a tridentate macrocyclic trithioether.

Preparation of bi-, tri-, and polinuclear metal compounds by utilizing dithiane as core centers have investigated by *Yamamoto*. Reactions of $[(\text{arene})\text{RuCl}_2]_2$ (arene = p-cymene, C_6H_6) with 1,3-dithiane ($1,3\text{-S}_2\text{C}_4\text{H}_8$) gave $[(\text{L}\text{RuCl}_2)_2(1,3\text{-S}_2\text{C}_4\text{H}_8)]$ (L = p-cymene, C_6H_6) if the molar ratio between starting dimer and the ligand is 1:1, and $[(\text{LMCl}_2)(1,3\text{-S}_2\text{C}_4\text{H}_8)]$ if 1,3-dithiane is added in excess. The reaction in the presence of KPF_6 afforded the corresponding ionic complex $[(\text{LClRu}(1,3\text{-S}_2\text{C}_4\text{H}_8)_2)]^+ [\text{PF}_6]^-$. The dithiane and trithiane have potential as the bridging ligands in the construction of supramolecules and dendrimeric structures containing metal atoms.¹⁰⁵

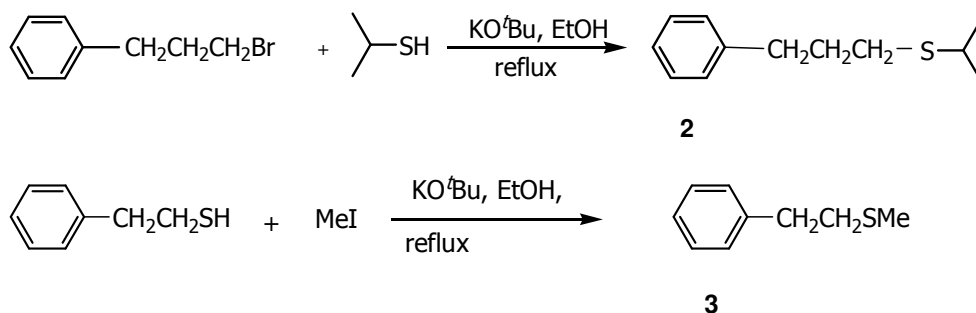
A question of our concern was, if it is possible to increase the stability of the inherently weakly coordinated simple thioether group by tethering. As it has been shown in various examples in the case of phosphine ruthenium complexes,⁷³ it should be possible to stabilize the ruthenium thioether bond by attaching the SR_2 moiety through a flexible side chain to the arene ligand rendering the functionalized arene a tetradentate hemilabile ligand.

2.2 Synthesis of half sandwich complexes $[(\eta^6\text{-arene})\text{RuCl}_2(\text{SRR}')]]$

With the aim to prepare tethered Ru(II) complexes $[(\eta^6:\eta^1\text{-arene-L})\text{RuCl}_2]$ (L = thioether derivatives), we have first synthesized $[(\eta^6\text{-arene})\text{RuCl}_2(\text{SRR}')]]$ complexes with the unsymmetrical simple aryl-alkyl or alkyl-allyl thioether ligands *i*-propyl(3-phenylpropyl)sulfide, ($\text{PhC}_3\text{H}_6\text{S}^i\text{Pr}$), methyl(2-phenylethyl)sulfide, ($\text{PhC}_2\text{H}_4\text{SMe}$), and allyl methylsulfide ($\text{MeSCH}_2\text{CH}=\text{CH}_2$).

The aryl alkyl thioether ligands were designed to possess pendant arene functionalities. Allyl methylsulfide was chosen as deprotonation typically occurs at a methyl substituent of the arene in $[(\eta^6\text{-HMB})\text{RuCl}_2(\text{L})]$ or $[(\eta^6\text{-p-cymene})\text{RuCl}_2(\text{L})]$. The resulting carbanion can then undergo Michael addition to the terminal propene carbon of the thioether allyl ligand and thus give rise to a tethered species.¹⁰⁶ As a point of comparison, similar derivatives containing pendant pyridine moieties were also investigated.

The synthesis of the new arylalkyl substituted thioethers, *i*-propyl(3-phenylpropyl)sulfide, ($\text{PhC}_3\text{H}_6\text{S}^i\text{Pr}$, **2**), and methyl(2-phenylethyl)sulfide, ($\text{PhC}_2\text{H}_4\text{SMe}$, **3**) follows established procedures¹⁰⁷ and is outlined in Scheme 12. Both rely on the nucleophilic substitution of bromide or iodide by the corresponding thiolate. The latter was produced from the parent thiol by deprotonation with KO^tBu prior to addition of the alkyl halide. The novel thioethers were obtained in good yields after distillation in vacuo.

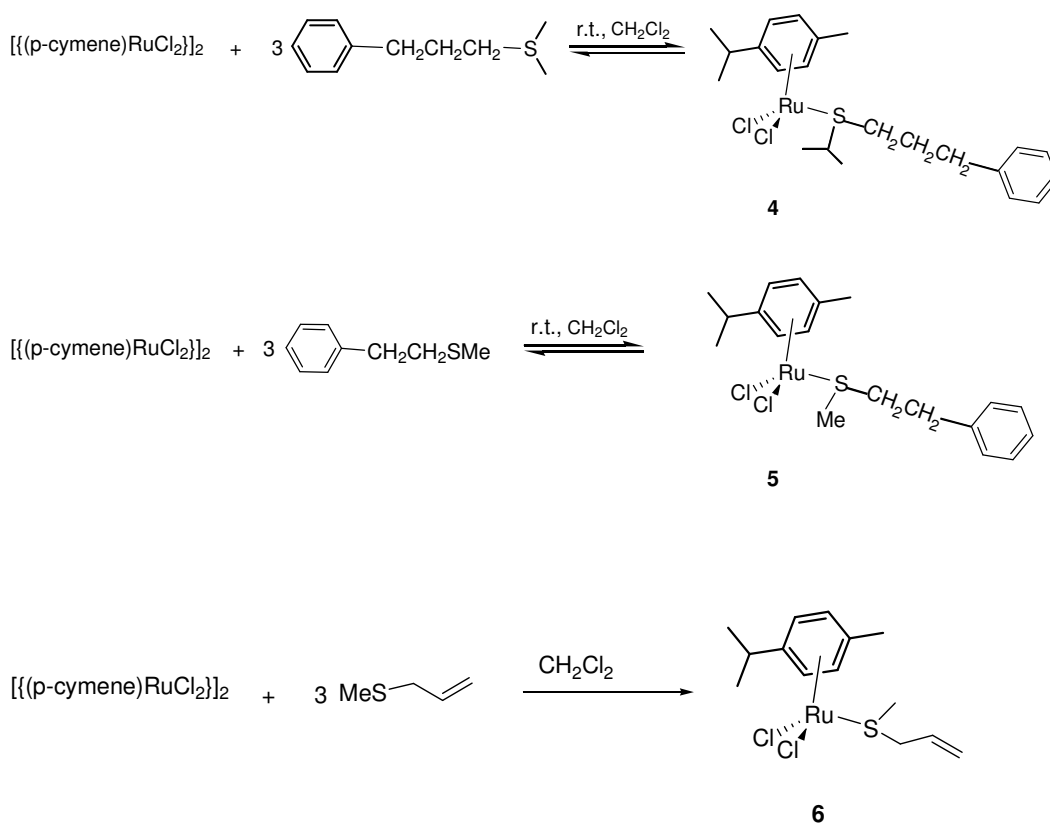


Scheme 12: Synthesis of the thioethers $\text{Ph}(\text{CH}_2)_n\text{SR}$.

Introducing a slight excess (ca. 1.5 eq) of thioether ligands **2**, **3** or of $\text{MeSCH}_2\text{CH}=\text{CH}_2$ to $[\{(\eta^6\text{-p-cymene})\text{RuCl}_2\}_2]$ (**1**) at room temperature in CH_2Cl_2 and stirring overnight gave equilibrium mixtures of mononuclear adducts $[(\eta^6\text{-p-cymene})\text{RuCl}_2(\text{SRR}')]]$ (**4**)-(6) as orange red solids and of the starting materials (Scheme 13). From these solutions pure

2. p-Cymene Ruthenium Thioether Complexes

thioether complexes **4-6** were obtained by crystallization from $\text{CD}_2\text{Cl}_2/\text{Et}_2\text{O}$ mixtures. Upon dissolution of the pure complexes in CD_2Cl_2 at ambient temperature the equilibria indicated in Scheme 13 were re-established. In the case of sterically more demanding thioethers (**4** and **5**) the obtained solids contained the thioether adducts along with the starting material whereas for **6** NMR data clearly show that the monoadduct is the only species formed in the reaction. These observations match well with reports by *Dixneuf and co-workers* for reactions of $[(\eta^6\text{-}1,3,5\text{-Me}_3\text{C}_6\text{H}_3)\text{RuCl}_2]_2$ with SMe_2 . They found that simple thioether adducts $(\eta^6\text{-arene})\text{RuCl}_2(\text{SRR}')$ are labile in solution and coexist in equilibrium with the dichloro bridged precursor **1** and free thioether.⁸⁰



Scheme 13: Monothioether $(\eta^6\text{-p-cymene})\text{Ru}$ complexes **4-6**.

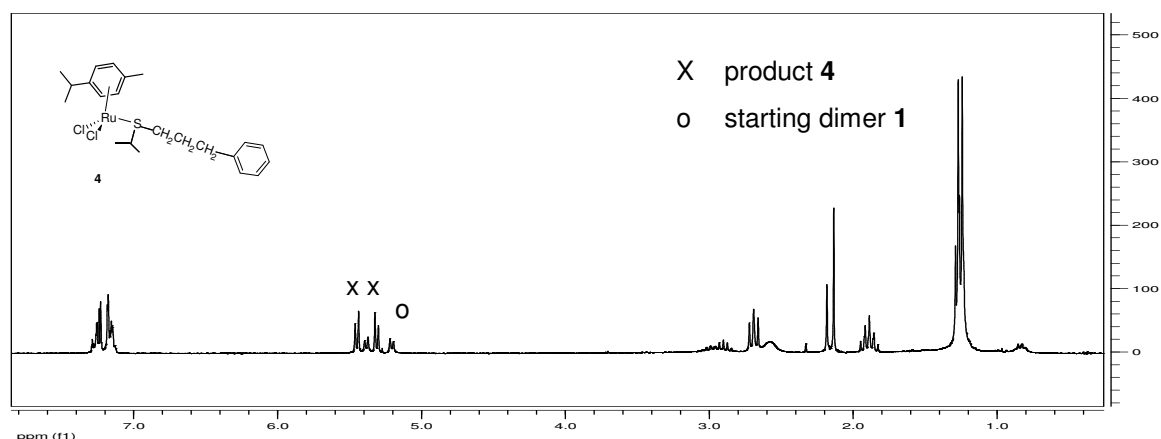
Ligand dissociation from complexes **4**, **5** is readily observed in NMR spectroscopy. NMR studies disclosed that pure complexes **4** and **5**, when dissolved in CD_2Cl_2 always give equilibrium mixtures between adduct, free thioether and starting dimer. The resonance signals of the dissociated thioether and the coordinated SRR' ligand are generally

2. p-Cymene Ruthenium Thioether Complexes

coalesced, giving only one set of signals (Figure 2a). Various different 2D-NMR methods such as H, C, HSQC HMBC, and NOE techniques were applied in order to distinguish between the resonances of free and bound thioether, but the thioether signals were always merged into a single set. Two dynamic processes account for the coalescence of the ^1H resonance signals of the thioethers in these mixtures: Ligand dissociation on one hand and sulfur inversion on the other.¹⁰⁸ Therefore, for every thioether complex, the resonance signals of the alkyl substituents neighboring the S atom are broadened. Discrimination between dinuclear **1** and the thioether adducts **4-6** in the equilibrium solution was nevertheless possible by the analysis of the ^1H -NMR signals in the regime of the coordinated p-cymene. Thus, signals ascribed to **1** and **4-6**, respectively, appeared as two sets of well resolved, separate doublets (see Figure 2a). Relative amounts of **1** and **4-6** in these equilibrium mixtures can be determined by ^1H -NMR integration of individual sets of CH resonances of the cymene ligand. Values of 12:1, 5:2 and 7.5:1 were obtained in CDCl_3 for **4-6**, respectively. This corresponds to the steric crowding around the sulfur atom of the thioether ligands, e.g. the bulkier the thioether substituents are, the larger is the amount of the starting dimer. Nearly identical values were obtained by comparing the peak currents of **4-6** and **1** in cyclic voltammetry experiments (see section 2.8). Figure 2b shows the ^1H -NMR spectrum immediately after dissolving the pure complex **4** in CD_2Cl_2 . Interestingly, in the shift region of the coordinated arene only one set of doublets could be observed indicating the presence of the desired monothioether adduct only. In toluene- d_8 , **4** initially forms a clear orange solution from which **1** slowly crystallizes. The final solution equilibrium mixture contains free $\text{PhC}_3\text{H}_6\text{S}^i\text{Pr}$ and **4** in an approximate 1:1 ratio as based on comparison of the integrals of the arene CH signals of **4** to those of the thioether methylene protons. A similar ratio of 1:0.88 (**4**:**1**) was observed in highly polar CD_3OD where **1** remains in solution.

2. p-Cymene Ruthenium Thioether Complexes

a)



b)

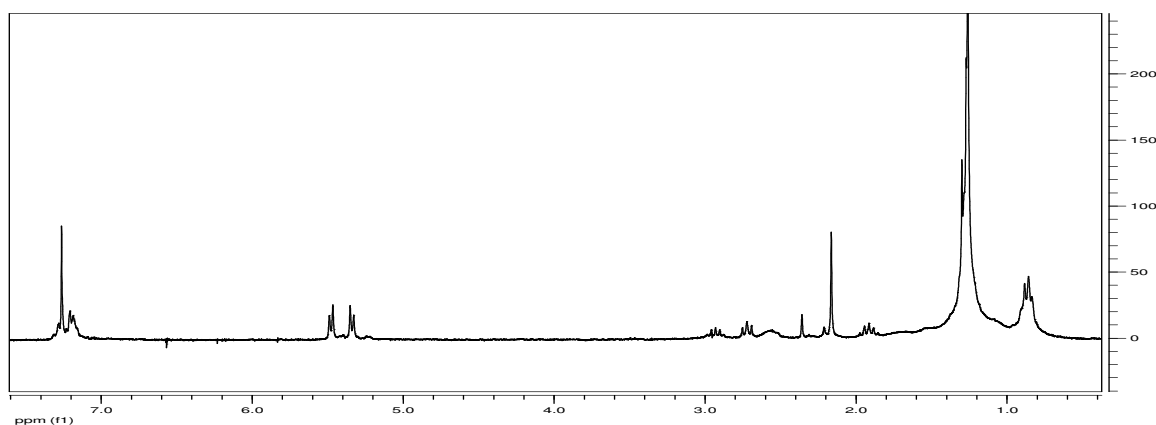


Figure 2: a) $^1\text{H-NMR}$ spectra of crude solid **4**.
b) NMR of microcrystalline **4** immediately after dissolving in CD_2Cl_2 .

In the course of our work we also prepared the cationic bis(thioether) adduct $[(\eta^6\text{-p-cymene})\text{RuCl}(\text{SR}_2)_2]^+ \text{SbF}_6^-$ (**7**) originally synthesized by *Dixneuf*.⁸⁰ As mentioned in the *Introduction*, those bisadducts are significantly more stable toward thioether dissociation. In our hands, following *Dixneuf*'s procedure, this complex was accompanied by small quantities of the trichloro bridged bis(arene) complex $\{[(\eta^6\text{-p-cymene})\text{Ru}]_2(\mu\text{-Cl})_3\}^+ \text{SbF}_6^-$ (**8**). Crystallization from a dichloromethane/ether mixture resulted in the crystallization of both **7** and **8**. Crystals of these compounds could be manually separated based on their different shapes. The structures of both complexes

were determined by X-ray diffraction and these will be discussed in the following section together with those of the monothioether Ru complexes.

2.3 X-ray structure determinations of $[(\eta^6\text{-p-cymene})\text{RuCl}_2(\text{SRR}')]$ (5), (6), $[(\eta^6\text{-p-cymene})\text{RuCl}(\text{SMe}_2)_2]^+ \text{SbF}_6^-$ (7), and $\{[(\eta^6\text{-p-cymene})\text{Ru}]\}_2(\mu\text{-Cl})_3\}^+ \text{SbF}_6^-$ (8)

Crystals of compounds **5**, **6**, **7** and **8** were grown by slow diffusion of ether into a concentrated solution of these complexes in CH_2Cl_2 and investigated by X-ray crystallography. The complexes, $[(\eta^6\text{-p-cymene})\text{RuCl}_2(\eta^1\text{-MeSC}_2\text{H}_4\text{Ph})]$ (**5**), $[(\eta^6\text{-p-cymene})\text{RuCl}_2(\text{MeSC}_3\text{H}_5)]$ (**6**) and $[(\eta^6\text{-p-cymene})\text{RuCl}(\text{SMe}_2)_2]^+ \text{SbF}_6^-$ (**7**) represent rare examples of structurally characterized $(\eta^6\text{-arene})\text{Ru}$ complexes bearing simple thioether ligands.

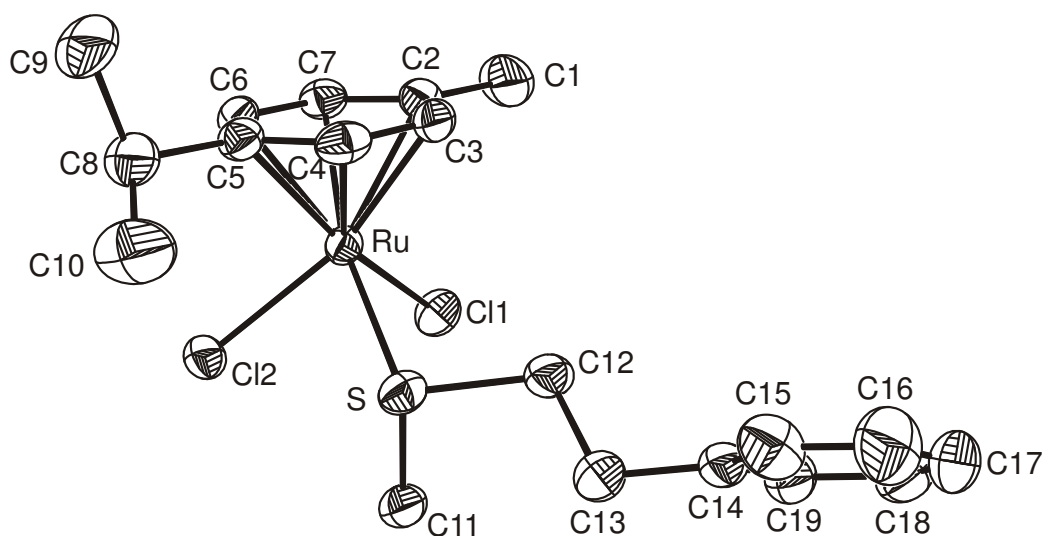


Figure 3: Structure of $[(\eta^6\text{-p-cymene})\text{RuCl}_2(\eta^1\text{-MeSC}_2\text{H}_4\text{Ph})]$ (**5**) in the solid state.

2. *p*-Cymene Ruthenium Thioether Complexes

Table 2: Selected structural parameters of $[(\eta^6\text{-}p\text{-cymene})\text{RuCl}_2(\text{MeSC}_3\text{H}_5)]$ (**6**).

Bond lengths (Å)		Bond angles (°)	
Ru-C2	2.191(2)	Cl-Ru-Cl	88.31(3)
Ru-C3	2.165(2)	Cl-Ru-S	80.37(3), 81.50(3)
Ru-C4	2.187(3)	C11-S-C12	100.50(18)
Ru-C5	2.207(2)	C11-S-Ru	109.18(12)
Ru-C6	2.200(2)	C12-S-Ru	107.82(12)
Ru-C7	2.190(2)		
Ru-Cl	2.4104(7), 2.4121(11)		
Ru-S	2.3978(8)		
S-C11	1.811(3)		
S-C12	1.824(4)		

Figures 3 and 4 display the structures of the complexes **5** and **6** in the solid states. The most important interatomic distances and bond angles are collected in Tables 1 and 2.

Complexes **5** and **6** crystallize in the monoclinic space groups $P2_1/n$ and $C2/c$, respectively. Two chloride and the thioether ligands occupy three coordination sites and form almost equally long legs of the piano-stool structure which is archetypical of half-sandwich arene complexes. The Ru-S bond lengths are close to 2.40 Å (2.403(1) Å in **5** and 2.3978(8) Å in **6**) and are thus notably longer than those in arene half sandwich complexes where the thioether moiety is part of a macrocycle¹⁰³ or a mixed thioether thiolate chelate ligand.^{103, 109} In these complexes Ru-S bonds usually range from 2.30 to 2.34 Å. The longer Ru-S distances reflect the inherent weakness of the unsupported Ru-S(thioether) bond as it is evident from the ready dissociation of the SR_2 ligand and partial formation of dichloro bridged $[(\eta^6\text{-arene})\text{RuCl}_2]_2$ dimers. Bond angles subtended by the ligands forming the legs and the ruthenium atom are all close 90° in **5** ($\text{Cl1-Ru-Cl2} = 89.52(3)^\circ$, $\text{Cl1-Ru-S} = 88.14(3)^\circ$, $\text{Cl2-Ru-S} = 84.51(3)^\circ$) and attest to the overall octahedral coordination of the metal atom. Larger deviations from this geometry are observed for **6**, where the S-Ru-Cl angles are somewhat acute at 80.37(2) and 81.50(2)°. The Ru-Cl bond lengths of 2.411(1) and 2.439(1) Å in **5** or 2.4104(7) and 2.4121(11) in **6** are unexceptional for monomeric dichloro arene ruthenium complexes featuring neutral two-electron donor ligands L like, e. g. $[(\eta^6\text{-C}_6\text{Me}_3\text{H}_3)\text{RuCl}_2(\text{pyridine})]$ (2.419(2) and 2.415(2) Å)¹¹⁰ or $[(p\text{-cymene})\text{RuCl}_2(2\text{-aminopyridine})]$ (2.405(3) and 2.402(3) Å).¹¹¹ Bond lengths to the carbon atoms of the cymene ring vary from 2.150 (3) Å to 2.216 (4) Å. In **5**,

2. p-Cymene Ruthenium Thioether Complexes

the longest Ru-C bond involves the methyl substituted carbon atom C2 as it is observed for many cymene ruthenium complexes, while this is not the case for **6**. The arene rings display a distinct C-C bond length alteration, and the average values of the long and short bonds differ by 0.02 Å. Essentially the same pattern is also observed for the bis(thioether) complex **7** and for one of the cymene ligands in the trichloro bridged dimer **8**.

Complex **7** crystallizes in the monoclinic space group $P2_1/c$. The structure of the complex cation of **7** (see Figure 5) resembles that of **5**, **6** in all its main structural characteristics, e.g. its three legged piano stool geometry with three essentially equally long legs. When comparing **7** with the structures of **5** and **6**, a small yet significant decrease in Ru-S bond lengths to 2.383(8) and 2.388(8) Å and of the Ru-Cl bond length to 2.394(7) Å is observed. This may be ascribed to the overall positive charge of the complex resulting in a stronger attraction between the metal atom and the electron-rich donor ligands and hence slightly shorter bond lengths. In contrast, the Ru-C bonds become slightly longer and their average value increases from 2.185 Å in **5** or 2.190 Å in **6** to 2.212 Å in **7**. In the crystalline state the two thioether ligands adopt a different orientation with respect to the arene ligand. While the methyl groups on S1 are in an *exo*-position with the methyl groups pointing away from the cymene ligand, the opposite is true for the second thioether ligand associated with S2.

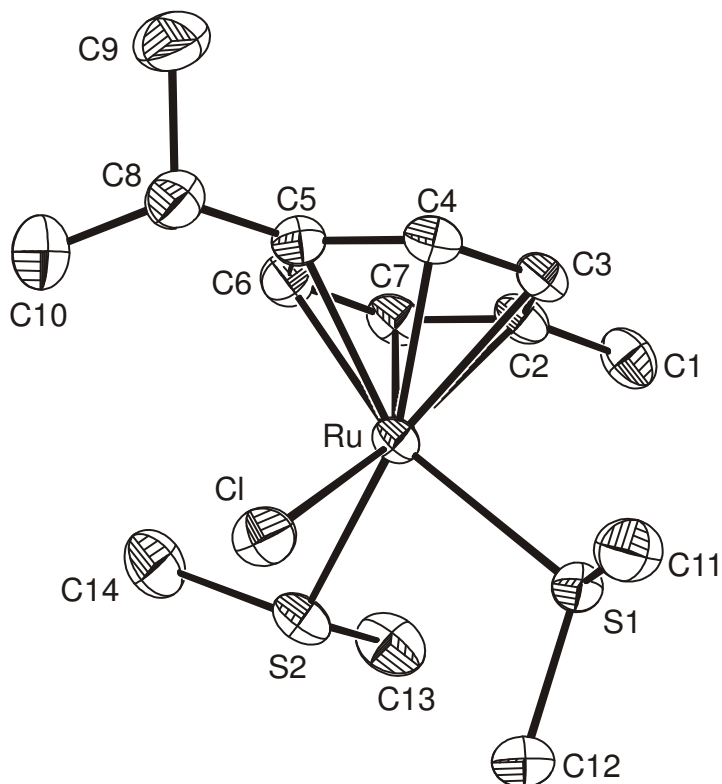


Figure 5: Structure of $[(\eta^6\text{-}p\text{-cymene})\text{RuCl}(\text{SMe}_2)_2]^+ \text{SbF}_6^-$ (**7**) in the solid state with the atom numbering.

Table 3: Selected structural parameters of $[(\eta^6\text{-arene})\text{RuCl}_2(\text{SMe}_2)_2]^+ \text{SbF}_6^-$ (**7**).

Bond lengths (Å)		Bond angles (°)	
Ru-C2	2.220(3)	Cl-Ru-S	87.69(3), 81.86(3)
Ru-C3	2.220(3)	S-Ru-S	87.50(3),
Ru-C4	2.197(3)	C11-S1-C12	97.90(2)
Ru-C5	2.240(3)	C11-S1-Ru	105.22(16)
Ru-C6	2.229(3)	C12-S1-Ru	112.70(14)
Ru-C7	2.183(3)	C13-S2-C14	100.70(3)
Ru-Cl	2.394(1)	C13-S2-Ru	110.40(17)
Ru-S	2.383(1), 2.388(1)	C14-S2-Ru	107.61(18)
S-C11, S-C13	1.801(4), 1.797(5)		
S-C12, S-C14	1.803(4), 1.798(5)		

The structure of the dinuclear complex **8** is shown in Figure 6. The complex cation adopts the familiar structure of two face-sharing octahedra with the arene ligands and the three chloride ligands as the opposite faces. This motif is highly common of complexes of the

2. p-Cymene Ruthenium Thioether Complexes

general composition $[L_3M(\mu-L')_3ML_3]^{n+}$ and has ample precedence in arene ruthenium chemistry.¹¹² Individual arene and Cl_3 planes are nearly parallel to each other with angles between their normals of 2.69° (Arene1- Cl_3), 0.28° (Arene2- Cl_3) and 2.87° (Arene1-Arene2), where Arene1 and Arene2 denote the arene ligands bonded to atom Ru1 and Ru2, respectively. The metal atoms are very slightly shifted off-center toward the common Cl_3 face of the bisoctahedron. Thus, the Ru- Cl_3 distances amount to 1.640 Å (Ru1- Cl_3) and 1.644 Å (Ru2- Cl_3) while the Ru atoms are 1.647 Å (Ru1) and 1.651 Å (Ru2) away from the corresponding arene planes. Ru-Cl distances range from 2.424(1) to 2.434(1) Å and are thus only slightly longer than typical bonds to terminal chloride ligands as in complexes **5-7**. The Ru-Cl distances in **8** also match well with the literature data of other complexes of the type $[\{(\eta^6\text{-arene})Ru\}_2(\mu-Cl)_3]^+$ where arene is C_6H_6 ,¹¹³ toluene,¹¹⁴ C_6Me_6 ,¹¹⁵ or ethoxybenzene,⁷⁹ and with the bis(p-cymene) complex $[\{(\eta^6\text{-p-cymene})Ru\}_2(\mu-Cl)_3]^+ BPh_4^-$.¹¹¹

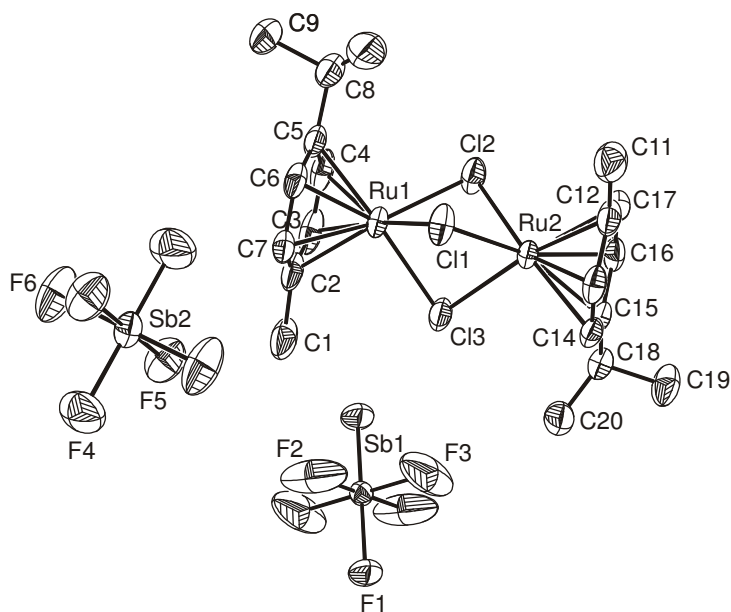


Figure 6: Structure of $[\{(\eta^6\text{-p-cymene})Ru\}_2Cl_3]^+ SbF_6^-$ (**8**) in the solid state. Note that the Sb atoms reside on special positions (Sb1/Sb1a: $(0,0,1/2)$ and $(0,1,1/2)$, respectively and Sb2/Sb2a $(1/2,1,0)$ bzw. $(1/2,0,1)$, respectively) and are thus related by an inversion center triclinic P-1. Thermal ellipsoids are drawn at a 50% probability level.

2. *p*-Cymene Ruthenium Thioether Complexes

Table 4: Interatomic distances and bond angles for **8**.

Bond lengths (Å)				Bond angles (°)	
Ru1-Cl1	2.4238(12)	Ru1-C5	2.184(5)	Cl1-Ru1-Cl2	79.61(4)
Ru2-Cl1	2.4341(11)	Ru1-C6	2.147(4)	Cl2-Ru1-Cl3	79.17(5)
Ru1-Cl2	2.4316(13)	Ru1-C7	2.174(5)	Cl1-Ru1-Cl3	79.53(5)
Ru2-Cl2	2.4307(12)	Ru2-C12	2.172(5)	Cl1-Ru2-Cl2	79.42(4)
Ru1-Cl3	2.4299(13)	Ru2-C13	2.139(5)	Cl2-Ru2-Cl3	79.14(4)
Ru2-Cl3	2.4324(13)	Ru2-C14	2.171(5)	Cl1-Ru2-Cl3	79.28(5)
Ru1-C2	2.176(6)	Ru2-C15	2.204(4)	Ru1-Cl1-Ru2	85.07(4)
Ru1-C3	2.157(6)	Ru2-C16	2.165(5)	Ru1-Cl1-Ru2	84.97(4)
Ru1-C4	2.143(6)	Ru2-C17	2.163(5)	Ru1-Cl3-Ru2	84.97(4)

Owing to restrictions imposed by face sharing, the Cl-Ru-Cl angles lie in a narrow range from 79.14(4) to 79.61(4)° and are even more acute as is observed for the monomeric thioether adducts. The Ru-Cl-Ru angles are all close to 85° and this again resembles the values of the tetraphenylborate salt, where these angles range from 84.1 to 86.1°. Ru-C bonds are in the range from 2.139(5) to 2.204(4) Å. For each cymene ligand, the longest Ru-C bond involves the C atom that bears the *i*Pr group. The cymene ligands at Ru(1) and Ru(2) differ in the orientation of the *i*Pr-substituents as it is shown by the torsional angles of C(4)-C(5)-C(8)-C(9) = 93.7(9)° for Ru(1), resembling an orthogonal orientation with respect to the ring plane, and C(14)-C(15)-C(18)-C(20) = 30.8(7)° for Ru(2).

The related complexes $[(\eta^6\text{-C}_6\text{H}_6)\text{Ru}]_2\text{Cl}_3]^+ \text{BF}_4^-$ and $[(\eta^6\text{-C}_6\text{H}_5\text{Me})\text{Ru}]_2\text{Cl}_3]^+ \text{BF}_4^-$ display interesting intermolecular interactions based on short CH...Cl and CH...F contacts between arene CH and the bridging chloride ligands or the F-atoms of the BF_4^- counterions.¹¹⁴ In **8**, the *i*Pr and the methyl substituents on the arene induce much larger anion/cation separations and prevent the formation of such a hydrogen bonding network (Figure 7). All CH...Cl contacts are longer than 2.93 Å and are thus, at best, only slightly shorter than the sum of the van der Waals radii. The same holds for possible interior contacts between hydrogen atoms and the SbF_6^- counteranion. Two notable exceptions are the short CH...F contacts between atoms F2 and the hydrogen atom attached to C17 (2.440 Å) and atoms F4 and the hydrogen atom at C7 (2.469 Å). All other CH...F distances are identical to or larger than 2.55 Å, the sum of the van der Waals radii.

2. p-Cymene Ruthenium Thioether Complexes

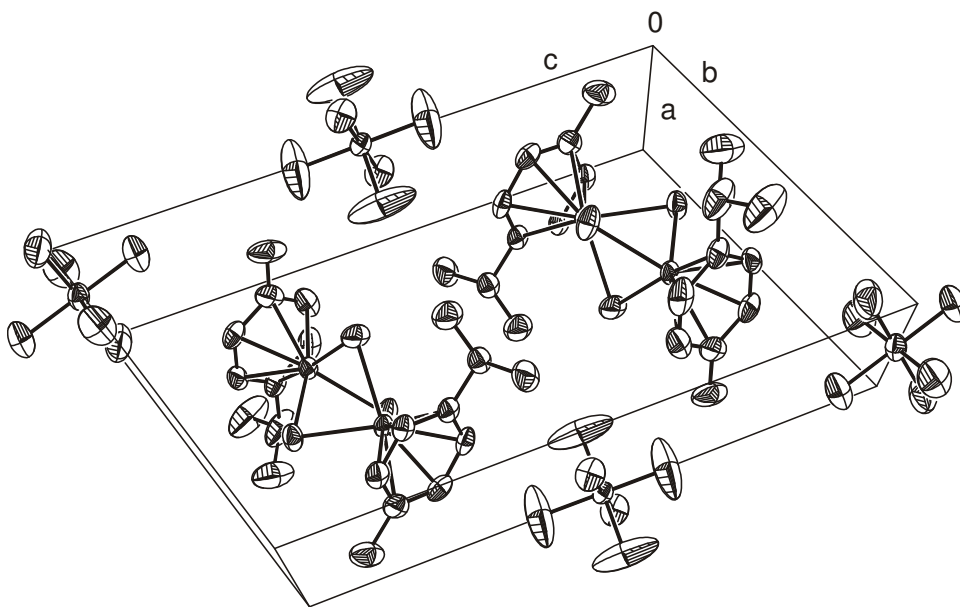


Figure 7: View of the unit cell of complex **8**. Thermal ellipsoids are drawn at a 50% probability level.

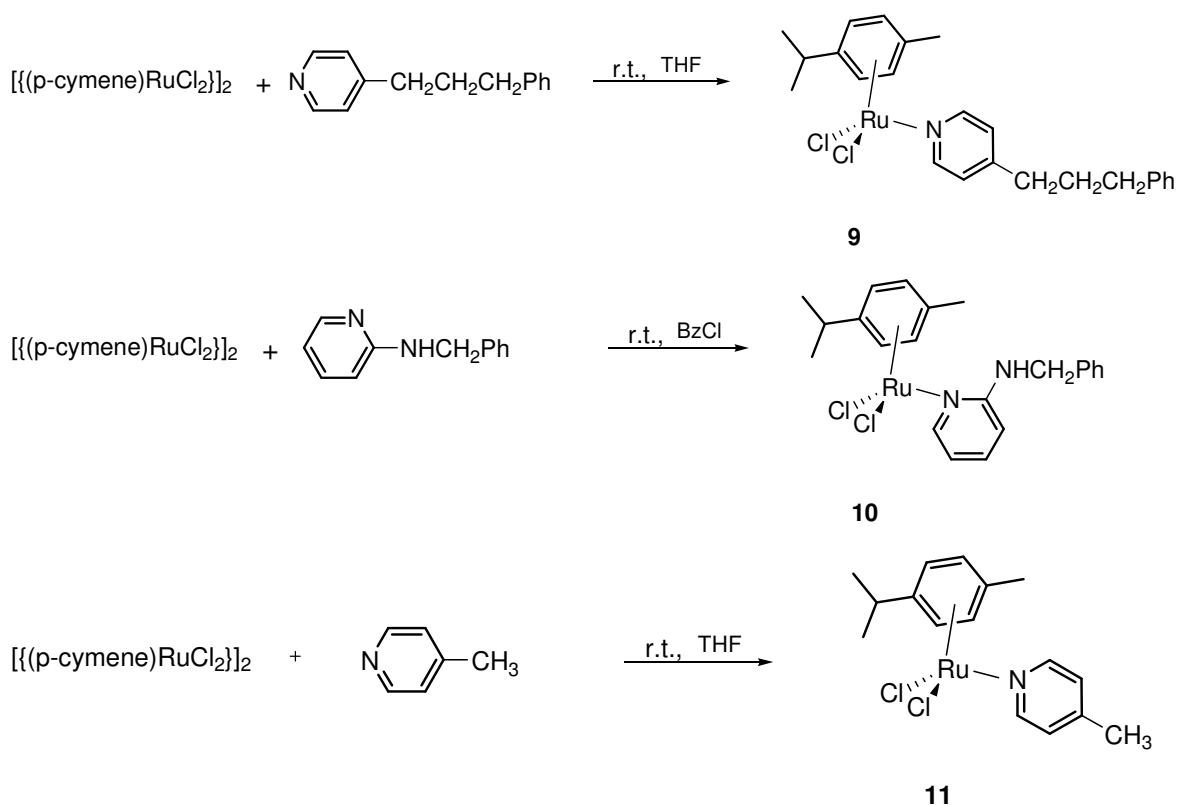
2.4 Complexes $[(\eta^6\text{-p-cymene})\text{RuCl}_2\text{L}]$ where L = substituted pyridine

We suspected that these rather detrimental equilibria in case of thioether ligands may also impede on the formation of the tethered target complexes $[(\eta^6:\eta^1\text{-C}_6\text{H}_5(\text{CH}_2)_n\text{SR})\text{RuCl}_2]$. Reports about high activity of the Grubbs carbene complexes $[(\text{IMesH}_2)\text{Cl}_2(\text{C}_5\text{H}_5\text{N})_2\text{Ru}=\text{CHPh}]$ and $[(\text{IMesH}_2(\text{l}_2)(\text{C}_5\text{H}_5\text{N})\text{Ru}=\text{CHPh}]^{16}$ containing pyridine ligands and the coordinative stability of Ru-pyridine bond led us to extend our work to Ru complexes containing substituted pyridine ligands with pendant arene moieties, aiming to convert them to tethered $[(\eta^6:\eta^1\text{-arene-L})\text{RuCl}_2]$ complexes.

The reaction of commercially available 4-(3-phenylpropyl)pyridine and $\{[(\eta^6\text{-p-cymene})\text{RuCl}_2]\}_2$ (**1**), in THF at room temperature leads to the simple addition product **9** (see Scheme 14). When this reaction was carried out in CH_2Cl_2 at room temperature the same product was obtained, although in smaller yield. We also observed the formation of the chloromethylpyridinium chloride salt $4\text{-PhC}_3\text{H}_6\text{-C}_6\text{H}_4\text{NCH}_2\text{Cl}^+ \text{Cl}^-$ resulting from the nucleophilic attack of the pyridine on the dichloromethane solvent. This species gives rise to a characteristic low field resonance in its $^1\text{H-NMR}$ spectrum at 9.34 ppm. This signal is attributed to the CH^+ protons in the 2,6 positions of the pyridinium nitrogen. Moreover, a singlet integrating as 2H at 6.00 ppm is attributed to the CH_2 group

2. p-Cymene Ruthenium Thioether Complexes

from the 1-chloromethylpyridinium moiety and was absent when the reaction is carried out in THF. These observations are confirmed by comparing with literature data of 1-chloromethylpyridinium chloride¹¹⁷ and other N-halomethylpyridinium halides.¹¹⁸ It is notable that pyridine itself does not react at atmospheric pressure with dichloromethane to form the 1-chloromethylpyridinium chloride. Upon coordination to the metal center, the ¹H resonances of the pyridine moiety in **9** are shifted to lower field by 0.4 ppm as compared to the free ligand (8.85 and 7.60 ppm for **9**, 8.45 ppm for H (3,5) and 7.28 for H (2,6) for free pyridine). Recrystallization from EtOH gave the pure product **9** but failed to produce any crystals suitable for X-ray structure determination.



Scheme 14: (η^6 -p-cymene)Ru complexes bearing pyridine ligands.

Similarly to **9**, we synthesized the aminopyridine complex **10** using commercially available 2-benzylaminopyridine and the Ru(II) dichloro bridged dimer **1** according to Scheme 14. Recrystallization from hot ethanol afforded pure **10** as a fine orange powder.

In contrast to **9**, NMR spectroscopic data were not completely conclusive at indicating the structure of **10**. Upon coordination, the protons at the 2,6 and the 3,5 positions of the pyridine ring and of the amine NH group all experience only a slight shift by about 0.1 ppm

2. p-Cymene Ruthenium Thioether Complexes

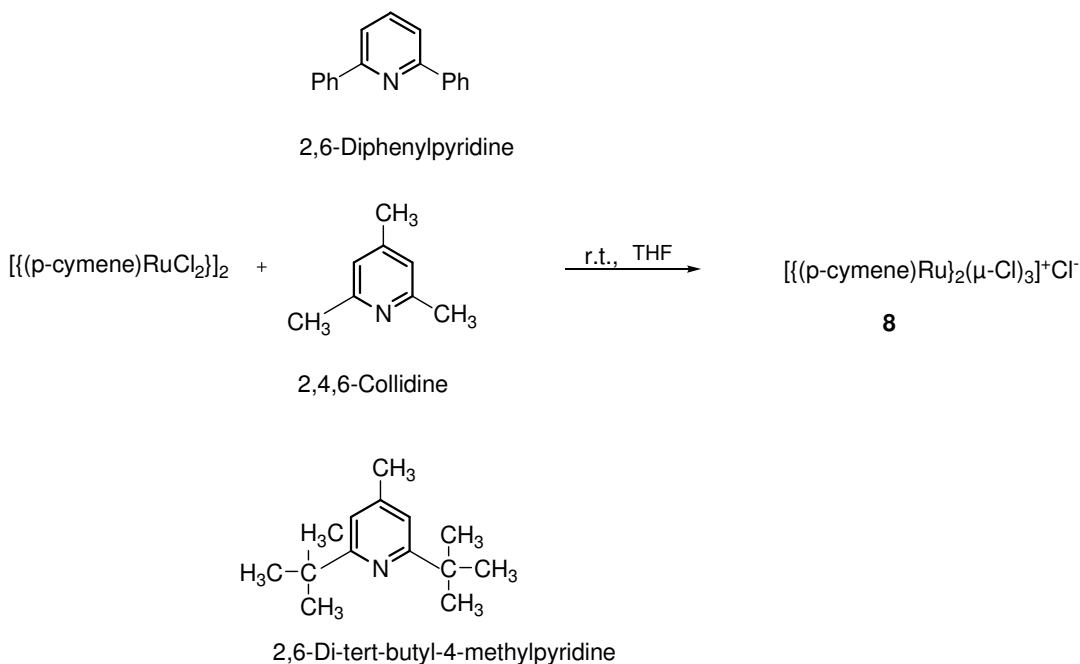
(pyridine H: 6.43 and 7.40 ppm in **10** and 6.51 and 7.33 ppm in the free pyridine; NH: 4.38 in complex **10**, 4.48 in the free ligand).

The reactions of $[(\eta^6\text{-arene})\text{RuCl}_2]_2$ compounds with a series of aminopyridine ligands together with X-ray crystal structures of some aminopyridine complexes were presented in the work of *Tocher*.¹¹¹ Here, exclusive coordination via the pyridine nitrogen was observed and we assume that the same holds for **10**.

Several unsuccessful pre-trials to convert **9** and **10** to tethered type Ru complexes (see Scheme 3) let us assume that restricted conformational flexibility of the alkyl or amine bridge connecting the pyridine and arene subunits of the ligands may prevent the approach of the dangling phenyl group to the ruthenium atom and thus impede on the displacement of the p-cymene ring. As a point of comparison we synthesized the 4-picoline derivative $[(\eta^6\text{-p-cymene})\text{RuCl}_2(\text{NC}_6\text{H}_4\text{CH}_3\text{-4})]$ (**11**) by treating dimer **1** with 2 equivalents of 4-picoline in THF (Scheme 14). Crystals of this complex were grown from an EtOH/ CHCl_3 mixture and its structure was established by X-ray crystallography as it will be discussed in following chapter.

In order to investigate whether sterically encumbered pyridines still may form simple 1:1 adducts $[(\eta^6\text{-p-cymene})\text{RuCl}_2(\text{L})]$, $[(\eta^6\text{-p-cymene})\text{RuCl}_2]_2$ (**1**) was reacted with 2,6-diphenylpyridine, 2,4,6-collidine and 2,6-di-*t*-butyl-4-methylpyridine in THF at room temperature under stirring for 16 hours. In every case, after evaporation of THF, washing with ether, the final product was the trichloro-bridged dimer $[(\eta^6\text{-p-cymene})\text{Ru}]_2\text{Cl}_3]^+ \text{SbF}_6^-$ (**8**) isolated as an intensively colored orange crystalline solid (Scheme 15). This directly relates to the formation of **8** as a side product in the reaction of **1** with 2 equivalents of SMe_2 forming **7** and shows that these pyridines are even weaker ligands as thioethers.

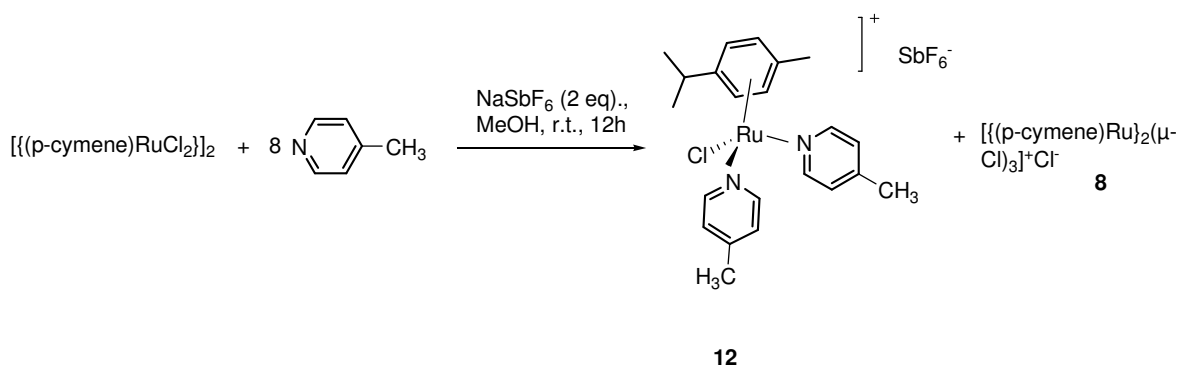
2. p-Cymene Ruthenium Thioether Complexes



Scheme 15: Reaction of **1** with bulky pyridines resulting in **8** as the major product.

Furthermore, in order to compare the reactivities of the cationic bithioether complex $[(\eta^6\text{-p-cymene})\text{RuCl}(\text{SMe}_2)]^+$ (**7**) and of similar cationic bispyridine complexes towards alkynes, we synthesized the $[(\eta^6\text{-p-cymene})\text{RuCl}(4\text{-methylpyridine})_2]^+\text{SbF}_6^-$ (**12**) (Scheme 16). In analogy to the reaction depicted in Scheme 14, $[\{(\eta^6\text{-p-cymene})\text{RuCl}_2\}]_2$ (**1**) was reacted with 8 equivalents of 4-methylpyridine and 2 equivalents of NaSbF_6 in MeOH and left to stir for 12h at room temperature. After usual routine work-up, NMR investigation of the resulting orange powder indicates formation of **12**. Again, a sizable amount of the cationic trichloro bridged complex **8** was formed as a byproduct. This newly synthesized complex was subjected to reaction with various propargylic alcohols in an attempt to synthesize novel allenylidene complexes as will be outlined in Chapter 3.6, but without success.

2. p-Cymene Ruthenium Thioether Complexes



Scheme 16: Synthesis of $[(\eta^6\text{-p-cymene})\text{RuCl}(4\text{-methylpyridine})_2]^+ \text{SbF}_6^-$ (**12**).

2.5 X-ray structure determination of $[(\eta^6\text{-p-cymene})\text{RuCl}_2(4\text{-methylpyridine})]$ (**11**)

Despite several reports on pyridine substituted complexes $[(\eta^6\text{-arene})\text{RuCl}_2(\text{py}')]$ ($\text{py}' = \text{pyridine or substituted pyridine}$), only few of them have been investigated by crystallography. Figure 8 shows the molecular structure of **11** in the crystal. It should be noted that in **11** Ru-Cl distances are slightly different: 2.4155(13) and 2.4202(14). Three related structures have already been reported, namely that of the pyridine adduct $[(\eta^6\text{-C}_6\text{H}_3\text{Me}_3)\text{RuCl}_2(\text{py})]$,¹¹⁰ $[(\text{p-cymene})\text{RuCl}_2(\text{py})]$ and paracyclophane compound $[(\eta^6\text{-[2}_2\text{]}(1,4)\text{C}_{16}\text{H}_{16})\text{RuCl}_2(\text{py})]$.¹¹¹ All these pyridine adducts display similar structural parameters with Ru-Cl bond lengths between 2.416(4) and 2.436(2) Å and Ru-N bonds that range from 2.120(4) to 2.160(6) Å. The Ru-N bond distance in **11** is 2.134(4) Å correlating well with literature data. The bond angles N-Ru-Cl in $[(\eta^6\text{-C}_6\text{H}_6)\text{RuCl}_2(\text{py})]$ are 86.16(10) and 86.12(10) and are slightly larger¹¹⁹ than the ones observed in **11** (N-Ru-Cl(1) = 84.96(12) and 85.94(12)). The Cl(1)-Ru-Cl(2) bond angle in $[(\eta^6\text{-C}_6\text{H}_6)\text{RuCl}_2(\text{py})]$ of 89.98(5) also matches well with the value of 88.39(5) observed in **11**. Ru-C bond distances are in the range of 2.179(5) to 2.212(5) Å. The longest bond is again formed with the carbon atom C7 which carries the methyl group. All important bond parameters are collected in Table 5.

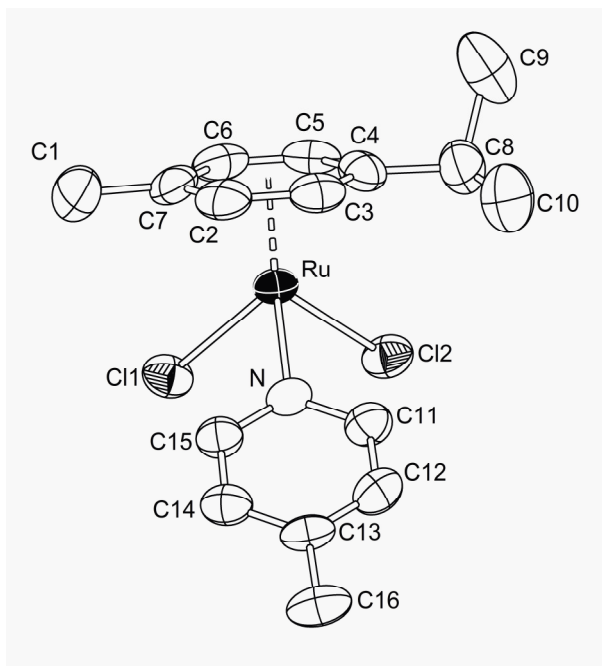


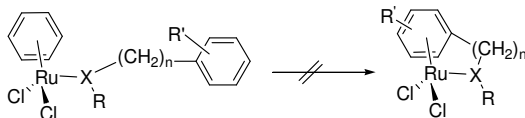
Figure 8: Crystal structure of $[(\eta^6\text{-p-cymene})\text{RuCl}_2(4\text{-methylpyridine})]$ (**11**) in the solid state.

Table 5: Selected bond lengths (Å) and angles (°) for **11**.

Bond lengths (Å)		Bond angles (°)	
Ru-N	2.134(4)	N-Ru-Cl2	85.94(12)
Ru-Cl1	2.416(13)	N-Ru-Cl1	84.96(12)
Ru-Cl2	2.420(14)	Cl1-Ru-Cl2	88.39(5)
Ru-C2	2.189(5)	C15-N-C11	117.1(4)
Ru-C3	2.189(5)	C15-N-Ru	121.9(3)
Ru-C4	2.211(5)	C11-N-Ru	120.8(4)
Ru-C5	2.178(5)		
Ru-C6	2.185(6)		
Ru-C7	2.211(5)		
N-C11	1.343(7)		
N-C15	1.335(7)		

2. p-Cymene Ruthenium Thioether Complexes

2.6 Attempted synthesis of $[(\eta^6:\eta^1\text{-arene-L})\text{RuCl}_2]$ where L = thioether or pyridine pendant functionalities



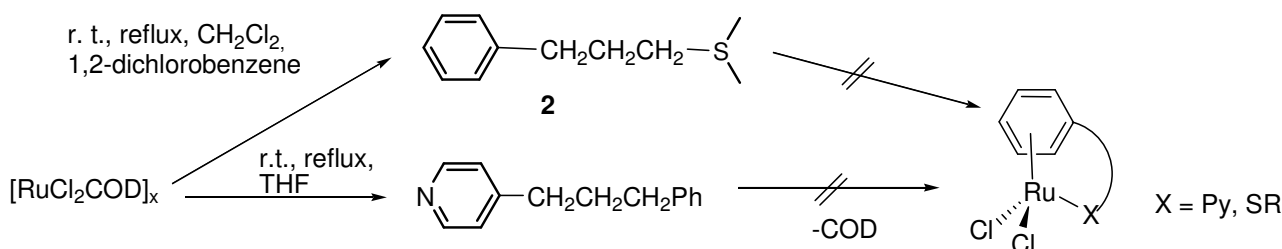
Recent work on similar $(\eta^6\text{-arene})\text{dichloro}$ ruthenium complexes bearing arylalkyl substituted phosphines with flexible alkyl chains has disclosed, that, upon thermal treatment, the coordinated arene is readily replaced by a dangling aryl substituent.^{67, 69, 120, 121} This reaction provides an easy access to tethered complexes where the phosphine substituted arene serves as an eight electron donor chelate ligand. Some of these complexes display reactivities that markedly differ from those of their non-tethered analogs.^{73, 75} In contrast, complexes **4** and **5** do not undergo such arene substitution in CH_2Cl_2 , CHCl_3 , or even in hot chlorobenzene and decompose at higher temperatures. Refluxing in 1,2-dichlorobenzene at temperatures of up to 150° provides dark oily mixtures of different complexes which were not further purified.

Conventional routes for the synthesis of functionalized arene complexes $[(\eta^6\text{-arene})\text{RuCl}_2]_2$ require Birch reduction of the parent arene using liquid ammonia and alkali metals to reduce the arene to the corresponding cyclohexadiene. The cyclohexadiene then serves as a reducing agent toward RuCl_3 , generating the desired arene complexes. Unfortunately, the conditions of Birch reduction are not compatible with the thioether functionality. Alternative routes such as treatment of *in situ* generated “ RuCl_2 ” with a donor-substituted arene¹²² or the photochemical displacement were also explored. Numerous *in situ* reductions of RuCl_3 to with activated Zn powder under reflux and reacting the resulting green solutions of “ RuCl_2 ” with tethered thioether ligands **2** and **3** as well as with 4-(3-phenylpropyl)pyridine and 2-benzylaminopyridine failed to give tethered (arene)Ru complexes.

It has also been reported that $[\text{Ru}(\text{COD})\text{Cl}_2]_x$ (COD = cis,cis-1,5-cyclooctadiene) can easily undergo COD ligand replacement due to its high lability, thus opening a free coordination site and lowering the energy barrier for coordination of other ligand. Assuming that the pendant donor group L (L = pyridine, thioether) may serve to anchor the correspondingly functionalized arene to the ruthenium atom and then aid in COD displacement by the

2. p-Cymene Ruthenium Thioether Complexes

arene, we synthesized $[\text{Ru}(\text{COD})\text{Cl}_2]_x$ and investigated its reaction with $\text{PhC}_3\text{H}_6\text{S}^i\text{Pr}$ and $\text{PhC}_3\text{H}_6\text{-4-C}_5\text{H}_4\text{N}$ (Scheme 17). In both cases, $^1\text{H-NMR}$ signals indicated only the presence of the uncoordinated ligands even if the reaction was heated under reflux. This probably attests to the weak coordinating ability of simple thioethers. One possible reason for our failure to displace the p-cymene ligand by the dangling arene group is the higher electron richness of the p-cymene resulting in more stable arene ruthenium coordination.



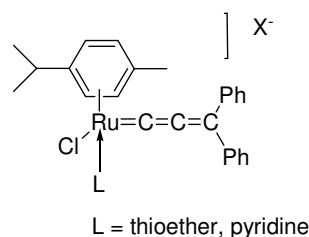
Scheme 17: Attempts of replacing the COD ligand of $[\text{Ru}(\text{COD})\text{Cl}_2]_x$ by functionalized arenes.

Similar subsequent experiments were therefore carried out with $[\{(\eta^6\text{-C}_6\text{H}_6)\text{RuCl}_2\}_2]$ and functionalized arenes (thioethers, pyridines) as the coordinated benzene is less electron rich and therefore more weakly bonded to the metal. However, under varying reaction conditions such as solvents and temperature, conversion to tethered complexes was not observed. Upon prolonged heating $^1\text{H-NMR}$ spectra showed only complex mixtures of products which we were not investigated in detail. This also applies to $[\{(\eta^6\text{-C}_6\text{Me}_6)\text{RuCl}_2\}_2]$ where the six methyl groups on the arene provide an electron rich surrounding and hence a particularly strong ruthenium arene bond.

2. p-Cymene Ruthenium Thioether Complexes

2.7 Attempts toward the synthesis of novel pyridine and thioether analogs of Dixneuf's metathesis catalysts $[(\eta^6\text{-p-cymene})\text{Cl}(\text{L})\text{Ru}=\text{C}=\text{C}=\text{CPh}_2]^+ \text{X}^-$

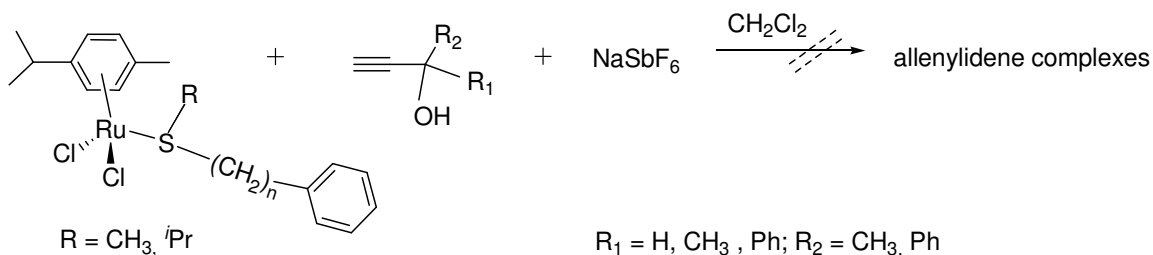
2.7.1 Attempted synthesis by chloride substitution from $[(\eta^6\text{-p-cymene})\text{Ru}(\text{L})\text{Cl}_2]^+ \text{X}^-$



The reaction of thioether and bis(thioether) chloro ruthenium complexes with terminal alkynes in methanol was reported to give methoxycarbene complexes $[(\eta^6\text{-arene})\text{Cl}(\text{SMe}_2)\text{Ru}=\text{C}(\text{OMe})\text{CH}_2\text{Ph}]^+$, most probably via vinylidene intermediates.⁸⁰ Assuming that alkynes and alkynols would behave similarly, we applied a similar strategy. Following *Dixneuf's* procedure¹²³ for the synthesis of analogous phosphine complexes, a first possible route to novel allenylidene complexes $[(\eta^6\text{-p-cymene})\text{Cl}(\text{L})\text{Ru}=\text{C}=\text{C}=\text{CPh}_2]^+$, or vinylidene complex $[(\eta^6\text{-p-cymene})\text{Cl}(\text{L})\text{Ru}=\text{C}=\text{CH}-\text{C}(\text{OH})\text{Ph}_2]^+$ was designed in a similar way. The newly synthesized thioether complexes **4**, **5** and **7**, and the pyridine complexes **9-12** $[(\text{p-cymene})\text{RuCl}_2(\text{L})]$ were treated with AgX ($\text{X} = \text{PF}_6^-$, OTf^- , BF_4^-) or NaSbF_6 in the presence of three equivalents of 1,1-diphenyl-2-propyn-1-ol, 1-phenylbut-3-yn-1-ol, or 2-methylbutynol in MeOH or CH_2Cl_2 . These reactions either did not proceed at all or led to the formation of oily mixtures from which no pure product could be isolated (Scheme 18).

In the case of 1-phenylbut-3-yn-1-ol we could observe only two main products in the reaction mixture. IR spectra showed no characteristic bands for allenylidene ligands in the range of 2000 to 1920 cm^{-1} or for vinylidene ligands which normally appear in the range of 1670 to 1600 cm^{-1} . We did not consider this outcome promising enough to attempt to separate this mixture or to characterize the resulting products.

2. p-Cymene Ruthenium Thioether Complexes



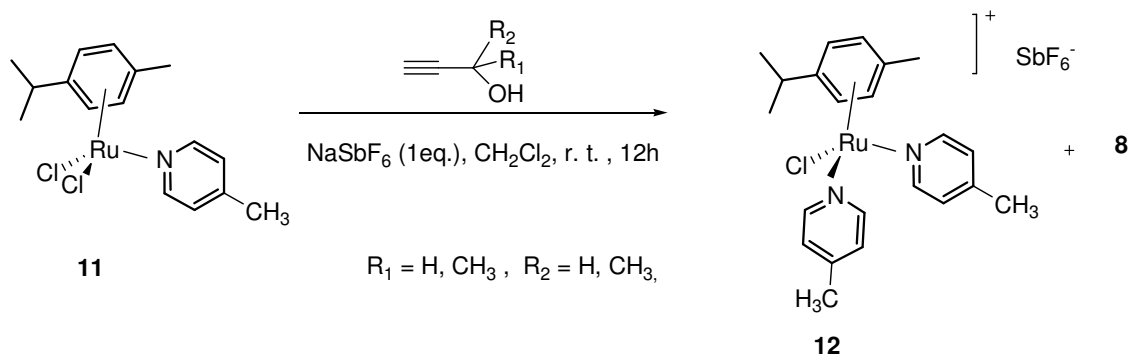
Scheme 18: Reactions of (η^6 -p-cymene)Ru thioether complexes with propargylic alcohols.

The same reaction pattern is observed when $[(\eta^6\text{-p-cymene})\text{RuCl}_2(\text{Ph}(\text{CH}_2)_3\text{S}^i\text{Pr})]$ (**4**) was treated with the mentioned propargylic alcohols, giving oily mixtures. Furthermore, we reacted $[(\eta^6\text{-p-cymene})\text{RuCl}_2(2\text{-benzylaminopyridine})]$ (**10**) according to *Dixneuf's* protocol,¹²³ with 1.2 equivalents of AgSbF_6 and 1.6 equivalents of 1,1-diphenyl-2-propyn-1-ol in CH_2Cl_2 . Again, no evidence for the formation of any allenylidene species was observed. $^1\text{H-NMR}$ results showed two major products which again could not be identified. A sharp IR band at 1658 cm^{-1} points to a possible vinylidene species, but all attempts at its isolation and further characterization were met with failure.

$[(\eta^6\text{-p-Cymene})\text{RuCl}_2(4\text{-methylpyridine})]$ was also reacted with different propargylic alcohols such as 1-methylpropynol, simple propargyl alcohol (1-propynol), and 1,1 dimethylpropynol. All $^1\text{H-NMR}$ spectra point to the formation of a mixture of the bis-picoline derivative $[(\eta^6\text{-p-cymene})\text{RuCl}(4\text{-methylpyridine})_2]^+\text{SbF}_6^-$ (**12**) and the trichloro-bridged dimer **8** as it is shown in Scheme 19.

From the reaction mixture obtained from $[(\eta^6\text{-p-cymene})\text{RuCl}_2(4\text{-methylpyridine})]$ and 1-methylpropynol, crystals of **8** and of $[(\text{p-cymene})\text{RuCl}(4\text{-methylpyridine})_2]^+\text{SbF}_6^-$, **11**, could be obtained by layering a CH_2Cl_2 solution with EtOH. When $[(\eta^6\text{-p-cymene})\text{RuCl}_2(4\text{-methylpyridine})]$ was stirred in CH_2Cl_2 in the presence of AgX ($\text{X} = \text{PF}_6^-, \text{OTf}^-, \text{BF}_4^-$) or NaSbF_6 and 4 equivalents of methylpyridine, but without added propargylic alcohol, only $[(\eta^6\text{-p-cymene})\text{RuCl}(4\text{-methylpyridine})_2]^+\text{SbF}_6^-$ (**12**) as a final product was obtained. With other propargylic alcohols, NMR spectra of the crude reaction products were indicative in showing mixtures of **12**, **11** and **8**.

2. p-Cymene Ruthenium Thioether Complexes



Scheme 19: Dismutation of **11** in the presence of different alkynols.

2.7.2 Attempted phosphine ligand substitution in

$[(\eta^6\text{-p-cymene})\text{Cl}(\text{PCy}_3)\text{Ru}=\text{C}=\text{C}=\text{CPh}_2]^+$

Another possible route to novel arene (allenylidene) complexes of ruthenium was to prepare first $[(\eta^6\text{-p-cymene})\text{RuCl}(\text{PCy}_3)(=\text{C}=\text{C}=\text{CPh}_2)]^+ \text{PF}_6^-$ in MeOH and then to try to replace the PCy_3 ligand with any of the pyridine or thioether ligands used in this study. In our hands, the original procedure,¹²³ e.g. stirring previously synthesized $[(\eta^6\text{-p-cymene})\text{RuCl}_2(\text{PCy}_3)]$, with 2 equivalents of 1,1-diphenylpropyn-1-ol and 1 equivalent of NaSbF_6 in MeOH for 3 hours at ambient temperature, did not give pure samples of the allenylidene complex $[(\eta^6\text{-p-cymene})\text{Cl}(\text{PCy}_3)\text{Ru}=\text{C}=\text{C}=\text{CPh}_2]^+$. It was previously reported that the allenylidene complex in MeOH solution may undergo nucleophilic attack at the C¹ atom of the allenylidene ligand to give the methoxycarbene complex $[(\eta^6\text{-p-cymene})(\text{PCy}_3)\text{Ru}=\text{C}(\text{OMe})\text{CH}=\text{CPh}_2]$.^{38, 124} We therefore also performed this reaction in CH_2Cl_2 or acetone and varied the silver salt and the reaction time from one to three hours. In every case, ¹H spectra were very complex and ³¹P-NMR spectra indicated the formation of a mixture of at least more than three products with only minor amounts of the allenylidene complex.

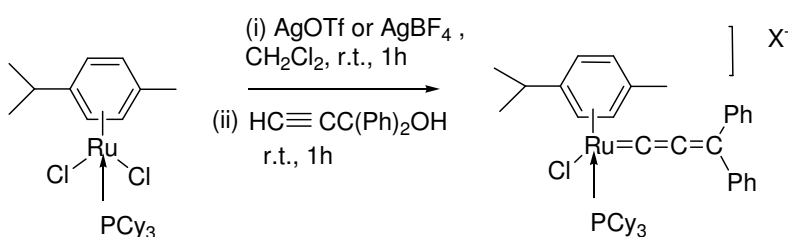
As was reported by *Dixneuf*,¹²³ reacting the $[(\eta^6\text{-p-cymene})\text{RuCl}_2(\text{PCy}_3)]$ complex and 1 equivalent of silver triflate, AgO_3SCF_3 ($\text{CF}_3\text{SO}_3^- = \text{OTf}^-$) in MeOH for 1 hour and filtering off the AgCl gave $[(\eta^6\text{-p-cymene})\text{RuCl}(\text{PCy}_3)]^+ \text{OTf}^-$. Furthermore, treatment of $[(\eta^6\text{-p-cymene})\text{RuCl}(\text{PCy}_3)]^+ \text{OTf}^-$ with 1.6 equivalents of 1,1-diphenylprop-2-yn-1-ol for 1 hour at room temperature affords the complex $[(\eta^6\text{-p-cymene})\text{Cl}(\text{PCy}_3)\text{Ru}=\text{C}=\text{C}=\text{CPh}_2]^+ \text{OTf}^-$ (**a**) as a violet powder (Scheme 20). In our hands this was the only route which afforded an analytically pure allenylidene complex. The

2. p-Cymene Ruthenium Thioether Complexes

^{31}P -NMR spectrum of the allenylidene complex **a** obtained after evaporation of the solvent and washing the residue with diethylether displays only one singlet at 59.6 ppm arising from the PCy_3 ligand. This is a substantial shift to lower field comparing to the 29.3 ppm assigned to the starting complex $[(\eta^6\text{-p-cymene})\text{RuCl}_2(\text{PCy}_3)]$. In addition, a sharp, intense band at 1958 cm^{-1} in the IR spectra points to the presence of an allenylidene species. All the results agree with the literature data.¹²³

We also examined the reaction of $[(\eta^6\text{-p-cymene})\text{RuCl}_2(\text{PCy}_3)]$ with silver tosylate in the absence of a propargylic alcohol in CH_2Cl_2 in order to examine the effect of the counter ion. A ^{31}P -NMR spectrum recorded after 2 hours of stirring followed by the same work-up procedure as for the triflate salt, revealed two doublets centered at 34.44 and 29.75 ppm ($J_{\text{PP}} = 35.20\text{ Hz}$) highly reminiscent of the signal patterns of the trichloro-bridged dimeric complex with Binap ligands synthesized by *Pregosin*.¹²⁵

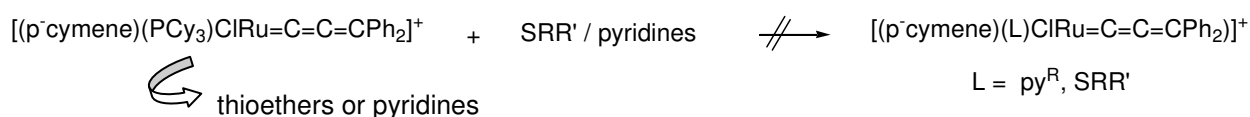
The allenylidene complex $[(\eta^6\text{-p-cymene})(\text{PCy}_3)\text{ClRu}=\text{C}=\text{C}=\text{CPh}_2]^+ \text{OTf}^-$ was treated with our newly synthesized thioether ligands **2** and **3**, with sterically bulky pyridine ligands, and 4-picoline in attempt to replace the PCy_3 ligand.



Scheme 20: Synthesis of the allenylidene complex **a**.

^{31}P -NMR monitoring of these reactions indicates the decrease, or vanishing, of the intensity of the characteristic singlet at 59.60 ppm arising from the coordinated PCy_3 ligand of complex **a** (Scheme 20) with the appearance of a singlet at 32.17 ppm indicating the release of free PCy_3 .¹²⁶ Various other signals with smaller intensities were also present. Most importantly, upon addition of the thioether or pyridine ligands, the IR band of compound **a** also decreased in intensity but no new band in the typical allenylidene region appeared. Further attempts at replacing the PCy_3 ligand of compounds in our search of novel allenylidene complexes $[(\eta^6\text{-p-cymene})\text{Cl}(\text{L})\text{Ru}=\text{C}=\text{C}=\text{Ph}_2]^+$ were therefore abandoned (Scheme 21).

2. p-Cymene Ruthenium Thioether Complexes



Scheme 21: Attempts to replace the phosphine ligand in **a** by substituted pyridines (py^R) or thioethers SRR'.

We also tried to synthesize the tosylate salt $[(\eta^6\text{-p-cymene})\text{RuCl}(\text{4-methylpyridine})]^+ \text{OTs}^-$ for subsequent reaction with 1,1-diphenylprop-2-yn-1-ol or other propargylic alcohols. ¹H-NMR spectra indicate a very complex reaction mixture, different from the one obtained with PCy₃, providing no useful information.

Nevertheless, complexes $[(\eta^6:\eta^1\text{-C}_6\text{H}_5(\text{CH}_2)_n\text{OR})\text{Ru}(\text{PR}'_3)\text{Cl}]^+$ (PR₃ = PCy₃, PⁱPr₃, P(CH₂OH)₃) react with 1,1-diphenyl-2-propyn-1-ol to form $[(\text{C}_6\text{H}_5(\text{CH}_2)_n\text{OR})(\text{PR}'_3)\text{ClRu}=\text{C}=\text{C}=\text{CPh}_2]^+$ as it will be discussed in Chapter 3.6.

2.8 Electrochemical investigations on the thioether ruthenium complexes

The thioether complexes **4-6**, $[(\eta^6\text{-p-cymene})\text{RuCl}_2(\text{SMe}_2)]$ (**7a**), and bis(thioether) adduct **7** were studied by cyclic voltammetry. Relevant data are compiled in Table 6.

Table 6: Voltammetric data for complexes **1**, **4-7**, and **7a** (CH₂Cl₂/0.1 M NBu₄PF₆). Potentials are reported versus the ferrocene/ferrocenium couple.

Compound	E ^{1/2} _{ox} (V)	E _{p,c} ^{a)} (V)	E _{p,a follow} (V) ^{b)}
4	0.85	^{c)}	-0.58
5	0.85	-2.09	-0.58
6	0.845	-2.02	-0.58
7a	0.83	-2.19	-0.58
7	1.44	-1.57	-0.50
1	1.04	-1.36, -1.98	-0.57

^{a)} peak potentials of an irreversible process.

^{b)} potential of the irreversible anodic peak following reduction.

^{c)} reduction peak overlapped with the second irreversible multielectron reduction wave of **1**.

2. p-Cymene Ruthenium Thioether Complexes

All complexes undergo one partially to nearly reversible oxidation and one chemically completely irreversible reduction within the potential window of the $\text{CH}_2\text{Cl}_2/\text{NBu}_4\text{PF}_6$ supporting electrolyte. The one-electron nature of these waves was ascertained from peak potential separations (cyclic voltammetry) and peak half-widths (square wave voltammetry) that correspond to the values expected for this stoichiometry and from nearly identical peak currents associated with the oxidation and the reduction processes. Chemical processes following oxidation could be fully suppressed by applying higher sweep rates or lowering the temperature, and full chemical reversibility was attained at 195 K in each case. Reduction, however, remained a completely irreversible process. The mono(thioether) complexes undergo oxidation at potentials near 0.85 V whereas the cationic bis(thioether) derivative **7** is much harder to oxidize and gives an $E_{1/2}$ of +1.44 V. The oxidation potentials of **4-6** and of the neutral mono SMe_2 derived complex **7a** are by about 100 mV higher than those of similar phosphine derivatives,^{3, 69, 127} and this indicates that SR_2 ligands are inferior electron donors compared to phosphines. A similar anodic shift is seen for the reduction peak potential of **7** compared to **4-6**. The strong influence of the complex charge on the oxidation and reduction potentials indicates that both processes are centered on the metal rather than at a ligand. Such behavior is common for half-sandwich ruthenium complexes. Irreversibility of the reduction step usually arises from ligand dissociation from a reactive Ru(I) species.¹²⁸ When the scan is reversed following reduction a new anodic peak appears. This feature is noticed in every thioether complex **4-6** and has a peak potential of -0.58 V (see Figure 10 and Figure 11). Upon the reverse anodic scan after reduction of $[\{(\eta^6\text{-p-cymene})\text{RuCl}_2\}_2]$ (**1**) an anodic peak at exactly the same potential is observed. This latter feature has been assigned as arising from the oxidation of $[(\text{p-cymene})\text{RuCl}]_2$ that is formed from **1** by a sequence of reduction and chloride dissociation steps.¹²⁸ Although the exact potential match may be fortuitous, formation of a common product from the reduction of thioether complexes **4-6** still suggests decomposition of the reduced forms by dissociation of the SRR' ligand.

Voltammograms of **4-6** (see Figure 10-12) also displayed a distinct reduction peak at -1.37 V. This peak was identified as arising from the reduction of $[\{(\text{p-cymene})\text{RuCl}_2\}_2]$ (**1**) by comparison with an authentic sample and by comparing voltammograms before and after addition of small amounts of **1** to the solutions of **4-6**. Relative amounts of **4-6** or **7a** and **1** were estimated as 11:1, 5:2, 7:1, and 12:1 by comparing the peak currents of the

2. p-Cymene Ruthenium Thioether Complexes

partially reversible oxidation of **4-6** and of the reduction peak of **1**. These values agree well with the ratios determined by NMR spectroscopy.

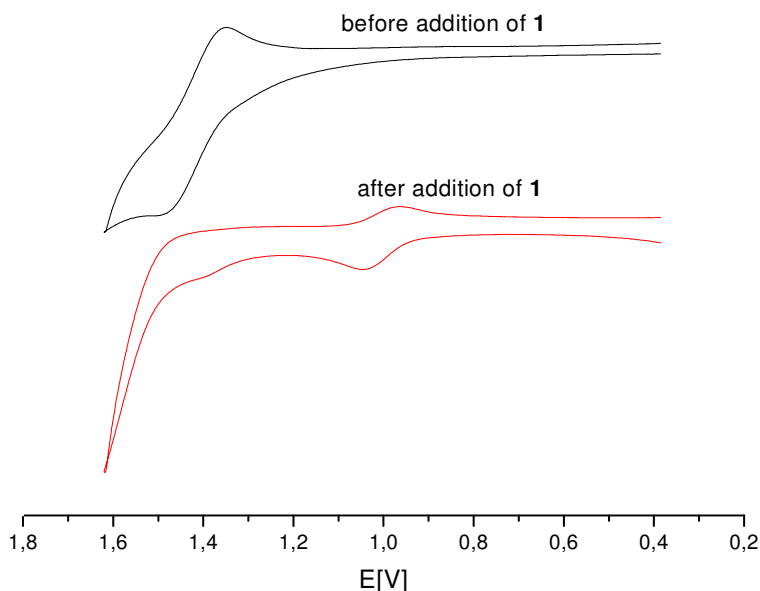


Figure 9: Cyclic voltammograms of complex **7** in $\text{CH}_2\text{Cl}_2/\text{NBu}_4\text{PF}_6$ (0.1 M) at RT and $v = 0.2$ V/s before (a) and after (b) addition of **1**.

As it is shown in Figures 10 and 12, the peak at -1.37 V of **1** present in the equilibrated solutions is enhanced when the partially reversible oxidation is scanned first. Thioether dissociation thus also constitutes a likely degradation pathway for the $[(p\text{-cymene})\text{RuCl}_2(\text{SRR}')^+]^+$ radical cations formed during the oxidation step. This is also in line with the observation that complex **5** with $\text{PhC}_3\text{H}_6\text{S}^i\text{Pr}$ as the sterically most demanding and most weakly coordinated thioether gives the least stable radical cation, i.e. the one with the smallest $i_{p,c}/i_{p,a}$ peak current ratio.

When increasing quantities of dimer **1** were stepwise added to a solution of the bis(thioether) complex **7**, the disappearance of the original waves of **7** and the appearance of a new, partially reversible couple at the considerably lower oxidation potential of +0.83 V was observed (Figure 9). After addition of about one equivalent of **1** this new couple constituted the prominent feature in the anodic regime. The product formed under these conditions was readily identified as the known mono(thioether) complex $[(\eta^6\text{-}p\text{-cymene})\text{RuCl}_2(\text{SMe}_2)]$ (**7a**) by comparison with authentic material synthesized independently.⁸⁰ We also verified clean formation of **7a** when **1** and **7** were combined in an

2. p-Cymene Ruthenium Thioether Complexes

NMR tube and dissolved in CD_2Cl_2 . This reaction provides another instance of the ready exchange of one SMe_2 ligand from bis(thioether) complex **7**.

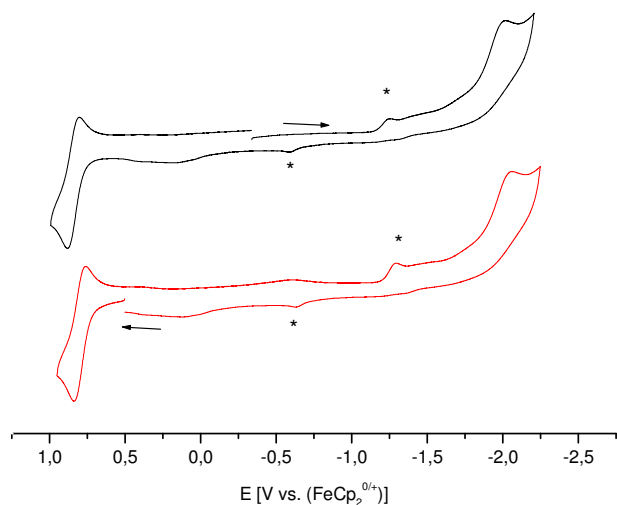


Figure 10: Cyclic voltammograms of complex **6** in $\text{CH}_2\text{Cl}_2/\text{NBu}_4\text{PF}_6$ (0.1 M) at RT and $\nu = 0.1$ V/s. Upper curve: reduction scanned first, lower curve: oxidation scanned first. The peaks due to the reduction of **1** and to the oxidation of the electroactive product formed from the radical anion of **1** are indicated by a star symbol.

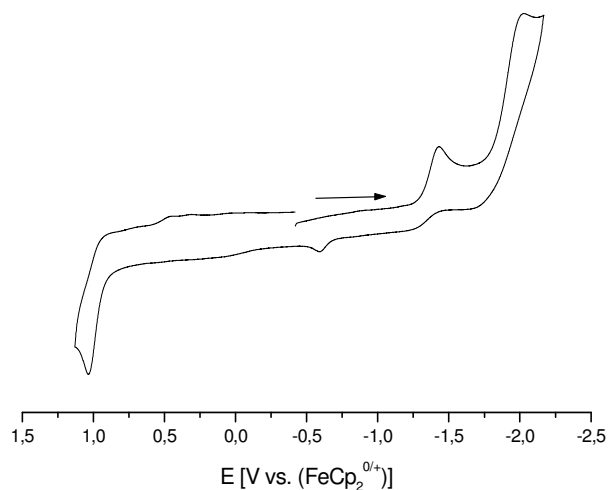


Figure 11: Cyclic voltammograms of complex **1** in $\text{CH}_2\text{Cl}_2/\text{NBu}_4\text{PF}_6$ (0.1 M) at RT and $\nu = 0.1$ V/s.

2. p-Cymene Ruthenium Thioether Complexes

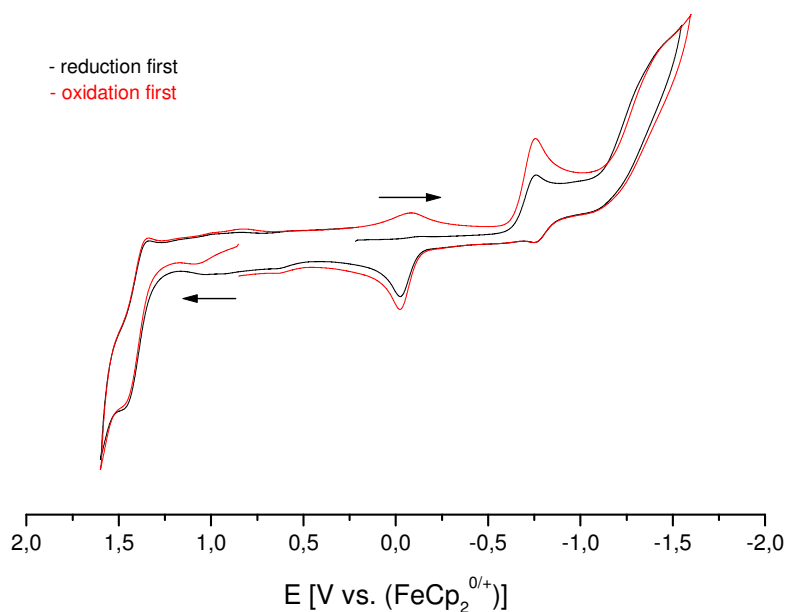


Figure 12: Cyclic voltammograms of complex **4** in CH₂Cl₂/NBu₄PF₆ (0.1 M) at RT and $v = 0.1$ V/s.

2.9 Electronic spectra

The UV-visible spectra of the thioether complexes were recorded in dichloromethane and are presented spectra in Figure 13 . Absorption maxima for all complexes are positioned at approximately the same wavelength. The prominent band at ca. 240 nm arises from $\pi-\pi^*$ transition and the ones with lower intensities at ca. 350 nm are probably due to metal to ligand charge transfer (Ru(II)- π^* arene) or d-d transitions.

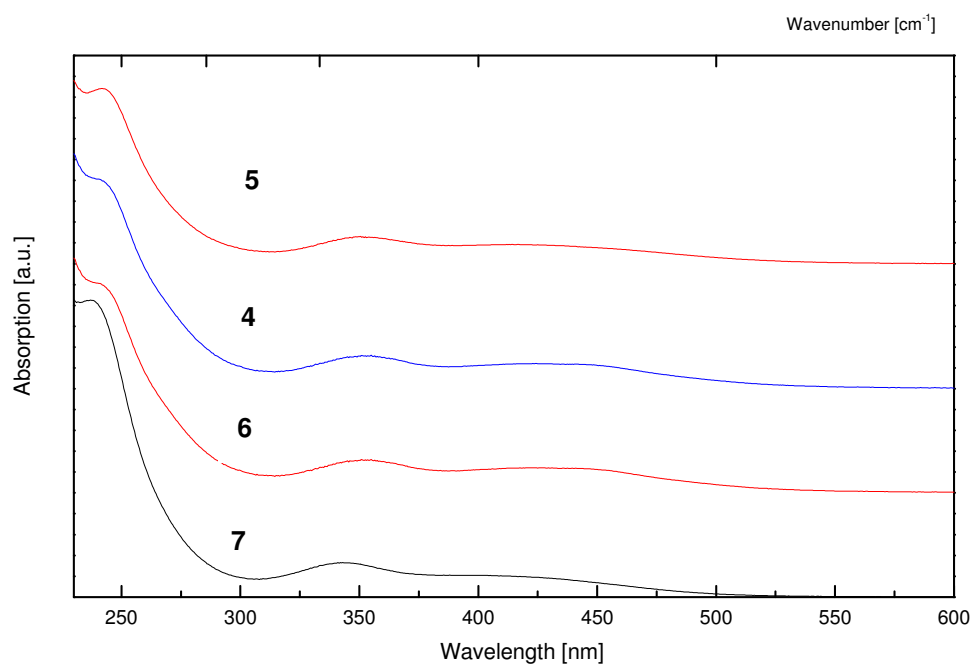
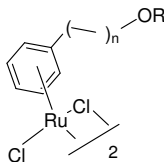


Figure 13: Electronic spectra of thioether complexes **4-7** in dichloromethane.

3 Half sandwich complexes bearing alcohol or ether functionalities on the arene



3.1 Introduction

Aryl substituted thioethers can not be reduced under Birch conditions to their corresponding cyclohexadienes due to the cleavage of the sulfur carbon bond. This is however possible for aryl alkyl ethers and alcohols, which offers a convenient access route to $[\{\eta^6\text{-arene}(\text{CH}_2)_n\text{OR}\}\text{RuCl}_2]_n$ complexes with alkoxy or hydroxy substituents on the side chain. Nevertheless, relatively little is known about them.⁷⁹ Ring closing metathesis of α,ω -dienes and cycloisomerization catalyzed by arene ruthenium complexes with side arm alcohol moieties was reported by *Kurosawa*.⁸³ Similar studies have briefly reported on neutral $[\{\{\eta^6\text{-C}_6\text{H}_5(\text{CH}_2)_n\text{OH}\}\text{RuCl}_2\}]$ ($n = 2, 3$) complexes, assuming them to possess dimeric structures with two chloride bridges connecting the $\{\{\eta^6\text{-arene}\}\text{RuCl}\}$ units, as it is usually found for this type of complexes. However, no spectroscopic characterisation that would provide evidence for these conclusions has been presented.^{66, 82} When the arene ruthenium complex $[\{\eta^6:\eta^1\text{-C}_6\text{H}_5(\text{CH}_2)_3\text{OH}\}\text{RuCl}_2]_n$ was treated with 2-aminoethanol and NaBF_4 in CH_3CN , the complex $[\{\eta^6:\eta^1\text{-C}_6\text{H}_5(\text{CH}_2)_3\text{O}\}_2\text{Ru}_2(\mu\text{-Cl})]^+ \text{BF}_4^-$ was formed. This complex adopts the structure of two face sharing octahedra with both alkoxo groups tethered to the arene ligand and one chloride atom as the bridges. Upon treatment of $[\{\eta^6:\eta^1\text{-C}_6\text{H}_5(\text{CH}_2)_3\text{O}\}_2\text{Ru}_2(\mu\text{-Cl})]^+ \text{BF}_4^-$ with AgBF_4 in acetonitrile the dicationic dimeric complex $[\{\{\eta^6:\eta^1\text{-C}_6\text{H}_5(\text{CH}_2)_3\text{O}\}_2\text{Ru}(\text{CH}_3\text{CN})_2\}_2]^{2+}(\text{BF}_4^-)_2$ was formed and structurally characterized.¹²⁹ Furthermore, the cationic derivatives $[\{\eta^6:\eta^1\text{-C}_6\text{H}_5(\text{CH}_2)_3\text{OH}\}\text{Ru}(\text{PR}_3)\text{Cl}]^+$ ($\text{PR}_3 = \text{PPh}_3, \text{PEt}_3$) and $[\{\eta^6:\eta^1\text{-C}_6\text{H}_5(\text{CH}_2)_3\text{OH}\}\text{RuL}_2]^{2+}$, where L_2 is a chelating diimine donor ligand such as 2,2'-bipyridine or 1,10-phenanthroline or a bisoxazolonyl ligand, clearly show the coordinating ability of the appended hydroxy group. According to NMR studies, these cationic derivatives preserve their tethered structures with the oxygen atom bonded to the metal even in methanolic solution,⁶⁶ despite the coordination ability of this

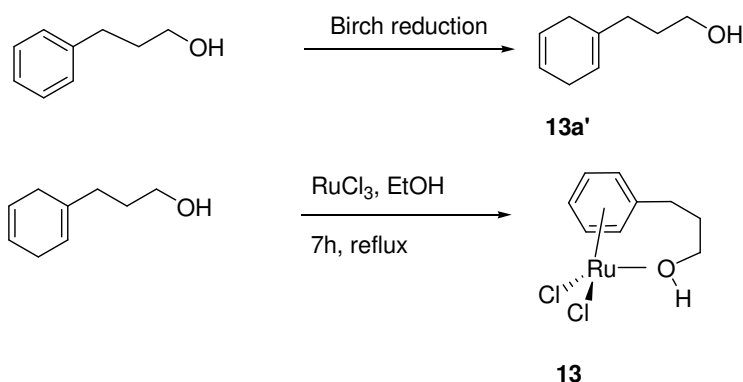
solvent and its propensity to form hydrogen bridges with the OH group and to possibly interfere with metal coordination.

As a part of our research on using arene dichloro ruthenium complexes as templates for cyclooligomerization and co-cyclization reactions³ we have also prepared and investigated ruthenium dichloro half-sandwich complexes with a hydroxypropyl- or methoxypropyl side arm, **13** and **14**, as well as the shorter chain ethyl alcohol **15** as it is shown in Scheme 22-24. Full characterization of these complexes along with the crystal structures of the hydroxypropyl derivatives **13** and its propyl methyl ether derivative **14** reveals a different behavior for neutral complexes with a free alcohol side chain and an ether functionality. Contrary to previous reports, the latter complex turned out to be monomeric in the solid state with the hydroxy function coordinated to the metal and intermolecular hydrogen bonding between the OH proton and a chloride ligand of a neighboring molecule. In this study we have also prepared the tripropylphosphine adducts **13a–15a** as well as the tricyclohexylphosphine adducts **13b** and **14b** and the P(CH₂OH)₃ containing complexes **13c,d**. The electrochemical behavior of these complexes was studied in detail by cyclic voltammetry and will be discussed in section 3.5.

3.2 Synthesis of half sandwich complexes [$\{\eta^6\text{-C}_6\text{H}_5(\text{CH}_2)_m\text{OR}\}\text{RuCl}_2\}_n$ ($n = 1, 2$; $m = 2$ or 3)

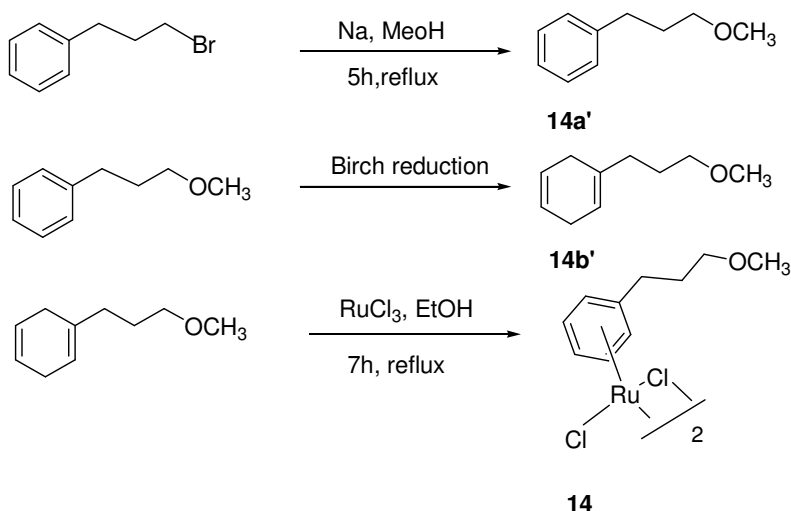
The synthesis of the functionalized arene complexes from the corresponding cyclohexadienes followed established methods.^{66, 130} First the parent arenes Ph(CH₂)_nOH and Ph(CH₂)_nOMe were reduced to the corresponding cyclohexadiene under Birch conditions¹³¹. The cyclohexadienes were then reacted upon reflux in EtOH with commercial hydrated RuCl₃ where they simultaneously serve as reductant and ligand to give the respective arene complexes [$\{\eta^6\text{-C}_6\text{H}_5(\text{CH}_2)_m\text{OR}\}\text{RuCl}_2\}_n$ ($m = 3, n = 1, R = \text{H}$: **13**, $m = 3, n = 2, R = \text{Me}$: **14**; $m = 2, n = 1$ or $2, R = \text{H}$: **15**) in good yields. These complexes were obtained as orange solids by slowly cooling the concentrated mother liquors (**13**, **14**) or as an orange brown powdery precipitate (**15**, see Scheme 22).

3. Chemistry of oxo and ether functionalized arene Ru complexes



Scheme 22: Synthesis of $[\{\eta^6:\eta^1\text{-C}_6\text{H}_5(\text{CH}_2)_3\text{OH}\}\text{RuCl}_2]$ (**13**).

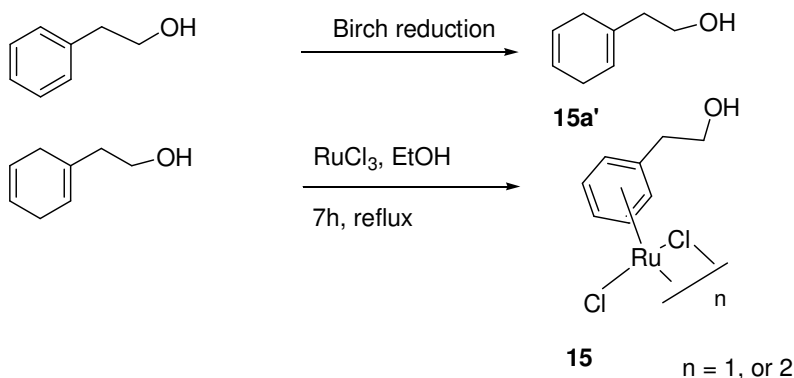
The hydroxy and methoxy substituted congeners **13** and **14** show markedly differing solubilities. While the ether is readily soluble in moderately polar organic solvents such as chloroform and methylene chloride, the hydroxypropyl derivative **13** is only moderately soluble in CH_2Cl_2 . The shorter chain hydroxyethyl analog **15** finally is very sparingly soluble even in boiling 1,2-dichloroethane and requires coordinating solvents like dimethylsulfoxide or dimethylformamide to allow for NMR spectroscopic characterization. This already points to the presence of significant intermolecular contacts via hydrogen bridges sustained by the OH group as the donor. In these donor solvents the arene protons and those of the ethyl side chain of **15** give rise to sharp, well resolved resonance signals. The ^{13}C -NMR spectra are likewise unsuspecting.



Scheme 23: Synthesis of $[\{\eta^6\text{-C}_6\text{H}_5(\text{CH}_2)_3\text{OMe}\}\text{RuCl}_2]$ (**14**).

3. Chemistry of oxo and ether functionalized arene Ru complexes

Asides from disrupting the intermolecular hydrogen bonds, donor solvents may also coordinate to the metal and cleave the Ru-Cl bridges of $[(\eta^6\text{-arene})\text{RuCl}_2]_2$ dimers or displace other donors. Dichloro bridged diruthenium complexes $[(\eta^6\text{-arene})\text{RuCl}_2]_2$ are known to form monomeric complexes $[(\eta^6\text{-arene})\text{RuCl}_2(\text{L})]$, $[(\eta^6\text{-arene})\text{RuCl}(\text{L})_2]^+$ or $[(\eta^6\text{-arene})\text{Ru}(\text{L}_3)]^{2+}$ in strong donor solvents ($\text{L} = \text{dmsO}, \text{dmf}, \text{H}_2\text{O}$).^{2, 132, 133} As positive charge accumulates upon chloride substitution, the resonance signals of the coordinated arene are commonly shifted to lower field.^{66, 132, 133} The exact nature of the species present in dmsO or dmf solutions of the hydroxyethylbenzene dichloro complex **15** still remains an open issue, but it is interesting to note a low field shift of 0.30 to 0.35 ppm for the aryl protons when dmf-d_7 is replaced by dmsO-d_6 . No such shift differences are observed for the protons of the hydroxyalkyl side chain. Similar trends also prevail for **13**. Here, a strong donor solvent is also likely to interfere with the intramolecular coordination of the hydroxy group, as it is present in the solid state (see following section) and probably also in a non-coordinating solvent like CD_2Cl_2 .



Scheme 24: Synthesis of $[(\eta^6\text{-C}_6\text{H}_5(\text{CH}_2)_2\text{OH})\text{RuCl}_2]$ (**15**).

3.3 X-ray structure determinations of $[(\eta^6:\eta^1\text{-C}_6\text{H}_5(\text{CH}_2)_3\text{OH})\text{RuCl}_2]$ (**13**) and $[(\eta^6\text{-C}_6\text{H}_5(\text{CH}_2)_3\text{OMe})\text{RuCl}_2]$ (**14**)

Crystals suitable for crystallographic determinations of the molecular structures have been obtained for the hydroxypropyl as well as the propyl methyl ether derived complexes by slowly cooling a hot saturated solution of the respective complex in ethanol. Plots of the molecular structures are provided as Figure 14 and 15. Table 7 lists important bond

3. Chemistry of oxo and ether functionalized arene Ru complexes

lengths and angles. The ether substituted complex crystallizes as a dimer, a structure which is commonly observed for complexes of the general composition $[(\eta^6\text{-arene})\text{RuCl}_2]_2$. Two chloride bridges tie the ruthenium atoms together forming a central Ru_2Cl_2 rhombus. There is a center of inversion located at the midpoint of the central Ru_2Cl_2 entity and the unit cell contains only one half molecule of **14**.

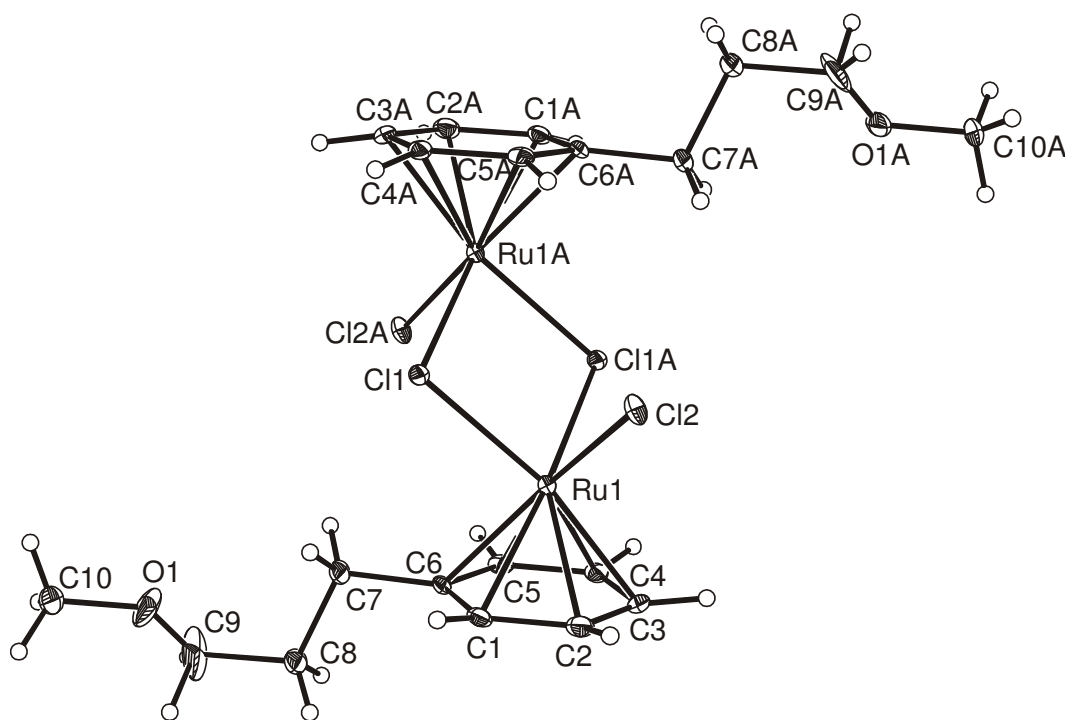


Figure 14: Molecular structure of $[(\eta^6\text{-C}_6\text{H}_5(\text{CH}_2)_3\text{OME})\text{RuCl}(\mu^2\text{-Cl})_2]$ (**14**) in the crystal. Thermal ellipsoids are drawn at a 50% probability level.

3. Chemistry of oxo and ether functionalized arene Ru complexes

Table 7: Selected bond lengths and angles for **14**.

Bond lengths (Å)				Bond angles (°)	
Ru1-Cl1	2.4427(8)	C1-C2	1.417(5)	Cl1-Ru1-Cl2	85.65(4)
Ru1-Cl1A	2.4481(18)	C2-C3	1.416(6)	Cl1-Ru1-Cl1A	82.60(5)
Ru1-Cl2	2.4067(8)	C3-C4	1.415(5)	Cl2-Ru1-Cl1A	87.35(5)
Ru1-C1	2.178(3)	C4-C5	1.426(5)	arene ^{a)} -Ru-Cl1	128.7(3)
Ru1-C2	2.164(4)	C5-C6	1.419(5)	arene ^{a)} -Ru1-Cl2	130.3(3)
Ru1-C3	2.174(3)	C1-C6	1.423(5)	arene ^{a)} -Ru-Cl1A	126.6(3)
Ru1-C4	2.150(3)	C6-C7	1.504(5)		
Ru1-C5	2.177(3)	C7-C8	1.533(5)		
Ru1-C6	2.185(3)				
arene ^{a)} -Ru1	1.643(3)				
C8-C91/C8-C92	1.526(9)/1.564(8)				
C91-O91/C92-O92	1.422(10)/1.436(10)				
O91-C10/O92-C10	1.543(8)/1.467(7)				

Arene^{a)} = midpoint of the arene ring.

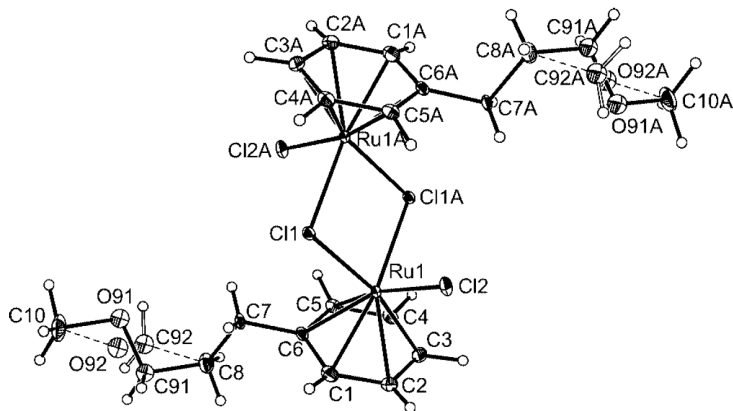


Figure 15: Molecular structure of (**14**) in the crystal showing disorder concerning atoms C9 and O9 of the methoxy side chains. Thermal ellipsoids are drawn at a 50% probability level.

As it is borne out by crystallographic symmetry, the arenes are situated on opposite sides of the central Ru₂Cl₂ ring to give the sterically preferred *transoid* arrangement. The methoxyalkyl side chains point away from the terminal chloride ligands and the central Ru₂Cl₂ ring such that the molecule displays a “stretched” conformation. There is some

3. Chemistry of oxo and ether functionalized arene Ru complexes

disorder concerning atoms C9 and O9 of the methoxypropyl side chains. As is indicated in Figure 16, these atoms are disordered over two positions (C91, C92, O91, O92) with occupancy factors of 0.47 and 0.53 with the C7 and C10 atoms common to both different orientations. The bonds to the bridging chloride ligands are somewhat longer (2.443(1) and 2.448(2) Å) than that to the terminal ones (2.407(1) Å), as it is usually observed for such chloro bridged dimers. These values compare favorably with those for $[(\eta^6\text{-C}_6\text{Me}_6)\text{RuCl}_2]_2$ (Ru-Cl(terminal) = 2.394(1), Ru-Cl(bridge) = 2.460(1) Å)¹³⁴ and the two independent molecules within the unit cell of $[(p\text{-cymene})\text{RuCl}_2]_2$ (Ru-Cl(terminal) = 2.416(3) Å, Ru-Cl(bridge) = 2.451(3) and 2.464(3) Å for the one and Ru-Cl(terminal) = 2.420(3) and 2.435(3) Å, Ru-Cl(bridge) = 2.437(3) and 2.488(3) Å for the other molecule).⁵² The Ru-Cl2 bond is roughly orthogonal to the central Ru₂Cl₂ plane (85.2°) while the planes of the arene rings are tilted at an angle of 54.6° against the Ru₂Cl₂ core. All other bond parameters, including the average Ru-C(arene) distances, are unremarkable and warrant no further discussion.

The hydroxypropyl derivative **13**, on the other hand, crystallizes as a monomer (Figure 16). The most relevant parameters are provided in Table 8. Intramolecular chelation makes the arene an eight electron donor ligand and renders the ruthenium atom an electronically saturated 18 valence electron center. The Ru-C6-C7-C8-C9-O1 six membered chelate adopts a half-chair conformation with the flap pointing toward Cl1 and is devoid of any notable strain. Thus, the Ru-C(arene) bond lengths fall in the same range as those observed in **14** and deviations of individual values from the average are no larger as in non-tethered **14**. The Ru-Cl distances of 2.409(1) and 2.421(1) Å compare well to those found for the plethora of neutral adducts of the type $[(\eta^6\text{-arene})\text{RuCl}_2(\text{L})]$ and phosphine tethered complexes like $[(\eta^6\text{-C}_6\text{H}_5(\text{CH}_2)_3\text{PMe}_2)\text{RuCl}_2]$ (2.405(2) to 2.421(2) Å), $[(\eta^6\text{-C}_6\text{H}_2\text{Me}_3\text{-2,4,6,-(1-C}_3\text{H}_6\text{PPh}_2))\text{RuCl}_2]$ (2.4159(10) and 2.4425(10) Å), or in $[(\eta^6\text{-C}_6\text{Me}_5(\text{C}_3\text{H}_6\text{PPh}_2))\text{RuCl}_2]$ (2.4016(12) and 2.4163(12) Å),⁶⁹ $[(\eta^6\text{-C}_6\text{H}_3\text{Me}_2\text{-3,5-(1-C}_3\text{H}_6\text{PPh}_2))\text{RuCl}_2]$ (2.397(2) and 2.420(2) Å), $[(\eta^6\text{-C}_6\text{H}_4\text{Et-4-(1-C}_3\text{H}_6\text{PPh}_2))\text{RuCl}_2]$ (2.4040(10) and 2.4073(11) Å),⁶⁸ or $[(\eta^6\text{-C}_6\text{H}_5(\text{CHMeC}_2\text{H}_4)_3\text{PPh}_2)\text{RuCl}_2]$ (2.4037(7) and 2.4271(6) Å).⁷⁴

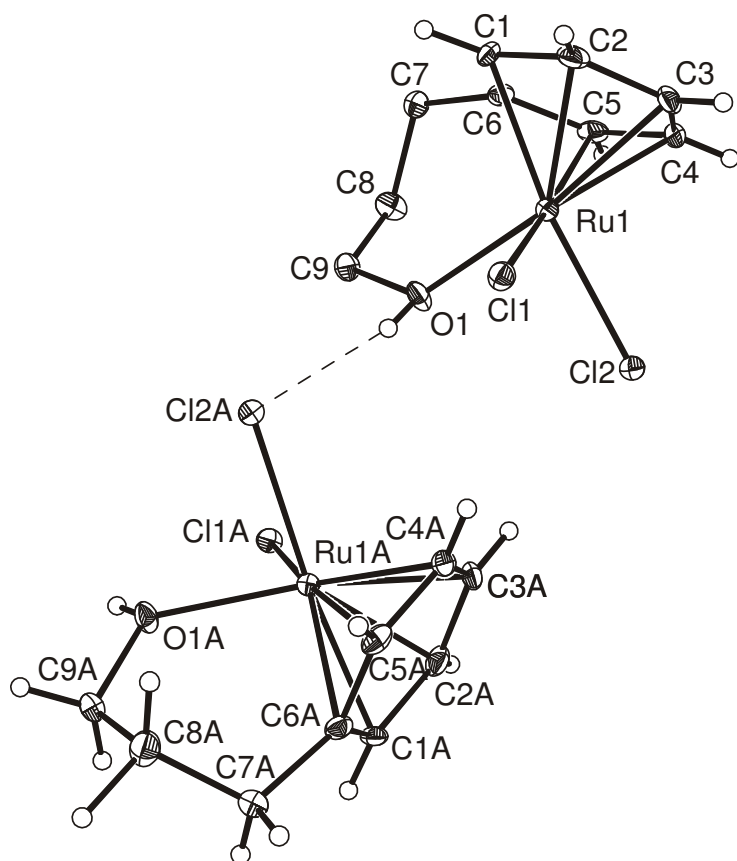


Figure 16: The molecular structure of $[\{\eta^6:\eta^1\text{-C}_6\text{H}_5(\text{CH}_2)_3\text{OH}\}\text{RuCl}_2]$ (**13**) in the crystal. Thermal ellipsoids are drawn at a 50% probability level.

Table 8: Selected bond lengths and angles for **13**.

Bond lengths (Å)				Bond angles (°)	
Ru1-Cl1	2.409(1)	C1-C2	1.419(7)	Cl1-Ru1-Cl2	87.28(4)
Ru1-Cl2	2.421(1)	C2-C3	1.422(7)	O1-Ru1-Cl1	83.57(10)
Ru1-O1	2.154(3)	C3-C4	1.400(8)	O1-Ru1-Cl2	82.37(10)
Ru1-C1	2.181(4)	C4-C5	1.422(7)	arene ^a -Ru-Cl1	129.3(1)
Ru1-C2	2.149(5)	C5-C6	1.433(7)	arene ^a -Ru-Cl2	128.2(1)
Ru1-C3	2.157(5)	C1-C6	1.422(7)	arene ^a -Ru-O1	129.9(1)
Ru1-C4	2.164(5)	C6-C7	1.508(7)		
Ru1-C5	2.194(5)	C7-C8	1.526(7)		
Ru1-C6	2.169(4)	C8-C9	1.496(7)		
arene ^a -Ru1	1.640(3)	C9-O1	1.448(6)		

Arene^a = midpoint of the arene ring.

3. Chemistry of oxo and ether functionalized arene Ru complexes

The Ru-O bond length of 2.153(3) Å is nearly identical to that observed in the dicationic chelate $[\{\eta^6:\eta^1\text{-C}_6\text{H}_5(\text{CH}_2)_3\text{OH}\}\text{Ru}(\text{phen})]^{2+} (\text{BF}_4^-)_2$ where phen denotes 1,10-phenanthroline (2.145(3) Å), but is notably longer as the Ru-O(alkoxylate) bond in $[\{\eta^6:\eta^1\text{-C}_6\text{H}_5(\text{CH}_2)_3\text{O}\}\text{Ru}(\text{bipy})]^+ \text{BF}_4^-$ (bipy = 2,2'-bipyridine, 2.050(5) Å).⁶⁶ The OH proton, like every other hydrogen atom of this structure, was directly located from the electron density map. It is found to point away from the metal and to project toward a chloride ligand of a neighbor molecule forming a grossly linear (154.87(1)°) OH...Cl bridge with a H...Cl separation of 2.24(1) Å and an O...Cl distance of 3.0513(2) Å. The OH...Cl bridge present in **13** is thus significantly shorter than the average hydrogen bond between an OH donor and a metal bonded chloride ligand as the acceptor ($d_{\text{av}}(\text{Cl}\cdots\text{H}) = 2.349(9)$ Å, $d_{\text{av}}(\text{O}\cdots\text{Cl}) = 3.272(8)$ Å, d_{av} = average distance).¹³⁵ This signals a rather strong OH...Cl interaction in **13**. A similar *intramolecular* OH...Cl contact with an O...Cl distance of 3.121(2) Å and an OH...Cl angle of 159.2° has been reported by Štěpnička, Therrien and their co-workers for $[\{\eta^6\text{-C}_6\text{H}_5(\text{CH}_2)_3\text{OH}\}\text{RuCl}_2(\text{PPh}_3)]$, the triphenylphosphine adduct of **13**.¹²⁷

In **13** these interactions also form a peculiar hydrogen bonding network that determines the packing in the crystal. Molecules of **13** arrange in double sheets that run parallel to the crystallographic *ab* plane. The Ru-Cl₂ vectors of the molecules belonging to the upper layer and those of the lower layer of each double sheet are roughly antiparallel to each others. Each molecule forms two OH...Cl contacts with different neighbors from the other layer of the double sheet, one via its OH group and one via its Cl₂ atom. As a whole, molecules interlinked by these hydrogen bonds form one-dimensional infinite zig-zag chains within the double sheets which propagate roughly along the *a* vector (Figure 17).

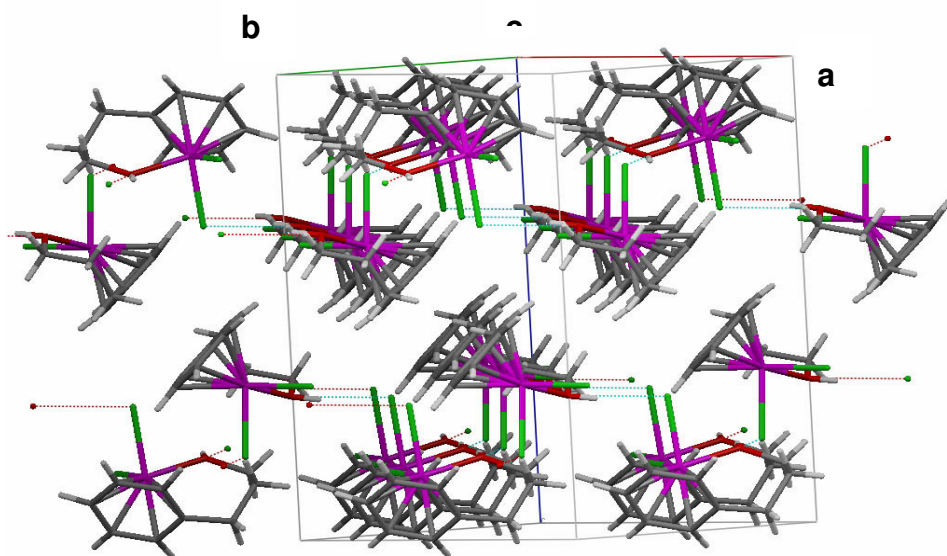
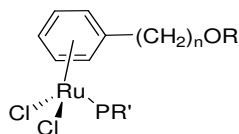


Figure 17: Plot showing packing and the OH...Cl contacts of **13**.

The coordinated arene rings of the molecules building the one layer within a double sheet tilt toward the Cl2 atom of the constituents of the other. These CH...Cl contacts, however, exceed 3.8 Å and are most probably too weak to allow for any significant interaction. Adjacent double sheets pack such that the arene rings are strictly parallel to each others. The distance between the arene planes of adjacent layers is 3.197 Å and is thus shorter as the distance between the individual layers in graphite (3.35 Å). Still, in **13** the arene rings of molecules belonging to different sheets are offset against each others.

The structure of **13** exemplifies how even only moderately strong hydrogen bridges are significant in determining the molecular conformation as well as the association and packing of individual molecules and the physical properties (such as solubilities) of compounds.

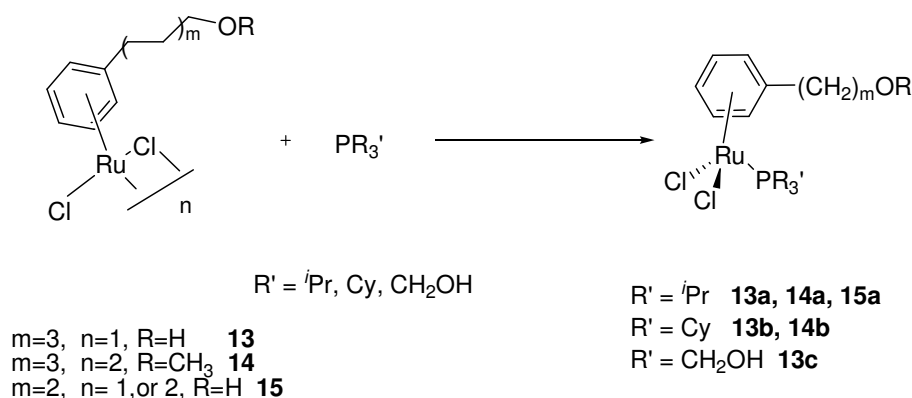
3.4 Phosphine derivatives of complexes 13-15



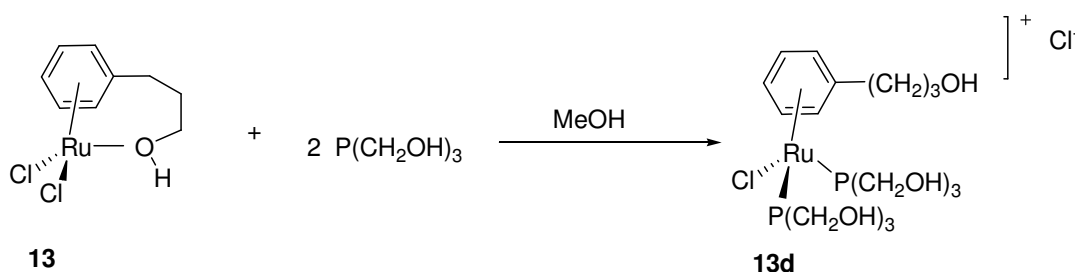
The development of metal mediated catalytic transformations in aqueous media is an important issue in modern organometallic chemistry, not only because of environmental considerations but also because the separation from the products is particularly facile using a two phase (water/organic solvent) system.¹³⁶ Introduction of hydrophilic ligands in the coordination sphere of a transition metal is probably the most popular method for preparation of water soluble catalysts. Thus, a vast number of functionalized phosphine ligands containing highly polar sulfonated, hydroxyalkyl, ammonium, phosphonium, or carboxylate groups are presently known and their effectiveness in biphasic catalysis has often been demonstrated.¹³⁷ In this context we prepared tris(hydroxymethyl)phosphine ($P(CH_2OH)_3$) complexes of **13-15** as well as tripropyl and tricyclohexylphosphine derivatives (Scheme 25).

Phosphine adducts of $[\{\eta^6-C_6H_5(CH_2)_nOR\}RuCl_2]_n$ are readily prepared by reacting the corresponding dichloro complex with a slight excess of the phosphine in CH_2Cl_2 . The ability of Ru dimers to form mononuclear complexes of the general formula $[(\eta^6\text{-arene})RuCl_2(L)]$ ($L = 2 e^-$ donor ligand) *via* cleavage of the chloride bridges is well known.¹³⁸ In the case of **13** and **15** which are only moderately or nearly insoluble in this medium, gradual dissolution of the starting complex occurred as the phosphine complex formed. The synthesis of the $P(CH_2OH)_3$ derived complexes **13c,d** requires the use of methanol as the solvent, and only intractable product mixtures were formed in CH_2Cl_2 . The $P(CH_2OH)_3$ ligand is moderately air sensitive. Referring to the work of *Therrien and Štěpnička*,¹²⁷ the decidedly higher solubility of the phosphine adducts may not only be due to the presence of solubilizing substituents on the phosphine, but also to a change of the nature of the $OH \cdots Cl$ contacts from intermolecular to intramolecular ones.

3. Chemistry of oxo and ether functionalized arene Ru complexes



Scheme 25: Synthesis of phosphine derivatives of **13-15**.



Scheme 26: Synthesis of **13d**.

All phosphine adducts are characterized by sharp singlet resonances in their ^{31}P -NMR spectra with resonance shifts near 30 ppm for the tricyclohexyl phosphine and the tris(hydroxymethyl)phosphine and of about 40 ppm for the tri*i*propylphosphine derivatives. The proton and carbon-13 NMR spectra likewise show the resonances of the ring protons and of the tri*i*propylphosphine substituent (for **13a-15a**) in a symmetric environment, which indicates the presence of a molecular mirror plane. For the tricyclohexylphosphine complex **14b** the appropriate number of CH_2 multiplets appears in the ^1H - and ^{13}C -NMR spectra. Attempts to prepare the monophosphine adduct of the hydroxypropylbenzene derivative **13c** initially led to slightly impure products with some admixture of another phosphine complex, as it was indicated by the presence of a second singlet resonance at somewhat lower field. This second symmetric phosphine complex was finally identified as the cationic bis(phosphine) adduct $[\{\eta^6\text{-C}_6\text{H}_5(\text{CH}_2)_3\text{OH}\}\text{RuCl}\{\text{P}(\text{CH}_2\text{OH})_3\}_2]^+ \text{Cl}^-$ **13d**. It was subsequently prepared and fully characterized by reacting $[\{\eta^6\text{-C}_6\text{H}_5(\text{CH}_2)_3\text{OH}\}\text{RuCl}_2]$ and $\text{P}(\text{CH}_2\text{OH})_3$ in a stoichiometric ratio of 1:2. Mixtures of $[\{\eta^6\text{-C}_6\text{H}_5(\text{CH}_2)_3\text{OH}\}]$

3. Chemistry of oxo and ether functionalized arene Ru complexes

$\text{RuCl}\{\text{P}(\text{CH}_2\text{OH})_3\}_2^+ \text{Cl}^-$ and $[\{\eta^6\text{-C}_6\text{H}_5(\text{CH}_2)_3\text{OH}\}\text{RuCl}_2]$ in CD_2Cl_2 are gradually transformed to give predominantly $[\{\eta^6\text{-C}_6\text{H}_5(\text{CH}_2)_3\text{OH}\}\text{RuCl}_2\{\text{P}(\text{CH}_2\text{OH})_3\}]$. Formation of the cationic bisadduct $[\{\eta^6\text{-C}_6\text{H}_5(\text{CH}_2)_2\text{OH}\}\text{RuCl}\{\text{P}(\text{CH}_2\text{OH})_3\}_2]^+ \text{Cl}^-$ of **15** was even more favored in polar media, where its formation besides the expected monoadduct $[\{\eta^6\text{-C}_6\text{H}_5(\text{CH}_2)_2\text{OH}\}\text{RuCl}_2\{\text{P}(\text{CH}_2\text{OH})_3\}]$ **15** accounted to about 30% of phosphine containing species even when substoichiometric amounts of the phosphine were employed. Owing to the low solubility of **15** in CH_2Cl_2 and the formation of several side products, reactions of **15** with $\text{P}(\text{CH}_2\text{OH})_3$ had to be performed in methanol as the solvent. The highly polar methanol solvent considerably aids in dissociating a chloride ligand, thus opening a coordination site which is then occupied by a second equivalent of the phosphine. The outcome of the reactions with less than one equivalent of $\text{P}(\text{CH}_2\text{OH})_3$ indicates, that under these conditions chloride substitution occurs at a similar rate as adduct formation. Of note is the finding, that $\text{P}(\text{CH}_2\text{OH})_3$ here coordinates without any loss of formaldehyde from the phosphine. Reactions utilizing this phosphine sometimes provide complexes that contain partially deformed $\text{PH}_n(\text{CH}_2\text{OH})_{3-n}$ ligands, mostly with high chemoselectivity. A notable example in ruthenium chemistry was recently published by *Whittlesey*.¹³⁹ The factors that are responsible for and influence the degree of deformylation from this phosphine are presently unknown. All the new complexes bearing the $\text{P}(\text{CH}_2\text{OH})_3$ ligand described herein are hygroscopic as is $\text{P}(\text{CH}_2\text{OH})_3$ itself and readily dissolve in water. Closely related complexes $[(\eta^6\text{-arene})\text{RuCl}_2\{\text{P}(\text{CH}_2\text{OH})_3\}]$ have found use in the catalytic conversion of allylic alcohols into corresponding aldehydes or ketones under biphasic conditions.¹⁴⁰ Reports by *Higham* on intra- and intermolecular hydrogen bonding involving the hydroxyalkyl side chains on the arene and the phosphine hydroxymethyl groups¹³⁹ could not be confirmed in these studies due to our failure to crystallize any of the $\text{P}(\text{CH}_2\text{OH})_3$ derived phosphine complexes.

3.5 Electrochemistry

The electrochemistry of half-sandwich dichloro complexes of the type $[(\eta^6\text{-arene})\text{RuCl}_2]_2$ has been probed by various authors and displays a rather intricate behavior with a rich chemistry following or even preceding each electron transfer step. As it is evidenced by these investigations, prototypical $[(\eta^6\text{-p-cymene})\text{RuCl}_2]_2$, in supporting electrolyte

3. Chemistry of oxo and ether functionalized arene Ru complexes

solution, is in equilibrium with the salt $[\{(p\text{-cymene})\text{Ru}\}_2(\mu\text{-Cl}_3)]^+ \text{Cl}^-$. This dissociation step is promoted by media of high ionic strength and is virtually complete in $\text{CH}_2\text{Cl}_2/\text{NBu}_4\text{PF}_6$. The trichloro bridged dimer gives a cathodic peak which precedes the reduction of the neutral dichloro bridged dimer. Authentic $[\{(\eta^6\text{-p-cymene})\text{RuCl}_2\}_2]$ is reduced in a chemically partially reversible and kinetically quasi-reversible one-electron step, and the resulting reduction product was assigned the unsymmetrical dichloro bridged structure $[\{(\eta^6\text{-p-cymene})\text{Ru}\}(\mu\text{-Cl})_2\{\text{RuCl}(\eta^6\text{-p-cymene})\}]$. This latter species dissociates another equivalent of chloride or may be back oxidized to the starting dimer by a sequence involving electron transfer and chloride association steps.¹²⁸ Anodic oxidation of $[(\eta^6\text{-C}_6\text{Me}_6)\text{RuCl}_2]_2$ was observed to proceed in two sequential one-electron steps. Both processes are prone to fast chemical follow processes which ultimately yield $[(\eta^6\text{-C}_6\text{Me}_6)\text{RuCl}_3]$ and oligomeric $[(\eta^6\text{-C}_6\text{Me}_6)\text{RuCl}]^+$ by disproportionation.¹⁴¹

We investigated the electrochemical properties of $[\{(\eta^6\text{-C}_6\text{H}_5(\text{CH}_2)_3\text{OMe})\text{RuCl}_2\}_2]$ (**14**) in $\text{CH}_2\text{Cl}_2/\text{NBu}_4\text{PF}_6$. Voltammograms at room temperature show a close to reversible reduction at -0.79 V (peaks A/A') and an irreversible anodic oxidation at $E_p = +0.33$ V (peak C). Peaks A and C are associated with about the same peak currents under all conditions (Figure 18-Figure 20). When the scan is reversed after traversing peak C, the new cathodic peak D is observed at $E_p = -0.42$ V. As the sweep rate is increased or the temperature is lowered, the reversibility of the oxidation step increases and the associated counter peak C' appears ($E_{1/2} = +0.285$ V) with the concomitant disappearance of peak D (see Figure 19).

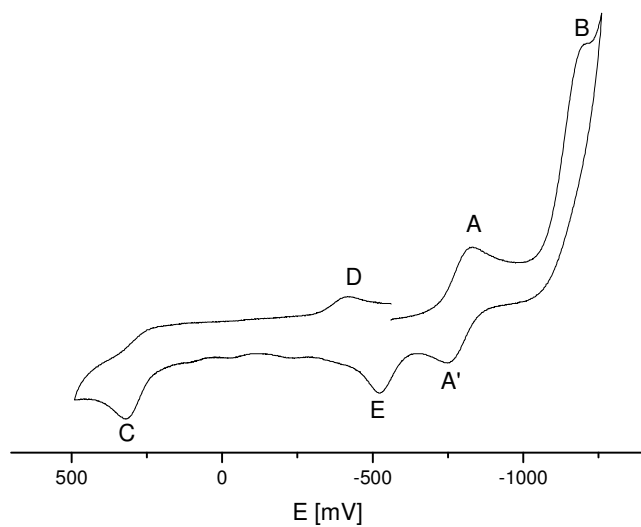


Figure 18: Cyclic voltammograms of complex **14** in $\text{CH}_2\text{Cl}_2/\text{NBu}_4\text{PF}_6$ at $V = 0.1 \text{ V/s}$ at 298 K.

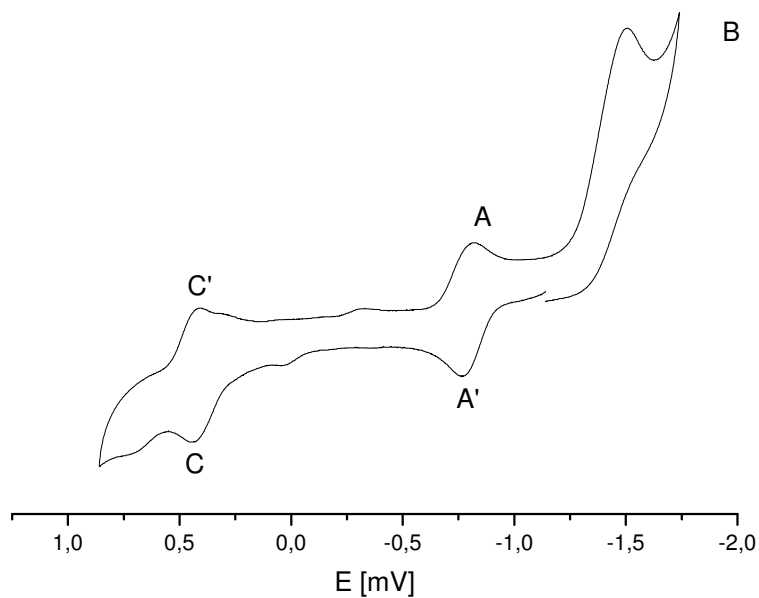


Figure 19: Cyclic voltammograms of complex **14** in $\text{CH}_2\text{Cl}_2/\text{NBu}_4\text{PF}_6$ at $V = 0.1 \text{ V/s}$ at 196 K in a CO_2 /propanol slush bath.

3. Chemistry of oxo and ether functionalized arene Ru complexes

This behavior is highly reminiscent of other dichloro bridged ruthenium dimers such that peaks A and C are ascribed to the reduction and the oxidation of $[(\eta^6\text{-C}_6\text{H}_5(\text{CH}_2)_3\text{OMe})\text{RuCl}_2]_2$. In the case of $[(\eta^6\text{-p-cymene})\text{RuCl}_2]_2$, a peak corresponding to D has been ascribed to the reduction of the monomeric $[(\eta^6\text{-C}_6\text{Me}_6)\text{RuCl}_3]$ formed in the disproportionation process following oxidation. Compared to $[(\eta^6\text{-C}_6\text{Me}_6)\text{RuCl}_2]_2$, wave C/C' is shifted by about 450 mV to more negative potentials and this may indicate some remarkable stabilization of the oxidized form through intramolecular solvation by the appended ether moiety. When the cathodic sweep is continued past the A/A' couple, another irreversible reduction peak is observed at ca. -1.20 V (peak B in Figures 18-20). This feature is associated with considerably higher currents as the A/A' couple and peak C. Peak B is followed by additional, broad and ill-defined features at even more cathodic potentials (not shown in Figures 18-20). On the reverse scan, an additional anodic feature, peak E, at -0.53 V indicates the formation of a new electroactive follow product.

Table 9: Redox potentials of the complex **14** and its follow products; peak-to-peak separations are given in parantheses.

Compound	$E^{1/2}_{\text{ox}}$ (V) (C/C')	$E^{1/2}_{\text{red}}$ (V) (A/A')	E_p (V) (B)	E_p (V) (E)	E_p (V) (F)	E_p (V) (D)
14	+0.295(60)	-0.790(65)	-1.20	-0.53	-0.43	-0.42

a) Potentials are provided relative to the Fc/Fc⁺ scale.

Table 10: Redox potentials of the complexes; peak-to-peak separations are given in parantheses.

Compound	$E^{1/2}_{\text{ox}}$ (V)
13a	+ 0.705(82)
13b	+ 0.735(81)
13c	+ 0.895(81)
14a	+ 0.770(73)
14b	+ 0.685(75)
15a	+ 0.775(77)

a) Potentials are provided relative to the Fc/Fc⁺ scale.

3. Chemistry of oxo and ether functionalized arene Ru complexes

Addition of the mild chloride scavenger NaSbF₆ to the supporting electrolyte solution has the effect of further increasing the intensity of peak B and decreasing the chemical reversibility of the A/A' couple, most probably by accelerating the rate of chloride dissociation from reduced [$\{\eta^6\text{-C}_6\text{H}_5(\text{CH}_2)_3\text{OMe}\}\text{RuCl}_2\}_2^-$] (Figure 20). Given the known propensity of [$\{\eta^6\text{-arene}\}\text{RuCl}_2\}_2$] to chloride loss in ionizing media and the qualitative changes induced by the presence of NaSbF₆, peak B is assigned as the reduction of such a chloride dissociation product.

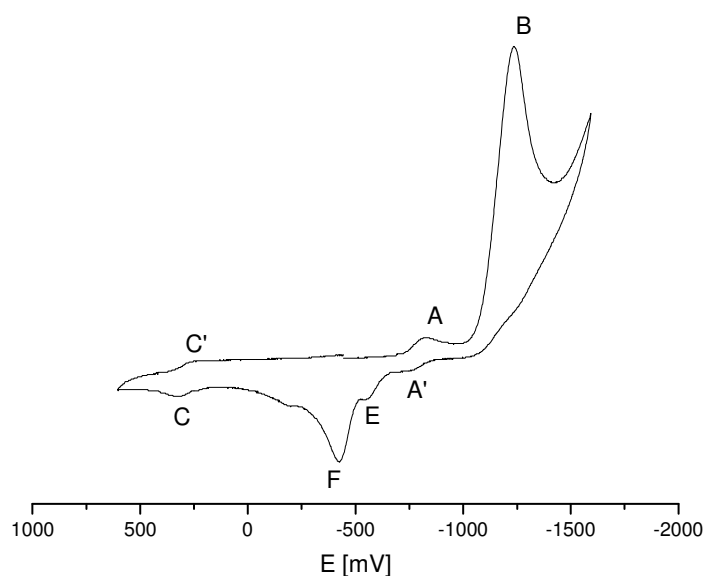


Figure 20: Cyclic voltammograms of complex **14** in CH₂Cl₂/NBu₄PF₆ at V = 0.1 V/s at 298 K but in the presence of excess of NaSbF₆.

Possible candidates are trichloro bridged [$\{\eta^6\text{-C}_6\text{H}_5(\text{CH}_2)_3\text{OMe}\}\text{Ru}(\mu\text{-Cl}_3)\text{Ru}\{\eta^6\text{-C}_6\text{H}_5(\text{CH}_2)_3\text{OMe}\}\}^+$] or an unsymmetric complex [$\{\eta^6:\eta^1\text{-C}_6\text{H}_5(\text{CH}_2)_3\text{OMe}\}\text{Ru}(\mu\text{-Cl}_2)\text{RuCl}\{\eta^6\text{-C}_6\text{H}_5(\text{CH}_2)_3\text{OMe}\}\}^+$] with the appended ether moiety coordinated to the ruthenium center. While additional experiments are necessary in order to unambiguously establish the nature of this species, we favor the latter structure since trichloro bridged dimers are commonly easier reduced as their neutral dichloro bridged precursors. The hydroxy appended complexes gave only ill defined, broad voltammetric responses and were not further investigated. This is possibly due to a combination of limited solubility and

a coupling of proton transfer from the side chain hydroxy group to the electron transfer processes.

Half-sandwich phosphine complexes of the type $[(\eta^6\text{-arene})\text{RuCl}_2(\text{PR}_3)]$, on the other hand, display much simpler electrochemical responses and usually undergo a chemically reversible oxidation at fairly positive potentials.^{69, 127, 142} This oxidation is assigned as the Ru(II/III) couple, i. e. as an essentially metal centered process. Electrochemical studies on $[(\eta^6\text{-C}_6\text{H}_6)\text{RuCl}_2(\text{PPh}_3)]$ by Dyson¹⁴³ reveal very similar results. The half-wave potentials thus reflect the electron density at the ruthenium atom and electron donation from the ancillary ligands. Phosphine adducts **13a-c**, **14a,b** and **15a** display essentially the same behavior. There is just one anodic wave within the $\text{CH}_2\text{Cl}_2/\text{NBu}_4\text{PF}_6$ electrolyte window, and this wave always constitutes a chemically reversible couple with $i_{p,c}/i_{p,a}$ ratios of at least 0.95, even at low sweep rates. The voltammetric response of compound **14a** is displayed as Figure 21 and may serve as a representative example. Peak potential differences slightly exceed the values of the internal ferrocene/ferrocenium standard with larger differences as the sweep rate is increased. Such findings are diagnostic of somewhat sluggish electron transfer kinetics (quasi-reversible behavior). Half-wave potentials and peak-to-peak separations are listed in Table 10.

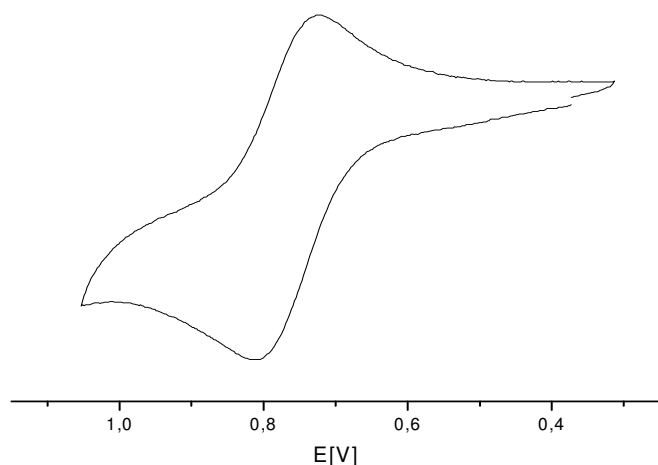


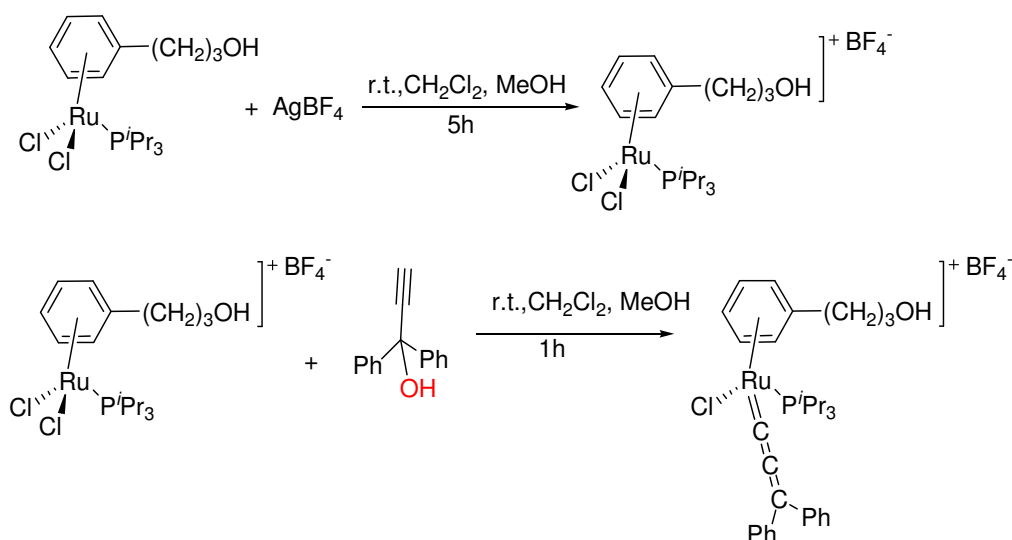
Figure 21: CV of compound $[(\eta^6\text{-C}_6\text{H}_5(\text{CH}_2)_3\text{OMe})\text{RuCl}_2(\text{P}^i\text{Pr}_3)]$ (**14a**) in $\text{CH}_2\text{Cl}_2/\text{NBu}_4\text{PF}_6$, 298 K, $\nu = 0.1$ V/s.

3. Chemistry of oxo and ether functionalized arene Ru complexes

Comparison of the data shows that the half-wave potentials are sensitive to both, the identity of the phosphine and of the arene ligands. The more basic P^iPr_3 and PCy_3 adducts lead to distinctly lower $E_{1/2}$ values as the tris(hydroxylated) $P(CH_2OH)_3$ with a difference of 190 mV between **13a** and **13c**. No clear trend arises from the substitution of the arene ligand. While the 3-hydroxypropylbenzene derived complex **13a** is somewhat easier to oxidize than its methyl ether **14a**, the opposite holds for the PCy_3 complexes **13b**, **14b**.

3.6 Synthesis of $[\{\eta^6-C_6H_5(CH_2)_nOR\}(PR'_3)ClRu=C=C=CPh_2]^+$

Following the well established protocol for conversion of propargylic alcohols to allenylidene ruthenium complexes, we attempted to synthesize a family of cationic allenylidene complexes starting from neutral ruthenium phosphine complexes **13a-c**, **14a,b** and **15a**. Chloride abstraction from phosphine adducts $[\{\eta^6-C_6H_5(C_nH_{2n})OR\}RuCl_2(PR'_3)]$ **13a-c**, **15a** with Tl^+ or Ag^+ salts led to the formation of cationic $[\{\eta^6-C_6H_5(C_nH_{2n})OR\}RuCl(PR'_3)]^+$ (OTf^- ($OTf^- = CF_3SO_3^-$)) $[\{\eta^6-C_6H_5(C_nH_{2n})OR\}RuCl(PR'_3)]^+$ SbF_6^- , and $[\{\eta^6-C_6H_5(C_nH_{2n})OR\}RuCl(PR'_3)]^+ BF_4^-$ complexes. Thallium salts are commonly used as non-oxidizing alternatives to silver salts in halide abstraction reactions. Further possible advantages of Tl^+ salts are, that they are not as photosensitive as Ag^+ salts, and that Tl^+ less readily coordinates to phosphine ligands giving rise to $M(PR_3)_3$.



Scheme 27: Synthesis of $[\{\eta^6-C_6H_5(CH_2)_3OH\}(P^iPr_3)ClRu=C=C=CPh_2]^+$.

3. Chemistry of oxo and ether functionalized arene Ru complexes

Nevertheless, in our hands, only abstraction with Ag^+ salts delivered pure cationic complexes which could be isolated and fully characterized. In reactions with thallium salts, ^{31}P -NMR spectra always showed more than one signal. Literature provides examples of incomplete chloride abstraction and so called “arrested states of abstraction” in which the chloride remains bond to the original ruthenium metal center but is also associated with the Tl^+ ion. The overall structure is that of a one dimensional coordination polymer that consists of individual ruthenium units being connected to an adjacent thallium ion via pendant side arms on the coordinated phosphine.¹⁴⁴ (see Figure 22)

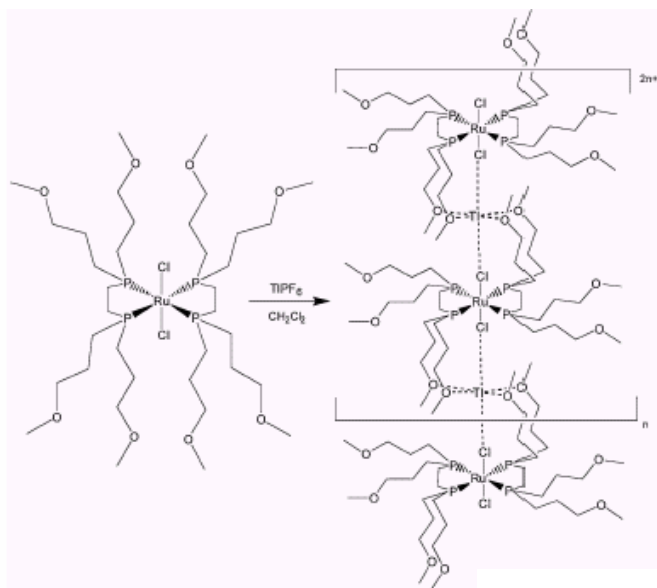


Figure 22: Arrested chloride abstraction with TlPF_6 .

All synthesized cationic complexes were reacted with 1,1-diphenyl-2-propyn-1-ol but only in the case of complex **13a** with P^iPr_3 as the phosphine and BF_4^- as the counter ion a sufficiently stable allenylidene complex was isolated. Attempts to synthesize allenylidene complexes $[\{\eta^6\text{-C}_6\text{H}_5(\text{CH}_2)_n\text{OR}\}(\text{PR}_3)\text{ClRu}=\text{C}=\text{C}=\text{CPh}_2]^+$ were therefore carried out at low temperature. Reactions were completed within a couple of hours at -40°C . Upon slow warming of these solutions in the NMR spectrometer several other signals in the ^{31}P spectrum appeared and a color change from the characteristic deep violet to orange brown appeared upon degradation. Depending on the substituents on the arene, these allenylidene complexes show variable stability at temperatures of -40 to -20°C . Under these conditions the characteristic spectroscopic resonance signals and intense absorption bands at $\text{ca } 1920\text{ cm}^{-1}$ in infrared spectroscopy were observed. The reaction of

3. Chemistry of oxo and ether functionalized arene Ru complexes

15a with 1,1-diphenyl-2-propyn-1-ol in CD_2Cl_2 was first carried out at $-78\text{ }^\circ\text{C}$ (dry ice/propanol) and the solution was then slowly warmed to $-10\text{ }^\circ\text{C}$. Low temperature monitoring by ^{31}P -NMR spectroscopy shows after 10 min formation of the allenylidene complex with the concomitant appearance of a new intense singlet at 70 ppm. This is at significantly lower field in comparison to the singlet at ca. 60 ppm arising from the coordinated PCy_3 ligand in previously reported allenylidene complexes $[\{\eta^6\text{-arene}\}(\text{P}^i\text{Pr}_3)\text{Cl}_2\text{Ru}=\text{C}=\text{C}=\text{CRR}'^+]$.¹²⁶ Warming the reaction to $0\text{ }^\circ\text{C}$ provided almost complete transformation of the propargylic alcohol, while the signal of the starting cationic phosphine complex **15a** at 46.1 ppm almost vanished. Further warming in steps of $5\text{ }^\circ\text{C}$ assists in complete conversion of propargylic alcohol, but was followed by the appearance of many other unidentified products arising from decomposition of the allenylidene complex. These observations were additionally proven when the cationic complex $[\{\eta^6\text{-C}_6\text{H}_5(\text{CH}_2)_3\text{OH}\}\text{ClRu}(\text{P}^i\text{Pr}_3)]^+ \text{BF}_4^-$ (**13a**) was reacted with 1,1-diphenyl-2-propyn-1-ol (Scheme 27) at 78 K and the reaction was monitored by IR spectroscopy by taking samples in short intervals. The blue curve in Figure 23 shows the spectrum recorded 51 min after reaction was started. The characteristic allenylidene band at 1984 cm^{-1} is clearly observed. When the reaction mixture was slowly warmed to $23\text{ }^\circ\text{C}$, the intensity of allenylidene band diminished whereas the intensities of other bands increased. This agrees well with our previous observations of formation of many other products. OH bands at 2937 cm^{-1} and 2884 cm^{-1} gain maximum intensity upon longer reaction times which probably indicates the loss of water due to the dehydration process during the reaction.

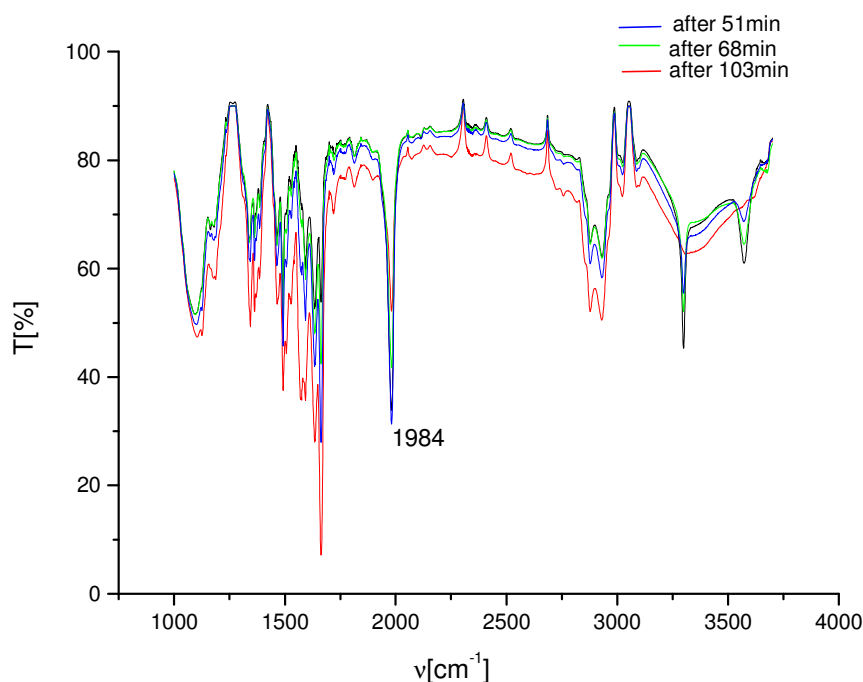


Figure 23: IR spectra recorded during reaction of $[(\eta^6\text{-C}_6\text{H}_5(\text{CH}_2)_3\text{OH})\text{ClRu}(\text{P}^i\text{Pr}_3)]^+\text{BF}_4^-$ (**13a**) and 1,1-diphenyl-2-propyn-1-ol.

Further warming to room temperature led to rapid degradation of the allenylidene complex and the appearance of prominent ^{31}P -NMR signals at lower field. This leads to the conclusion that all reactions involving such allenylidene complexes must be carried out at around or below $0\text{ }^\circ\text{C}$ *in situ*. However, our interest was directed more towards examining the catalytic activity of these allenylidene complexes in olefin metathesis. Therefore we probed the catalytic activity of these allenylidene derivatives in ring closing metathesis reactions at $10\text{ }^\circ\text{C}$ with *N,N*-diallyltosylamine and diallylmalonate. Unfortunately, at this temperature no sign of catalysis could be observed. Studies by *Fürstner* and *Dixneuf* had shown, that allenylidene complexes $[(\eta^6\text{-arene})\text{Cl}(\text{PR}'_3)\text{Ru}=\text{C}=\text{C}=\text{CPh}_2]^+$ are not catalytically active themselves but rather serve as precatalysts. Two different pathways accounts for their conversion to catalytically active species: Thermal or irradiative loss of the coordinated arene or dissociation of the phosphine. Both pathways would provide a coordinatively unsaturated metal center. Upon slow warming to room temperature the indicative singlet for free P^iPr_3 at 47.37 ppm appeared, but along with many other species. Our efforts to design catalysts possessing reactivities like the Grubbs and Fürster-Dixneuf

3. Chemistry of oxo and ether functionalized arene Ru complexes

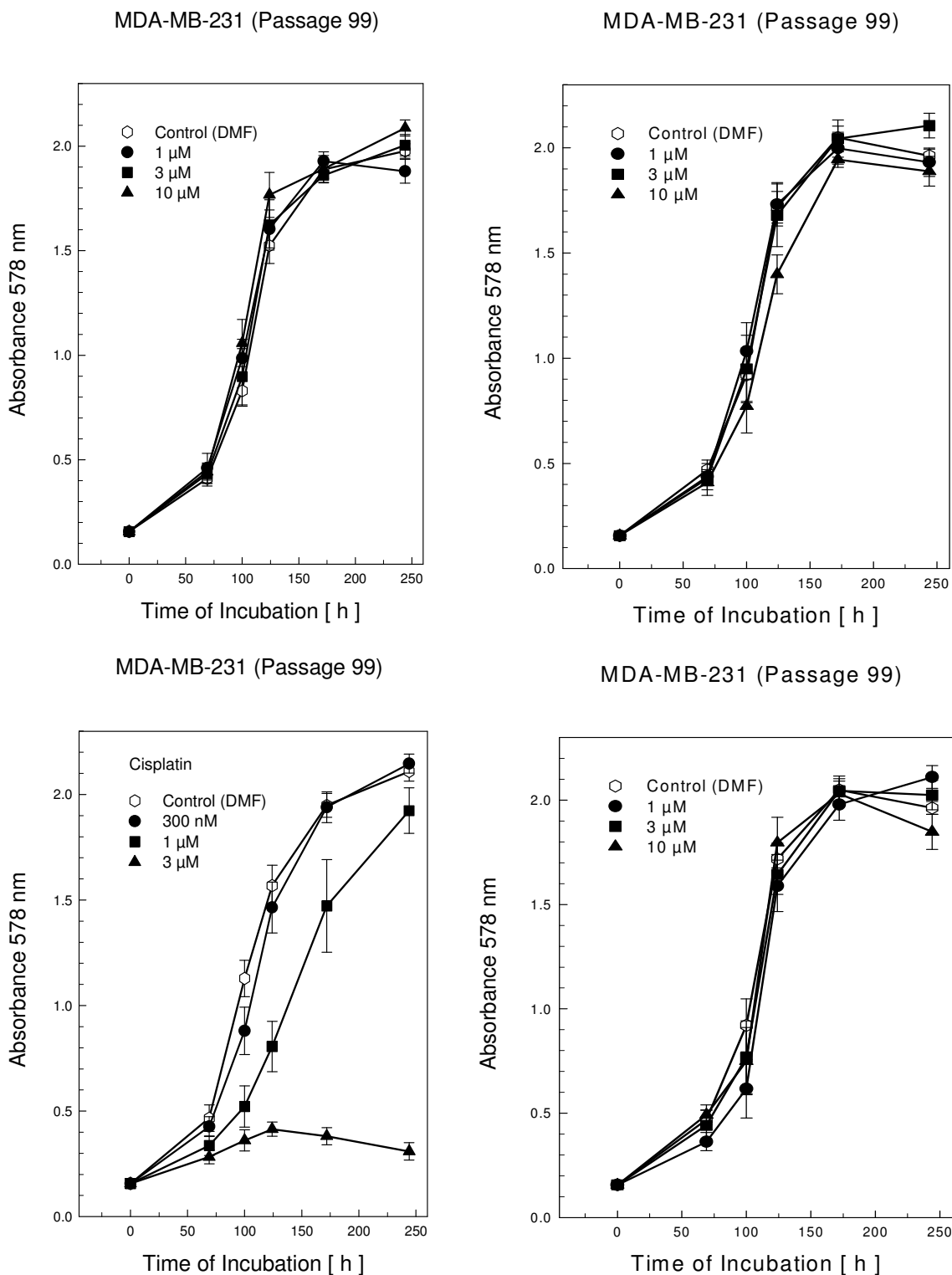
class of metathesis active compounds were thus not met with success. Therefore, we decided to investigate the reactivities of arene ruthenium complexes towards alkynols in cyclodimerization or cyclotrimerization reactions. Our results in this area will be presented in Chapter 4.

3.7 Assessment of the biological activity of complexes $[\{\eta^6\text{-C}_6\text{H}_5(\text{CH}_2)_n\text{OR}\}\text{RuCl}(\text{PR}_3)]$

After finding that allenylidene complexes $[\{\eta^6\text{-C}_6\text{H}_5(\text{CH}_2)_n\text{OR}\}(\text{PR}_3)\text{ClRu}=\text{C}=\text{C}=\text{CRR}'\text{]}^+$ are rather unstable and catalytically inactive at the temperature where they may be generated, we decided to examine if the congeners that dissolve in water or other highly polar solvents possess anticancerogenic properties. This is set against the background that some water soluble ruthenium(II) arene complexes with phosphine ligands have already been found to exhibit antimicrobial and antiviral properties showing remarkable toxicity towards microbes and viruses.⁵² Werner type coordination complexes of ruthenium commonly form various species in aqueous solution which complicates the assessment of their biological activity. These difficulties might be overcome using organometallic compounds which exhibit different ligand exchange kinetics. Ruthenium(II) arene complexes were also shown to form adducts with nucleosides and nucleotides,^{145, 146} and these have been demonstrated to exhibit anticancer activity.¹¹²

For investigation of their anticancer properties we chose complexes **13**, **13c** and **15c**. Cisplatin was purchased SIGMA, Munich, Germany. 10 mM stock solutions of the test compounds were prepared in DMF. The stock solutions were stored at -20 °C. The results (mean values \pm standard deviation) were plotted as growth curves.

3. Chemistry of oxo and ether functionalized arene Ru complexes

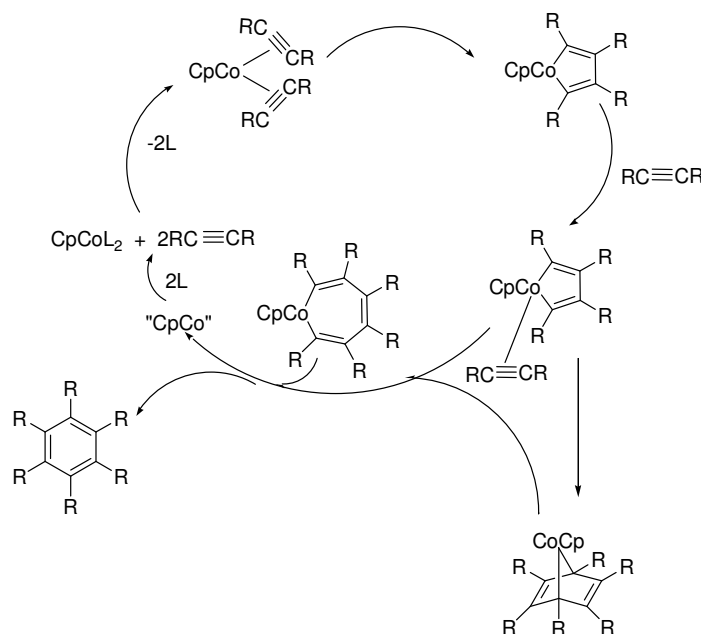


By this method, the chemosensitivity assay is based on quantification of biomass by staining cells with crystal violet. The crystal violet technique measures the total dye binding capacity of a given cell population which correlates to the total biomass. Results show the half sandwich ruthenium complexes do not exhibit anticancer activities toward MDA-MB-231 cell lines.

4 The coupling of alkynols on arene ruthenium platforms

4.1 Cyclotrimerization of 2-methylbut-3-yn-1-ol

Transition-metal catalyzed alkyne cyclotrimerization is a straightforward approach for the assembly of substituted benzenes and non-aromatic carbocycles from simple acyclic precursors. Co-trimerization reactions widen the scope of such reactions and provide access to a broad variety of heterocycles such as pyridines or phosphonines (see Scheme 5 on page 16). These are of vital interest in chemistry, biology and pharmacy, e.g. for the synthesis of natural products. The first organometallic compound that efficiently catalyzed the cyclotrimerization of alkynes to benzenes was $\text{CpCo}(\text{CO})_2$.¹⁴⁷ In the meantime it has been found that complexes of other transition metals are equally active in the cyclotrimerization of alkynes to aromatic hydrocarbons. Cyclotrimerization reactions generally involve coordination of two molecules of an alkyne, formation of a metallacyclopentadiene, coordination of another molecule of alkyne, and a coupling to arene products with regeneration of the catalyst.¹⁴⁸ The accepted mechanism for CpCo based systems is presented in Scheme 28.



Scheme 28: Catalytic cycle of CpCoL_2 catalyzed cyclotrimerization of alkynes.

4. Coupling of alkynols on {Arene-Ru} platforms

Considering the linear or cyclic oligomerization of alkynes, CpCo and CpRu entities (see Scheme 7 on page 18) have been a long standing success story and have provided access to a vast number of substrates.¹⁴⁸ The ruthenium catalyzed cyclooligomerization of three molecules of an alkyne or two molecules of an alkyne and one molecule of an alkene to benzenes or cyclohexadienes,¹⁴⁹ respectively, has been studied by the *Kirchner* group,⁹³ both experimentally and theoretically. In this case the crucial species is CpRuCl, which is another 14 valence electron entity. It differs from CpCo and (arene)Ru in that it has another ligand in addition to a cyclic π -perimeter bonded to the metal. This leads to distinctly different intermediates along the reaction path when compared to the cobalt-case (Scheme 28). From the reaction with three equivalents of an alkyne a metallocyclopentatriene instead of a metallocyclopentadiene (or metallol) is produced after the coupling of two molecules of the alkyne. The final product preceding the release of the arene following insertion of the third alkyne molecule, is a η^2 -bonded arene rather than a η^4 -bonded one as in the case of cobalt (see Figure 24). Amongst the various other metal complexes that may also effect such coupling reactions,¹⁵⁰⁻¹⁵³ half sandwich ruthenium complexes $[\text{Cp}^{\text{R}}\text{RuL}_2\text{Cl}]$ and $[\text{Cp}^{\text{R}}\text{RuL}_3]^+$ (Cp^{R} = substituted η^5 -coordinated cyclopentadienyl or indenyl ligand, L = neutral ligand) have recently emerged as equally powerful tools for novel alkyne couplings.^{93, 98, 154, 155} Despite increased interest in cyclopentadienyl ruthenium promoted couplings of alkynes, similar reactions of isoelectronic $[(\eta^6\text{-arene})\text{RuL}_n]^+$ entities have seemingly not been utilized to date and our study encloses a contribution to this field.

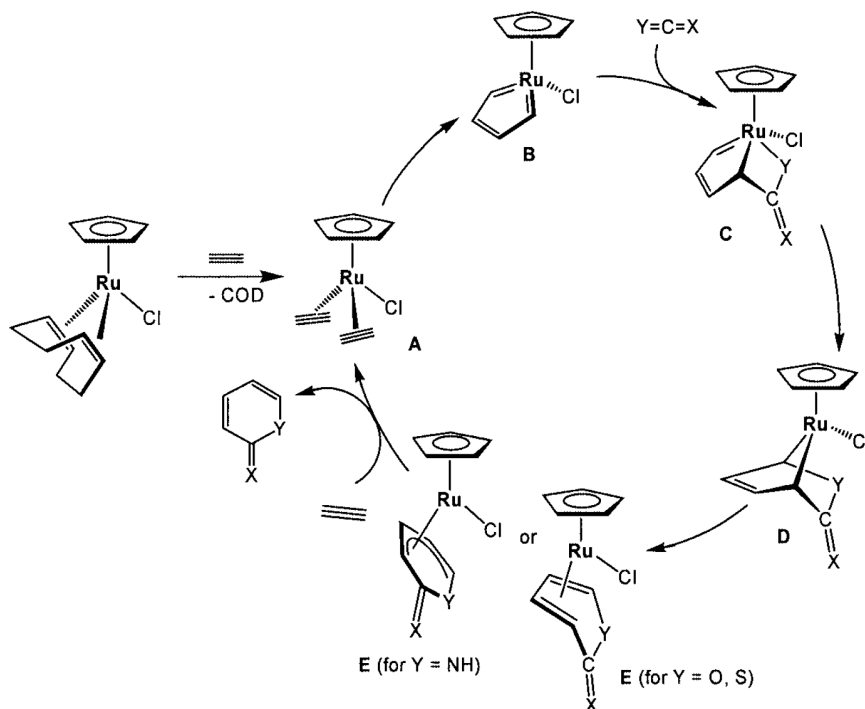
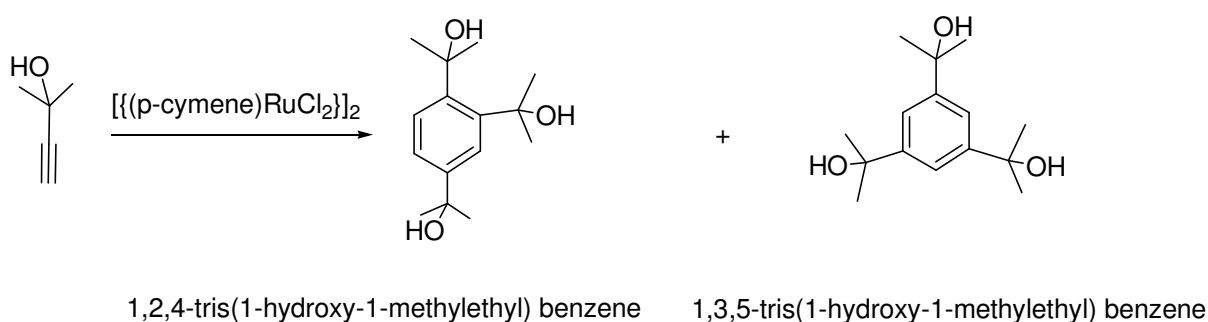


Figure 24: CpRu(COD)Cl initiated cyclotrimerization of alkynes.

While alkyne cyclotrimerizations have been highly successful, there has been limited success with the cyclizations of alkynols presumably because the catalytically active metal center is deactivated by reaction with the OH group of the alkynol. Due to the comparatively low oxophilicity of ruthenium, complexes of this element may also be employed in catalytic reactions involving alkynols. Some investigations on the cyclization of alkynols have been already carried out by other authors,^{99, 100, 156} and mixtures of 1,2,4- and 1,3,5- substituted benzene derivatives as well as polymeric materials were obtained. The unsymmetrical 1,2,4 isomer usually predominates over the symmetrical 1,3,5-trisubstituted benzene derivative in the reaction mixtures and separation of the two isomers is often tedious and difficult. However, the regiospecific catalytic cyclotrimerization of 2-methylbut-3-yn-2-ol by some nickel and platinum complexes were studied by the group of *Furlani*. In a systematic study of the $[\text{NiX}_2\text{L}_2]$ ($\text{X} = \text{halogen}, \text{NO}_3, \text{NCS}$; $\text{L} = \text{phosphine}$) catalyzed cyclotrimerization of 2-methylbut-3-yn-2-ol it was found that $[\text{NiBr}_2\text{L}_2]$ gave the 1,3,5-trisubstituted benzene derivative in high yields,¹⁰⁰ while $[\text{NiI}_2(\text{Ph}_3\text{P})_2]$ converts the same alkynol into 1,2,4-isomer.⁹⁹

4. Coupling of alkynols on {Arene-Ru} platforms



Scheme 29: Cyclization of 2-methylbut-3-yn-2-ol to substituted benzenes.

Interestingly, there is some evidence of cobalt catalyzed cyclotrimerizations of dialkynols in aqueous solution using the complex $\text{Cp}'\text{Co}(\text{COD})$. One problem of using $\text{CpCo}(\text{CO})_2$ in water stems from the difficulty of substituting the CO ligand, which may be due in part to enhanced back-bonding in this high dielectric constant solvent. Therefore, $\text{Cp}'\text{Co}(\text{COD})$ complexes were designed with substituent R on the Cp ring that aided its water solubility and a cyclooctadiene that would control steric access to the cobalt coordination sphere. In this reaction dissociative coordination of alkynol implies slippage of the Cp ligand from η^5 to η^3 and subsequent coordination of the first alkyne.¹⁰¹ A crucial aspect in CpCo alkyne cyclotrimerization in organic solvents is the dissociative formation of 16 valence electron complexes at several points in the reaction¹⁵⁷ to allow the alkyne to approach to the metal center and there is the possibility that or Cp or COD dissociate from the metal center. In the mechanism proposed by *Kirchner* it is evident that dissociation of COD ligand provides free coordination sites for coordination of two alkynes.

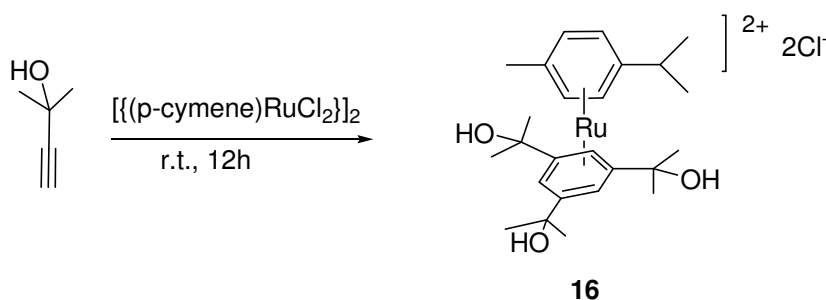
In general, $[(\eta^6\text{-arene})\text{RuCl}_2]_2$ complexes readily react with neutral two-electron donor ligands to give neutral complexes which, in polar solvents, easily dissociate one chloride ligand, thus opening a free coordination site next to the new ligand L. An accessible free coordination site in *cis* position to the coordinated alkyne or alkyldiene ligands is a requirement for subsequent direct coupling of 3 equivalents of alkynols to give benzene derivatives. Therefore, amongst the first reactions explored in this work were direct reactions of a variety of propargylic alcohols with $[(\eta^6\text{-p-cymene})\text{RuCl}_2]_2$ (**1**) in different stoichiometric ratios in the presence of different chloride-abstracting agents including AgOTf , AgOTs , NaSbF_6 , NaPF_6 , AgSbF_6 , and NaBPh_4 or in their absence, in a mixture of MeOH and CH_2Cl_2 as the solvent. Treatment of $[(\eta^6\text{-p-cymene})\text{RuCl}_2]_2$ (**1**) with 3

4. Coupling of alkynols on {Arene-Ru} platforms

equivalents of 1,1-dimethylprop-2-yn-1-ol per monomeric unit and 4 equivalents of NaSbF₆ afforded only the trichloro-bridged dimer $[(\eta^6\text{-p-cymene})\text{Ru}]_2(\mu\text{-Cl})_3]^+ \text{SbF}_6^-$ (**8**). In the presence of all other halide-abstracting agents, some of the alkynol is slowly consumed but only unidentifiable mixtures are obtained.

When the dichloro-bridged complex $[(\eta^6\text{-p-cymene})\text{RuCl}_2]_2$ (**1**) was separately reacted with 3 equivalents of 1,1-diphenylprop-2-yn-1-ol or 1-phenylprop-2-yn-1-ol, ¹H-NMR spectroscopy of the orange crude reaction mixture obtained after 14 hours of stirring at room temperature, evaporation of the solvents and washing the residue with ether showed a complex mixture of organometallic species which we were not able to separate by chromatography. Monitoring the reaction of **1** with 7.5 equivalents of 1,1-dimethylprop-2-yn-1-ol by ¹H-NMR spectroscopy in CD₂Cl₂ solution, revealed a gradual conversion of the alkynol to new organic products. ¹H-NMR spectra recorded after 1 hour showed a mixture of the starting alkynol and a variety of organic products. The parallel growth of six doublets in the aromatic regime in the range from 6.13 to 7.25 ppm, indicates the formation of a new unsymmetrical organometallic species (Scheme 29). Despite the comparatively low field, this indicates that η^6 -coordination of this arene is maintained while the molecular mirror plane is lost. This intermediate species has not been identified at this point. Following the progress of this reaction continuously during the next 5 hours showed, that the starting alkynol is slowly consumed. Moreover, the intensities of the signals for the initially formed organic and organometallic species slowly decrease. This is accompanied by the rise of two sets of signals in the aromatic region at $\delta = 7.09$ and 7.47 ppm and singlets for OH groups at 2.46 and 3.26 ppm showing a 2:1 integral ratio. A new resonance signal for methyl protons appears at $\delta = 1.49$ ppm.

From the reaction mixture some colorless crystals were obtained. Their investigation by X-ray structure analysis provided a possible key for the understanding of the outcome of this reaction. The crystalline solid turned out to be the novel, bis(arene)Ru complex $[(\eta^6\text{-p-cymene})(\eta^6\text{-C}_6\text{H}_3(\text{CMe}_2\text{OH})_3\text{-1,3,5})\text{Ru}]^{2+} (\text{Cl}^-)_2 \times 2 \text{H}_2\text{O}$ (**16**). Importantly, the trisubstituted arene ring must have originated from the cyclotrimerization of the starting alkynol at the $\{(\eta^6\text{-p-cymene})\text{Ru}\}^{2+}$ template.



Scheme 30: Synthesis of $[(\eta^6\text{-p-cymene})(\eta^6\text{-C}_6\text{H}_3(\text{CMe}_2\text{OH})_{3-1,3,5})\text{Ru}]^{2+} (\text{Cl}^-)_2$ (**16**).

Our results are in a good correlation with *Dinjus's* reports on the cyclotrimerization of alkynes with Cp^*RuCl which are isolobal to the CpCo fragment.¹⁵⁸ Interestingly, in these reactions isolable organometallic products are formed. Phenylacetylene reacts with $\text{Cp}^*\text{Ru}(\text{COD})\text{Cl}$ and, depending on the reaction conditions, gives rise to a neutral ruthenacyclopentatriene with the the 1,4-diphenyl-but-2-en-1,4-diyl ligand which was structurally characterized or the cationic sandwich compound $[\text{Cp}^*\text{Ru}\{(\eta^6\text{-1,2,4-triphenyl)benzene}\}]^+$.¹⁵⁹ This report indicates that longer reaction times are necessary in order to form the cationic sandwich complex, which is consistent with our observations.

4.2 Crystal structure of $[(\eta^6\text{-p-cymene})$

$\{\eta^6\text{-C}_6\text{H}_3(\text{CMe}_2\text{OH})_{3-1,3,5}\}\text{Ru}]^{2+} (\text{Cl}^-)_2 \times 2 \text{H}_2\text{O}$ (**16**)

A crystal structure determination of **16** was carried out on an irregularly shaped colorless crystal. Complex **16** crystallizes in the monoclinic space group $P 2_1/c$. In **16**, the metal ion is coordinated to two arene rings and binds in a η^6 manner to each of them (see Figure 25). The distance of the Ru atom to the centers of the arene planes are 1.739 for plane of the (p-cymene) ligand and 1.745 Å for the plane of the $\{\eta^6\text{-C}_6\text{H}_3(\text{CMe}_2\text{OH})_{3-1,3,5}\}$ ligand. The comparable distance of the ruthenium center from the arene ring in $[\text{Cp}^*\text{Ru}\{(1,2,4\text{-triphenyl)benzene}\}]$ is 1.72 Å. The Ru-C bonds in **16** are longer than those in typical half sandwich complexes but compare well to values found for similar dicationic bis(arene) complexes of ruthenium such as $[(\eta^6\text{-biphenyl})_2\text{Ru}]^{2+} (\text{BF}_4^-)_2$ where they range from 2.229(6) to 2.302(9) Å.¹⁶⁰ The three CMe_2OH groups at the one arene ligand are all oriented in a way such that one Me substituent is directed away from the metal. Two of the OH-groups form hydrogen bonds to the Cl^- counter anions. It is worth noting that the

4. Coupling of alkynols on {Arene-Ru} platforms

hydrogen atoms were directly located in the Fourier map and could be refined. Each of the chlorine atoms is additionally hydrogen bonded to a co-crystallized molecule of water. Selected bond angles and distances are given in Table 11. Both six membered rings are planar with very small deviations of individual atomic positions to the best planes and they are almost perfectly parallel to each other (angle 2.4°). Carbon atoms directly attached to the six membered rings are almost coplanar with the respective ring planes. The substituents are only slightly bent away from the ruthenium center.

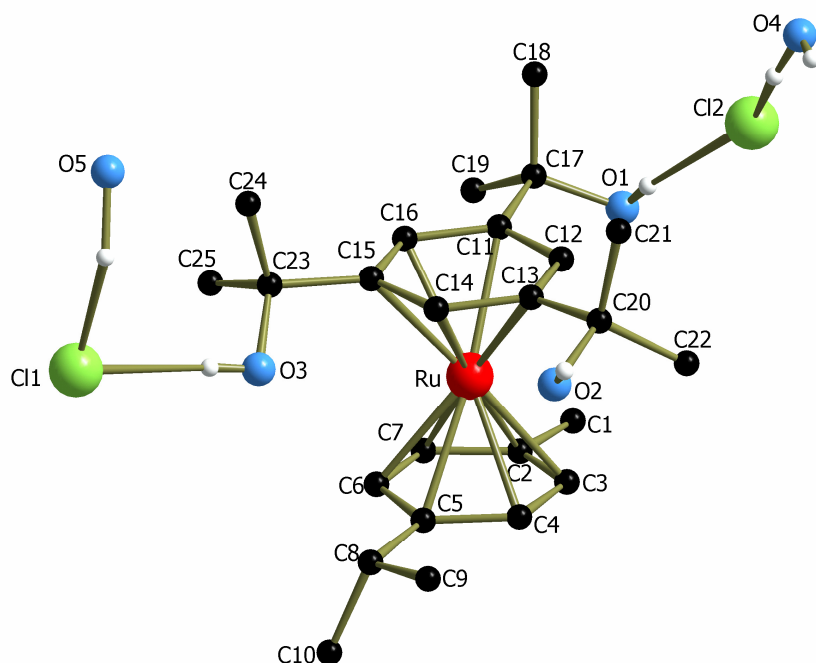


Figure 25: Crystal structure of the dicationic bis-sandwich complex $[(\eta^6\text{-p-cymene})\{\eta^6\text{-C}_6\text{H}_3(\text{CMe}_2\text{OH})_{3-1,3,5}\}\text{Ru}]^{2+} (\text{Cl}^-)_2 \times 2 \text{H}_2\text{O}$ (**16**) in the solid state.

4. Coupling of alkynols on {Arene-Ru} platforms

Table 11: Selected bond lengths (Å) and angles (°) for **16**.

Bond lengths (Å)				Bond angles (°)	
Ru-C2	2.289(3)	C1-C2	1.502(6)	O1-C17-C19	107.5(4)
Ru-C3	2.227(4)	C2-C3	1.412(6)	O1-C17-C18	111.6(4)
Ru-C4	2.230(4)	C3-C4	1.410(6)	O1-C17-C11	109.6(3)
Ru-C5	2.269(3)	C4-C5	1.408(5)	O2-C20-C21	111.7(4)
Ru-C6	2.211(4)	C5-C6	1.418(5)	O2-C20-C22	109.4(4)
Ru-C7	2.231(3)	C6-C7	1.407(6)	O3-C23-C15	105.5(3)
Ru-C11	2.273(3)	C7-C2	1.414(6)	O3-C23-C25	110.5(3)
Ru-C12	2.232(4)	C12-C11	1.418(5)	O3-C23-C24	111.7(4)
Ru-C13	2.250(3)	C12-C13	1.404(5)		
Ru-C14	2.203(4)	C14-C13	1.412(5)		
Ru-C15	2.252(3)	C14-C15	1.409(5)		
Ru-C16	2.239(3)	C16-C15	1.425(5)		
		C16-C11	1.414(5)		
		C23-O3	1.420(5)		
		C17-O1	1.418(5)		
		C20-O2	1.420(5)		

Despite the low yield of complex **16** it was attempted to record its $^1\text{H-NMR}$ spectrum in CD_2Cl_2 . Due to its low concentration no valuable information could, however, be obtained. Dicationic bis(arene) complexes of Ru(II) $[(\eta^6\text{-arene})(\eta^6\text{-arene}')\text{Ru}]^{2+}$ are well known in the literature. Derivatives with two identical arene rings can be obtained by the *Fischer-Hafner* method,¹⁶¹ whereas derivatives with two different arene rings coordinated to ruthenium are conveniently prepared in high yields by refluxing dichlorobridged bis(arene) ruthenium dimers in the presence of another arene in CF_3COOH as the solvent.¹⁶¹⁻¹⁶³ In order to verify the formation of **12** and to characterize it by NMR and IR spectroscopy, we tried to prepare this complex from **1** and six equivalents of 1,1-dimethyl-prop-2-yn-1-ol in the presence or absence of various Cl^- abstracting agents, but without success. Free $\text{C}_6\text{H}_3(\text{CMe}_2\text{OH})_3$ is not easily available such that the preparation of **16** from the dimer **1** and the trisubstituted arene according to the *Rybinskaya* method¹⁶²⁻¹⁶⁴ could not be investigated.

The structural characterization of **16** as containing an arene which is formed upon the

4. Coupling of alkynols on {Arene-Ru} platforms

cyclotrimerization of the starting alkynol allowed us to identify the final organic product formed in the reaction of **1** and a large excess of HC≡C-CMe₂OH. The resonance shifts observed for the aromatic CH protons at $\delta = 7.47$ and 7.09 ppm, the OH protons at $\delta = 3.26$ and 2.46 ppm and the resonance signals for CH₃ groups at 1.49 ppm match the literature values for C₆H₃(CMe₂OH)_{3-1,2,4}.¹⁰⁰ Thus, the final product is surprisingly another regioisomer as that found in the structure of **16**. At this stage we can, however, not say, whether **16** (or other bis(arene)Ru complexes) are active catalysts for the cyclotrimerization of 1,1-dimethyl-prop-2-yn-1-ol or whether **16** is just an inactive byproduct formed in small quantities during this reaction. It is, however, certain that entities [{{(η^6 -p-cymene)RuCl₂}}₂] or some species derived thereof during the reaction with 1,1-dimethyl-prop-2-yn-1-ol, are active in converting this alkynol to a cyclotrimer.

Previous reactions strongly support a close analogy of [Cp^RRuL₂Cl], [Cp^RRuL₃]⁺ and {(arene)RuL_n}⁺ counterparts and the possible catalytic utility of {arene-Ru}²⁺ units in such coupling reactions. This reactions also showed that {(arene-Ru)}²⁺ fragments are capable of cyclotrimerizing alkynols just like their {CpRu}⁺ relatives.

4.3 NMR studies on the activity of [{{(η^6 -p-cymene)RuCl₂}}₂] in the cyclotrimerization of alkynols

Our approach to investigate the cyclotrimerization of different alkynols with [{{(η^6 -arene)RuCl₂}}₂] complexes was to monitor the course of these reactions by NMR spectroscopy at regular intervals. Subsequent experiments were carried out at room temperature or by heating, the alkynol/catalyst mixtures of various ratios at different temperatures.

At room temperature, 3 mol% of catalyst, [{{(η^6 -p-cymene)RuCl₂}}₂] was added to 1,1-dimethyl-prop-2-yn-1-ol in CDCl₃ and ¹H-NMR samples were collected in equal intervals. After 48 h two singlets in the aromatic region at 7.18 and 7.48 ppm were observed signaling that some of alcohol had cyclotrimerized to a substituted benzene. These two signals could originate from the unsymmetrical cyclotrimer. However, the appearance of many other peaks of higher field suggests many other side products are formed after such long reaction time. After 48 h a doublet resonance at 1.22 ppm and new singlets at 1.31 ppm, 1.48 ppm and 2.27 ppm were observed in addition to the prominent

4. Coupling of alkynols on {Arene-Ru} platforms

signal of the starting alkynol at 1.51ppm (CH_3) 2.13ppm (OH) and 2.40ppm ($-\text{CH}$) group. In order to isolate the organic products, CDCl_3 was evaporated and crude product was extracted in to diethylether. $^1\text{H-NMR}$ spectra recorded on the ether extracts failed to show any aromatic product. Seemingly there is not sufficient energy for the cyclotrimerization reaction to occur.

Upon increases the temperature to 60 °C conversion takes place after a shorter induction period but the amount of polymeric material increases.¹⁰⁰ In that respect, we heated the same reaction mixture and recorded spectra at 20 min intervals. It was indeed observed that upon heating two aromatic singlets at 7.05 and 7.55 ppm developed in $^1\text{H-NMR}$ spectra already after a short period of time along with prominent signals from unconsumed propargylic alcohol and the dimeric precatalysts. After heating for 40 min, the intensities of aromatic signals increased. The signals of the educts were still present after 5 h of heating. Longer heating times did not further increase the intensity of the aromatic signals and a numerous of other overlapping signals in alkyl regime were observed. To avoid degradation, the reaction was repeated at 45 °C but with the same overall result.

The results of these experiment may be summarized as follows: $^1\text{H-NMR}$ spectroscopic monitoring of these reactions and the isolation of complex **16** provide evidence, that alkynols can undergo cyclotrimerization reactions on $(\eta^6\text{-arene})\text{Ru}$ templates. These reactions are, however, rather unselective and no pure products could be isolated from the reaction mixtures. This makes all the investigated arene ruthenium complexes inferior to the established $[\text{NiX}_2(\text{PR}_3)_2]$ systems.

The isolation of a dicationic mixed bis(arene) ruthenium complex during our previous investigations led us to ask whether such complexes are directly involved in the catalytic cycle. Complexes of this type are logical intermediates in alkyne cyclotrimerization. Replacement of one of the arene ligands by free molecules of the respective alkyne would release the free trisubstituted arene and start another reaction cycle. In this case, isolated bis-arene sandwich complex should themselves be catalytically active. On the other hand it is also possible that the actual catalysts still has one or more chloride ligands attached such that the bis arene complexes simply represent a “dead end” and catalyst decomposition. In that case, no catalytic activity of bis arene sandwich complexes is to be expected. In order to answer this point, we prepared some symmetrically and unsymmetrically substituted arene complexes $[(\eta^6\text{-arene})_2\text{Ru}]^{2+} (\text{Cl})_2$ and $[(\eta^6\text{-arene})(\eta^6\text{-arene}^1)\text{Ru}]^{2+} (\text{Cl})_2$ applying *Rybinskaya's* method^{162, 164 165} and investigated

4. Coupling of alkynols on {Arene-Ru} platforms

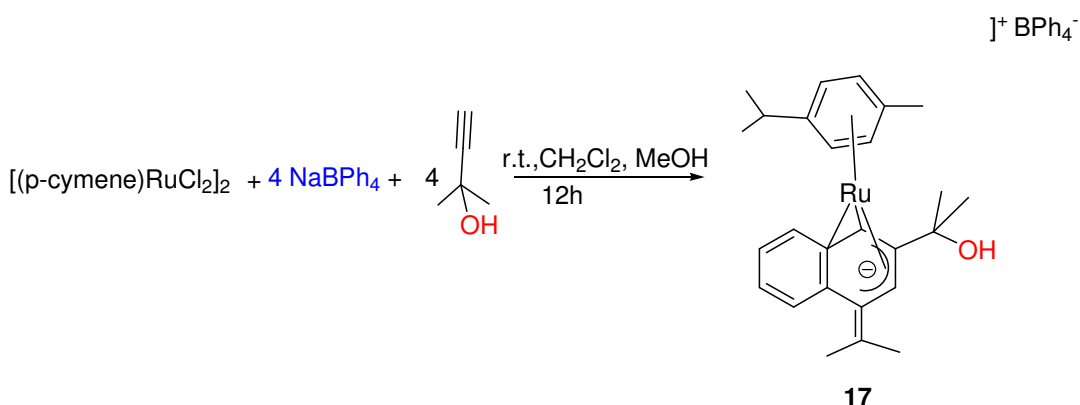
their reactivity against 2-methyl-but-3-yn-2-ol. All these derivatives including substitutionally rather labile did not react with the excess 2-methyl-but-3-yn-2-ol. The results showed that such bis (arene) complexes are not performing as catalysts in cyclotrimerization reactions of alkynols.

4.4 Cocyclization of 2-methylbut-3-yn-1-ol and of a phenylate group from tetraphenylborate

Based on our previous results that $\{(arene)Ru\}^{2+}$ fragments are probably capable of cyclotrimerizing alkynols just like their $\{CpRu\}^+$ counterparts, we decided to examine reactions of the $\{(\eta^6\text{-p-cymene})RuCl_2\}_2$ (**1**) dimer with alkynols in the presence of different halogen abstracting agents such as $NaSbF_6$, $AgBF_4$, AgO_3SCF_3 or $TIPF_6$. *Dixneuf et al.* have recently reported that $[Cp^*RuCl(COD)]$ promotes the head to head coupling of two terminal alkynols in the presence of carboxylic acids transforming them into alkyldiene cyclobutenes.⁹⁷ Linear tail-to-tail dimerization of alkynols gave hydroxy substituted butadienones.⁹⁶

Treatment of **1** with $NaSbF_6$ and excess 2-methyl-but-3-yn-2-ol gave only the known trichloro bridged dimer $\{[(\eta^6\text{-p-cymene})Ru]_2(\mu\text{-Cl})_3\}^+ SbF_6^-$ (**8**) which was characterized by NMR spectroscopy. When other halide abstracting agents were employed, intractable product mixtures were obtained. In the presence of tetraphenylborate, however, a single clean product **17** was formed as was indicated by NMR spectroscopy. The NMR spectra of **17** showed fundamentally different characteristics than expected for **16** or any of the dimeric complexes encountered in the other reactions of $\{(\eta^6\text{-p-cymene})RuCl_2\}_2$.

Much more unexpected was the discovery, that the same dimeric ruthenium complex, in the presence of stoichiometric quantities of tetraphenylborate, effects the co-cyclization of two molecules of disubstituted alkynols and of a phenylate group to a 1-methylene-1,2-dihydronaphthalenide ligand. The corresponding complex has been identified by extensive 1D- and 2D NMR spectroscopic investigations such as H, C, HSQC, HMBC and NOE experiments. The 1-methylene-1,2-dihydronaphthalenide ligand has no precedence in the literature and represents a wholly novel architecture. The annellated phenyl ring in the backbone of this ligand originates from the tetraphenylborate anion. The reaction scheme is presented in Scheme 31.



Scheme 31: Synthesis of the ruthenium dihydronaphthalenide complex **17**.

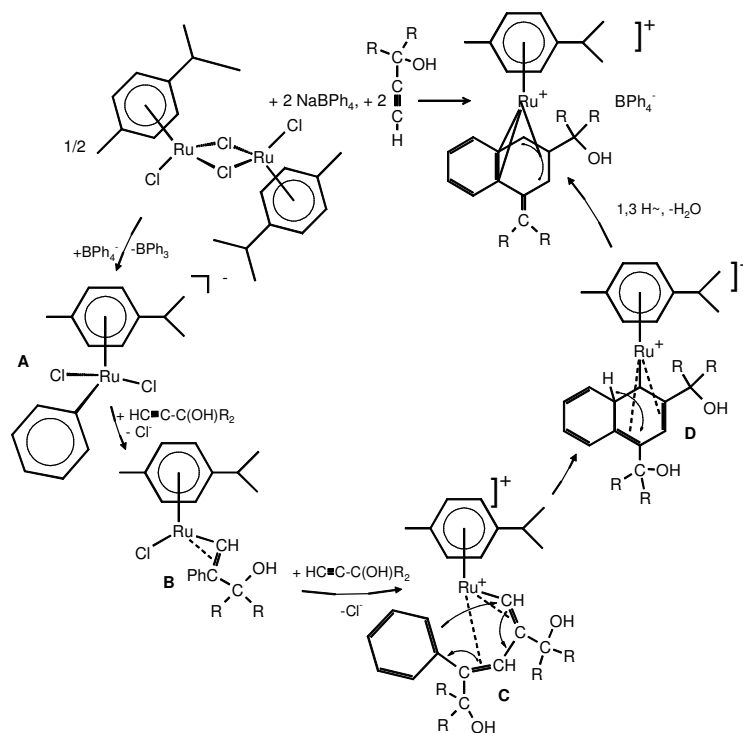
Since all our attempts to grow X-ray quality crystals of this product have failed up to now, its identification rests on the results from NMR spectroscopy (1D and 2D NMR), IR, mass spectrometry and analytical data. The ¹H- and ¹³C-NMR spectra display the resonances of an intact BPh₄⁻ counterion and a π-conjugated cymene ligand that are present in a 1:1 ratio. The ¹H-NMR spectrum of complex **17** is depicted in Figure 26. The appearance of four distinguishable sets of π-coordinated CH-units and anisochronic methyl groups for the *i*-propyl substituent of the cymene unit indicate that the plane of symmetry through this ligand has been lost. The observation of four additional methyl signals suggests that two equivalents of the propargylic alcohol have been incorporated into the product. The single OH proton signal (δ = 1.78) in the ¹H-NMR and strong bands at 3545 cm⁻¹ and 1175 cm⁻¹ arising from the OH and out-of-phase C-C-O stretches in the IR spectrum are characteristic of a tertiary alcohol. The presence of just one OH group in the product suggests that one equivalent of water was lost during the reaction. The remaining ¹H- and ¹³C- resonances comprise the signals of four quaternary carbon atoms and two more olefinic CH-units that resonate at rather high field. These are attributable to ruthenium coordinated =CH moieties. Four additional =CH-signals are partially overlapped by the resonances of the counterion and are characteristic of non-coordinated arenes.

4. Coupling of alkynols on {Arene-Ru} platforms

further one-bond and long-range correlations in H,C HSQC and HMBC spectra suggests that the terminal carbon atom of the isobutylidene unit, two π -coordinated CH carbon units ($\delta(^{13}\text{C}) = 48.5, 77.4$), and the three remaining quaternary carbon atoms form a six membered ring. The carbon atom resonating at $\delta = 113.8$ ppm is substituted by the CMe_2OH group while the two remaining ones ($\delta(^{13}\text{C}) = 81.7, 101.4$) and the four residual $=\text{CH}$ -units comprise a second six-membered ring that is annellated with the first one to give a naphthalene skeleton (see Figure 27). The positions and the spatial arrangement of the exocyclic propylidene and CMe_2OH moieties were substantiated by the detection of NOE correlations between the CH proton at 4.70 ppm and the methyl protons at 1.57 ppm, the CH proton at 6.70 ppm and the CH_3 protons at 1.44 and 1.77 ppm, and between one of the aromatic protons at 7.48 ppm and the proton of the second propylidene CH_3 group at 1.66 ppm. The observation of characteristic upfield shifts for five of the six atoms in the disubstituted ring suggests that the naphthalene framework is bonded in an η^5 -coordination mode and, since all carbon atoms in the fused ring system and the exocyclic methylene unit are three-coordinated, carries a negative charge. The whole complex cation may thus be described in terms of a Ru(II) atom that is coordinated by a neutral η^6 -bonded cymene and a uninegative benzanellated 1-methylene-1,2-dihydrocyclohexadienide ligand which behaves essentially as a pentadienyl equivalent. Positive ion EI (70 eV) and CI MS spectra (NH_3 reactand gas) gave the mole peak at m/z 462.1 in 88% intensity with the correct isotope pattern. The base peak at m/z 444.1 results from the loss of water from the CMe_2OH entity.

As to the formation of the dihydronaphthalenide ligand we suggest the reaction sequence outlined in Scheme 32. In the first step NaBPh_4 acts as a phenylating agent toward the *p*-cymene ruthenium dimer, giving $[(\eta^6\text{-}p\text{-cymene})\text{RuCl}_2(\text{Ph})]^-$, **A**. Substitution of one chloride by one equivalent of the propargylic alcohol would then render $[(\eta^6\text{-}p\text{-cymene})\text{RuCl}(\text{Ph})(\eta^2\text{-HCCMe}_2\text{OH})]$. Migratory insertion of the phenylate ligand into the Ru-alkyne bond, possibly via the corresponding vinylidene $[(\eta^6\text{-}p\text{-cymene})\text{Cl}(\text{Ph})\text{Ru}=\text{C}=\text{CHCMe}_2\text{OH}]$, would give the coordinatively unsaturated vinyl intermediate **B**. Chloride loss, coordination of one further equivalent of the alkynol followed by another insertion step would result in the 4-phenylpentadienyl intermediate **C**. Electrocyclic ring closure would then generate intermediate **D** which transforms into the final product via 1,3 hydrogen shift with concomitant aromatization followed by dehydration.

4. Coupling of alkynols on {Arene-Ru} platforms



Scheme 32: Proposed reaction sequence in the formation of complex **17**.

4.5 Mechanistic aspects and investigation of the proposed mechanism by DFT calculations

While all intermediates along the proposed reaction path are speculative, as we were not able to isolate any intermediates, we performed DFT calculations using Gaussian98 on the of conversion of **1** and propargylic alcohol to the product **17**. Using Density Functional Theory (DFT) treatment, the geometries of the proposed reaction intermediates have been optimized and their electronic structures and energies have been evaluated.

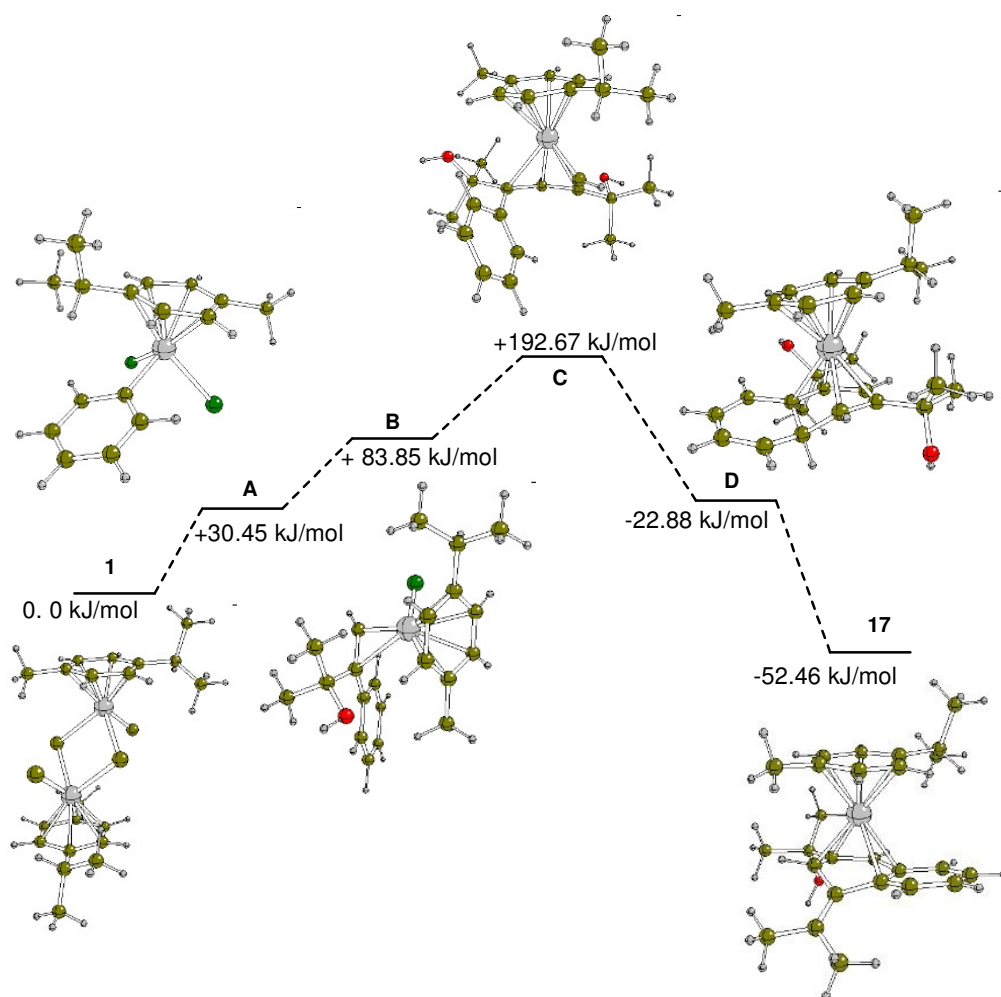


Figure 28: Energy profile for the reaction of $[(\eta^6\text{-p-cymene})\text{RuCl}_2]_2$ (**1**) to give complex **17** (in kJ/mol, relative to **1**).

The energy data and energy differences have been calculated for the gas phase at absolute temperature. It is expected that charged particles are stabilized in a polar solvent with respect to neutral ones. Therefore, it is assumed that the formation of the ionic intermediate **C** (step 3 of the reaction) is more favorable in polar solvents due to the stabilization of the ions by the solvent.

In the initial step a phenylate ligand is added and the chloro bridges are split, leading to intermediate **A**. Intermediate **A** is 30.45 kJ/mol higher in energy than a half unit of the starting dimer. In line with analogous reactions reported recently, complex **A** probably undergoes a migratory insertion of one equivalent of the alkynol into the Ru-phenyl bond to give intermediate **B**. The formation of **B** is still an endothermic process, requiring further 53.40 kJ/mol. Along these lines, **B** is able to accommodate another molecule of alkynol in step by chloride displacement and to undergo another insertion step to afford **C**.

4. Coupling of alkynols on {Arene-Ru} platforms

Intermediate **C** is another 108.78 kJ/mol higher in energy. It should be noted however that these energy differences may be lower in polar solvents. There is evidence that solvation of the ions significantly decreases energy barriers in comparison to gas phase calculations.¹⁶⁶ The reactivity of **C** is guided by the availability of the electrocyclic ring closure to generate intermediate **D**. This reaction is energetically highly favorable releasing 215.48 kJ/mol. The final step is the transformation into the product **E** via 1,3 hydrogen shift and dehydration resulting in the aromatic ring of product **E**. The overall reaction starting from the (η^6 -p-cymene)Ru dimer **1** to **E** is moderately exothermic by -52.46 kJ/mol.

In conclusion, we have shown that the overall reaction is thermodynamically feasible and that all postulated intermediates **A** to **E** are local minima on the energy hypersurface. Still, alternative pathways involving different intermediates can not be ruled out at this point.

4.6 Labeling studies as a mechanistic support to origin of the phenyl ring of the naphthalenide skeleton

As was discussed before, product **17** was not obtained when other chloride abstracting agents were employed. This led us to think that one part of naphthalenide ring must have derived from a phenylate group of the BPh_4^- anion and the other part from two molecules of the propargylic alcohol such that this reaction constitutes a cyclotrimerization of “Ph” and two alkynols with concomitant dehydration.

With the aim to investigate the mechanism of this reaction we tried to synthesize the bis(arene) sandwich complex $[(\eta^6\text{-p-cymene})\text{Ru}(\eta^6\text{-C}_6\text{H}_5\text{BPh}_3)]^+ \text{BPh}_4^-$ as a possible starting compound or another possible intermediate of this reaction by reacting $[(\eta^6\text{-p-cymene})\text{RuCl}_2]_2$ and four equivalents of NaBPh_4 . NMR spectroscopy of the resulting product showed, that it is a mixture of three different organometallic species displaying three sets of two CH doublets each in the region for coordinated p-cymene ligands. One pair of doublets at 5.94 and 5.71 ppm with $^3J = 6.29$ Hz could be assigned to the trichloro-bridged dimer **8** while two doublets at 5.44 and 5.36 ppm belong to the starting complex **1**. The remaining doublets at 5.78 and 5.54 ppm represent a third organometallic compound which we could not identify until now. Three pairs of doublets derived from isopropyl CH_3 methyl groups also indicate the presence of three compounds, each having a molecular mirror plane. There were, however, no further signals that could be assigned to

the CH-protons of a metal coordinated ($\eta^6\text{-C}_6\text{H}_5$)BPh₃⁻ anion.

In order to have an additional spectroscopic handle, we repeated the reaction using four equivalents of NaB(C₆H₄F-4)₄ and recorded non-coupled ¹⁹F-NMR spectra. These showed only one main signal at -119.72 ppm for free B(C₆H₄F-4)₄⁻ and small one at -109.61 ppm. ¹H-NMR investigation again showed the presence of three products: Starting material **1**, the trichloro-bridged dimer **8** and a third component giving rise to a triplet at $\delta = 6.70$ ppm and a multiplet at $\delta = 7.30$ ppm. These signals appear at unusually low field for metal coordinated arene rings but may still correspond to the signals observed at $\delta = 5.78$ ppm and $\delta = 5.44$ ppm in the case of the reaction with B(C₆H₅)₄⁻.

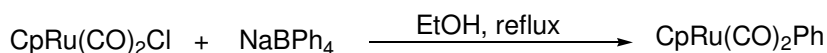
Next we investigated the reaction of the chloro-bridged dimer **1** with four equivalents of NaB(C₆H₄F-4)₄ and 7.5 equivalents of 1,1-dimethyl-prop-2-yn-1-ol. The crude product obtained after the usual work-up was a mixture of several species exhibiting a multitude of CH₃-signals, OH-signals and CH- signals attributable to the cymene ligand. Most notably, there are also signals at similar fields as those for the coordinated CH-units of the alkylidene dihydro naphthalenide rings in **17**. In ¹⁹F-NMR spectra displayed small signals at $\delta = -119.39$, -112.10 , -105.17 ppm in addition to those of the B(C₆H₄F-4)₄⁻ anion that could possibly originate from regioisomers of the naphthalenide ring differing in the position of the fluoride or from species with another core structure of the additional ligand. The reaction between **1**, NaB(C₆H₄F-4)₄ and 1,1-dimethyl-prop-2-yn-1-ol thus provided only some hint, but no direct evidence that the phenyl group of the dihydronaphthalenide ligands of **17** originates from the BPh₄⁻ anion.

However, we could still show, that the uncoordinated phenyl ring of the naphthalenide skeleton as well as the hydrogen atom lost in the dehydration step both arise from the BPh₄⁻ anion. Utilizing perdeuterated BPh₄-d₂₀ instead of tetraphenylborate itself results in tetra- and pentadeuterated complexes, where the four hydrogens of the unsubstituted benzene and of the dihydronaphthalenide ligand and, in part, the OH proton of the CMe₂OH side chain have been replaced by deuterium (Scheme 34). The partial H/D exchange of the OH proton points to the fact, that the fifth deuterium label has been released in the form of water, HOD, and then undergone H/D exchange with the free OH group of the complex. All these findings are accommodated by the proposed reaction scheme (Scheme 34). All of the CH resonance signals of the non coordinated part of the naphthalenide ring appeared as non-binomial quartets in ¹³C-NMR spectroscopy by coupling to a D atom and none of the corresponding proton resonance signals could be

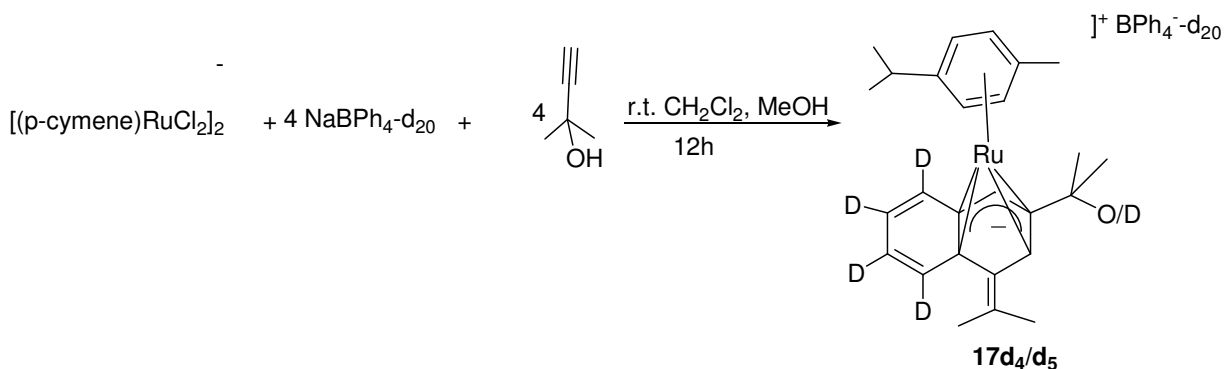
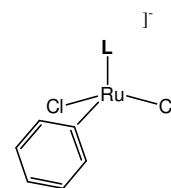
4. Coupling of alkynols on {Arene-Ru} platforms

observed (see Figure 29). Likewise, the OH signal at 1.78 ppm and the IR OH band at 3545 cm^{-1} were considerably weakened, and the latter is partially replaced by a sharp intense band at 2242 cm^{-1} . This again points to partial H/D exchange with the water liberated as DOH in the dehydration process. In the EI MS the mole peak shifts by five mass units, attesting to the incorporation of up to five D atoms. The BPh_3 released in this reaction is further converted to triphenylboroxine by reaction with methanol and water as is indicated by NMR and MS data.

We note that action of the BPh_4^- anion as a phenylating agent, although rare, is not without precedence, especially in ruthenium chemistry. Thus, $[\{\text{CpRu}(\text{CO})_2\}_2(\mu\text{-X})]^+$ ($\text{X} = \text{Cl}, \text{Br}$) reacts with NaBPh_4 to give a mixture of $[\text{CpRu}(\text{CO})_2\text{X}]$ and $[\text{CpRu}(\text{CO})_2(\text{Ph})]$ (Scheme 33).¹⁶⁷ Any of the other reaction steps in Scheme 32 are elementary processes in many transition metal catalyzed or mediated conversions of alkynes. We also note the high regioselectivity observed in each of the addition/insertion steps. In fact, we have not been able to detect any other regioisomer of **17** in the crude product by NMR spectroscopy.



Scheme 33: Evidence that NaBPh_4 behaves as a phenylating agent.



Scheme 34: Synthesis of complex **17d₄/d₅**.

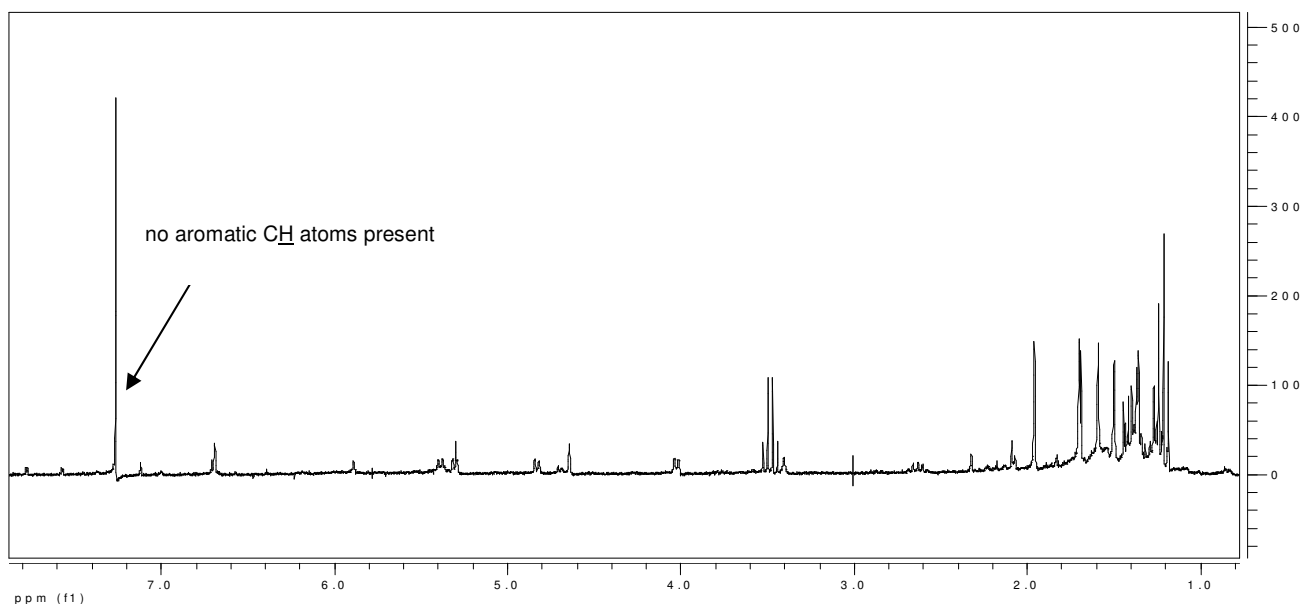
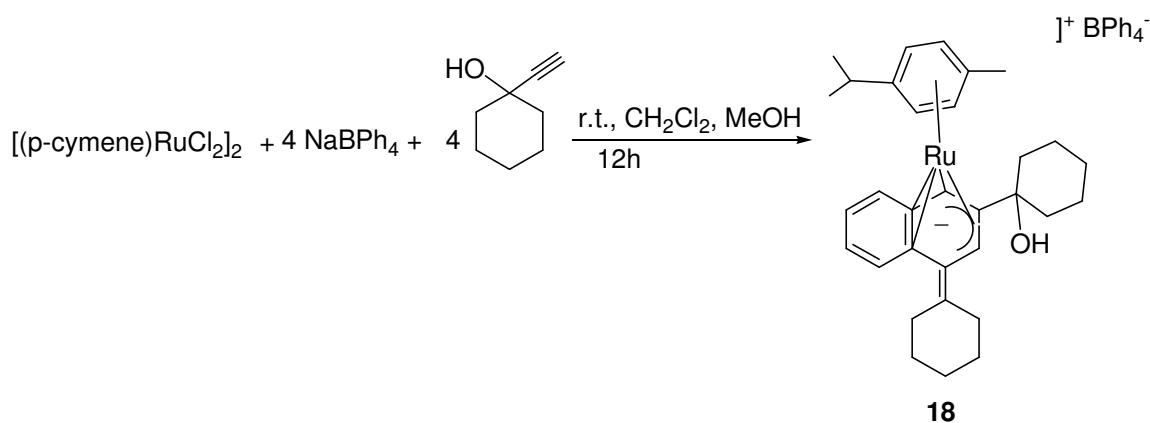


Figure 29: $^1\text{H-NMR}$ spectra of complex **17d₄/d₅** showing absence of aromatic protons.

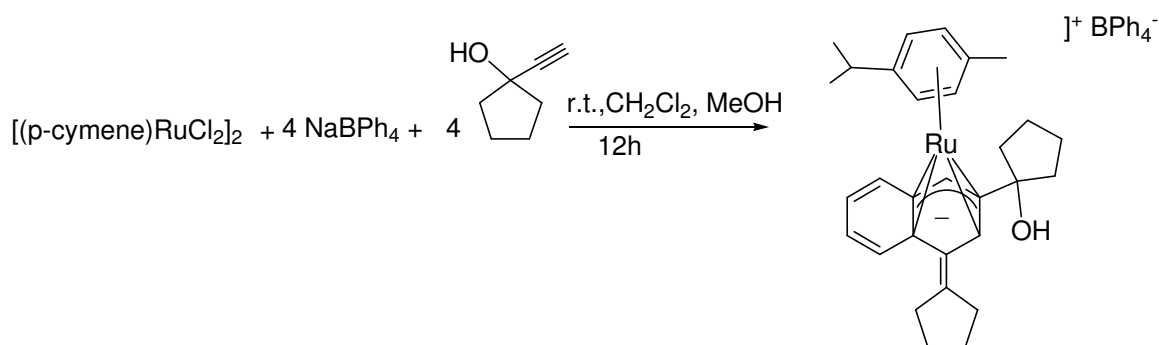
4.7 Cocyclization reactions involving different propargylic alcohols

In order to widen the scope of this reaction, we also examined the conversion of other alkynols. Products containing ligands with the same dihydronaphthalenide skeleton were obtained with 1-ethynylcyclohexanol and 1-ethynylcyclopentanol, giving complexes **18**, **19**.



Scheme 35: Synthesis of complex **18**.

4. Coupling of alkynols on {Arene-Ru} platforms



Scheme 36: Synthesis of complex **19**.

2-Phenylbutynol and 1,1-diphenylprop-2-yn-1-ol, on the other hand, gave complex mixtures from which no clean products could be obtained or identified. ¹Butylacetylene also failed to react. The related dimer $[(\eta^6\text{-C}_6\text{Me}_6)\text{RuCl}_2]_2$ gave only small amounts of a complex corresponding to **17** when treated with NaBPh_4 and 2-methylbut-3-yn-2-ol either at room temperature or under reflux conditions. This may be related to a higher energy barrier for phenylate addition to a more electron rich $[(\eta^6\text{-arene})\text{RuCl}_2]_2$ dimer.

Complexes $[(\eta^6\text{-C}_6\text{H}_5(\text{CH}_2)_3\text{OH})\text{RuCl}_2]_2$ **13** and $[(\eta^6\text{-C}_6\text{H}_5(\text{CH}_2)_3\text{OMe})\text{RuCl}_2]_2$ **14** when treated with 2-methyl-3-yn-1-ol in the presence of NaBPh_4 gave the dicationic complex **20** and **21** where the newly formed isocycle coordinates as a neutral naphthalene ligand. The assignment of the ¹H- and ¹³C-NMR signals for complex **21** were derived from 1D and 2D NMR techniques are shown in Figure 30. The quaternary carbon atom bearing the 2-hydroxy-2-propyl substituent could not be identified.

The functionalized naphthalene ring of **20** and **21** closely relates to the dihydronaphthalenide ligand of **17-19**; it is the protonated form of its isomer where the CMe₂OH and the exocyclic methylene group have been interchanged. Such a process may be triggered by a shift of the proton from an intermediate immediately preceding dehydration to the other substituted carbon atom of the carbocyclic ring, subsequent dehydration of the other hydroxypropyl substituent and final protonation (see Scheme 39)

Although it is not directly evident from the ¹H-NMR shifts, naphthalene is still coordinated to the metal center as it is shown by the combustion analysis for complex **20** (calculated C 75.27, H 6.66%; found C 72.00, H 6.66%) and **21** (calculated C 66.65, H 6.15%; found C 66.00, H 6.52%). ¹H-NMR shifts of coordinated naphthalene ligands that resemble those of free naphthalenes are, however, not wholly unexpected as the example of

4. Coupling of alkynols on {Arene-Ru} platforms

$[\eta^6\text{-}(\text{C}_6\text{H}_3\text{Me}_3\text{-1,3,5})(\text{C}_{10}\text{H}_8)\text{Ru}]^{2+}$ shows. Here, the coordinated naphthalene ligands shows ^1H -NMR resonances ranging from 7.0 to 8.15 ppm.¹⁶⁴ More evidence that the naphthalene ligand is retained in complex **20** and **21** comes from their electrochemical characterization as it is discussed in the following section.

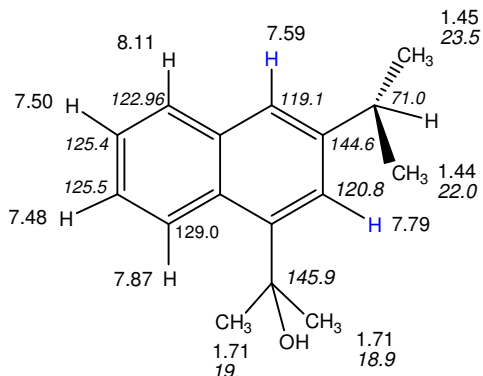
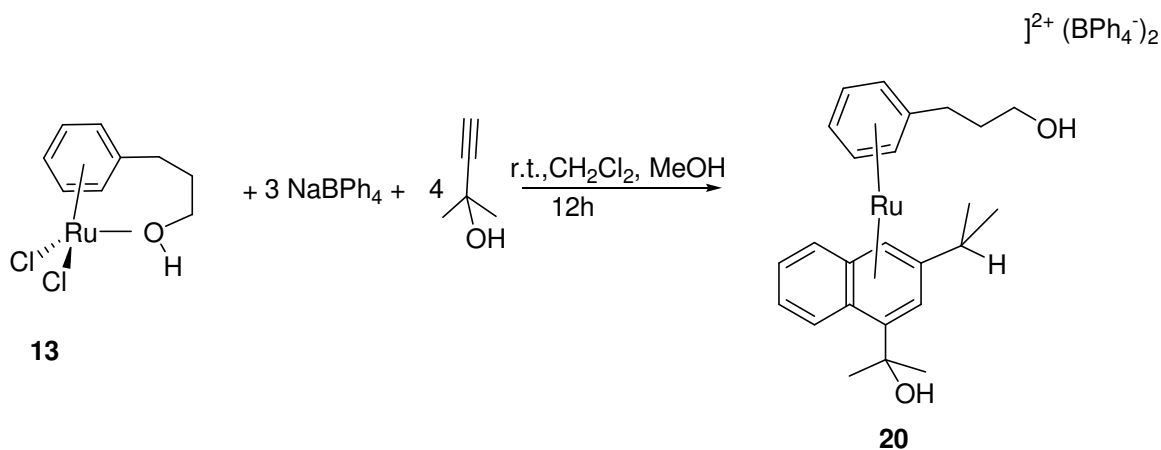
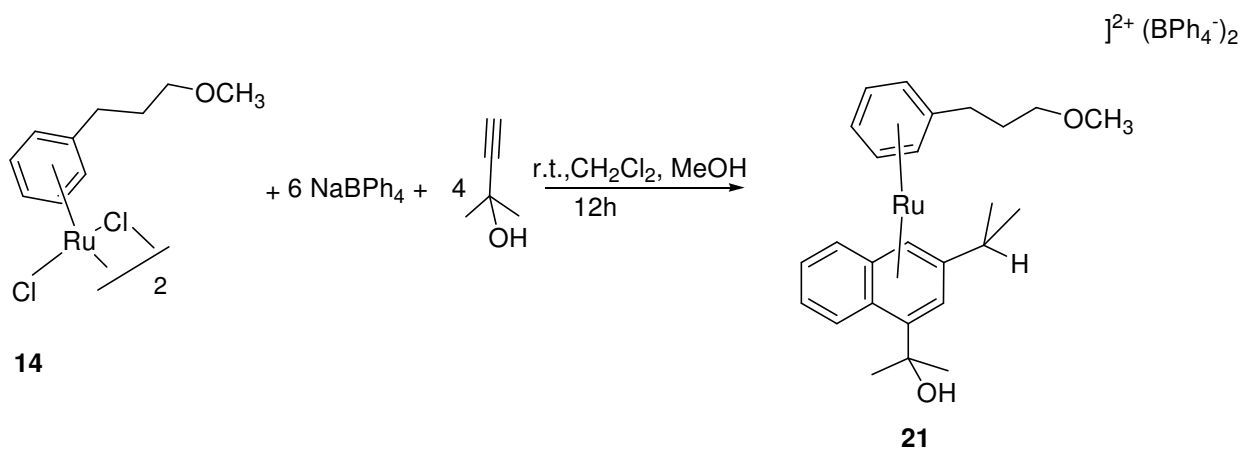


Figure 30: ^1H and ^{13}C shifts (in italics) of the naphthalene ligand of **21**.

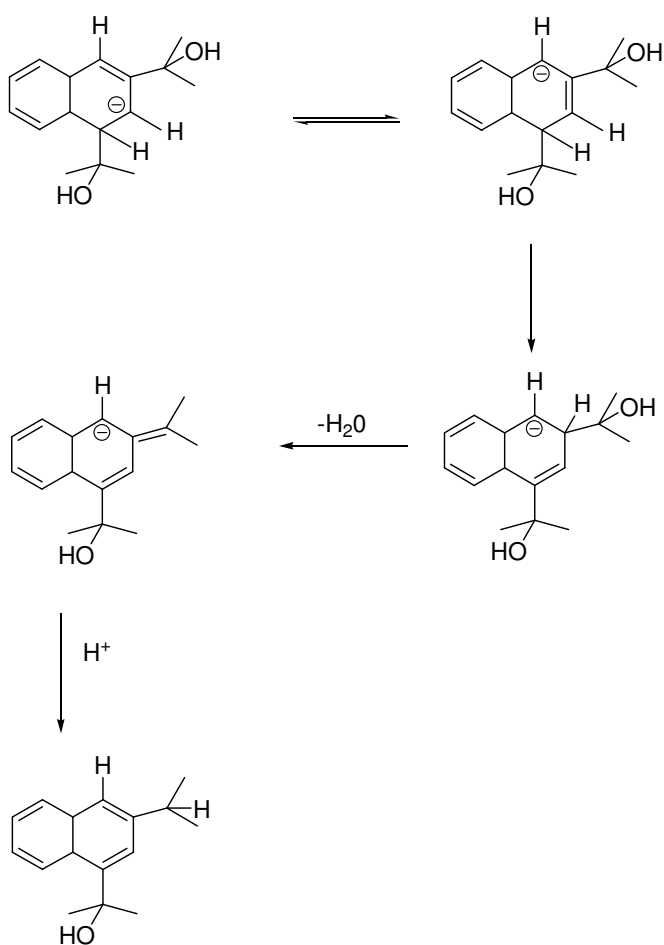


Scheme 37: Synthesis of complex **20**.

4. Coupling of alkynols on {Arene-Ru} platforms



Scheme 38: Synthesis of complex **21**.



Scheme 39: Proposed mechanism for the formation of the naphthalene ligand.

4.8 Electrochemical investigations on the dihydronaphthalenide complexes

Electrochemical investigations of dihydronaphthalenide complexes showed these are chemically irreversibly oxidized and reduced. Both processes are followed by fast chemical processes. Within the voltammetric time scale, we could observe two electroactive products which, on the other hand, could be reversibly oxidized or reduced. In Figure 31, the waves denoted as C/D and E/F are both formed either after scanning in anodic direction first or after scanning towards negative potentials first.

Voltammograms at room temperature of **17** (see Figure 31) show a irreversible oxidation at $E_p = -0.453$ V which is far less positive potential as that of the neutral dichloro bridged dimer $[(\eta^6\text{-p-cymene})\text{RuCl}_2]_2$ ($E_p = +1.04$ V). The oxidation remains completely irreversible, even when the sweep rate was increased up to 10 V/s or upon cooling to -78° C. Furthermore, the peak height and half width, when compared to that of the irreversible reduction, suggests a multi electron process. The chemical process following anodic oxidation at peak A gives rise to two new species which are reduced (and oxidized) in peaks C/D and E/F. The half-wave potentials for both processes are -0.59 V (C/D) and -0.72 V (E/F). Peak potential separations and half-width comparable to that of the ferrocene/ferrocenium standard argue for one-electron processes, each. Interestingly, the same couple C/D and E/F also arise from the irreversible cathodic reduction, peak B as it is shown in Figure 35. Both couples are not present in the solution unless the potential is scanned past peaks A or B. In Figure 32-34 can be seen that peaks C/D and E/F are not present in the solution, only after formation of peak A or peak B. The identity of the species underlying these couples and the fate of the oxidized/reduced forms of parent **17** still is an open issue.

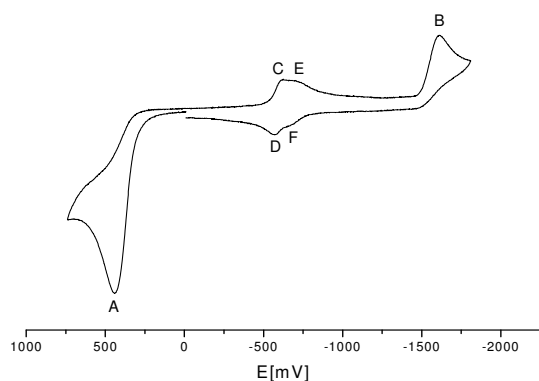


Figure 31: Cyclic voltammogram of complex **17** in $\text{CH}_2\text{Cl}_2/\text{NBu}_4\text{PF}_6$ at $v = 0.1$ V/s at

4. Coupling of alkynols on {Arene-Ru} platforms

298K (oxidation scanned first).

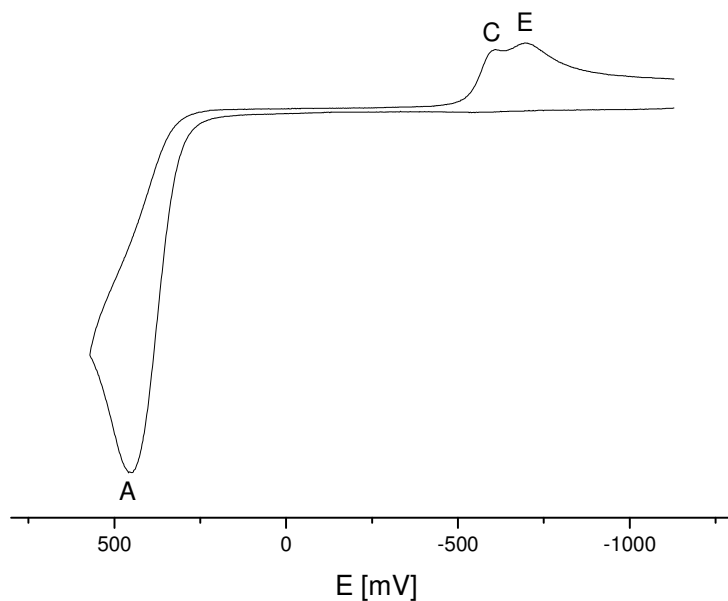


Figure 32: Anodic scan of **17** was initiated negative of couples E/F resulting in no appearance of peak D and F. ($\text{CH}_2\text{Cl}_2/\text{NBu}_4\text{PF}_6$ at $v = 0.1$ V/s at 298 K (oxidation scanned first)).

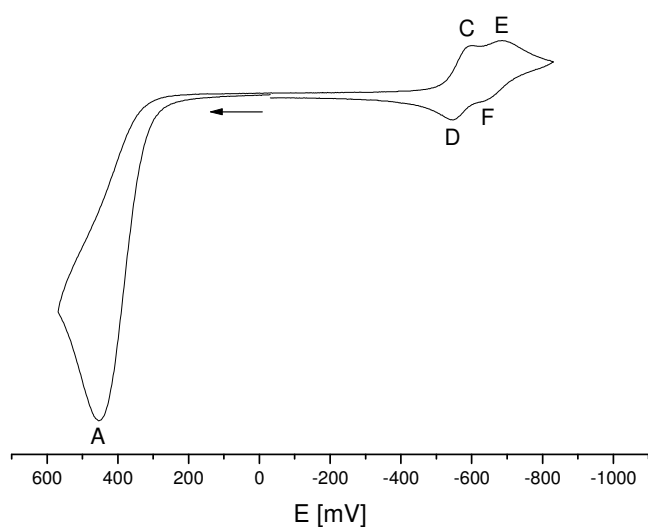


Figure 33: Anodic scan of **17** was clipped on the reverse scan after going through peaks E/F and only anodic scan is shown. ($\text{CH}_2\text{Cl}_2/\text{NBu}_4\text{PF}_6$ at $v = 0.1$ V/s at 298 K (reduction scanned first)).

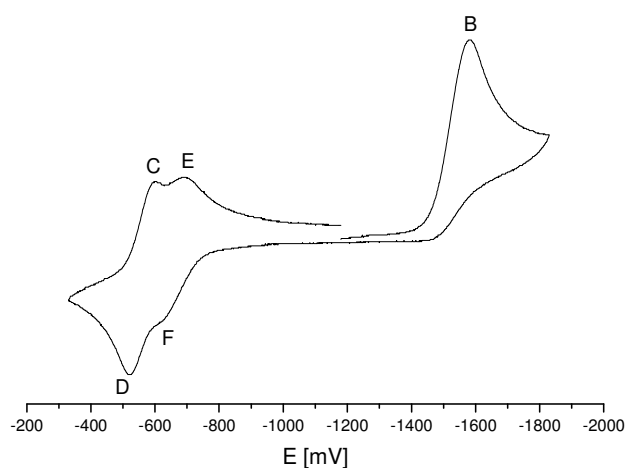


Figure 34: Cathodic scan of **17** was clipped on the reverse scan after going through peaks D/C and only cathodic scan is shown. ($\text{CH}_2\text{Cl}_2/\text{NBu}_4\text{PF}_6$ at $v = 0.1 \text{ V/s}$ at 298 K (reduction scanned first)).

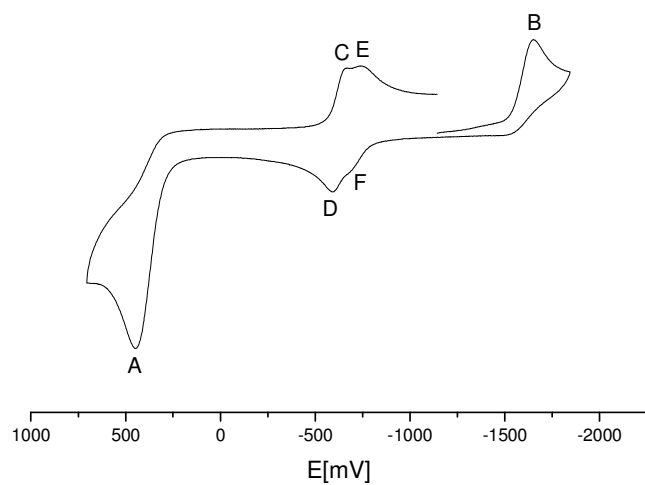


Figure 35: Cyclic voltammogram of complex **17** in $\text{CH}_2\text{Cl}_2/\text{NBu}_4\text{PF}_6$ at $v = 0.1 \text{ V/s}$ at 298 K (reduction scanned first).

4. Coupling of alkynols on {Arene-Ru} platforms

In contrast, compound **18** results into only one pair of peaks C/D at $E_{1/2} = -0.67$ V which is by about 80 mV higher than C/D in **17**. Reversible C/D peaks are formed independently of the direction of the first scan, suggesting chemical stability of the electroactive species formed. Oxidation potential $E_p = 0.517$ (not shown in Figure) and of the cathodic peak B ($E_p = -1.70$ V) are shifted by approximately the same value of approximately 70 mV when compared to **17**. The potential of the irreversible oxidation ($E_p = 0.517$ V, not shown in Figure). Compound **19** proved to be not sufficiently stable to allow for electrochemical measurements.

We also performed electrochemical investigations on the systems with substituted arenes, even though extensive 2D NMR studies suggest mixture of free ligands and no organometallic species which is rather different to naphthalenide skeleton compounds **17** and **18**. Conclusions drawn from NMR studies about dissociation of the free naphthalene ligand and free arene in the solution are in slight contradictory to observations evident from electrochemical studies. As it is shown in Figure 36, complex **20** assumes the same electrochemical behaviour as compounds **17** and **18**. Pair of peaks C/D at $E_{1/2} = -0.73$ V are formed upon both irreversible oxidation ($E_p = +0.4$ V) and irreversible reduction ($E_p = 1.93$ V).

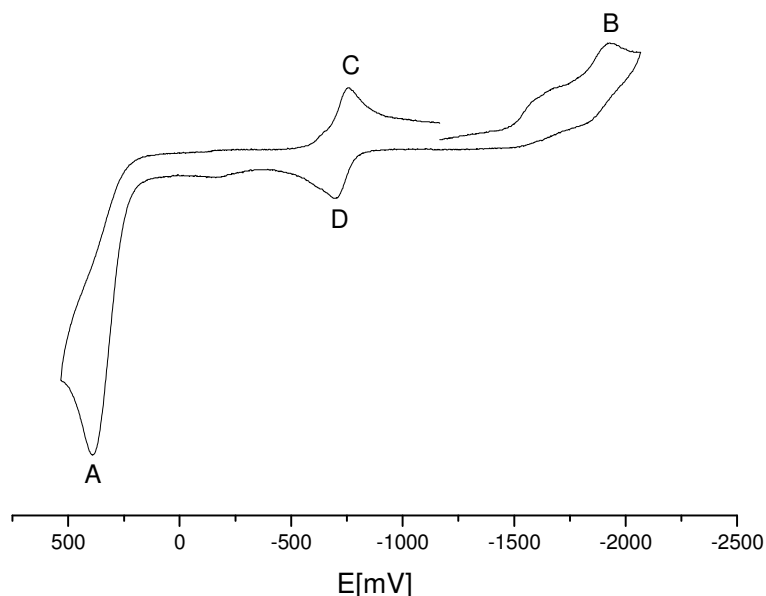


Figure 36: Cyclic voltammogram of complex **20** in $\text{CH}_2\text{Cl}_2/\text{NBu}_4\text{PF}_6$ at $v = 0.1$ V/s at 298 K (reduction scanned first).

5 Experimental Part

5.1 General methods and procedures

All synthetic operations were performed under an argon atmosphere using standard Schlenk techniques.

5.1.1 Solvents

All solvents were distilled under argon by using conventional methods, over appropriate drying agents (tetrahydrofuran over potassium, dichloromethane, dichloroethane and ethanol over calcium hydride, methanol over calcium oxide, and acetone over CaCl_2). Distilled solvents were stored in Schlenk glassware with activated molecular sieves (4Å).

Solvents for spectroscopic investigations were of the highest possible purity (dichloromethane from Fluka, Burdick&Jackson grade "high purity solvent", < 0.005% H_2O).

For electrochemical investigations highly pure solvents mentioned above were distilled twice, and saturated with argon.

5.1.2 Commercially available starting compounds were purchased in the specifications given from the following suppliers:

1-Bromo-3-phenylpropane (98% Aldrich), 4-(3-Phenylpropyl)pyridine (98%, Lancaster), Methyl iodide (98%, Aldrich), Dimethylsulfide (>99%, Merck-Schuchardt), 2-Benzylaminopyridine (98% Lancaster), 1,1-Diphenyl-2-propyl-1-ol (purum > 98%, Fluka), 3-Phenyl-1-butyne-3-ol (98%, Aldrich), 1,1-Dimethylprop-2-yn-1-ol (98%, Aldrich), Propargylic alcohol (98%, Aldrich).

Sodium hexafluoroantimonate (V) (Alfa Aesar), Silver hexafluoroantimonate (V) (98%, Aldrich), Sodium tetraphenylborate (99.5%, A.C.S. Aldrich) 1-Ethynylcyclopentanol, (98%, Lancaster), 1-Ethynylcyclohexanol, (99%, Lancaster), 2,6-Diphenylpyridine, (97%, Lancaster), 2,4,6-Collidine, (99% Lancaster), 2,6-Di-tert-butyl-4-methylpyridine (97%, Lancaster)

1-Hexyne (> 98%, Merck-Schuchardt), 3,3-Dimethyl-1-butyne (98%, Lancaster),

5. Experimental part

Isopropyl thiol (98%, Lancaster), 1-Thio-3-phenylethane (97%, Lancaster), 4-Methylpyridine (99%, Lancaster), tricyclohexylphosphine (97%, Alfa Aesar), AgOTf (98 %, Aldrich), Na(BPh₄F-4)₄ (99%, Aldrich), RuCl₃ (Ru content 42.41%, Johnsson Matthey), triisopropylphosphine, (Strem), tricyclohexylphosphine, (Strem), tris(hydroxymethyl)phosphine (Strem).

5.2 Analytical and spectroscopic instruments

5.2.1 NMR-spectroscopy

NMR spectra were recorded on either a Bruker AC 250 or a Bruker AS 200 series spectrometer, at 293 K, in the indicated solvent. Resonance shifts were referenced to residual, partially protonated solvent (¹H), the solvent signal itself (¹³C) or external H₃PO₄ (³¹P) and (¹⁹F). 2D NMR spectra were recorded on Bruker AMX 400 NMR spectrometer.

5.2.2 IR-spectroscopy

IR spectra were recorded on a Perkin Elmer FTIR Paragon 1000 PC instrument. For spectra in solution, a cell equipped with CaF₂ windows was used. For solid compounds spectra were recorded as KBr pellets.

5.2.3 CHN analysis

The CHN analyses were performed on a Perkin Elmer Analyzer 240 at in house facilities.

5.2.4 Biological activity assessment

The human estrogen receptor negative MDA-MB-231 (HTB 26) breast cancer cells were obtained from the American Type Culture Collection (ATCC), Rockville, USA. Cell banking and quality control were performed according to the "seed stock concept". Cells were cultured in McCoy's 5A medium (SIGMA, Munich, Germany) containing L-glutamine, 2.2 g/l NaHCO₃ and 5 % fetal calf serum (BIOCHROM, Berlin, Germany). Cells were maintained in a water saturated atmosphere (95 % air / 5 % carbon dioxide) at 37°C in

75-cm² culture flasks (NUNC, Wiesbaden, Germany), and were serially passaged following trypsinization using 0.05% trypsin/0.02% EDTA (ROCHE DIAGNOSTICS, Mannheim, Germany). Mycoplasma contamination was routinely monitored, and only Mycoplasma free cultures were used.

The chemosensitivity assay was performed as described previously¹⁴⁵. In brief, tumor cell suspensions (100 μ l/well) were seeded into 96-well flat bottomed microtitration plates (GREINER, Frickenhausen, Germany) at a density of ca. 15 cells/microscopic field (magnification 320x). After 2-3 days the culture medium was removed by suction and replaced by fresh medium (200 μ l/well) containing varying drug concentrations or vehicle (DMF or DMSO). Drugs were added as 1000-fold concentrated feed solutions. On every plate 16 wells served as controls and 16 wells were used per drug concentration. After various times of incubation the cells were fixed with glutardialdehyde (Merck, Darmstadt, Germany) and stored in a refrigerator. At the end of the experiment all plates were processed simultaneously (staining with 0.02 % aqueous crystal violet (SERVA, Heidelberg, Germany) solution (100 μ l/well)). Excess dye was removed by rinsing the trays with water for 20 min. The stain bound by the cells was redissolved in 70 % ethanol (180 μ l/well) while shaking the microplates for about 3 hours. Absorbance (proportional to cell mass) was measured at 578 nm using a BIOTEK 309 Autoreader (TECNOMARA, Fernwald, Germany).

5.2.5 X-ray analysis

X-ray-quality crystals were obtained as described in the Experimental Section. Crystals were removed from Schlenk tubes and immediately covered with a layer of viscous hydrocarbon oil (Paratone N, Exxon). A suitable crystal was selected, attached to a glass fiber. All data were collected at 293 K or 173 K using either a Bruker-Nonius Kappa CCD) or a rebuilt Syntex P2₁/Siemens P3 diffractometer. Calculations were carried out with the SHELXTL PC 5.03¹⁴¹ and SHELXL-97¹⁶⁸ program system installed on a local PC. The structures were solved by direct methods and refined on F_o^2 by full-matrix least-squares refinement. An absorption correction was applied by using semiempirical ψ -scans or by a numerical absorption correction.¹⁶⁹

The structure refinement was done by full matrix least squares refinement method. Formulas below applies for every crystal structure.

5. Experimental part

$$a) F_0 \geq 4\sigma$$

$$b) R_1 = \sum \|F_0 - F_c\| / \sum \|F_0\|$$

$$c) wR_2 = \left\{ \sum w(F_0^2 - F_c^2)^2 / \sum w(F_0^2)^2 \right\}^{1/2}$$

$$d) GooF = \left\{ \sum w(F_0^2 - F_c^2)^2 / (n - p) \right\}^{1/2} : n = \text{Reflection number}; p = \text{Parameter number}$$

5.2.6 Cyclic voltammetry

Electrochemistry was performed in a home-built cylindrical vacuum tight one compartment cell. A spiral shaped Pt wire and a Ag wire as the counter and reference electrodes are sealed into opposite sides of the glass wall while the respective working electrode (Pt or glassy carbon 1.1 mm polished with 0.25 μm diamond paste (Buehler-Wirtz) before each experiment) is introduced via a teflon screw cap with a suitable fitting. The cell may be attached to a conventional Schlenk line via two sidearms equipped with teflon screw valves and allows experiments to be performed under an atmosphere of argon with approximately 2.5 ml of analyte solution. CH_2Cl_2 for electrochemical work was obtained from Fluka (Burdick&Jackson Brand) and freshly distilled from CaH_2 before use. NBu_4PF_6 (0.25 mM) was used as the supporting electrolyte. All potentials are referenced versus the ferrocene/ferrocenium couple. Electrochemical data were acquired with a computer controlled EG&G model 273 potentiostat utilizing the EG&G 250 software package.

5.3 Synthesis of the starting materials

5.3.1 Synthesis of $[(\eta^6\text{-p-cymene})\text{RuCl}_2]_2$ (1)

The $[(\eta^6\text{-p-cymene})\text{RuCl}_2]_2$ was prepared according to well established synthetic procedure.¹⁷⁰ A solution of hydrated ruthenium trichloride (approximating $\text{RuCl}_3 \times 3 \text{H}_2\text{O}$, containing 38-39% Ru) (2 g, approx 7.7 mmole) in 100 ml ethanol is treated with 10 ml of α -phellandrene and heated under reflux in a 150 ml round-bottomed flask for 4 hours. The solution is allowed to cool to room temperature, and the red-brown, microcrystalline product is filtered off. Additional product is obtained by evaporating the orange-yellow filtrate under reduced pressure to approximately half-volume and cooling over night to 4 °C. After drying in vacuo the yield is 1.8-2.0 g (78%).

Analysis Calcd for $\text{C}_{20}\text{H}_{28}\text{Cl}_4\text{Ru}_2$: C: 39.2%, H: 4.6% (611.94 g/mol); found: C: 39.4%, H: 4.5%.

5.3.2 Synthesis of $[(\eta^6\text{-C}_6(\text{CH}_3)_6)\text{RuCl}_2]_2$

A mixture of $[(\eta^6\text{-p-cymene})\text{RuCl}_2]_2$ (1.0 g, 1.63 mmol) and hexamethylbenzene (10 g, excess) is heated to 180-185 °C with stirring for 2 hours. The reaction is carried out in stoppered flask in an oil bath. The crystals of hexamethylbenzene which sublime to the upper walls of the flask are periodically scraped down into the melt. $[(\eta^6\text{-p-cymene})\text{RuCl}_2]_2$ and some of the excess of hexamethylbenzene are removed by washing with diethyl ether or hexane, the residual hexamethylbenzene is best removed by sublimation. The solid was washed with chloroform and dichlormethane until the washings are colorless. The compound is crystallized by addition of hexane and evaporation of the orange-red solution. Yield (0.87 g, 80%), Analysis Calcd for $\text{C}_{24}\text{H}_{36}\text{Cl}_4\text{Ru}_2$: C: 43.1%, H: 5.4% (669 g/mol); found: C: 43.3%, H: 5.5%.

5.3.3 Synthesis of $[(\eta^6\text{-p-cymene})(\eta^6\text{-C}_{10}\text{H}_8)\text{RuCl}_2]^{2+}(\text{BF}_4^-)_2$

The synthesis of the dicationic bis(sandwich) complex was performed following the procedure of *Bennett*.¹⁶⁴ 0.1g (0.163 mmol) of $[(\eta^6\text{-p-cymene})\text{RuCl}_2]_2$ was dissolved in

5. Experimental part

2.5 ml of acetone and 0.126 g (0.65 mmol) of AgBF_4 was added and the mixture was stirred vigorously at room temperature for 15 min. The solution was filtered over cannula and the filtrate was treated with excess naphthalene, 0.108 g (0.845 mmol) and 2.5 ml of CF_3COOH . Then the reaction was heated under reflux for 3 h. The brown solution was filtered over cannula and the filtered solution was washed 3 x 2 ml of Et_2O and dried in vacuo to give 0.056 g (0.212 mmol), 65% of the product.

$^1\text{H-NMR}$ (acetone- d_6): δ (ppm) = 1.32 (6H, d, $^3J_{\text{HH}} = 6.95$ Hz, $\text{CH}_3(\text{iPr})$), 2.15 (3H, s, $\text{CH}_3(\text{cym})$), 2.67 (1H, hept, $^3J_{\text{HH}} = 6.95$ Hz, $\text{CH}(\text{iPr})$), 6.75, 6.41 (each 2H, d, $^3J_{\text{HH}} = 5.65$ Hz, $\text{CH}(\text{cym})$), 7.29, 8.13, 8.26, 8.33 (each 2H, m).

5.3.4 Synthesis of $[(\eta^6\text{-C}_6\text{H}_6)\text{RuCl}_2]_2$

Preparation of $[(\eta^6\text{-C}_6\text{H}_6)\text{RuCl}_2]_2$ followed *Bennett* method.⁴⁰ Hydrated RuCl_3 (2 g) in 100 ml of ethanol was heated under reflux with 10 ml of cyclohexadiene (either 1,3- or 1,4-) for 4 hours. The brown precipitate was filtered off, washed with methanol, and dried in vacuo (1.83g, 95%).

5.3.5 Synthesis of $\text{NaB}(\text{C}_6\text{H}_5)_4\text{-d}_{20}$

The preparation of $\text{NaPh}_4\text{-d}_{20}$ was carried out upon modified procedure of *Wittig* and *Raff*.¹⁷¹ To bromobenzene- d_5 (1.9 g, 11.6 mmol) in 10ml of diethylether was added dropwise n-butyllithium (12.1 mmol) in hexanes, and the solution was stirred for 10 min. An ethereal solution of $\text{BF}_3\text{xEt}_2\text{O}$ (0.4 g, 2.8 mmol) was added dropwise and the mixture refluxed for 1 hour. The ether was removed and the residue was dissolved in water (30 ml) and washed with ligroin (2 x 30 ml). The aqueous layer was saturated with solid NaCl and the product isolated by filtration. Recrystallization from acetone/toluene gave 0.34 g (34%) of $\text{NaBPh}_4\text{-d}_{20}$.

Analysis calcd. for $\text{NaC}_{24}\text{D}_{20}\text{B}$ (669 g/mol) C 79.55, D 5.56; found C 79.32, D 5.77%.

5.3.6 Synthesis of 3-phenyl-1-propylmethylether, $\text{C}_6\text{H}_5(\text{CH}_2)_3\text{OCH}_3$

The synthesis of aliphatic ethers is known as Williams-ether synthesis. In a three necked flask with a reflux condenser, 1.3 g Na (0.057 mol) was dissolved in 11.53 ml (0.285 mol)

of MeOH. To the methanolic solution 7.23 ml (0.048 mol) of 3-phenylpropylbromide was added dropwise and the reaction mixture was heated under reflux in argon atmosphere for 6 hours. To the cooled reaction mixture 80 ml H₂O was added and the organic phase was extracted in 50 ml of ether. Collected organic phase was washed 2 x 30 ml of H₂O, dried with CaCl₂ and distilled. The product was obtained as a slightly yellowish oil.

¹H-NMR (CDCl₃): 1.84 (2H, q, ³J_{HH} = 7.45 Hz, CH₂CH₂CH₂), 2.63 (2H, t, ³J_{HH} = 7.42 Hz, PhCH₂), 3.28 (3H, s, OCH₃), 3.32 (2H, t, ³J_{HH} = 6.37 Hz, OCH₂), 7.18 (5H, m, CH(Ph)).

¹³C-NMR (CDCl₃): 29.85 (s, CH₂), 31.00 (s, PhCH₂), 59.20 (s, OCH₃), 71.95 (s, CH₂O), 125.65 (s, *p*-CH), 128.46 (s, *m*-CH), 129.00 (s, *o*-CH), 142.55 (s, C_{quart}).

5.3.7 Synthesis of 3-(1,4-cyclohexadiene)-1-propyl methyl ether

Substituted arenes in this work were reduced to the corresponding cyclohexadienes under Birch conditions. Reactions were carried out under a modified *Fujimoto* procedure.¹⁷² In a 1l three-necked flask, 7 ml (0.044 mol) of Ph(CH₂)₃OCH₃ was added to 16.5 ml (0.283 mol) of absolute ethanol and reaction mixture was cooled to -78 °C using a dry ice/propanol slush bad. Using a long cannula, 400 ml of liquid ammonia were condensed into the reaction mixture over 3 hours. Without removing the cooling bath, small pieces of lithium were added until the blue color persisted. After dropwise addition of 7 ml (0.12 mol) of absolute ethanol, more lithium was added until the color persisted. After the mixture was stirred for 30 min, 10 g of NH₄Cl was added and the ammonia was allowed to evaporate over night. The residue was dissolved in 250 ml of water and extracted inot 3 x 20 ml of CH₂Cl₂. The combined organic layers were washed with a saturated solution of NaCl and then dried with Na₂SO₄. The solvent was removed in vacuo to give 3 g of a yellow oil sufficiently pure to be used without further purification. Yield 44.85% (3 g, 0.0197 mol).

¹H-NMR (CDCl₃): 1.65 (2H, q, ³J_{HH} = 7.45 Hz, CH₂CH₂CH₂), 2.1 (4H, t, ³J_{HH} = 7.1 Hz, CH₂), 2.55 (2H, m, PhCH₂), 3.25 (3H, s, OCH₃), 3.32 (2H, t, ³J_{HH} = 6.56 Hz, OCH₂), 5.35 (1H, bs, CH), 5.65 (2H, m, CH).

¹³C-NMR (CDCl₃): 25.95 (s, *o*-CH₂), 27.85 (s, CH₂), 31.00 (s, PhCH₂), 59.20 (s, OCH₃), 71.95 (s, CH₂O), 124.52 (s, *p*-CH), 127.32 (s, *m*-CH), 140.76 (s, C_{quart}).

5. Experimental part

5.3.8 Synthesis of 3-(1,4-cyclohexadiene)-1-propanol

In a 1l three-necked flask, 9.92 ml (0.073 mol) of $\text{Ph}(\text{CH}_2)_3\text{OH}$ was added to 24.0 ml (0.41 mol) of absolute ethanol and the reaction mixture was cooled to $-78\text{ }^\circ\text{C}$ using a dry ice/propanol slush bad. Using a long cannula, 600 ml of liquid ammonia was condensed into the reaction mixture over 3 hours. Without removing the cooling bath, small pieces of lithium were added until the blue color persisted. After the dropwise addition of 10 ml (0.17 mol) of absolute ethanol, more lithium was added until the color persisted. After the mixture was stirred for 30 min, 16 g of NH_4Cl was added and the ammonia was allowed to evaporate over night. The residue was dissolved in 300 ml of water and extracted into 3 x 30 ml of CH_2Cl_2 . The combined organic layers were washed with a saturated solution of NaCl and then dried with Na_2SO_4 . The solvent was removed in vacuo to give 3.97 g of a yellow oil that could be used without further purification. Yield 39.31% (3.97 g, 0.0287 mol).

$^1\text{H-NMR}$ (CDCl_3): 1.65 (2H, q, $^3J_{\text{HH}} = 7.45\text{ Hz}$, $\text{CH}_2\text{CH}_2\text{CH}_2$), 2.0 (4H, t, $^3J_{\text{HH}} = 7.69\text{ Hz}$, CH_2), 2.15 (1H, s, OH), 2.59 (2H, m, PhCH_2), 3.65 (2H, t, $^3J_{\text{HH}} = 6.70\text{ Hz}$, OCH_2), 5.40 (1H, bs, CH), 5.70 (2H, m, CH).

$^{13}\text{C-NMR}$ (CDCl_3): 27.95 (s, $\sigma\text{-CH}_2$), 28.79 (s, CH_2), 31.00 (s, PhCH_2), 71.95 (s, CH_2O), 126.74 (s, $p\text{-CH}$), 128.57 (s, $m\text{-CH}$), 138.92 (s, C_{quart}).

5.3.9 Synthesis of 2-(1,4-cyclohexadiene)ethanol

In a 500 ml three-necked flask, 4 g (0.0328 mol) of $\text{Ph}(\text{CH}_2)_2\text{OH}$ was added to 15.0 ml (0.257 mol) of absolute ethanol and the reaction mixture was cooled to $-78\text{ }^\circ\text{C}$ using a dry ice/propanol slush bad. Using a long cannula, 200ml of liquid ammonia was condensed into the reaction mixture over 3 hours. Without removing the cooling bath, small pieces of lithium were added until the blue color persisted. After the dropwise addition of 5 ml (0.086 mol) of absolute ethanol, more lithium was added until the color persisted. After the mixture was stirred for 30 min, 8 g of NH_4Cl was added and the ammonia was allowed to evaporate over night. The residue was dissolved in 100 ml of water and extracted into 3 x 20 ml of CH_2Cl_2 . The combined organic layers were washed with a saturated solution of NaCl and then dried with Na_2SO_4 . The solvent was removed in vacuo to give 1.8 g of yellow oil that was not further purified. Yield 45.50% (1.8 g, 0.0145 mol).

$^1\text{H-NMR}$ (CDCl_3): 2.12 (2H, q, $^3J_{\text{HH}} = 7.45$ Hz, PhCH_2CH_2), 2.25 (1H, s, OH), 2.54 (4H, m, CH_2), 3.57 (2H, t, $^3J_{\text{HH}} = 6.45$ Hz, OCH_2), 5.41 (1H, bs, CH), 5.59 (2H, m, CH).

$^{13}\text{C-NMR}$ (CDCl_3): 24.23 (s, $o\text{-CH}_2$), 29.00 (s, PhCH_2), 68.70 (s, CH_2O), 125.02 (s, $p\text{-CH}$), 127.56 (s, $m\text{-CH}$), 139.98 (s, C_{quart}).

5.3.10 Synthesis of (2-phenylpropyl)isopropyl sulfide

In a 250 ml three-necked flask 9.780 g (87.15 mmol) of KO^tBu was dissolved under stirring in 50 ml of EtOH. After complete dissolution, 7.43 ml (79.96 mmol) of i -propylthiol was added dropwise. 12.2 ml (80.0 mmol) of $\text{Ph}(\text{CH}_2)_3\text{Br}$ was then dissolved in 40 ml of EtOH and added dropwise to the reaction mixture and refluxed for 30 min. EtOH and the remaining KO^tBu were removed by distillation at atmospheric pressure. The residue was treated with 80 ml of water and the aqueous layer was extracted with 3 x 40 ml portions of ether. The ethereal layer was washed with 20 ml of water and stirred over anhydrous Na_2SO_4 for 30 min. After filtering, the ether layer was removed by distillation. Compound $\text{Ph}(\text{CH}_2)_3\text{S}^i\text{Pr}$ was then collected by distillation at 70-76 °C in vacuo as a colorless ill-smelling liquid in 74.20% yield (11.53 g; 59.35 mmol).

$^1\text{H-NMR}$ (CDCl_3): δ (ppm) = 0.86 (6H, d, $^3J_{\text{HH}} = 6.69$ Hz, $\text{CH}_3(^i\text{Pr})$), 1.92 (2H, q, $^3J_{\text{HH}} = 7.35$ Hz, $\text{CH}_2\text{CH}_2\text{CH}_2$), 2.92 (1H, hept, $^3J_{\text{HH}} = 6.80$ Hz, $\text{CH}(^i\text{Pr})$), 2.55 (2H, t, $^3J_{\text{HH}} = 7.31$ Hz, CH_2Ph), 2.73 (2H, t, $^3J_{\text{HH}} = 7.58$ Hz, CH_2S), 7.24 (5H, m, $\text{CH}(\text{Ph})$).

$^{13}\text{C-NMR}$ (CDCl_3): δ (ppm) = 23.48 ($\text{CH}_3(^i\text{Pr})$), 29.95 (s, CH_2), 32.42 (s, CH_2Ph), 34.81 (s, $\text{CH}(^i\text{Pr})$), 35.01 (s, CH_2S), 125.90 (s, $p\text{-CH}$), 128.38 (s, $m\text{-CH}$), 128.52 (s, $o\text{-CH}$), 141.55 (s, C_{quart}).

5.3.11 Synthesis of methyl(2-phenylethyl)sulfide

Analogously to the synthesis of $\text{Ph}(\text{CH}_2)_3\text{S}^i\text{Pr}$, in a 250 ml three-necked flask 8.120 g (72.4 mmol) of KO^tBu was dissolved under stirring in 50 ml of EtOH. After complete dissolution, 10.0 g (72.4 mmol) of $\text{Ph}(\text{CH}_2)_2\text{SH}$ was dissolved in 30 ml of EtOH and added dropwise. After stirring for 15 min, 4.5 ml (72.4 mmol) of MeI was added dropwise to the reaction mixture and then refluxed for 30 min. EtOH and the rest of formed HO^tBu were removed by distillation at atmospheric pressure. The residue was treated with 80 ml of

5. Experimental part

water and the aqueous layer was extracted with 3 x 40 ml portions of ether. The ether layer was washed with 20 ml of water and left to stir over anhydrous Na₂SO₄ for 30 min. After filtration, the ether was removed by distillation. Product Ph(CH₂)₂SMe was collected by vacuum distillation at 65° C as a colorless foul-smelling liquid in 76% yield (8.368 g; 59.35 mmol).

¹H-NMR (CDCl₃): δ (ppm) = 2.13 (3H, s, CH₃S), 2.76 (2H, t, ³J_{HH} = 8.0 Hz, CH₂Ph), 2.89 (2H, t, ³J_{HH} = 8.0 Hz, CH₂S), 7.26 (5H, m, CH(Ph)).

¹³C-NMR (CDCl₃): δ (ppm) = 15.63 (s, CH₃S), 35.75 (s, CH₂Ph), 35.85 (s, CH₂S), 127.2 (s, *p*-CH), 128.15 (s, *m*-CH), 128.57 (s, *o*-CH_{Ph}), 140.13 (s, C_{quart}).

5.4 Synthesis of compounds

5.4.1 Synthesis of [(η⁶-*p*-cymene)RuCl₂(PhC₃H₆S^{*i*}Pr)] (4)

193 μl (0.98 mmol) of Ph(CH₂)₃S^{*i*}Pr was added to 0.200 g (0.326 mmol) of [(η⁶-*p*-cymene)RuCl₂]₂ dissolved in 5 ml of CH₂Cl₂. The reaction mixture was stirred for 14 h at room temperature, then layered with 4 ml of EtOH and left 5 days at room temperature. A small amount of a microcrystalline solid of **1** was formed and removed by cannula filtration. The filtered solution was dried in vacuo. The dry residue was washed with 3 x 4 ml of Et₂O and the Et₂O removed after washing by cannula filtration. The residue was then recrystallized two times from CH₂Cl₂/Et₂O to give **4** as orange microcrystals. Yield 0.296 g (0.59 mmol, 90.5%).

Analysis calcd. for C₂₂H₃₂Cl₂RuS (500.53): C 52.79, H 6.44; found C 53.01, H 6.55%.

¹H-NMR (CDCl₃): δ (ppm) = 1.27 (12H, m, CH₃(^{*i*}Pr)), 1.88 (2H, q, ³J_{HH} = 7.57 Hz, CH₂CH₂CH₂), 2.18 (3H, s, CH₃(cym)), 2.64 (4H, m, CH₂), 2.93 (2H, m, CH(^{*i*}Pr)), 5.21, 5.38 (each 2H, d, ³J_{HH} = 5.85 Hz, CH(cym)), 7.21 (5H, m, CH(Ph)).

¹³C-NMR (CDCl₃): δ (ppm) = 18.90 (CH₃(cym)), 22.14 (CH₃(^{*i*}Pr)), 30.36 (CH₂), 30.61 (CH₂Ph), 31.20 (CH(^{*i*}Pr)), 34.89 (CH(^{*i*}Pr)), 37.46 (CH₂S), 80.53, 81.29 (CH(cym)), 96.74, 101.23 (C_{quart}(cym)), 125.90 (*p*-CH(Ph)), 128.38 (s, *m*-CH(Ph)), 128.50 (s, *o*-CH(Ph)), 141.55 (s, C_{quart}(Ph)).

5.4.2 Synthesis of $[(\eta^6\text{-p-cymene})\text{RuCl}_2(\text{PhC}_2\text{H}_4\text{SMe})]$ (5)

A Schlenk tube was charged with 0.300 g (0.49 mmol) of $[(\eta^6\text{-p-cymene})\text{RuCl}_2]_2$ and a 223 μl of $\text{PhC}_2\text{H}_4\text{SMe}$ and the mixture stirred at room temperature overnight in 4 ml of CH_2Cl_2 . The solvent was evaporated and the crude product was washed with 2 x 5 ml of Et_2O . The orange powder obtained after drying in vacuo was dissolved in 3 ml CH_2Cl_2 , cautiously layered with the same quantity of Et_2O and left to cool in a refrigerator. Compound **5** crystallized as long orange needles. Yield 65.4% (0.147 g, 0.32 mmol).

Analysis calcd. for $\text{C}_{19}\text{H}_{26}\text{Cl}_2\text{RuS}$ (458.45): C 49.78, H 5.72; found: C 49.73, H 5.79%.

$^1\text{H-NMR}$ (CDCl_3): δ (ppm) = 1.26 (6H, d, $^3J_{\text{HH}} = 6.86$ Hz, $\text{CH}_3(\text{iPr})$), 2.18, 2.24 (each s, 3H, $\text{CH}_3(\text{cym})$, CH_3S), 2.90 (2H, m CH_2Ph), 2.92 (2H, m, CH_2S), 3.03 (1H, hept, $^3J_{\text{HH}} = 6.86$ Hz, $\text{CH}(\text{iPr})$), 5.18, 5.77 (each 2H, d, $^3J_{\text{HH}} = 6.04$ Hz, $\text{CH}(\text{cym})$), 7.26 (5H, m, $\text{CH}(\text{Ph})$).

$^{13}\text{C-NMR}$ (CDCl_3): δ (ppm) = 18.29, 19.70 ($\text{CH}_3(\text{cym})$, CH_3S), 22.20 ($\text{CH}_3(\text{iPr})$), 30.62 ($\text{CH}(\text{iPr})$), 33.97 (CH_2Ph), 41.09 (CH_2S), 82.89 ($\text{CH}(\text{cym})$), 83.93 (s, $\text{CH}(\text{cym})$), 99.30 (s, $\text{C}_{\text{quart}}(\text{cym})$), 104.58 (s, $\text{C}_{\text{quart}}(\text{cym})$), 126.78 (s, $p\text{-CH}$), 128.67 (s, $m\text{-CH}$), 128.72 (s, $o\text{-CH}$), 139.15 (s, C_{quart}).

5.4.3 Synthesis of $[(\eta^6\text{-p-cymene})\text{RuCl}_2(\text{SMeC}_3\text{H}_5)]$ (6)

0.120 g (0.196 mmol) of $[(\eta^6\text{-p-cymene})\text{RuCl}_2]_2$ was dissolved in 6 ml of CH_2Cl_2 and 52 μl (0.591 mmol) of SMeC_3H_5 was added dropwise. The reaction mixture was stirred for 12 h at room temperature. The solvent was evaporated from the dark orange solution. The dry residue was washed with 3 x 4 ml of Et_2O and the Et_2O removed in vacuo. The resulting orange powder was dissolved in 3 ml of CH_2Cl_2 and layered with 3 ml of ether. After 3 days orange crystals were obtained. Yield 74.4% (0.115 g, 0.294 mmol).

Analysis calcd. for $\text{C}_{14}\text{H}_{22}\text{Cl}_2\text{RuS}$ (394.36): C 46.41, H 6.12; found C 46.76, H 6.14%.

$^1\text{H-NMR}$ (CDCl_3): δ (ppm) = 1.24 (6H, d, $^3J_{\text{HH}} = 6.95$ Hz, $\text{CH}_3(\text{iPr})$), 2.15, 2.17 (each 3H, s, $\text{CH}_3(\text{cym})$, CH_3S), 2.92 (1H, hept, $^3J_{\text{HH}} = 6.95$ Hz, $\text{CH}(\text{iPr})$), 3.36 (2H, d, $^3J_{\text{HH}} = 7.3$ Hz, CH_2S), 5.17 (2H, d(br), $^3J_{\text{HH}} = 16$ Hz, $\text{CH}=\text{CH}$), 5.19 (d, br, $\text{CH}=\text{CH}$, $^3J_{\text{HH}} = 10.8$ Hz), 5.25, 5.41 (each 2H, d, $^3J_{\text{HH}} = 5.66$ Hz, $\text{CH}(\text{cym})$), 5.71 (1H, ddt, $\text{CH}=\text{CH}$, $^3J_{\text{HH}} = 16.0$,

5. Experimental part

10.8, 7.3 Hz).

^{13}C -NMR (CDCl_3): δ (ppm) = 18.12, 18.90 (CH_3S , $\text{CH}_3(\text{cym})$), 22.14 ($\text{CH}_3(\text{iPr})$), 30.42 ($\text{CH}(\text{iPr})$), 40.69 (CH_2S), 82.87 ($\text{CH}(\text{cym})$), 83.46 ($\text{CH}(\text{cym})$), 98.76 ($\text{C}_{\text{quart}}(\text{cym})$), 104.42 ($\text{C}_{\text{quart}}(\text{cym})$), 120.91 (s, $=\text{CH}$), 130.87 (s, $=\text{CH}_2$).

5.4.4 Synthesis of $[(\eta^6\text{-p-cymene})\text{RuCl}(\text{SMe}_2)_2]^+ \text{SbF}_6^-$ (**7**) and $\{[(\eta^6\text{-p-cymene})\text{Ru}]_2(\mu\text{-Cl})_3\}^+ \text{SbF}_6^-$ (**8**)

Following the procedure of *Dixneuf*,⁸⁰ 0.200 g (0.326 mmol) of $\{[(\eta^6\text{-p-cymene})\text{RuCl}_2]_2\}$, 0.176 g (0.68 mmol) of NaSbF_6 and 190 μl (2.61 mmol) of dimethyl sulfide were stirred with 8ml of MeOH for two days at room temperature. The resulting yellow mixture was evaporated to dryness and the residue was dissolved in 4 ml of CH_2Cl_2 . The solution was then filtered and the orange filtrate layered with 15 ml of Et_2O . Orange crystals of **7** along with a small quantity of **8** formed upon slow diffusion of ether and were isolated by decantation of the solvent, dried in vacuo and then manually separated (**7**: orange diamonds, **8** orange needles). Yields were 230 mg (55.9 %) of **7** and 21 mg (7.9 %) of **8**.

Analysis calcd. for $\text{C}_{20}\text{H}_{28}\text{Cl}_3\text{F}_6\text{Ru}_2\text{Sb}$ (812.68): C 29.55, H 3.47; found C 30.02, H 3.55%.

7: ^1H -NMR (CDCl_3): δ (ppm) = 1.27 (6H, d, $^3J_{\text{HH}} = 7.00$ Hz, $\text{CH}_3(\text{iPr})$), 2.21 (3H, s, $\text{CH}_3(\text{cym})$), 2.27 (6H, s, CH_3S), 2.96 (2H, hept, $^3J_{\text{HH}} = 7.00$ Hz, $\text{CH}(\text{iPr})$), 5.20, 5.40 (each 2H, d, $^3J_{\text{HH}} = 6.01$ Hz, $\text{CH}(\text{cym})$).

^{13}C -NMR (CDCl_3): δ (ppm) = 18.03, 18.90 (CH_3S , $\text{CH}_3(\text{cym})$), 21.90 ($\text{CH}_3(\text{iPr})$), 31.44 (s, $\text{CH}(\text{iPr})$), 78.81 (s, CH), 88.57 (s, CH), 101.83 ($\text{C}_{\text{quart}}(\text{cym})$), 111.62 ($\text{C}_{\text{quart}}(\text{cym})$).

Analysis calcd. for $\text{C}_{14}\text{H}_{16}\text{ClF}_6\text{RuS}_2\text{Sb}$ (620.66): C 26.66, H 4.15; found: C 26.85, H 4.15.

8: ^1H -NMR (CDCl_3): δ (ppm) = 1.30 (6H, d, $^3J_{\text{HH}} = 6.9$ Hz, $\text{CH}_3(\text{iPr})$), 2.22 (3H, s, $\text{CH}_3(\text{cym})$), 2.78 (1H, hept, $^3J_{\text{HH}} = 6.9$ Hz, $\text{CH}(\text{iPr})$), 5.46, 5.64 (each 2H, d, $^3J_{\text{HH}} = 6.20$ Hz, CH).

^{13}C -NMR (CDCl_3): δ (ppm) = 18.96 ($\text{CH}_3(\text{cym})$), 22.17 ($\text{CH}_3(\text{iPr})$), 30.63 ($\text{CH}(\text{iPr})$), 80.55, 81.32 ($\text{CH}(\text{cym})$), 96.77 ($\text{C}_{\text{quart}}(\text{cym})$), 101.24 ($\text{C}_{\text{quart}}(\text{cym})$).

5.4.5 Synthesis of $[(\eta^6\text{-p-cymene})\text{RuCl}_2(\text{PhC}_3\text{H}_6\text{Py})]$ (**9**)

In a 50 ml evacuated Schlenk tube, 0.500 g (0.817 mmol) of $[(\eta^6\text{-p-cymene})\text{RuCl}_2]_2$, was reacted with 380 μl (1.63 mmol) of $\text{PhC}_3\text{H}_6\text{Py}$ in 10 ml of THF. The suspension was left to stir at ambient temperature over night. The solvent was evaporated under vacuum and the crude product was washed with 2 x 6 ml of petrol ether and dried in vacuo. Recrystallization in order to remove excess non-reacted pyridine was done by slowly cooling a solution in hot EtOH. Yield 76.25% (0.313 g, 0.623 mmol).

When the same reaction was performed in CH_2Cl_2 as solvent the starting materials and product was much better soluble. After workup as above, complex **8** was, however, contaminated with the chloromethylammonium salt of the pyridine ligand, which gives rise to $^1\text{H-NMR}$ signals at $\delta = 9.04$ ppm. Removal of this impurity required 3 successive recrystallizations.

Analysis calcd. for $\text{C}_{24}\text{H}_{29}\text{RuNCl}_2$ (503.47): C 57.26, H 5.81, N 2.78; found C 57.75, H 5.94, N 2.80%.

$^1\text{H-NMR}$ (CDCl_3): δ (ppm) = 1.27 (6H, d, $^3J_{\text{HH}} = 6.80$ Hz, $\text{CH}_3(\text{Pr})$), 1.88 (2H, q, $^3J_{\text{HH}} = 7.56$ Hz, $\text{CH}_2\text{-CH}_2\text{-CH}_2$), 2.07 (3H, s, $\text{CH}_3(\text{cym})$), 2.64 (4H, tt, $^3J_{\text{HH}} = 3.85$ Hz, CH_2), 2.95 (1H, hept, $^3J_{\text{HH}} = 6.80$ Hz, $\text{CH}(\text{Pr})$), 5.18 (2H, d, $^3J_{\text{HH}} = 5.70$ Hz, $\text{CH}(\text{cym})$), 5.40 (2H, d, $^3J_{\text{HH}} = 5.70$ Hz, $\text{CH}(\text{cym})$), 7.12 (5H, m, $\text{CH}(\text{ph})$), 8.85 (4H, d, $^3J_{\text{HH}} = 6.58$ Hz, $\text{CH}(\text{py})$).

$^{13}\text{C-NMR}$ (CDCl_3): δ (ppm) = 19.20 (s, $\text{CH}_3(\text{cym})$), 22.34 (s, $\text{CH}_3(\text{Pr})$), 32.91 (s, $\text{CH}(\text{Pr})$), 33.85 (s, CH_2), 36.62 (s, $\text{CH}_2(\text{Ph})$), 37.49 (s, $\text{CH}_2(\text{py})$), 82.35 (s, $\text{CH}(\text{cym})$), 83.35 (s, $\text{CH}(\text{cym})$), 98.40 (s, $\text{C}_{\text{quart}}(\text{cym})$), 101.7 (s, $\text{C}_{\text{quart}}(\text{cym})$), 126.10 (s, $\text{CH}(\text{ph})$), 128.24 (s, $\text{CH}(\text{ph})$), 130.58 (s, $\text{CH}(\text{ph})$), 151.7 (s, $\text{CH}(\text{py})$), 154.0 (s, $\text{C}_{\text{quart}}(\text{py})$), 156 (s, $\text{CH}(\text{py})$).

5.4.6 Synthesis of $[(\eta^6\text{-p-cymene})\text{RuCl}_2(2\text{-benzylaminopyridine})]$ (**10**)

In a routine run, 0.200 g (0.326 mmol) of $[(\eta^6\text{-p-cymene})\text{RuCl}_2]_2$ was combined with 0.12 g (0.652) with PhCH_2NHPy , dissolved in 8 ml of chlorobenzene and stirred over night. The mother solvent was pipetted out and the residue was dissolved in dichloromethane and left to stir for 1 hour. The solution was then filtered by cannula filtration and the filtrate was evaporated in vacuum. **10** was obtained as an orange powder in 67% yield (0.1 g, 0.22 mmol).

5. Experimental part

Analysis calcd. for $C_{22}H_{24}RuN_2Cl_2$ (489.43): C 53.98, H 5.14, N 5.72; found C 54.34, H 5.50, N 5.65%.

1H -NMR ($CDCl_3$): δ (ppm) = 0.86 (2H, t, $^3J_{HH}=6.13$ Hz, \underline{CH}_2), 1.25 (6H, d, $^3J_{HH} = 6.90$ Hz, $\underline{CH}_3(iPr)$), 1.95 (3H, s, $\underline{CH}_3(cym)$), 2.9 (1H, hept, $^3J_{HH} = 7.90$ Hz, $\underline{CH}(iPr)$), 4.38 (2H, d, $^3J_{HH} = 5.67$ Hz, \underline{NH}), 5.22 (2H, d, $^3J_{HH} = 5.72$ Hz, $\underline{CH}(cym)$), 5.45 (2H, d, $^3J_{HH} = 5.72$ Hz, $\underline{CH}(cym)$), 6.43 (2H, d, $^3J_{HH} = 8.44$ Hz, o- $\underline{CH}(ph)$), 6.59 (2H, t, $^3J_{HH} = 6.48$ Hz, m- $\underline{CH}(py)$), 7.4 (1H, m, p- $\underline{CH}(py)$), 8.08 (t, \underline{NH}) 8.70 (4H, d, $^3J_{HH} = 4.95$ Hz, $\underline{CH}(py)$).

^{13}C -NMR ($CDCl_3$): δ (ppm) = 18.05 (s, $\underline{CH}_3(cym)$), 22.22 (s, $\underline{CH}_3(iPr)$), 30.04 (s, $\underline{CH}(iPr)$), 33.85 (s, \underline{CH}_2), 47.65 (s, $\underline{CH}_2(ph)$), 81.27 (s, $\underline{CH}(cym)$), 82.63 (s, $\underline{CH}(cym)$) 97.44 (s, $C_{quart}(cym)$), 103.3 (s, $C_{quart}(cym)$), 107.62 (s, $\underline{CH}(py)$), 113.61 (s, $\underline{CH}(py)$), 127.53 (s, $\underline{CH}(ph)$), 128.8 (s, $\underline{CH}(ph)$), 137.38 (s, $C_{quart}(ph)$), 138.92 (s, $\underline{CH}(ph)$), 153.50 (s, $\underline{CH}(py)$), 161.76 (s, $C_{quart}(py)$).

5.4.7 Synthesis of $[(\eta^6\text{-p-cymene})RuCl_2(4\text{-methylpyridine})]$ (**11**)

In a typical run, 0.350 g (0.57 mmol) of $[(\eta^6\text{-p-cymene})RuCl_2]_2$ was reacted with 110.9 μ l (1.14 mmol) of 4-picoline, MePy, in 8 ml of THF and stirred for 14 h at room temperature. The solvent was removed by evaporation and the crude product was dissolved in dichloromethane and stirred for 1 h. After filtration, the CH_2Cl_2 was removed in vacuo and the residue was washed with 3 x 10 ml of petrol ether. Recrystallization from EtOH and a very small quantity of $CHCl_3$ just necessary to dissolve the crude product afforded orange crystals as small round pearls. X-ray structure determination points to structure **11**, which agrees with the results from NMR. Yield 84% (0.19 g, 0.48 mmol).

1H -NMR ($CDCl_3$): δ (ppm) = 1.27 (6H, d, $^3J_{HH} = 6.80$ Hz, $\underline{CH}_3(iPr)$), 2.06 (3H, s, $\underline{CH}_3(cym)$), 2.37 (3H, s, $\underline{CH}_3(py)$), 2.95 (1H, hept, $^3J_{HH} = 6.80$ Hz, $\underline{CH}(iPr)$), 5.17 (2H, d, $^3J_{HH} = 6.02$ Hz, $\underline{CH}(cym)$), 5.39 (2H, d, $^3J_{HH} = 6.02$ Hz, $\underline{CH}(cym)$), 7.08 (2H, d, $^3J_{HH} = 6.03$ Hz, m- $\underline{CH}(py)$), 8.82 (2H, d, $^3J_{HH} = 6.03$ Hz, o- $\underline{CH}(py)$).

^{13}C -NMR ($CDCl_3$): δ (ppm) = 18.07 (s, $\underline{CH}_3(cym)$), 20.70 (s, $\underline{CH}_3(iPr)$), 22.11 (s, $\underline{CH}_3(py)$) 30.44 (s, $\underline{CH}(iPr)$), 33.85 (s, \underline{CH}_2), 81.94 (s, $\underline{CH}(cym)$), 82.64 (s, $\underline{CH}(cym)$), 96.89 (s, $C_{quart}(cym)$), 103.06 (s, $C_{quart}(cym)$), 125.38 (s, m- $\underline{CH}(py)$), 149.45 (s, p- $C_{quart}(py)$),

153.50 (s, o-CH(py))

Analysis calcd. for $C_{16}H_{21}RuNCl_2$ (398.07): C 48.13, H 5.30, N 3.51; found C 48.56, H 5.53, N 3.30%.

5.4.8 Synthesis of $[(\eta^6\text{-p-cymene})RuCl\text{-bis}(4\text{-methylpyridine})]^+ PF_6^-$ (**12**)

Compound **11** (0.150 g, 0.34 mmol) was reacted with 53.0 μ l (0.67 mmol) of 2-methyl-3-butyn-2-ol and 0.0875 g (0.034 mmol) of $NaSbF_6$ in 8 ml of CH_2Cl_2 . After stirring over night, the solvent was evaporated. The residue residues was washed under standard procedure with Et_2O and brought to dryness in vacuo. The residue was dissolved in 4 ml of dichloromethane and layered with 4 ml of EtOH. Recrystallization afforded only small quantities of **8** as shown by 1H -NMR spectroscopy. The mother liquor was evaporated to dryness and identified as a mixture of **8** and **12**. Yield 72% (0.091g, 0.2 mmol).

Pure **12** was then obtained in another route:

In a typical run 0.1700 g (0.28 mmol) of $[(\eta^6\text{-p-cymene})RuCl_2]_2$ was combined with 216.0 μ l (2.22 mmol) of 4-picoline, MePy, and 0.150 g (0.58 mmol) of $NaSbF_6$. The reactants were dissolved in 10 ml of MeOH. The reaction mixture was stirred for 16 h at room temperature after which time MeOH was evaporated to dryness. The crude product was washed with 2 x 8 ml of Et_2O and dried in vacuo.

1H -NMR ($CDCl_3$) : δ (ppm) = 1.10 (6H, d, $^3J_{HH} = 6.9$ Hz, $\underline{CH}_3(iPr)$), 1.71 (3H, s, $\underline{CH}_3(cym)$), 2.34 (6H, s, $\underline{CH}_3(py)$), 2.65 (1H, hept, $^3J_{HH} = 6.12$ Hz, $\underline{CH}(iPr)$), 5.49 (2H, d, $^3J_{HH} = 6.06$ Hz, $\underline{CH}(cym)$), 5.78 (2H, d, $^3J_{HH} = 6.06$ Hz, $\underline{CH}(cym)$), 7.18 (4H, d, $^3J_{HH} = 6.09$ Hz, m- $\underline{CH}(py)$), 8.61 (4H, d, $^3J_{HH} = 6.03$ Hz, o- $\underline{CH}(py)$).

^{13}C -NMR ($CDCl_3$) : δ (ppm) = 17.48 (s, $\underline{CH}_3(cym)$), 20.68 (s, $\underline{CH}_3(iPr)$), 21.93 (s, $\underline{CH}_3(py)$), 30.52 (s, $\underline{CH}(iPr)$), 33.85 (s, \underline{CH}_2), 81.71 (s, $\underline{CH}(cym)$), 88.10 (s, $\underline{CH}(cym)$) 101.394 (s, $C_{quart}(cym)$), 102.71 (s, $C_{quart}(cym)$), 126.88 (s, m- $\underline{CH}(py)$), 151.35 (s, p- $C_{quart}(py)$), 153.04 (s, o- $\underline{CH}(py)$).

5. Experimental part

5.4.9 Synthesis of $[\{\eta^6\text{-C}_6\text{H}_5(\text{CH}_2)_3\text{OH}\}\text{RuCl}_2]_2$ (**13**)

In a typical run, 9.30 g (67.30 mmol) of (1,4-cyclohexadienyl)-1-propanol was combined with 2.78 g (11.66 mmol) of hydrated RuCl_3 in 70 ml of ethanol. The mixture was heated under reflux for 6 h. The microcrystalline solid obtained after storing the mother liquor in the fridge overnight was recrystallized from hot ethanol to give orange crystals of **13** in a yield of 2.79 g (77.6 %).

Analysis calcd. for $\text{C}_9\text{H}_{12}\text{Cl}_2\text{ORu}$ (308.17): C 35.08, H 3.93; found C 35.43, H 3.97%.

$^1\text{H-NMR}$ (CDCl_3): δ (ppm) = 1.85 (2H, tt, $^3J_{\text{HH}} = 7.2, 7.0$ Hz, $\text{CH}_2\text{CH}_2\text{CH}_2$), 2.63 (2H, t, $^3J_{\text{HH}} = 7.2$ Hz, PhCH_2), 3.38 (2H, t, $^3J_{\text{HH}} = 7.0$ Hz, CH_2O), 5.39 (2H, d, $^3J_{\text{HH}} = 5.4$ Hz, CH), 5.57 (2H, t, $^3J_{\text{HH}} = 5.1$ Hz, CH), 5.64 (1H, dt, $^3J_{\text{HH}} = 5.4, 5.1$ Hz, CH).

$^1\text{H-NMR}$ (dmsO-d_6): δ (ppm) = 1.81 (2H, tt, $^3J_{\text{HH}} = 7.2, 7.0$ Hz, $\text{CH}_2\text{CH}_2\text{CH}_2$), 2.43 (2H, t, $^3J_{\text{HH}} = 7.6$ Hz, PhCH_2), 3.36 (2H, t, $^3J_{\text{HH}} = 6.3$ Hz, CH_2O), 5.73 (1H, t, $^3J_{\text{HH}} = 5.5$ Hz, CH), 5.74 (2H, d, $^3J_{\text{HH}} = 5.5$ Hz, CH), 5.98 (2H, t, $^3J_{\text{HH}} = 5.5$ Hz, CH).

$^{13}\text{C-NMR}$ (CDCl_3): δ (ppm) = 29.76 (s, CCH_2), 30.05 (s, PhCH_2), 71.79 (s, CH_2O), 80.17, 80.86, 84.37 (each s, CH), 111.89 (C_{quart}).

$m_p = 230.5$ °C.

5.4.10 Synthesis of $[\{\eta^6\text{-C}_6\text{H}_5(\text{CH}_2)_3\text{OH}\}\text{Ru}(\text{P}^i\text{Pr}_3)\text{Cl}_2]$ (**13a**)

0.30g (0.97 mmol) of **13** was reacted with 185 μl (0.48 mmol) of P^iPr_3 in 5 ml of CH_2Cl_2 . The reaction mixture was stirred overnight and filtered by cannula. The clear solution was dried in vacuo. Then the residue was washed with 3 x 4 ml of Et_2O . Drying in vacuo gave 354 mg of **13a** (77.7%).

Analysis calcd. for $\text{C}_{18}\text{H}_{33}\text{Cl}_2\text{OPRu}$ (468.49): C 46.16, H 7.10; found C 47.10, H 7.46%.

$^1\text{H-NMR}$ (CDCl_3): δ (ppm) = 1.28, 1.34 (each d, $^3J_{\text{HH}} = 7.2$ Hz, 9 H, $\text{CH}_3(\text{P}^i\text{Pr}_3)$), 1.92 (2H, tt, $^3J_{\text{HH}} = 8.55, 6.2$ Hz, $\text{CH}_2\text{CH}_2\text{CH}_2$), 2.71 (2H, t, $^3J_{\text{HH}} = 8.55$ Hz, PhCH_2), 2.77 (3H, m, $\text{CH}(\text{P}^i\text{Pr}_3)$), 3.43 (2H, t, $^3J_{\text{HH}} = 6.2$ Hz, OCH_2), 5.31 (2H, t, $^3J_{\text{HH}} = 5.6$ Hz), 5.42 (2H, d, $^3J_{\text{HH}} = 5.8$ Hz), 5.57 (1H, dt, $^3J_{\text{HH}} = 5.8, 5.6$ Hz).

$^{13}\text{C-NMR}$ (CDCl_3): δ (ppm) = 19.84 (s, CCH_3) 25.58 (d, $J_{\text{P-C}} = 20.43$ Hz, CH), 29.12 (s, CCH_2), 29.72 (s, PhCH_2), 71.72 (s, CH_2O), 77.67, 85.20 (each s, CH), 87.94 (d, $^2J_{\text{P-C}} = 5.8$ Hz, CH), 111.89 (d, C_{quart} , $^2J_{\text{P-C}} = 7.2$ Hz).

^{31}P (CDCl_3): δ (ppm) = 36.52 (s, PPr_3).

m_p = 115.0 °C.

5.4.11 [$\{\text{C}_6\text{H}_5(\text{CH}_2)_3\text{OH}\}\text{Ru}(\text{PCy}_3)\text{Cl}_2$] (**13b**)

Compound **13** (0.30g, 0.97 mmol) and 0.273 g (0.49 mmol) of PCy_3 were dissolved in 6 ml of CH_2Cl_2 and stirred overnight. The filtered solution was dried in vacuo and the residue was washed with 3 x 4ml of Et_2O and dried. Compound **13b** was obtained as an orange brown fluffy powder in a yield of 396 mg (69.2%).

Analysis calcd. for $\text{C}_{27}\text{H}_{45}\text{Cl}_2\text{OPRu}$ (588.60): C 55.16, H 7.71; found C 56.00, H 8.25%.

$^1\text{H-NMR}$ (CDCl_3): δ (ppm) = 1.14-1.55 (16 H, m, br.), 1.6-1.9 (10 H, m.), 2.23 (4H, m.), 2.49 (3H, m.), all CH_2 , CH (PCy_3), 1.93 (2H, tt, $^3J_{\text{HH}} = 7.7, 6.2$ Hz, $\text{CH}_2\text{CH}_2\text{CH}_2$), 2.71 (2H, t, $^3J_{\text{HH}} = 7.7$ Hz, PhCH_2), 3.46 (2H, t, $^3J_{\text{HH}} = 6.2$ Hz, CH_2O), 5.39 (3H, m), 5.52 (2H, t, $^3J_{\text{HH}} = 5.0$ Hz).

$^{13}\text{C-NMR}$ (CDCl_3): δ (ppm) = 27.9, 28.05, 29.36, 30.00, 30.26 (each s, CH_2), 36.16 (d, $J_{\text{P-C}} = 18.9$ Hz, $\text{CH}(\text{PCy}_3)$), 72.13 (s, OCH_2), 77.60, 84.97 (s, CH), 88.75 (d, $^2J_{\text{P-C}} = 5.1$ Hz, CH), 112.05 (d, $^2J_{\text{P-C}} = 6.3$ Hz, C_{quart}).

^{31}P (CDCl_3): δ (ppm) = 31.61 (s, PCy_3).

m_p = 141.0 °C.

5.4.12 [$\{\eta^6\text{-C}_6\text{H}_5(\text{CH}_2)_3\text{OH}\}\text{RuCl}_2\{\text{P}(\text{CH}_2\text{OH})_3\}$] (**13c**)

134 mg (0.43 mmol) of $\{\eta^6\text{-C}_6\text{H}_5(\text{CH}_2)_3\text{OH}\}\text{RuCl}_2$ (**13**) was reacted with 50 mg (0.40 mmol) of tris(hydroxymethyl)phosphine, $\text{P}(\text{CH}_2\text{OH})_3$, in 5 ml of CH_2Cl_2 . The reaction mixture was allowed to stir overnight and filtered by cannula to remove some undissolved material. The vacuum dried residue was washed with 3 x 2 ml of Et_2O . After drying under vacuum 106 mg (57%) of a brown, hygroscopic powder was obtained.

Analysis calcd. for $\text{C}_{12}\text{H}_{21}\text{O}_4\text{PRuCl}_2$ (432.24): C 33.34, H 4.90; found C 31.68, H 5.34%.

$^1\text{H-NMR}$ (CD_3OD): δ (ppm) = 1.93 (2H, m, $\text{CH}_2\text{CH}_2\text{CH}_2$), 2.55 (2H, t, $^3J_{\text{HH}} = 7.8$ Hz, PhCH_2), 3.32 (3H, t, $^3J_{\text{HH}} = 0.9$ Hz, $\text{P}(\text{CH}_2\text{OH})_3$, 3H), 3.47 (6H, d, $^3J_{\text{HH}} = 0.9$ Hz, $\text{P}(\text{CH}_2\text{OH})_3$), 4.83 (s, br, OH), 5.51 (2H, t, $^3J_{\text{HH}} = 6.8$ Hz), 5.62 (2H, dd, $^3J_{\text{HH}} = 6.8, 4.6$ Hz), 5.89 (1H, t, $^3J_{\text{HH}} = 4.6$ Hz).

$^{13}\text{C-NMR}$ (CDCl_3): δ = 30.19 (s, CH_2) 30.58 (s, PhCH_2), 57.38 (d, $J_{\text{P-C}} = 33.08$ Hz,

5. Experimental part

P(CH₂OH)₃, 72.74 (s, CH₂O), 78.28 (s, CH), 87.52 (s, CH), 88.70 (d, ²J_{P-C} = 5.3 Hz, CH), 111.5 (d, ²J_{P-C} = 4.21, C_{quart}).

³¹P (CDCl₃): δ (ppm) = 29.06 (s, P(CH₂OH)₃).

m_p = 106° C.

5.4.13 [{η⁶-C₆H₅(CH₂)₃OH}]RuCl(P(CH₂OH)₃)₂⁺ Cl⁻ (**13d**)

0.052 g (0.176 mmol) of [{η⁶-C₆H₅(CH₂)₃OH}]RuCl₂ was reacted with 45 mg (0.36 mmol) of tris(hydroxymethyl)phosphine, P(CH₂OH)₃, in 5 ml of CH₂Cl₂. The reaction mixture was allowed to stir overnight and filtered by cannula to remove some undissolved material. The filtered solution was dried in vacuo and the residue was washed with 3 x 2 ml of Et₂O. After removing of Et₂O in vacuo 56 mg (59.3%) of **13d** was obtained as a brown, waxy, hygroscopic solid. C₁₅H₃₀Cl₂O₇P₂Ru (556.3)

¹H-NMR (CD₃OD): δ (ppm) = 1.98 (2H, tt, ³J_{HH} = 7.75, 6.10 Hz, CH₂CH₂CH₂), 2.48 (2H, t, ³J_{HH} = 7.75 Hz, PhCH₂), 3.48 (2H, dt, ³J_{HH} = 6.1, 2.5 Hz, CH₂O), 4.07 (1H, d, ³J_{HH} = 2.5 Hz, OH) 4.38 (12H, dd, ²J_{PH} = 18.7, ²J_{HH} = 11.6 Hz, P(CH₂OH)₃), 4.82 (6H, s(br), P(CH₂OH)₃), 5.41 (1H, t, ³J_{HH} = 5.90 Hz), 6.25 (2H, d, ³J_{HH} = 5.9 Hz), 6.58 (2H, t, ³J_{HH} = 5.9 Hz).

¹³C-NMR (CDCl₃): δ (ppm) = 35.90 (s, CH₂) 37.40 (s, PhCH₂), 57.37 (d, J_{P-C} = 32.91 Hz, P(CH₂OH)₃), 72.00 (s, CH₂O), 78.72 (s, CH), 87.08 (s, CH), 89.72 (d, ²J_{P-C} = 5.7 Hz, CH), C_{ipso} quaternary carbon atom was not observed.

³¹P (CDCl₃): δ (ppm) = 38.18 (s, P(CH₂OH)₃).

5.4.14 [{η⁶-C₆H₅(CH₂)₃OMe}]RuCl₂ (**14**)

Compound **14** was prepared analogously to **13** from 7.31g (48.00 mmol) of (1,4-cyclohexadienyl)-1-propyl methyl ether and 1.97 g (8.27 mmol) of RuCl₃ in 60 ml of ethanol. The orange red solution was allowed to cool overnight at 4 °C, which gave **14** as a crystalline solid. The mother liquor was removed by filtration and concentrated by distillation to 15 ml. A further crop of microcrystals was obtained by cooling this solution overnight in a fridge. The combined yield was 2.02 g (73.5 %).

Analysis calcd. for C₂₀H₄₈Cl₄O₂Ru₂ (664.55): C 37.28, H 4.38; found C 37.43, H 4.52%.

¹H-NMR (CDCl₃): δ (ppm) = 1.81 (2H, tt, ³J_{HH} = 7.2, 5.9 Hz, CH₂CH₂CH₂), 2.57 (2H, t, ³J_{HH}

= 7.2 Hz, PhCH₂), 3.22 (3H, s, OCH₃), 3.32 (2H, t, ³J_{HH} = 5.9 Hz, CH₂O), 5.32 (2H, d, ³J_{HH} = 5.7 Hz), 5.55 (1H, t, ³J_{HH} = 5.2 Hz), 5.63 (2H, dd, ³J_{HH} = 5.7, 5.2 Hz).

¹³C-NMR (CDCl₃): δ (ppm) = 29.76 (s, CH₂), 30.05 (s, PhCH₂), 58.90 (s, OCH₃), 71.79 (s, CH₂O), 80.17, 80.86, 84.37 (each s, CH), 101.41 (C_{quart}).

m_p = 245 °C.

5.4.15 Synthesis of [(η⁶-C₆H₅(CH₂)₃OCH₃)Ru(PⁱPr₃)Cl₂] (14a)

0.20 g (0.31 mmol) of **14** was reacted with 237 μl (0.62 mmol) of PⁱPr₃ in 8 ml of CH₂Cl₂. The reaction mixture was stirred overnight at room temperature and filtered via a paper-tipped cannula. The solvent was then removed under vacuum and the dry residue was washed with 3 × 4 ml of Et₂O. The solid was then vacuum dried to yield 254 mg of **14a** (85%).

Analysis calcd. for C₁₉H₃₅Cl₂OPRu (483.43): C 47.30, H 7.31; found C 47.34, H 7.30 %.

¹H-NMR (CDCl₃): δ (ppm) = 1.29, 1.34 (9H, each d, ³J_{HH} = 7.2 Hz, CH₃(PⁱPr₃)), 1.93 (2H, tt, ³J_{HH} = 7.3, 6.2 Hz, CH₂CH₂CH₂), 2.71 (2H, t, ³J_{HH} = 7.3 Hz, PhCH₂), 2.82 (3H, m, CH(PⁱPr₃)), 3.30 (s, 3H, OCH₃), 3.47 (2H, t, ³J_{HH} = 6.2 Hz, CH₂O), 5.36 (2H, t, ³J_{HH} = 5.4 Hz), 5.4 (2H, d, ³J_{HH} = 5.0 Hz), 5.58 (1H, dd, ³J_{HH} = 5.4, 5.0 Hz).

¹³C-NMR (CDCl₃): δ (ppm) = 20.53 (s, CH₃(PⁱPr₃)), 25.94 (d, J_{P-C} = 20.47 Hz, CH(PⁱPr₃)), 29.52 (s, CH₂), 30.16 (s, PhCH₂), 58.86 (s, OCH₃), 72.15 (s, CH₂O), 77.05, 87.89 (s, CH), 88.47 (d, ²J_{P-C} = 5.0 Hz, CH), 112.39 (C_{quart}).

³¹P (CDCl₃): δ = 41.45 (s, PⁱPr₃).

m_p = 117 °C.

5.4.16 [(C₆H₅(CH₂)₃OCH₃)Ru(PCy₃)Cl₂] (14b)

Compound **14** (0.100 g, 0.150 mmol) and 0.103 g (0.31 mmol) of PCy₃ were dissolved in 4 ml of CH₂Cl₂ and stirred overnight. The filtered solution was dried under vacuum and the residue was washed with 3 × 4 ml of Et₂O and dried. Compound **14b** was obtained as an orange brown fluffy powder in a yield of 130 mg (72%).

Analysis calcd. for C₂₈H₄₇Cl₂OPRu (602.63): C 55.81, H 7.86; found C 56.00, H 8.25%.

¹H-NMR (CDCl₃): δ (ppm) = 1.26 (12 H, m, br), 1.41 (3H, t, ³J_{HH} = 12.2 Hz), 1.76 (9H, m,

5. Experimental part

br), 2.1 (6H, m), 2.42 (m, 3H), all $\underline{\text{CH}}_2$, $\underline{\text{CH}}$ (PCy₃), 1.94 (2H, tt, $^3J_{\text{HH}} = 7.8, 6.4$ Hz, $\text{CH}_2\text{CH}_2\text{CH}_2$), 2.65 (2H, t, $^3J_{\text{HH}} = 7.8$ Hz, Ph $\underline{\text{CH}}_2$), 3.31 (s, 3H, O $\underline{\text{CH}}_3$), 3.45 (2H, t, $^3J_{\text{HH}} = 6.4$ Hz, $\underline{\text{CH}}_2\text{O}$), 5.37 (3H m), 5.57 (2H, m).

^{13}C -NMR(CDCl₃): δ (ppm) = 26.8 (d, $J_{\text{PC}} = 1.05$ Hz, $\underline{\text{C}}\text{H}_2$), 27.9, 28.1 (s, $\underline{\text{C}}\text{H}_2$), 29.5 (d, $^5J_{\text{P-C}} = 1.05$ Hz, $\underline{\text{C}}\text{H}_2$), 30.2 (d, $^4J_{\text{P-C}} = 2.1$ Hz, Ph $\underline{\text{C}}\text{H}_2$), 36.3 (d, $^1J_{\text{PC}} = 18.9$ Hz, $\underline{\text{C}}\text{H}(\text{PCy}_3)$), 58.65 (s, $\underline{\text{C}}\text{H}_2\text{O}$), 72.0 (s, O $\underline{\text{C}}\text{H}_3$), 77.45, 77.5, 85.6 (s, $\underline{\text{C}}\text{H}$), 88.3 (d, $^2J_{\text{P-C}} = 5.3$ Hz, $\underline{\text{C}}\text{H}$), 111.9 (d, $^2J_{\text{P-C}} = 5.8$ Hz, C_{quart}).

^{31}P (CDCl₃): δ (ppm) = 32.91 (s, PCy₃).

$m_p = 234$ °C.

5.4.17 [$\{\eta^6\text{-C}_6\text{H}_5(\text{CH}_2)_2\text{OH}\}\text{RuCl}_2$] (15)

In a typical run, 3.60 g (29.03 mmol) of 2-(1,4-cyclohexadienyl)ethanol was reacted with 1.20 g (5.03 mmol) of RuCl₃ in 20 ml of ethanol. The reaction mixture was heated under reflux for 6 h and the solution was left to cool down overnight in a fridge. Ethanol was removed by cannula filtration and the microcrystalline solid was recrystallized by slowly cooling a hot solution in ethanol. After drying under vacuum, 1.09 g (73.7%) were obtained as orange microcrystals.

Analysis calcd. for C₈H₁₀Cl₂ORu (294.14): C 32.67, H 3.43; found C 33.16, H 3.46%.

^1H -NMR (dmf-d₇): δ (ppm) = 2.57 (2H, t, $^3J_{\text{HH}} = 6.0$ Hz, Ph $\underline{\text{C}}\text{H}_2$), 3.70 (2H, dt, $^3J_{\text{HH}} = 6.0, 5.4$ Hz, $\underline{\text{C}}\text{H}_2\text{O}$), 4.66 (1H, t, $^3J_{\text{HH}} = 5.4$ Hz, O $\underline{\text{H}}$), 5.46 (3H,m), 5.61 (2H, t, $^3J_{\text{HH}} = 5.6$ Hz).

^1H -NMR (dms_o-d₆): δ (ppm) = 2.56 (2H, t, $^3J_{\text{HH}} = 6.1$ Hz, $\underline{\text{C}}\text{H}_2\text{O}$), 3.66 (2H, br, $\underline{\text{C}}\text{H}_2\text{O}$), 4.75 (1H, br, O $\underline{\text{H}}$), 5.76 (3H m), 5.96 (2H, t, $^3J_{\text{HH}} = 5.9$ Hz).

^{13}C -NMR (dmf-d₇): δ (ppm) = 37.0 (s, $\underline{\text{C}}\text{H}_2$), 61.0 (s, O $\underline{\text{C}}\text{H}_2$), 78.0 (s, $\underline{\text{C}}\text{H}$), 80.9, 84.0 (each s, $\underline{\text{C}}\text{H}$), 98.6 (C_{quart})

$m_p = 211$ °C.

5.4.18 [$\{\eta^6\text{-C}_6\text{H}_5(\text{CH}_2)_2\text{OH}\}\text{Ru}(\text{P}^i\text{Pr}_3)\text{Cl}_2$] (15a)

A suspension of 0.175 g (0.59 mmol) of **15** in 7 ml of CH₂Cl₂ was treated with 112.5 μl (0.59 mmol) of PⁱPr₃. After stirring overnight, the reaction mixture had turned into a brown solution. Small quantities of undissolved material were removed by cannula filtration. The

filtered solution was dried in vacuo and the residue was washed with 3 x 4 ml of Et₂O and vacuum dried. Compound **15a** was obtained as a brown solid in a yield of 220 mg (82%). Analysis calcd. for C₁₇H₃₁Cl₂OPRu (454.38): C 44.94, 6.88 H; found C 46.28, H 7.02%.

¹H-NMR (CD₂Cl₂): δ (ppm) = 1.29 and 1.36 (9H, each d, ³J_{HH} = 7.22 Hz, CH₃(PⁱPr₃), 2.72 (3H, m, CH(PⁱPr₃)), 2.84 (2H, t, ³J_{HH} = 5.7 Hz, PhCH₂), 4.07 (2H, t, ³J_{HH} = 5.7 Hz, CH₂O), 5.31 (3H m), 5.76 (2H, m).

¹³C-NMR (CD₂Cl₂): δ (ppm) = 21.77 (d, ³J_{P-C} = 1.8 Hz, CH₃(PⁱPr₃)), 27.74 (d, J_{P-C} = 20.4 Hz, CH(PⁱPr₃)), 31.51 (s, CCH₂), 62.13 (s, CH₂O), 80.12, 84.79 (s, CH), 92.31 (d, ²J_{P-C} = 4.7 Hz, CH), 110.89 (C_{quart}, ²J_{P-C} = 4.8 Hz).

³¹P-NMR(CDCl₃): δ (ppm) = 41.25 (s, PⁱPr₃).

m_p = 121 °C.

5.4.19 Synthesis of [{η⁶-C₆H₅(CH₂)₃OCH₃}Ru(PⁱPr₃)ClRu=C=C=CPh₂]⁺ BF₄⁻

0.112 g (0.232 mmol) of [{η⁶-C₆H₅(CH₂)₃OCH₃}Ru(PⁱPr₃)Cl₂] (**14a**) was dissolved in a mixture of 1 ml of CH₂Cl₂ and 0.6 ml of methanol. To the orange solution 0.0586 g (0.300 mmol) of AgBF₄ was added and the reaction mixture was stirred for 1 hour. ¹H-NMR spectra for [{η⁶-C₆H₅(CH₂)₃OCH₃}RuCl(PⁱPr₃)]⁺ BF₄⁻ showed the same chemical shifts as for **14a**.

³¹P-NMR (CD₂Cl₂) δ (ppm) = 48.26 (s, PⁱPr₃). Yield for C₁₉H₃₅ClOPRuAgBF₄ (533.792) 58% (0.072 g, 0.134 mmol).

0.021 g (0.0393 mmol) of [{η⁶-C₆H₅(CH₂)₃OCH₃}RuCl(PⁱPr₃)]⁺ BF₄⁻ was dissolved in CD₂Cl₂ and the solution was cooled to -78 °C using a dry ice/*i*propanol slush bath. 0.0114 g (0.055 mmol) of 1,1-diphenyl-2-propyn-1-ol was added and the solution was transferred to a NMR tube. The solution was slowly warmed up to -40 °C while the progress of the reaction was monitored by low temperature NMR spectroscopy.

³¹P-NMR (CD₂Cl₂) δ (ppm) = 68.68 ppm (s, PⁱPr₃).

IR (solution):

ν_{ccc} : 1920 cm⁻¹

5. Experimental part

5.4.20 Synthesis of $[(\eta^6\text{-p-cymene})\text{Ru}(\text{1-methylene-1,2-dihydro-naphthalenide})]^+ \text{BPh}_4^-$ (17)

In a typical run, 0.150 g (0.245 mmol) of $[(\eta^6\text{-p-cymene})\text{RuCl}_2]_2$ was reacted with 178 μl (0.245 mmol) of 2-methyl-3-butyn-2-ol and 0.336 g (0.98 mmol) of NaBPh_4 in 4 ml of CH_2Cl_2 and 4 ml of MeOH. After stirring over night, the reaction mixture was filtered by cannula filtration and filtrate was evaporated to dryness in vacuum. The residue was again dissolved in CH_2Cl_2 stirred for 45 min, filtered again, and the filtrate was evaporated under vacuum. The product was obtained as a red powder and was washed with 3 x 8 ml Et_2O and dried in vacuum. Yield 69.4% (0.132 g, 0.17mmol).

Analysis calcd. for $\text{C}_{50}\text{H}_{53}\text{RuOB}$ (781.85): C 76.81, H 6.83; found 74.78, 6.61%.

$^1\text{H-NMR}$ (CD_2Cl_2): δ (ppm) = 1.28 (3H, d, $\text{CH}_3(\text{iPr})$, $^3J_{\text{HH}} = 6.88$ Hz), 1.41 (3H, d, $\text{CH}_3(\text{iPr})$, $^3J_{\text{HH}} = 6.88$ Hz), 1.44 (3H, s, $\text{CH}_3(\text{naph})$), 1.57 (3H, s, $\text{CH}_3(\text{naph})$), 1.66 (3H, s, $\text{CH}_3(\text{naph})$), 1.77 (3H, s, $\text{CH}_3(\text{naph})$), 1.90 (1H, s(br.), OH), 2.05 (3H, s, $\text{CH}_3(\text{cym})$), 2.65 (1H, hept, $\text{CH}(\text{iPr})$, $^3J_{\text{H-H}} = 6.88$ Hz), 4.18 (1H, d, $\text{CH}(\text{cym})$, $^3J_{\text{HH}} = 6.2$ Hz), 4.7 (1H, s, CH], 4.82 (1H, d, $\text{CH}(\text{cym})$, $^3J_{\text{HH}} = 6.2$ Hz), 5.31 (1H, d, $\text{CH}(\text{cym})$, $^3J_{\text{HH}} = 6.2$ Hz), 5.36 (1H, d, $\text{CH}(\text{cym})$, $^3J_{\text{HH}} = 6.2$ Hz), 6.7 (1H, s, $\text{CH}(\text{naph})$), 7.31 (1H, t, $\text{CH}(\text{naph})$, $^3J_{\text{HH}} = 7.12$ Hz), 7.34 (1H, t, $\text{CH}(\text{naph})$, $^3J_{\text{HH}} = 7.18$ Hz), 7.42 (1H, t, $\text{CH}(\text{naph})$), 7.48 (1H, m, $\text{CH}(\text{naph})$).

$^{13}\text{C-NMR}$ (CD_2Cl_2): δ (ppm) = 18.91 (s, $\text{CH}_3(\text{naph})$), 19.17 (s, $\text{CH}_3(\text{cym})$), 19.75 (s, $\text{CH}_3(\text{naph})$), 21.95 (s, $\text{CH}_3(\text{naph})$), 24.20 (s, $\text{CH}_3(\text{iPr})$), 31.27 (s, $\text{CH}_3(\text{naph})$), 31.8 (s, $\text{CH}_3(\text{iPr})$), 33.85 (s, $\text{CH}(\text{iPr})$), 48.5 (s, CH), 70.0 (s, $\text{C}_{\text{quart}}(\text{alc})$), 77.4 (s, $\text{C}_{\text{quart}}(\text{naph})$], 81.7 (s, $\text{C}_{\text{quart}}(\text{naph})$) 84.70 (s, $\text{CH}(\text{cym})$), 88.2 (s, $\text{CH}(\text{cym})$), 86.7 (s, $\text{CH}(\text{cym})$), 90.6 (s, $\text{CH}(\text{cym})$), 101.4 (s, $\text{C}_{\text{quart}}(\text{naph})$), 105.6 (s, $\text{C}_{\text{quart}}(\text{cym})$), 116.2 (s, $\text{C}_{\text{quart}}(\text{cym})$), 121.5 (s, $\text{C}_{\text{quart}}(\text{alc})$), 123.0 (s, $\text{C}_{\text{quart}}(\text{naph})$), 127.2 (s, $\text{CH}(\text{naph})$), 127.6 (s, $\text{CH}(\text{naph})$), 130.6 (s, $\text{CH}(\text{naph})$), 134.4 (s, $\text{CH}(\text{naph})$).

IR (KBr): ν : 3545 cm^{-1} (OH), 1596 cm^{-1} (C=C).

5.4.21 Synthesis of complex 18

Under the same procedure as for **17**, 0.100 g (0.163 mmol) of $[(\eta^6\text{-p-cymene})\text{RuCl}_2]_2$ was reacted with 0.158 g (1.225 mmol) of 1-ethynylcyclohexanol and 0.213 g (0.652 mmol) of NaBPh_4 resulting in the product **18**.

Analysis calcd. (measured) for C₅₆H₆₁OBRu (861.98): C 78.03, 7.13 H; found C 76.31, H 7.46 %.

¹H-NMR (CD₂Cl₂): δ (ppm) = 1.32 (3H, d, CH₃(ⁱPr), ³J_{HH} = 6.88 Hz), 1.77 (3H, d, CH₃(ⁱPr), ³J_{HH} = 6.88 Hz), 1.56-2.00 (m, CH₂), 1.95 (1H, s(br), OH), 2.14 (3H, s, CH₃(cym)), 2.47 (1H, hept, CH(ⁱPr) ³J_{HH} = 6.88 Hz), 3.80 (1H, d, CH(cym), ³J_{HH} = 6.2 Hz), 4.53 (1H, s, CH), 4.70 (1H, d, CH(cym), ³J_{HH} = 6.2 Hz), 4.88 (1H, d, CH(cym), ³J_{HH} = 6.2 Hz), 5.05 (1H, d, CH(cym) ³J_{HH} = 6.2 Hz), 6.40 (1H, s, CH(naph)), 7.33 (1H, t, CH(naph), ³J_{HH} = 7.20 Hz), 7.34 (1H, t, CH(naph), ³J_{HH} = 7.20 Hz), 7.47 (1H, t, CH(naph), ³J_{HH} = 7.20 Hz), 7.48 (1H, m, CH(naph)).

¹³C-NMR (CD₂Cl₂): δ (ppm) = 16.13 (s, CH₃(cym)), 19.13 (s, CH₃(ⁱPr)), 26.21 (s, CH₂(alc)), 27.35 (s, CH₂(alc)), 28.74 (s, CH₂(alc)), 32.51 (s, CH₃(ⁱPr)), 38.36 (s, CH₂(alc)), 38.84 (s, CH₂(alc)), 39.13 (s, CH₂(alc)), 41.00 (s, CH(ⁱPr)), 46.82 (s, CH), 73.26 (s, C_{quart}(alc)), 80.06 (s, C_{quart}(naph)), 86.40 (s, C_{quart}(naph)), 88.56 (s, CH(cym)), 90.41 (s, CH(cym)), 92.94 (s, CH(cym)), 103.91 (s, CH(cym)), 107.44 (s, C_{quart}(naph)), 118.09 (s, C_{quart}(cym)), 122.65 (s, C_{quart}(cym)), 124.02 (s, C_{quart}(alc)), 127.95 (s, C_{quart}(naph)), 130.55 (s, CH(naph)), 132.86 (s, CH(naph)), 131.01 (s, CH(naph)), 138.18 (s, CH(naph)).

5.4.22 Synthesis of complex 19

Following the same procedure, 0.100 g (0.163 mmol) of [(η⁶-p-cymene)RuCl₂]₂ was reacted with 140 μl (1.225 mmol) of 1-ethynylcyclopentanol and 0.213 g (0.652 mmol) of NaBPh₄ resulting in the product **19**.

Analysis calcd. for C₅₄H₅₇OBRu (833.93): C 77.78, H 6.89; found 75.78, 6.87%.

¹H-NMR (CD₂Cl₂): δ (ppm) = 1.32 (3H, d, CH₃(ⁱPr), ³J_{HH} = 6.88 Hz), 1.77 (3H, d, ³J_{HH} = 6.88 Hz, CH₃(-Pr)), 1.56-2.00 (m, CH₂), 1.85 (1H, broad, OH), 2.14 (3H, s, CH₃(cym)), 2.47 (1H, hept, CH(ⁱPr), ³J_{HH} = 6.88 Hz), 3.98 (1H, d, CH(cym), ³J_{HH} = 6.2 Hz), 4.34 (1H, s, CH), 4.54 (1H, d, CH(cym), ³J_{HH} = 6.2 Hz), 4.80 (1H, d, CH(cym), ³J_{HH} = 6.2 Hz), 5.09 (1H, d, CH(cym) ³J_{HH} = 6.2 Hz), 6.66 (1H, s, CH(naph)), 7.33 (1H, t, CH(naph), ³J_{HH} = 7.20 Hz), 7.34 (1H, t, CH(naph), ³J_{HH} = 7.20 Hz), 7.47 (1H, t, CH(naph), ³J_{HH} = 7.20 Hz), 7.48 (1H, m, CH(naph)).

5. Experimental part

^{13}C -NMR (CD_2Cl_2): δ (ppm) = 21.07 (s, $\underline{\text{C}}\text{H}_3(\text{cym})$), 24.06 (s, $\underline{\text{C}}\text{H}_3(\textit{i}\text{Pr})$), 26.20 (s, $\underline{\text{C}}\text{H}_2(\text{alc})$), 26.35 (s, $\underline{\text{C}}\text{H}_2(\text{alc})$), 27.51 (s, $\underline{\text{C}}\text{H}_2(\text{alc})$), 31.89 (s, $\underline{\text{C}}\text{H}_3(\textit{i}\text{Pr})$), 35.81 (s, $\underline{\text{C}}\text{H}_2(\text{alc})$), 43.576 (s, $\underline{\text{C}}\text{H}(\textit{i}\text{Pr})$), 45.20 (s, $\underline{\text{C}}\text{H}$), 83.29 (s, $\text{C}_{\text{quart}}(\text{alc})$), 85.61 (s, $\text{C}_{\text{quart}}(\text{naph})$), 87.46 (s, $\text{C}_{\text{quart}}(\text{naph})$), 88.70 (s, $\underline{\text{C}}\text{H}(\text{cym})$), 88.76 (s, $\underline{\text{C}}\text{H}(\text{cym})$), 89.83 (s, $\underline{\text{C}}\text{H}(\text{cym})$), 91.64 (s, $\underline{\text{C}}\text{H}(\text{cym})$), 106.58 (s, $\text{C}_{\text{quart}}(\text{naph})$), 113.54 (s, $\text{C}_{\text{quart}}(\text{cym})$), 117.70 (s, $\text{C}_{\text{quart}}(\text{cym})$), 125.86 (s, $\text{C}_{\text{quart}}(\text{alc})$), 127.89 (s, $\text{C}_{\text{quart}}(\text{naph})$), 129.21 (s, $\underline{\text{C}}\text{H}(\text{naph})$), 129.54 (s, $\underline{\text{C}}\text{H}(\text{naph})$), 130.48 (s, $\underline{\text{C}}\text{H}(\text{naph})$), 138.18 (s, $\underline{\text{C}}\text{H}(\text{naph})$).

Analysis calcd. for $\text{C}_{54}\text{H}_{57}\text{OBRu}$ (833.93): C 77.78, H 6.89; found 75.78, 6.87%.

5.4.23 Synthesis of complex 17d₄/d₅

In a typical run, 0.060 g (0.196 mmol) of $\{(\eta^6\text{-p-cymene})\text{RuCl}_2\}_2$ was reacted with 71.3 μl (2.94 mmol) of 2-methyl-3-butyn-2-ol and 0.142 g (0.362 mmol) of $\text{NaBPh}_4\text{-d}_{20}$ in 4 ml of CH_2Cl_2 and 4 ml of MeOH. After stirring over night, the reaction mixture was filtered by cannula filtration and the filtrate was evaporated to dryness in vacuum. The residue was again dissolved in CH_2Cl_2 , stirred for 45 min, filtered again, and the filtrate was evaporated under vacuum. The product was obtained as red powder and was washed 3 x 5 ml Et_2O and dried in vacuum. Yield 70% (0.064 g, 0.14 mmol).

^1H -NMR (CD_2Cl_2): δ (ppm) = 1.27 (3H, d, $\underline{\text{C}}\text{H}_3(\textit{i}\text{Pr})$, $^3J_{\text{HH}} = 6.88$ Hz), 1.36 (3H, d, $\text{CH}_3(\textit{i}\text{Pr})$, $^3J_{\text{HH}} = 6.88$ Hz), 1.42 (3H, s, $\underline{\text{C}}\text{H}_3(\text{naph})$), 1.50 (3H, s, $\underline{\text{C}}\text{H}_3(\text{naph})$), 1.59 (3H, s, $\underline{\text{C}}\text{H}_3(\text{naph})$), 1.70 (3H, s, $\underline{\text{C}}\text{H}_3(\text{naph})$), 1.82 (1H, s(br.), $\underline{\text{O}}\text{H}$), 1.95 (3H, s, $\underline{\text{C}}\text{H}_3(\text{cym})$), 2.65 (1H, hept, $\underline{\text{C}}\text{H}(\textit{i}\text{Pr})$, $^3J_{\text{HH}} = 6.88$ Hz), 4.03 (1H, d, $\underline{\text{C}}\text{H}(\text{cym})$, $^3J_{\text{HH}} = 6.2$ Hz), 4.64 (1H, s, $\underline{\text{C}}\text{H}$), 4.82 (1H, d, $\underline{\text{C}}\text{H}(\text{cym})$, $^3J_{\text{HH}} = 6.2$ Hz), 5.31 (1H, d, $\underline{\text{C}}\text{H}(\text{cym})$, $^3J_{\text{HH}} = 6.2$ Hz), 5.36 (1H, d, $\underline{\text{C}}\text{H}(\text{cym})$, $^3J_{\text{HH}} = 6.2$ Hz), 6.71 (1H, s, $\underline{\text{C}}\text{H}(\text{naph})$).

^{13}C -NMR (CD_2Cl_2): δ (ppm) = 18.91 (s, $\underline{\text{C}}\text{H}_3(\text{naph})$), 19.17 (s, $\underline{\text{C}}\text{H}_3(\text{cym})$), 19.76 (s, $\underline{\text{C}}\text{H}_3(\text{naph})$), 21.96 (s, $\underline{\text{C}}\text{H}_3(\text{naph})$), 24.21 (s, $\underline{\text{C}}\text{H}_3(\textit{i}\text{Pr})$), 31.28 (s, $\underline{\text{C}}\text{H}_3(\text{naph})$), 31.87 (s, $\underline{\text{C}}\text{H}_3(\textit{i}\text{Pr})$), 32.39 (s, $\underline{\text{C}}\text{H}(\textit{i}\text{Pr})$), 48.51 (s, $\underline{\text{C}}\text{H}$), 70.0 (s, $\text{C}_{\text{quart}}(\text{alc})$), 77.4 (s, $\text{C}_{\text{quart}}(\text{naph})$), 81.7 (s, $\text{C}_{\text{quart}}(\text{naph})$), 84.70 (s, $\underline{\text{C}}\text{H}(\text{cym})$), 88.2 (s, $\underline{\text{C}}\text{H}(\text{cym})$), 86.71 (s, $\underline{\text{C}}\text{H}(\text{cym})$), 90.58 (s, $\underline{\text{C}}\text{H}(\text{cym})$), 101.40 (s, $\text{C}_{\text{quart}}(\text{naph})$), 105.57 (s, $\text{C}_{\text{quart}}(\text{cym})$), 116.19 (s, $\text{C}_{\text{quart}}(\text{cym})$), 122.50 (s, $\text{C}_{\text{quart}}(\text{alc})$), 123.20 (s, $\text{C}_{\text{quart}}(\text{naph})$), 127.25 (s, $\underline{\text{C}}\text{H}(\text{naph})$), 127.60 (s, $\underline{\text{C}}\text{H}(\text{naph})$), 130.6 (s, $\underline{\text{C}}\text{H}(\text{naph})$), 135.80 (s, $\underline{\text{C}}\text{H}(\text{naph})$).

MS (*m/z*) 467.1

6 Summary

Dimeric complexes $[(\eta^6\text{-arene})\text{RuCl}_2]_2$ constitute the most important entry point to the chemistry of $(\eta^6\text{-arene})\text{Ru}$ complexes. The vast number of catalytically active $(\text{arene})\text{Ru}$ complexes led our search for new $(\text{arene})\text{RuL}_n$ derivatives with potential utility in catalysis. These include allenylidene (propadienylidene, $=\text{C}=\text{C}=\text{RR}'$) complexes $[(\eta^6\text{-arene})\text{Cl}(\text{PR}_3)\text{Ru}=\text{C}=\text{C}=\text{RR}']^+$, derivatives $[(\eta^6\text{-C}_5\text{H}_5(\text{CH}_2)_m\text{OR})\text{RuCl}_2]_n$ ($m = 2$ or 3 ; $n = 1$ or 2 ; $R = \text{H}, \text{Me}$) bearing hemilabile hydroxy and ether functionalities, and simple thioether and pyridine adducts $[(\text{arene})\text{RuCl}_2(\text{L})]$ and $[(\text{arene})\text{RuCl}(\text{L})_2]^+$ ($\text{L} =$ substituted pyridine, thioether). Studies on transformations of alkynols widened our spectrum of interests from ruthenium allenylidene complexes to the cyclotrimerization of alkynols and the coupling of alkynols and a phenylate group on ruthenium templates. The latter transformations give rise to the highly selective assembly of unprecedented dihydronaphthalenide or naphthalene ligands.

One aspect of this work was the preparation of first examples of tethered ruthenium complexes containing arylalkyl substituted thioethers. Thioethers form substitutionally labile monomeric adducts $[(\eta^6\text{-p-cymene})\text{RuCl}_2(\text{SRR}')]_2$ upon treatment with the $[(\eta^6\text{-p-cymene})\text{RuCl}_2]_2$ dimer ($\text{p-cymene} = \eta^6\text{-MeC}_6\text{H}_4\text{-}i\text{Pr-1,4}$). Simple thioether adducts $[(\eta^6\text{-arene})\text{RuCl}_2(\text{SRR}')]_2$ are found to be labile in solution and are in equilibrium with the dichloro bridged precursor and the free thioether. Pure thioether adducts $[(\eta^6\text{-p-cymene})\text{RuCl}_2(\eta^1\text{-MeSC}_2\text{H}_4\text{Ph})]$ (**5**), $[(\eta^6\text{-p-cymene})\text{RuCl}_2(\text{MeSC}_3\text{H}_5)]$ (**6**), and $[(\eta^6\text{-p-cymene})\text{RuCl}(\text{SMe}_2)_2]^+ \text{SbF}_6^-$ (**7**) represent rare examples of $(\text{arene})\text{Ru}$ complexes bearing simple thioether ligands that have been structurally characterized (Figure 37).

The electrochemical properties of these complexes were studied in detail. All complexes undergo one partially to nearly reversible oxidation and one chemically completely irreversible reduction within the potential window of the $\text{CH}_2\text{Cl}_2/\text{NBu}_4\text{PF}_6$ supporting electrolyte. The mono(thioether) complexes undergo oxidation at potentials near $+0.85$ V whereas the cationic bis(thioether) derivative **7** is much harder to oxidize and gives an $E_{1/2}$ of $+1.44$ V. All our attempts to thermally or photochemically convert complexes $[(\eta^6\text{-p-cymene})\text{RuCl}_2(\eta^1\text{-MeSC}_2\text{H}_4\text{Ph})]$ or $[(\eta^6\text{-p-cymene})\text{RuCl}_2(\eta^1\text{-}i\text{PrSC}_3\text{H}_6\text{Ph})]$ to derivatives bearing tethered thioether ligand such as $[(\eta^6\text{-}\eta^1\text{-C}_6\text{H}_5(\text{CH}_2)_n\text{SR})\text{Cl}_2(\text{L})\text{Ru}]$ were, however, met with failure.

6. Summary

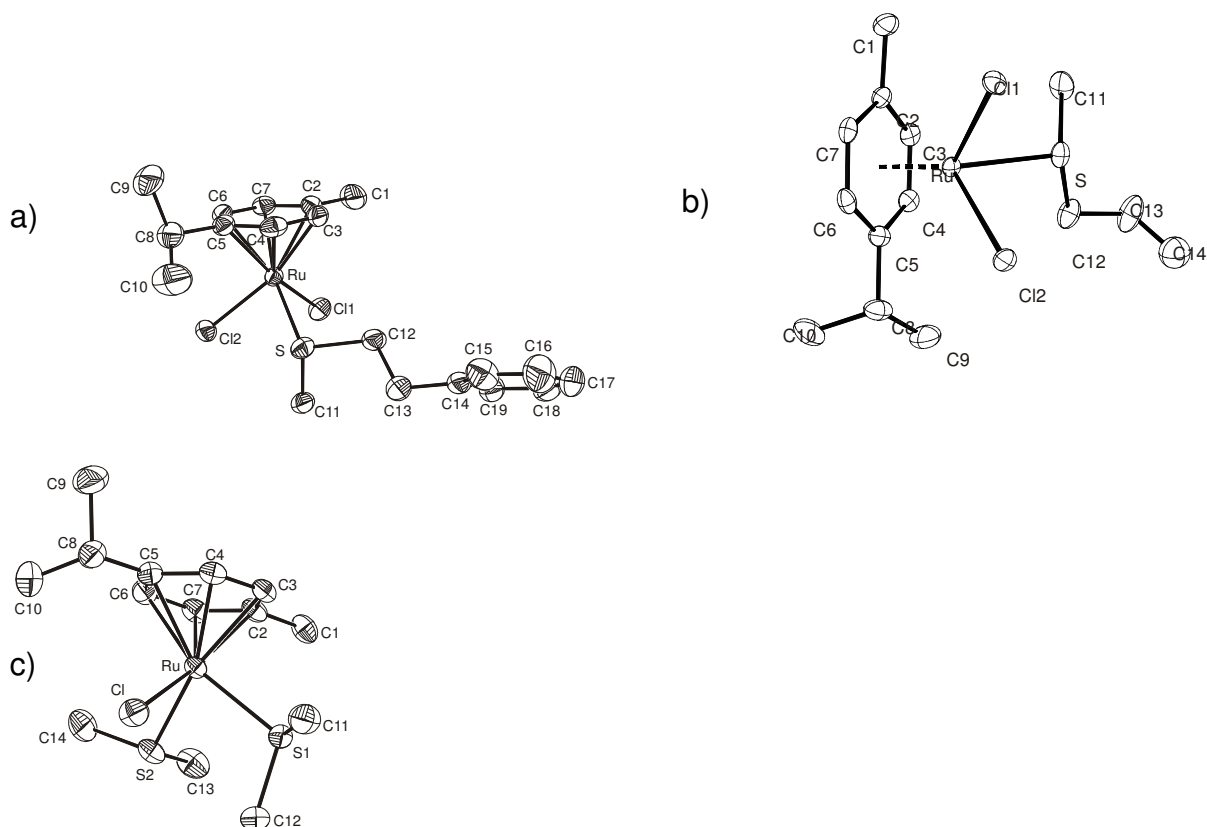


Figure 37: Molecular structures of a) $[(\eta^6\text{-p-cymene})\text{RuCl}_2(\eta^1\text{-MeSC}_2\text{H}_4\text{Ph})]$ (5), b) $[(\eta^6\text{-p-cymene})\text{RuCl}_2(\text{MeSC}_3\text{H}_5)]$ (6), c) $[(\eta^6\text{-p-cymene})\text{RuCl}(\text{SMe}_2)_2]^+ \text{SbF}_6^-$ (7).

Whereas a considerable number of arene ruthenium half-sandwich complexes with tethered phosphine donors are known in the literature, much less work has been done on complexes of arenes with oxygen containing groups such as ethers or alcohols. We here report on the hydroxyalkyl appended arene ruthenium half sandwich complexes $[(\eta^6\text{-C}_6\text{H}_5(\text{CH}_2)_m\text{OH})\text{RuCl}_2]_n$ ($m = 2$ or 3 ; $n = 1$ or 2) and the methyl ether of the hydroxypropyl derivative. Most significantly, the comparison between the hydroxypropyl complex and its methyl ether reveals significantly different structures (Figure 38). The methyl ether adopts the usual dichlorobridged dimeric structure with an uncoordinated dangling methoxy substituent. The corresponding hydroxy complex is, however, monomeric in the solid state with the OH group of the side chain coordinated to the metal. The arrangement of individual molecules in the crystal lattice is governed by hydrogen bridges between the OH proton of one and one Cl^- ligand of a neighboring molecule and by sheet-like arrangements of the coordinated arenes. The poor solubility of the hydroxy substituted complexes in non coordinating solvents suggests that these intermolecular interactions are rather strong.

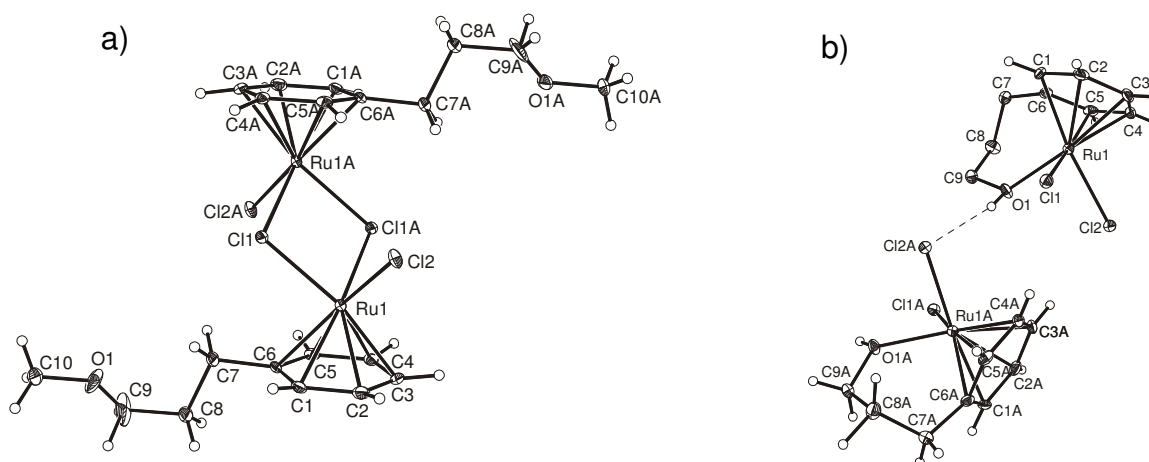


Figure 38: X-ray structures of a) $[\{\eta^6\text{-C}_6\text{H}_5(\text{CH}_2)_3\text{OMe}\}\text{RuCl}_2]_2$ (**14**),
 b) $[\{\eta^6:\eta^1\text{-C}_6\text{H}_5(\text{CH}_2)_3\text{OH}\}\text{RuCl}_2]$ (**13**).

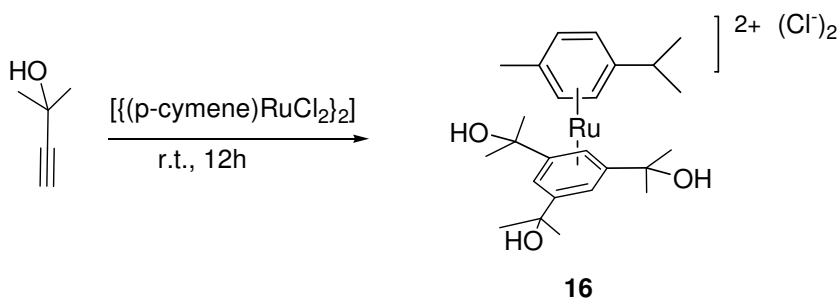
Several phosphine adducts have been prepared from the hydroxy or alkoxy functionalized $[\{\eta^6\text{-C}_6\text{H}_5(\text{CH}_2)_m\text{OR}\}\text{RuCl}_2]_n$ ($m = 2$ or 3 ; $n = 1$ or 2 ; $R = \text{H}, \text{Me}$) precursors. The electrochemical properties of the phosphine adducts and of the dichloro bridged aryl ether complex are also discussed. Half-sandwich dichloro complexes of the type $[(\eta^6\text{-arene})\text{RuCl}_2]_2$ display a rather intricate behavior with a rich chemistry following or even preceding each electron transfer step. We investigated the electrochemical properties of $[\{\eta^6\text{-C}_6\text{H}_5(\text{CH}_2)_3\text{OMe}\}\text{RuCl}_2]_2$ in $\text{CH}_2\text{Cl}_2/\text{NBu}_4\text{PF}_6$. Voltammograms at room temperature show a close to reversible reduction at -0.79 V and an irreversible anodic oxidation at $E_p = +0.33$ V. Half-sandwich phosphine complexes of the type $[(\eta^6\text{-arene})\text{RuCl}_2(\text{PR}_3)]$, on the other hand, display much simpler electrochemical responses and usually undergo a chemically reversible oxidation at potentials of $+0.69$ to $+0.77$ V.

Allenyldiene complexes $[\{\eta^6\text{-C}_6\text{H}_5(\text{CH}_2)_m\text{OH}\}\text{Cl}_2(\text{PR}_3)\text{Ru}=\text{C}=\text{C}=\text{CPh}_2]^+$ ($m = 2, 3$; $R = \text{H}, \text{Me}$) have been prepared from the dichloro phosphine precursors via a sequence involving chloride abstraction with AgX , activation of diphenylpropynol by the resulting, coordinatively unsaturated $[\{\eta^6\text{-C}_6\text{H}_5(\text{CH}_2)_m\text{OR}\}\text{RuCl}(\text{PR}_3)]^+$ and dehydration to the allenylidene complex. Their formation is firmly established by ^{31}P -NMR and IR spectroscopy, but they are thermally labile and decompose at temperatures above 0°C .

6. Summary

The low thermal stability renders these potential olefin metathesis precatalysts inactive in the ring closure metathesis (RCM) of diallylmalonate and N,N-diallyltosylamine.

Alkyne cyclotrimerizations have been highly successful in the formation of substituted benzenes. In contrast, similar reactions involving alkynols have been met with only limited success, presumably because of inactivation of the catalytic metal center by reaction with oxygen atom on the alkynol. We investigated whether arene dichloro ruthenium complexes can function as templates for cyclooligomerization and co-cyclization reactions of alkynols. From our attempts to effect the cyclotrimerization of 2-methyl-but-3-yn-2-ol, we isolated the complex $[(\eta^6\text{-p-cymene})\{\eta^6\text{-C}_6\text{H}_3(\text{CMe}_2\text{OH})_{3-1,3,5}\}\text{Ru}]^{2+} 2\text{Cl}^- \times 2\text{H}_2\text{O}$, which was identified by X-ray crystallography. The symmetrically trisubstituted arene ring originates from the cyclotrimerization of the starting alkynol on the $\{(\text{p-cymene})\text{Ru}\}^{2+}$ template (Figure 39). We also obtained some spectroscopic evidence for the formation of trisubstituted benzenes from the reaction of propargylic alcohols in the presence of catalytic amounts of $\{[\eta^6\text{-arene}\text{RuCl}_2]_2\}$ complexes, but the results are inferior to those of the established $[\text{Ni}(\text{PR}_3)\text{X}_2]$ ($\text{X} = \text{Cl}, \text{I}$) systems.



Scheme 40: Synthesis of $[(\eta^6\text{-p-cymene})\{\eta^6\text{-C}_6\text{H}_3(\text{CMe}_2\text{OH})_{3-1,3,5}\}\text{Ru}]^{2+} (\text{Cl}^-)_2 \times 2 \text{H}_2\text{O}$ (**16**).

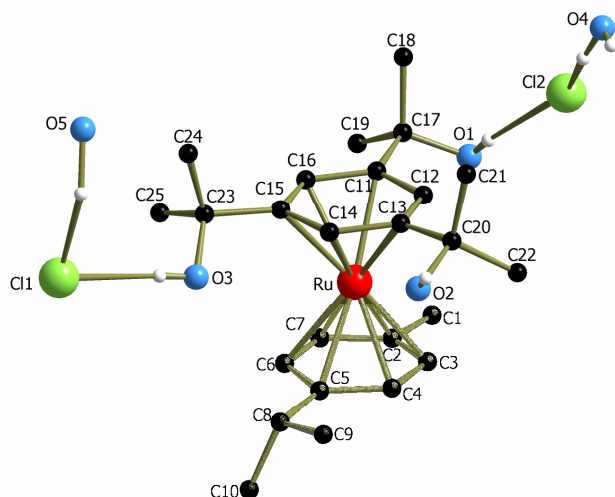
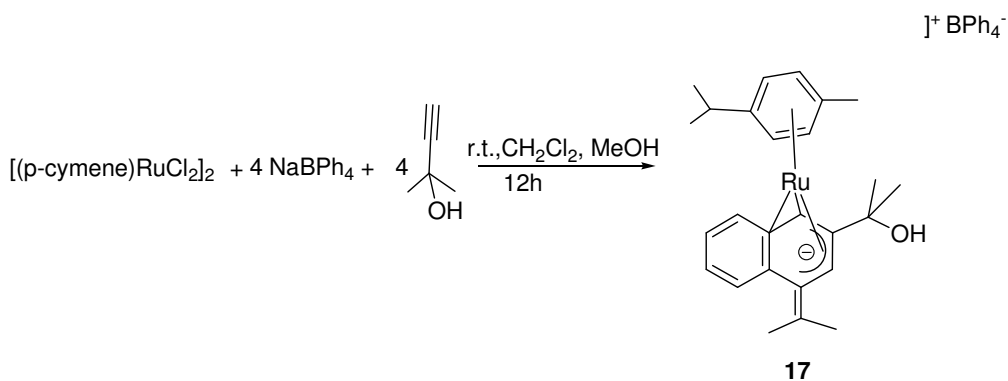


Figure 39: Molecular structure of $[(\eta^6\text{-p-cymene})\{\eta^6\text{-C}_6\text{H}_3(\text{CMe}_2\text{OH})_3\text{-1,3,5}\}\text{Ru}]^{2+} (\text{Cl}^-)_2 \times 2 \text{H}_2\text{O}$ (**16**).

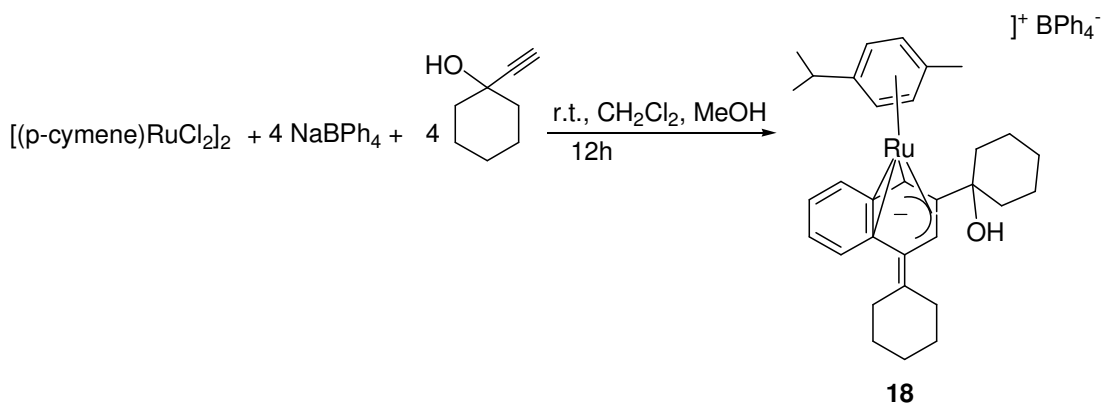
The co-cyclization and the stoichiometric coupling of a phenylate group and two equivalents of 2-methyl-but-3-yn-2-ol on $[(\eta^6\text{-p-cymene})\text{RuCl}_2]_2$ in the presence of NaBPh_4 affords, in a highly selective manner, unprecedented $\eta^5\text{-1-methylene-1,2-dihydronaphthalenide}$ ligands.



Scheme 41: Synthesis of $\eta^5\text{-1-methylene-1,2-dihydronaphthalenide}$ ruthenium complex (**17**).

The two-dimensional C,H and H,H correlation spectra allowed us to establish the ligand structure as it is depicted in Scheme 41. As to the formation of the dihydronaphthalenide ligand we suggest the reaction sequence outlined in Figure 40. Reactions with 1-ethynylcyclopentanol and 1-ethynylcyclohexanol provided complexes bearing dihydronaphthalenide ligands of the same architecture as in complex **18** (Scheme 42). In contrast, the reaction of 2-methyl-but-3-yn-2-ol with $[(\eta^6\text{-C}_6\text{H}_5(\text{CH}_2)_3\text{OMe})\text{RuCl}_2]_2$ under identical conditions provided the dicationic naphthalenide complex **21** (Scheme 43).

6. Summary



Scheme 42: Synthesis of complex **18**.

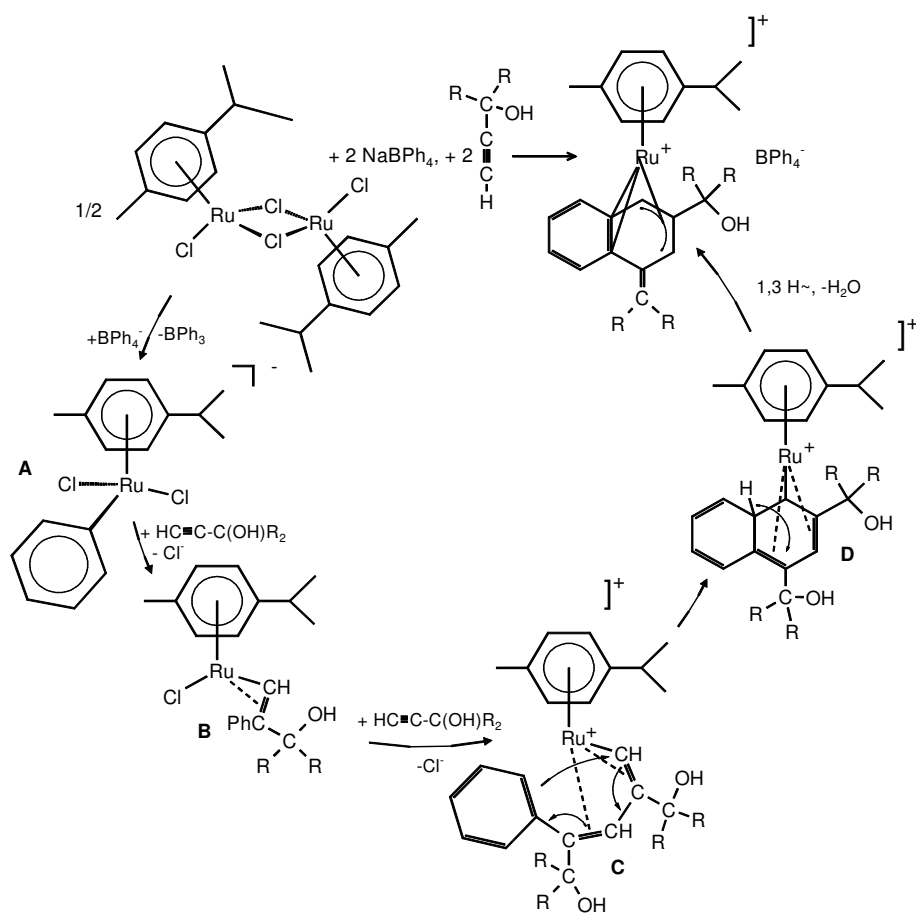
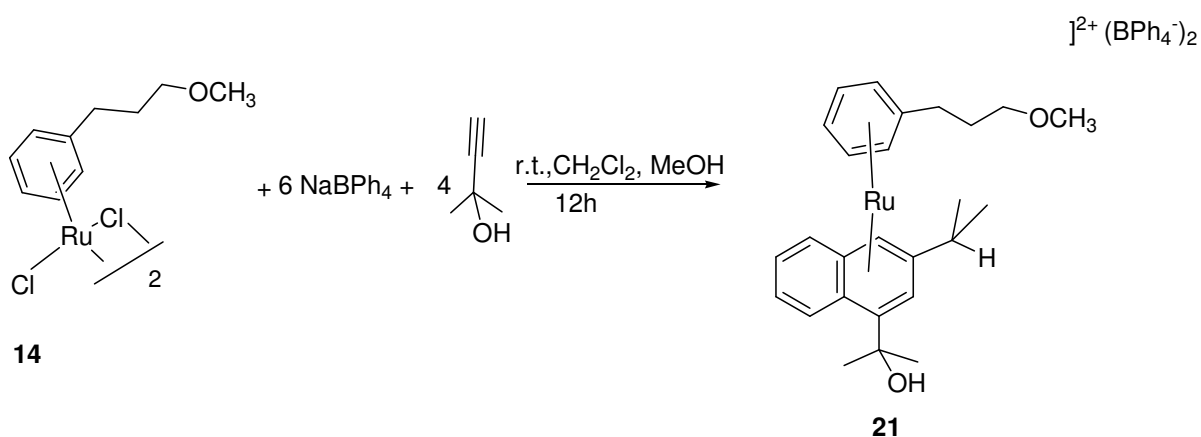


Figure 40: Proposed reaction sequence in the formation of complex **17**.



Scheme 43: Synthesis of complex **21**.

While all intermediates along the proposed reaction path are speculative, we performed DFT calculations using Gaussian98 on the conversion of **1** and 2-methyl-but-3-yn-2-ol to complex **17**. The geometries of the proposed reaction intermediates have been optimized and their energies have been evaluated. The results of this study confirm that the overall process is exergonic and that all postulated intermediates correspond to the minima on the energy hypersurface. The thermodynamic profile of this process is depicted as Figure 41.

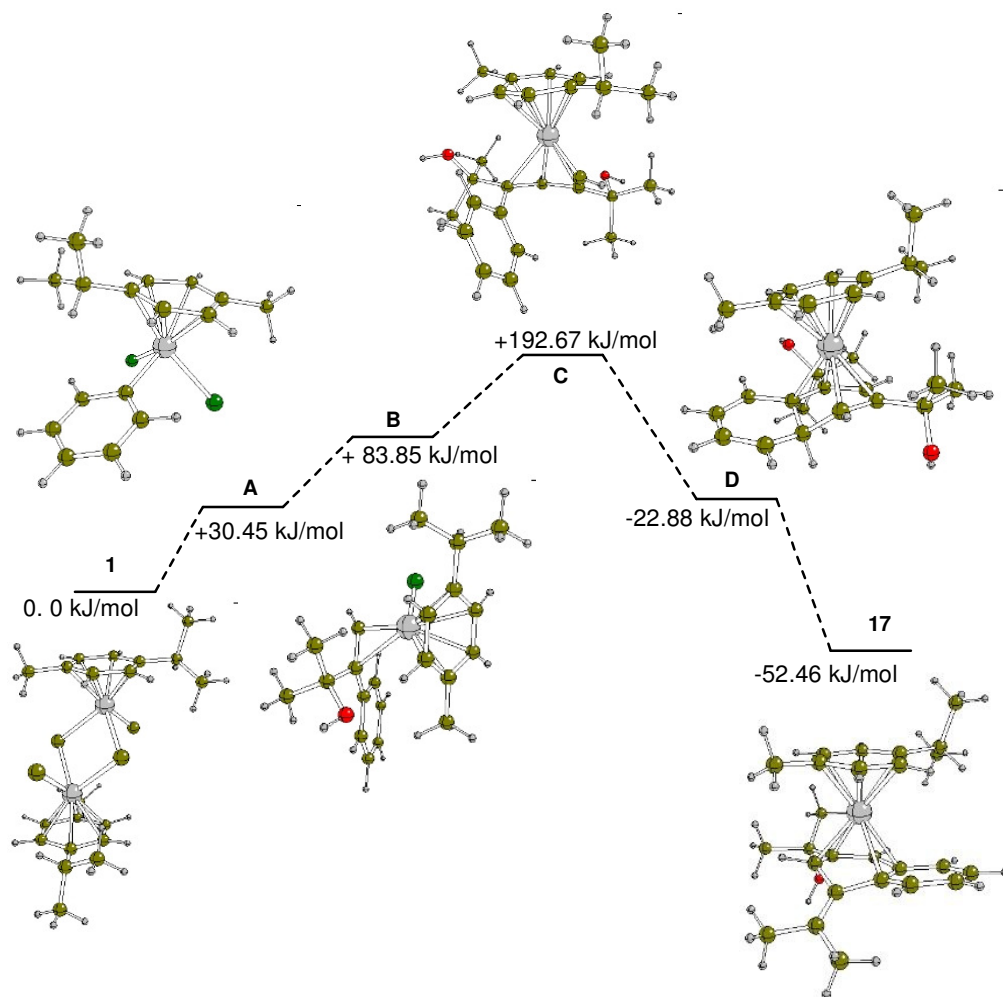


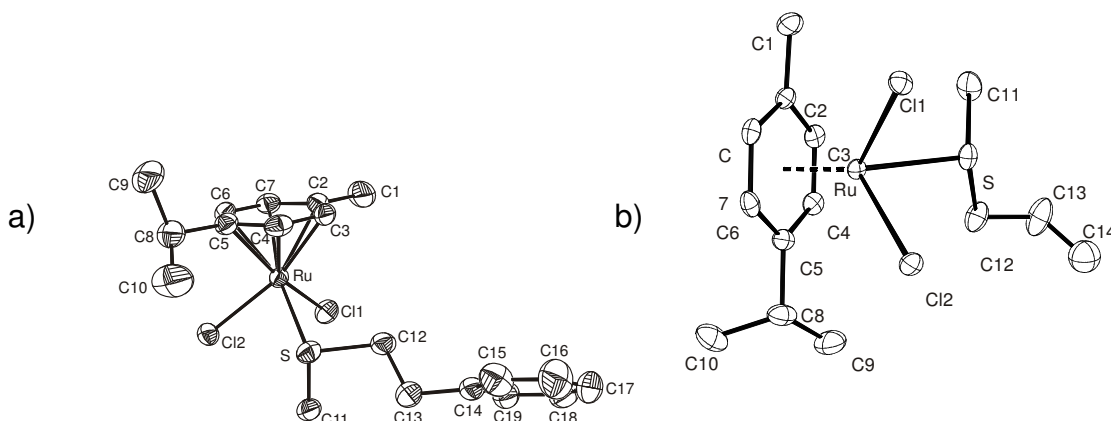
Figure 41: Energy profile for the reaction of $[\{(\eta^6\text{-p-cymene})\text{RuCl}_2\}_2]$ (**1**) with NaBPh_4 and 2-methyl-but-3-yn-2-ol to give complex **17** (energies are given in kJ/mol relative to a half molecule of **1**).

We have confirmed that the unsubstituted phenyl ring of the dihydronaphthalenide skeleton originates from the tetraphenyl borate counter ion employing $\text{BPh}_4^- \text{-d}_{20}$. All hydrogen atoms of this ring as well as one of H atoms of the water molecule released during the final dehydration step originate from a phenylate group of the BPh_4^- anion. Triphenylboroxine, $(\text{PhBO})_3$, and benzene have been identified by NMR and mass spectrometry as the methanolysis products of the released BPh_3 .

7 Zusammenfassung

Dimere Komplexe des Typs $[(\eta^6\text{-Aren})\text{RuCl}_2]_2$ stellen den wichtigsten Zugang zur Chemie der η^6 -Aren-Rutheniumkomplexe dar. Die Vielzahl katalytisch aktiver Aren-Rutheniumkomplexe führte zu unserer Suche nach neuen $(\text{Aren})\text{RuL}_n$ -Derivaten mit möglicher Verwendung in der Katalyse. Zu diesen gehören Allenyliden- (Propadienylden-, $=\text{C}=\text{C}=\text{RR}'$) Komplexe $[(\eta^6\text{-Aren})\text{Cl}(\text{PR}_3)\text{Ru}=\text{C}=\text{C}=\text{RR}']^+$, Derivate $[(\eta^6\text{-C}_5\text{H}_5(\text{CH}_2)_m\text{OR})\text{RuCl}_2]_n$ ($m = 2$ oder 3 ; $n = 1$ oder 2 ; $\text{R} = \text{H}, \text{Me}$) mit hemilabilen Hydroxy- und Ether-Funktionalitäten, sowie einfache Thioether- und Pyridin-Addukte $[(\text{Aren})\text{RuCl}_2(\text{L})]$ und $[(\text{Aren})\text{RuCl}(\text{L})_2]^+$ ($\text{L} =$ substituierte Pyridine oder Thioether). Untersuchungen zur Umwandlung von Alkinolen erweiterten unser Interessenspektrum von Rutheniumallenylidenkomplexen um die Cyclotrimerisierung von Alkinolen und um die Kupplung von Alkinolen und einer Phenylatgruppe am Rutheniumtemplat. Die letztgenannte Reaktion führt zur hochselektiven Bildung von Dihydronaphthalenid- oder Naphthalenliganden.

Ein Gesichtspunkt dieser Arbeit war die Darstellung der ersten Rutheniumkomplexe mit Arylalkyl-substituierten Thioethern als Henkelliganden. Bei Umsetzung mit dem $[(\eta^6\text{-p-Cymen})\text{RuCl}_2]_2$ -Dimer ($\text{p-Cymen} = \eta^6\text{-MeC}_6\text{H}_4\text{iPr-1,4}$) bilden Thioether substitutionslabile monomere Addukte $[(\eta^6\text{-p-Cymen})\text{RuCl}_2(\text{SRR}')]^+$. Einfache Thioetheraddukte $[(\eta^6\text{-Aren})\text{RuCl}_2(\text{SRR}')]^+$ sind in Lösung nicht stabil und stehen im Gleichgewicht mit dem zweifach chloroverbrückten Edukt und dem freien Thioether. Die reinen Thioetheraddukte $[(\eta^6\text{-p-Cymen})\text{RuCl}_2(\eta^1\text{-MeSC}_2\text{H}_4\text{Ph})]$ (5), $[(\eta^6\text{-p-Cymen})\text{RuCl}_2(\text{MeSC}_3\text{H}_5)]$ (6) und $[(\eta^6\text{-p-Cymen})\text{RuCl}(\text{SMe}_2)_2]^+ \text{SbF}_6^-$ (7) stellen daher seltene Beispiele für strukturell charakterisierte Arenrutheniumkomplexe mit einfachen Thioetherliganden dar (Abbildung 42).



c)

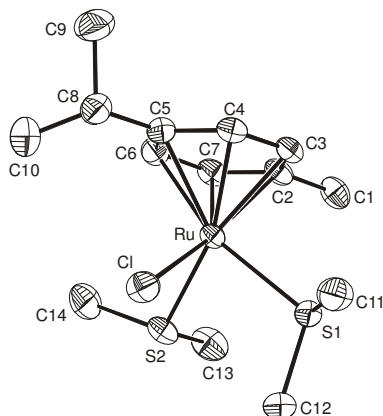


Abbildung 42: Molekülstrukturen von a) [(p-Cymen)RuCl₂(η¹-MeSC₂H₄Ph)] (**5**),
 b) [(p-Cymen)RuCl₂(MeSC₃H₅)] (**6**),
 c) [(p-Cymen)RuCl(SMe₂)₂]⁺ SbF₆⁻ (**7**).

Die elektrochemischen Eigenschaften dieser Komplexe wurden im Detail untersucht. Alle Komplexe zeigen eine teilweise bis nahezu reversible Oxidation und eine chemisch vollständig irreversible Reduktion innerhalb des Potentialfensters des CH₂Cl₂/NBu₄PF₆ Leitelektrolyten. Die Monothioetherkomplexe werden bei Potentialen von etwa +0.85 V oxidiert, während das kationische Bisthioetherderivat **7** viel schwerer zu oxidieren ist (E_{1/2} = +1.44 V). Alle Versuche, die Komplexe [(η⁶-p-Cymen)RuCl₂(η¹-MeSC₂H₄Ph)] oder [(η⁶-p-Cymen)RuCl₂(η¹-i-PrSC₃H₆Ph)] thermisch oder photochemisch zu Derivaten [(η⁶:η¹-C₆H₅(CH₂)_nSR)Cl₂Ru] mit Arenthioether-Henkelliganden umzuwandeln, schlugen fehl.

Während etliche verhenkelte Arenruthenium-Halbsandwichkomplexe mit Aralkyl-Phosphindonorgruppen existieren, gibt es deutlich weniger Beispiele für Arenkomplexe mit sauerstoffhaltigen Gruppen wie Ether oder Alkohole. Wir berichten hier über Arenruthenium-Halbsandwichkomplexe mit Hydroxyalkyl-Seitenketten [(η⁶-C₆H₅(CH₂)_mOH}RuCl₂]_n (m = 2 oder 3; n = 1 oder 2) und den Methylether des Hydroxypropylderivats. Interessanterweise zeigen sich im Vergleich zwischen dem Hydroxypropylkomplex und seinem Methylether signifikant unterschiedliche Strukturen (Abbildung 43). Der Methylether besitzt die übliche, zweifach chlorverbrückte dimere Struktur mit einem unkoordinierten Methoxysubstituenten. Der entsprechende Hydroxykomplex jedoch ist im festen Zustand monomer, wobei die OH-Gruppe der Seitenkette an das Metall koordiniert ist. Die Anordnung der einzelnen Moleküle im Kristall

wird durch die Wasserstoffbrücken zwischen den OH-Protonen des einen und einem Cl⁻-Liganden eines benachbarten Moleküls sowie eine schichtartige Anordnung der koordinierten Arene bestimmt. Die schlechte Löslichkeit der hydroxysubstituierten Komplexe in nicht-koordinierenden Lösungsmitteln weist darauf hin, dass diese intermolekularen Wechselwirkungen recht stark sind.

Mehrere Phosphinaddukte der hydroxy- oder alkoxyfunktionalisierten Komplexe $[\{\eta^6\text{-C}_6\text{H}_5(\text{CH}_2)_m\text{OR}\}\text{RuCl}_2]_n$ ($m = 2$ oder 3 ; $n = 1$ oder 2 ; $R = \text{H}, \text{Me}$) wurden dargestellt. Die elektrochemischen Eigenschaften der Phosphinaddukte und der dichlorverbrückten Aryletherkomplexe werden ebenfalls beschrieben. Die Elektrochemie der Halbsandwich-Komplexe des Typs $[\{(\eta^6\text{-Aren})\text{RuCl}_2\}_2]$ zeigt ein recht komplexes Verhalten. Jedem einzelnen Elektronentransferschritt sind chemische Folgeprozesse nachgelagert; teilweise gehen sie dem Elektronenübertrag sogar voraus. Wir haben die elektrochemischen Eigenschaften von $[\{\eta^6\text{-C}_6\text{H}_5(\text{CH}_2)_3\text{OMe}\}\text{RuCl}_2]_2$ in $\text{CH}_2\text{Cl}_2/\text{NBu}_4\text{PF}_6$ untersucht. Bei Zimmertemperatur zeigen die Voltammogramme eine nahezu reversible Reduktion bei -0.79 V und eine irreversible anodische Oxidation bei $E_p = +0.33 \text{ V}$.

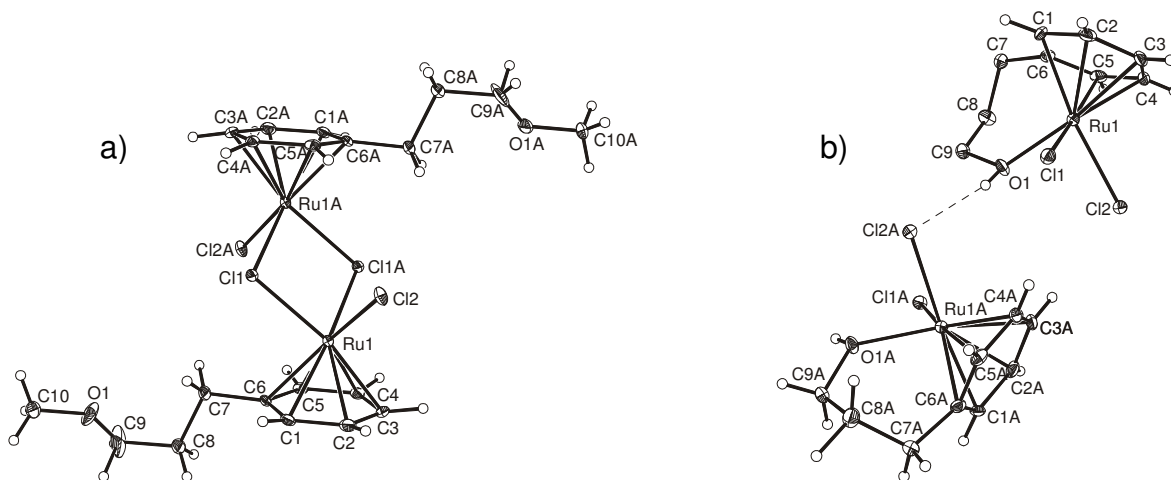


Abbildung 43: Molekülstrukturen von a) $[\{\eta^6\text{-C}_6\text{H}_5(\text{CH}_2)_3\text{OMe}\}\text{RuCl}_2]$ (**14**),
b) $[\{(\eta^6:\eta^1\text{-C}_6\text{H}_5(\text{CH}_2)_3\text{OH})\}\text{RuCl}_2]$ (**13**) im Kristall.

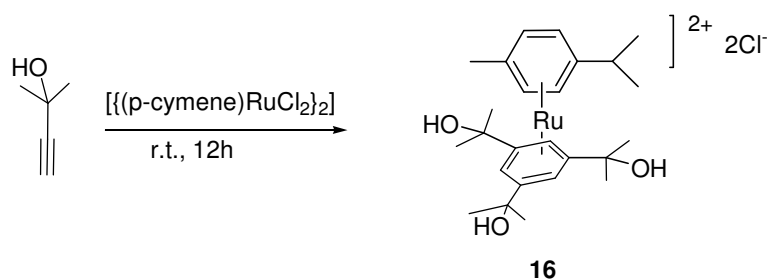
Halbsandwich-Phosphinkomplexe des Typs $[(\eta^6\text{-Aren})\text{RuCl}_2(\text{PR}_3)]$ zeigen ein weitaus einfacheres elektrochemisches Verhalten. Sie werden bei recht positiven Potentialen von $+0.69$ bis $+0.77 \text{ V}$ chemisch reversibel oxidiert.

Die Allenylidenkomplexe $[\{\eta^6\text{-C}_6\text{H}_5(\text{CH}_2)_m\text{OH}\}\text{Cl}_2(\text{PR}_3)\text{Ru}=\text{C}=\text{C}=\text{CPh}_2]^+$ ($m = 2$ oder 3 ; $R = \text{H}, \text{Me}$) wurden aus den Dichlorphosphinkomplexen über eine Schrittfolge aus Chloridabspaltung mit AgX , Aktivierung des Diphenylpropinols durch das entstehende, koordinativ ungesättigte $[\{\eta^6\text{-C}_6\text{H}_5(\text{CH}_2)_m\text{OR}\}\text{RuCl}(\text{PR}_3)]^+$ und Dehydratisierung zum

7. Zusammenfassung

Allenylidenkomplex dargestellt. Ihre Bildung konnte eindeutig durch ^{31}P -NMR- und IR-Spektroskopie nachgewiesen werden, jedoch sind die Verbindungen thermisch labil und zersetzen sich oberhalb von 0°C . Die geringe thermische Stabilität führt dazu, dass diese potenziellen Olefinmetathese-Präkatalysatoren keinerlei Aktivität hinsichtlich der Ringschlussmetathese (RCM) von Diallylmalonat und N,N-Diallyltosylamin zeigen.

Während die Cyclotrimerisierung von Alkinen einen der wichtigsten Zugangswege zu Aromaten darstellt, blieben Versuche zur Cyclotrimerisierung von Alkinolen bislang nur von begrenztem Erfolg. Dies ist vermutlich auf die Deaktivierung des katalytisch aktiven Metallzentrums durch die Reaktion mit dem Sauerstoffatom am Alkinol zurückzuführen. Wir untersuchten, ob sich einfache Dichlorarenrutheniumkomplexe als Template für die Cyclooligomerisierung und Cocyclisierung von Alkinolen eignen. Bei unseren Versuchen zur Cyclotrimerisierung von 2-Methyl-but-3-in-2-ol wurde der Komplex $[(\eta^6\text{-p-Cymen})\{\eta^6\text{-C}_6\text{H}_3(\text{CMe}_2\text{OH})_{3-1,3,5}\}\text{Ru}]^{2+} 2\text{Cl}^- \times 2\text{H}_2\text{O}$ isoliert und kristallographisch charakterisiert. Der symmetrische, dreifach substituierte Arenring ist tatsächlich ein Cyclotrimer des als Ausgangsmaterials verwendeten Alkinols (Abbildung 44). Auf spektroskopischem Wege erhielten wir zudem Hinweise auf die Bildung dreifach substituierter Benzole bei der Reaktion von katalytischen Mengen von $[(\eta^6\text{-Aren})\text{RuCl}_2]_2$ -Komplexen mit Propargylalkoholen. Allerdings sind die Ergebnisse weitaus schlechter als diejenigen, welche mit den etablierten $[\text{Ni}(\text{PR}_3)\text{X}_2]$ ($\text{X} = \text{Cl}, \text{I}$) - Systemen erzielt werden konnten.



Schema 44: Synthese von $[(\eta^6\text{-p-Cymen})\{\eta^6\text{-C}_6\text{H}_3(\text{CMe}_2\text{OH})_{3-1,3,5}\}\text{Ru}]^{2+} (\text{Cl})_2 \times 2 \text{H}_2\text{O}$ (**16**).

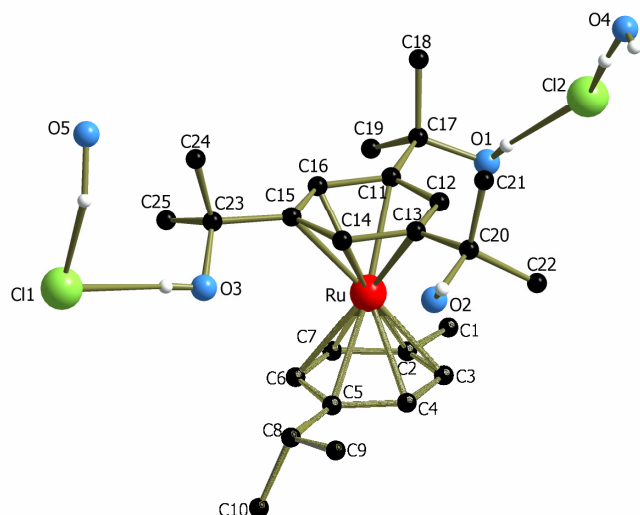
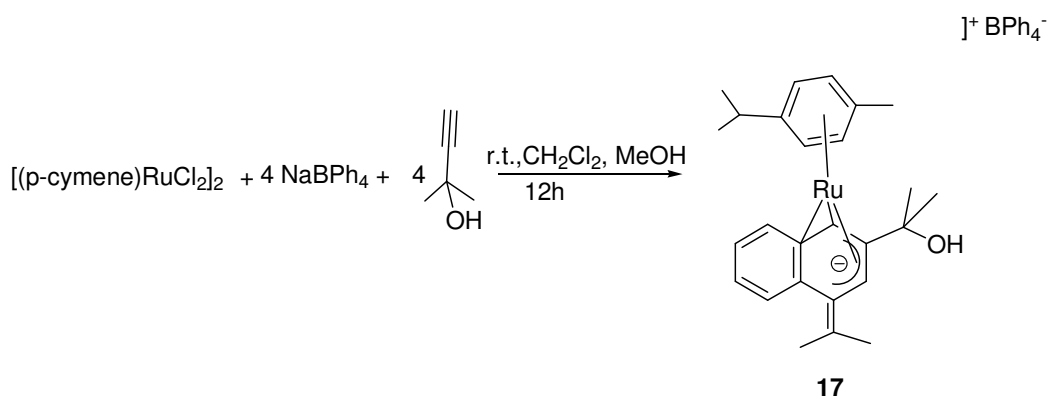


Abbildung 44: Molekülstruktur von $[(\eta^6\text{-p-Cymen})\{\eta^5\text{-C}_6\text{H}_3(\text{CMe}_2\text{OH})_3\text{-1,3,5}\}\text{Ru}]^{2+}(\text{Cl}^-) \times 2 \text{H}_2\text{O}$ (**16**).

Die Cocyclisierung und die stöchiometrische Kopplung von einem Phenylatrest und zwei Äquivalenten von 2-Methyl-but-3-in-2-ol durch $\{[(\eta^6\text{-p-Cymen})\text{RuCl}_2]_2\}$ in Gegenwart von NaBPh_4 ergibt hochselektiv einen Komplex mit dem bislang unbekanntem $\eta^5\text{-1-Methylen-1,2-dihydranaphtalenid-Liganden}$.



Schema 45: Synthese eines Komplexes mit dem neuartigen $\eta^5\text{-1-Methylen-1,2-dihydranaphtalenidliganden}$ (**17**).

Mit Hilfe zweidimensionaler C,H- und H,H-Korrelationspektren konnten wir die Ligandstruktur ermitteln; sie ist in Schema 45 dargestellt. Zur Bildung des Dihydranaphtalenidliganden schlagen wir die Reaktionsfolge in Abbildung 45 vor.

7. Zusammenfassung

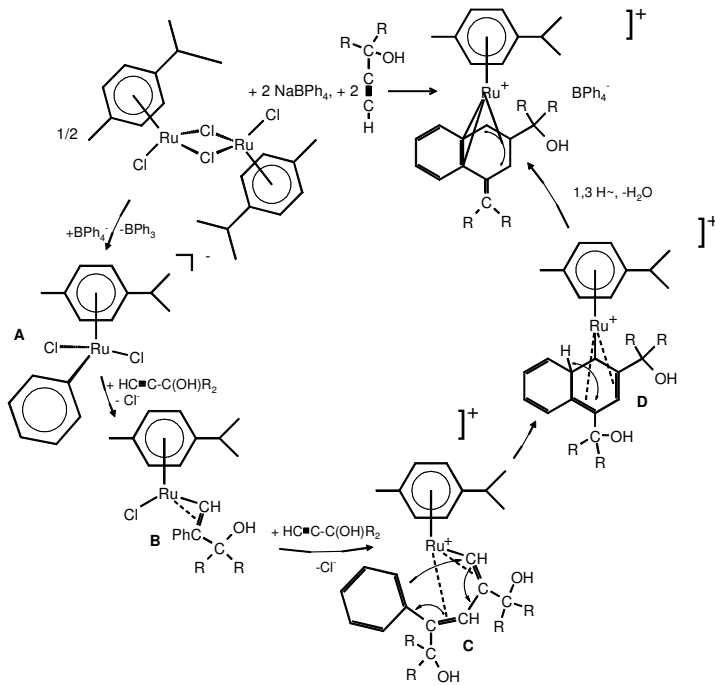
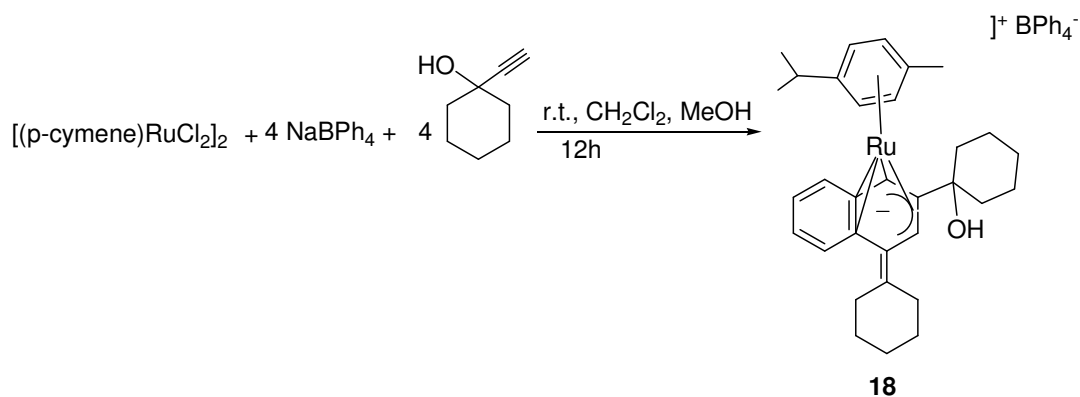
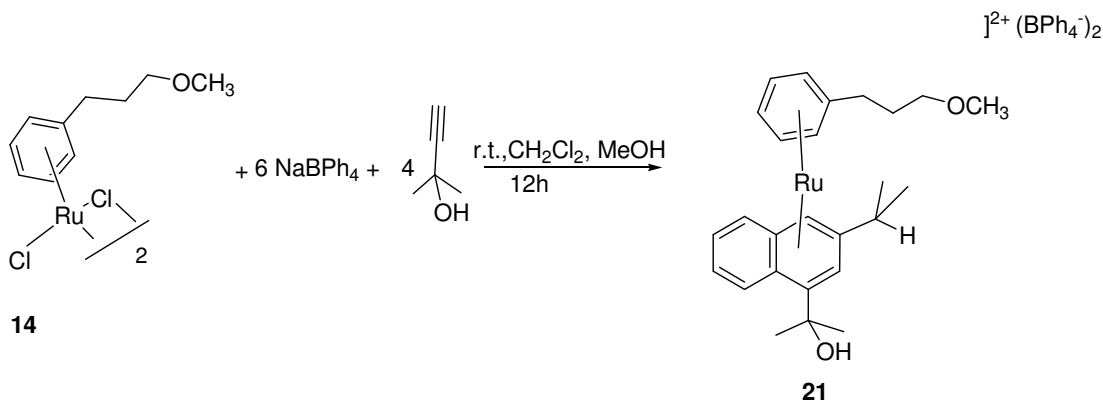


Abbildung 45: Vorgeschlagene Reaktionsfolge für die Bildung von Komplex 17.

Reaktionen mit unterschiedlichen Alkinolen wie 1-Ethynylcyclohexanol und 1-Ethynylcyclopentanol und mit unterschiedlichen substituierten Arenen ergab im Fall des 1-Ethynylcyclohexanols und -pentinols die gleiche Naphthalenidstruktur wie für Komplex 18 (Schema 46). Im Fall von $[\{\eta^6\text{-C}_6\text{H}_5(\text{CH}_2)_3\text{OMe}\}\text{RuCl}_2]$ entsteht dagegen der dikationische Naphthalenidkomplex 21 (Schema 47).



Schema 46: Synthese des Komplexes 18.



Schema 47: Synthese des Komplexes **21**.

Während die Zwischenstufen entlang des vorgeschlagenen Reaktionswegs spekulativ sind, konnten mit Gaussian98 DFT-Rechnungen zur Reaktion von **1** mit Tetraphenylborat und 2-Methylbut-3-in-2-ol zum Produkt **17** durchgeführt werden. Die Geometrien der vorgeschlagenen Reaktionsintermediate wurden optimiert und ihr Energieinhalt ermittelt. Die Ergebnisse dieser Rechnungen zeigen, dass die Reaktion insgesamt exergonisch ist und dass alle postulierten Zwischenstufen Minima auf der Potenzialhyperfläche entsprechen. Das thermodynamische Profil dieses Prozesses ist als Abbildung 46 dargestellt.

Durch Verwendung von $\text{BPh}_4^- \text{-d}_{20}$ konnten wir nachweisen, dass der unsubstituierte Phenylring des Naphthalenidliganden dem Tetraphenylborat-Gegenion entstammt. Alle Wasserstoffatome dieses Rings sowie eines der H-Atome des im letzten Dehydratisierungsschritt freigesetzten Wassermoleküls werden in Gegenwart von $\text{BPh}_4^- \text{-d}_{20}$ durch Deuterium ersetzt. Triphenylboroxin, $(\text{PhBO})_3$, und Benzol wurden als Methanolyseprodukte des während der Reaktion freigesetzten Triphenylborans NMR-spektroskopisch und massenspektrometrisch identifiziert.

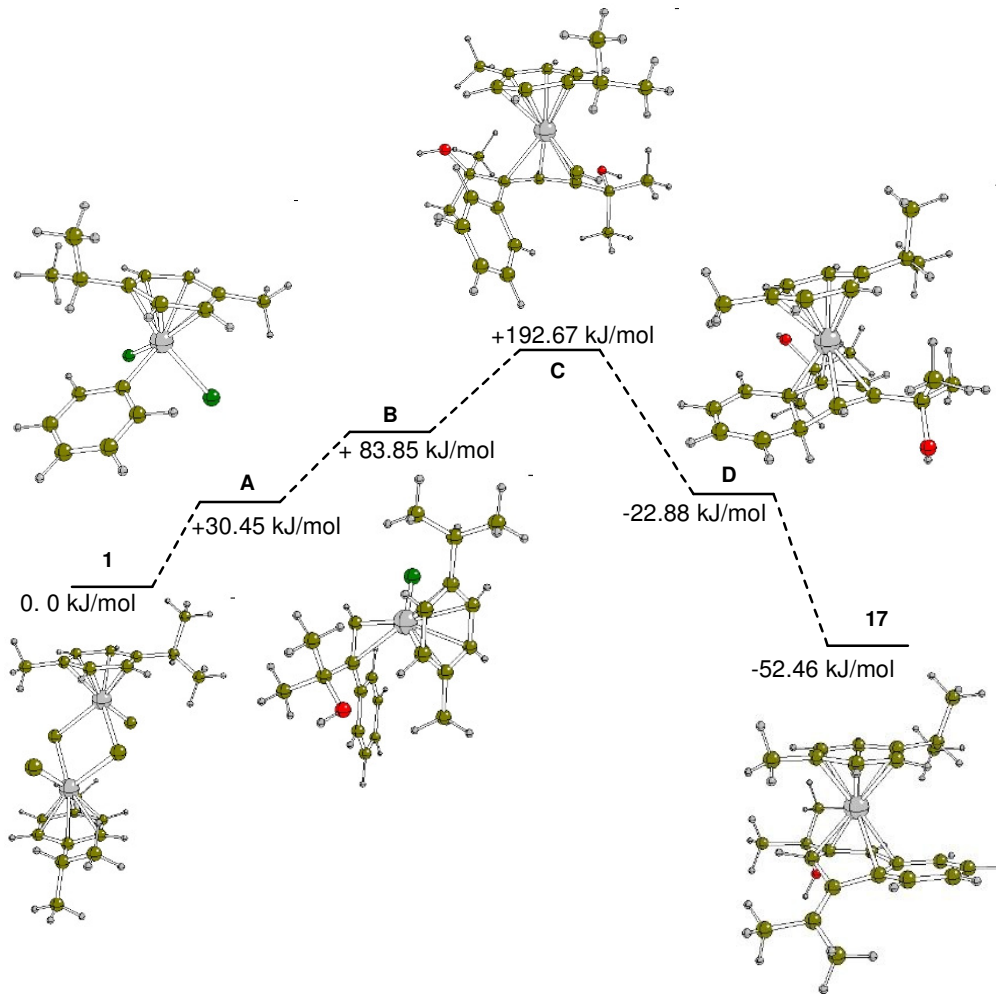


Abbildung 46: Energieprofil für die Reaktion von $[(\eta^6\text{-p-Cymen})\text{RuCl}_2]_2$ (**1**), NaBPh_4 und 2-methyl-but-1-in-2-ol (Energie in kJ/mol, bezogen auf eine $\{(\eta^6\text{-p-Cymen})\text{RuCl}_2\}$ -Einheit von **1**).

8 Appendix

8.1 Crystal data for $[(\eta^6\text{-p-cymene})\text{RuCl}_2(\text{MeSC}_2\text{H}_4\text{Ph})]$ (5)

Table 12: Crystal data and structure refinement for $[(\eta^6\text{-p-cymene})\text{RuCl}_2(\text{MeSC}_2\text{H}_4\text{Ph})]$

Empirical formula	$\text{C}_{19} \text{H}_{26} \text{Cl}_2 \text{Ru S}$
Formula weight	458.43 g/mol
Temperature	293(2) K
Wavelength	0.71073 Å
Crystal system	monoclinic
Space group	$P2_1/n$
Unit cell dimensions	$a = 11.2219(2) \text{ \AA}$ $\alpha = 90^\circ$. $b = 12.1458(2) \text{ \AA}$ $\beta = 90.455(1)^\circ$. $c = 14.8970(2) \text{ \AA}$ $\gamma = 90^\circ$.
Volume	$2030.38(6) \text{ \AA}^3$
Z, Calculated density	4, 1.500 g/cm^3
Absorption coefficient	1.135 mm^{-1}
F(000)	936
θ range for data collection	2.82 to 27.48° .
Limiting indices	$-14 < h < 14$, $-15 < k < 15$, $-19 < l < 19$

8. Appendix

Reflections collected / unique ^{a)}	41082 / 4639 [R(int) = 0.0499]
Completeness to $\theta = 27.48$	99.9 %
Refinement method	Full-matrix least-squares on F^2
Data / restraints / parameters	4639 / 0 / 313
Goodness-of-fit ^{d)} on F^2	1.076
Final R indices [$I > 2\sigma(I)$]	$R_1^{b)}$ = 0.0350, $wR_2^{c)}$ = 0.0813
R indices (all data)	$R_1^{b)}$ = 0.0445, $wR_2^{c)}$ = 0.0857
Extinction coefficient	0.0044(5)
Largest diff. peak and hole	0.593 and -0.518 eA ⁻³

Table 13: Atomic coordinates ($\times 10^4$) and equivalent isotropic displacement parameters ($\text{Å}^2 \times 10^3$) for $[(\eta^6\text{-p-cymene})\text{RuCl}_2(\text{MeSC}_2\text{H}_4\text{Ph})]$. U_{eq} is defined as one third of the trace of the orthogonalized U_{ij} -tensor.

	x	y	z	U(eq)
Ru	6705(1)	4218(1)	8736(1)	44(1)
S	8652(1)	4493(1)	8114(1)	59(1)
Cl(1)	7561(1)	4564(1)	10198(1)	67(1)
Cl(2)	6479(1)	6197(1)	8513(1)	61(1)
C(1)	6172(8)	2123(7)	10177(6)	124(3)
C(2)	6581(3)	2450(3)	8515(3)	69(1)
C(3)	6343(3)	3025(3)	7703(2)	64(1)
C(4)	5446(3)	3816(3)	7650(2)	56(1)
C(5)	4807(3)	4047(3)	8449(2)	54(1)

C(6)	5042(3)	3514(3)	9240(2)	59(1)
C(7)	5932(3)	2688(3)	9294(2)	68(1)
C(8)	5116(4)	4441(4)	6802(3)	81(1)
C(9)	4184(8)	3764(7)	6288(5)	118(2)
C(10)	6159(7)	4729(9)	6234(4)	138(3)
C(11)	9399(3)	5612(3)	8684(4)	71(1)
C(12)	9599(3)	3326(3)	8472(3)	66(1)
C(13)	10863(3)	3480(4)	8142(3)	80(1)
C(14)	11659(3)	2524(3)	8370(3)	65(1)
C(15)	11974(5)	1804(4)	7706(4)	94(1)
C(16)	12751(7)	1001(5)	7832(6)	123(2)
C(17)	13256(5)	868(5)	8650(7)	120(3)
C(18)	12955(4)	1533(5)	9340(4)	98(2)
C(19)	12132(4)	393(4)	9214(3)	78(1)

Table 14: Bond lengths (Å) and angles [°] for $[(\eta^6\text{-p-cymene})\text{RuCl}_2(\text{MeSC}_2\text{H}_4\text{Ph})]$

Ru-C(3)	2.149(3)	C(5)-C(6)	1.367(5)
Ru-C(2)	2.177(3)	C(6)-C(7)	1.417(5)
Ru-C(5)	2.179(3)	C(8)-C(10)	1.491(8)
Ru-C(6)	2.191(3)	C(8)-C(9)	1.531(7)
Ru-C(4)	2.194(3)	C(12)-C(13)	1.516(5)
Ru-C(7)	2.215(3)	C(13)-C(14)	1.502(5)
Ru-S	2.4031(8)	C(14)-C(15)	1.368(6)
Ru-Cl(1)	2.4109(8)	C(14)-C(19)	1.371(6)
Ru-Cl(2)	2.4390(8)	C(15)-C(16)	1.321(8)
S-C(11)	1.806(4)	C(16)-C(17)	1.350(10)
S-C(12)	1.848(4)	C(17)-C(18)	1.351(9)
C(1)-C(7)	1.507(6)	C(18)-C(19)	1.406(7)
C(2)-C(7)	1.405(5)	C(3)-Ru-C(2)	38.33(15)
C(2)-C(3)	1.421(5)	C(3)-Ru-C(5)	67.45(12)
C(3)-C(4)	1.393(5)	C(2)-Ru-C(5)	79.32(12)
C(4)-C(5)	1.422(4)	C(3)-Ru-C(6)	79.97(13)
C(4)-C(8)	1.516(5)	C(2)-Ru-C(6)	67.23(14)

8. Appendix

C(5)-Ru-C(6)	36.47(12)	C(4)-C(3)-C(2)	121.2(3)
C(3)-Ru-C(4)	37.40(13)	C(4)-C(3)-Ru	73.04(19)
C(2)-Ru-C(4)	68.23(13)	C(2)-C(3)-Ru	71.9(2)
C(5)-Ru-C(4)	37.96(12)	C(3)-C(4)-C(5)	117.2(3)
C(6)-Ru-C(4)	67.70(12)	C(3)-C(4)-C(8)	124.3(3)
C(3)-Ru-C(7)	68.34(14)	C(5)-C(4)-C(8)	118.5(3)
C(2)-Ru-C(7)	37.28(15)	C(3)-C(4)-Ru	69.56(18)
C(5)-Ru-C(7)	66.92(12)	C(5)-C(4)-Ru	70.43(17)
C(6)-Ru-C(7)	37.51(13)	C(8)-C(4)-Ru	130.9(2)
C(4)-Ru-C(7)	80.68(12)	C(6)-C(5)-C(4)	122.2(3)
C(3)-Ru-S	89.13(9)	C(6)-C(5)-Ru	72.24(18)
C(2)-Ru-S	97.84(10)	C(4)-C(5)-Ru	71.61(17)
C(5)-Ru-S	145.89(9)	C(5)-C(6)-C(7)	120.9(3)
C(6)-Ru-S	164.99(10)	C(5)-C(6)-Ru	71.28(18)
C(4)-Ru-S	109.19(8)	C(7)-C(6)-Ru	72.19(18)
C(7)-Ru-S	128.41(10)	C(2)-C(7)-C(6)	118.0(3)
C(3)-Ru-Cl(1)	146.71(11)	C(2)-C(7)-C(1)	122.5(5)
C(2)-Ru-Cl(1)	109.45(11)	C(6)-C(7)-C(1)	119.5(5)
C(5)-Ru-Cl(1)	125.12(9)	C(2)-C(7)-Ru	69.88(19)
C(6)-Ru-Cl(1)	95.30(9)	C(6)-C(7)-Ru	70.29(18)
C(4)-Ru-Cl(1)	162.64(8)	C(1)-C(7)-Ru	129.9(3)
C(7)-Ru-Cl(1)	87.79(9)	C(10)-C(8)-C(4)	113.7(5)
S-Ru-Cl(1)	88.14(3)	C(10)-C(8)-C(9)	112.2(5)
C(3)-Ru-Cl(2)	123.21(11)	C(4)-C(8)-C(9)	108.0(4)
C(2)-Ru-Cl(2)	160.91(11)	C(13)-C(12)-S	110.4(3)
C(5)-Ru-Cl(2)	88.11(9)	C(14)-C(13)-C(12)	112.8(3)
C(6)-Ru-Cl(2)	110.07(10)	C(15)-C(14)-C(19)	119.2(4)
C(4)-Ru-Cl(2)	93.04(9)	C(15)-C(14)-C(13)	119.2(4)
C(7)-Ru-Cl(2)	146.81(11)	C(19)-C(14)-C(13)	121.5(4)
S-Ru-Cl(2)	84.52(3)	C(16)-C(15)-C(14)	122.9(6)
Cl(1)-Ru-Cl(2)	89.52(3)	C(15)-C(16)-C(17)	119.3(6)
C(11)-S-C(12)	100.2(2)	C(16)-C(17)-C(18)	120.6(5)
C(11)-S-Ru	110.05(15)	C(17)-C(18)-C(19)	120.7(6)
C(12)-S-Ru	107.73(11)	C(14)-C(19)-C(18)	117.2(5)
C(7)-C(2)-C(3)	120.4(3)		
C(7)-C(2)-Ru	72.8(2)		
C(3)-C(2)-Ru	69.78(19)		

Table 15: Anisotropic displacement parameters [$\text{\AA}^2 \times 10^3$] for $[(\eta^6\text{-p-cymene})\text{RuCl}_2(\text{MeSC}_2\text{H}_4\text{Ph})]$. The anisotropic displacement factor exponent takes the form $-2\pi^2 [(ha^*)^2U_{11} + \dots + 2hka^*b^*U_{12}]$.

	U^{11}	U^{22}	U^{33}	U^{23}	U^{13}	U^{12}
Ru	40(1)	46(1)	47(1)	-2(1)	-2(1)	2(1)
S	45(1)	66(1)	66(1)	-4(1)	4(1)	-2(1)
Cl(1)	67(1)	81(1)	54(1)	-7(1)	-11(1)	-2(1)
Cl(2)	59(1)	49(1)	75(1)	3(1)	3(1)	4(1)
C(1)	133(6)	114(5)	126(5)	68(4)	-54(4)	-39(4)
C(2)	49(2)	44(2)	115(3)	-8(2)	-13(2)	6(1)
C(3)	54(2)	63(2)	73(2)	-21(2)	8(2)	-10(2)
C(4)	54(2)	62(2)	53(2)	2(1)	-6(1)	-8(1)
C(5)	43(1)	55(2)	64(2)	-1(1)	-4(1)	1(1)
C(6)	53(2)	68(2)	57(2)	1(2)	7(1)	-11(2)
C(7)	69(2)	60(2)	73(2)	17(2)	-16(2)	-14(2)
C(8)	91(3)	96(3)	56(2)	13(2)	-18(2)	-21(2)
C(9)	122(5)	149(6)	82(4)	27(4)	-52(4)	-39(5)
C(10)	151(6)	195(9)	67(3)	40(4)	-10(4)	-71(6)
C(11)	53(2)	59(2)	102(3)	-5(2)	-5(2)	-4(2)
C(12)	51(2)	54(2)	94(3)	-4(2)	12(2)	-2(1)
C(13)	56(2)	77(3)	108(3)	13(2)	17(2)	5(2)
C(14)	51(2)	54(2)	90(2)	0(2)	13(2)	-2(1)
C(15)	111(4)	83(3)	87(3)	-7(3)	16(3)	0(3)
C(16)	119(5)	104(4)	146(6)	-15(4)	38(4)	27(4)
C(17)	70(3)	75(3)	216(9)	-2(4)	31(4)	23(2)
C(18)	69(3)	111(4)	113(4)	28(3)	-15(3)	-12(3)
C(19)	71(2)	72(2)	91(3)	-6(2)	0(2)	3(2)

Table 16: Hydrogen coordinates ($\times 10^3$) and isotropic displacement parameters [$\text{\AA}^2 \times 10^3$] for $[(\eta^6\text{-p-cymene})\text{RuCl}_2(\text{MeSC}_2\text{H}_4\text{Ph})]$

	x	y	z	U(eq)
H(1C)	5640(60)	1470(60)	10300(40)	160(20)
H(1B)	6500(80)	2470(60)	10660(50)	190(30)
H(1A)	6860(50)	1890(50)	10070(40)	120(20)
H(2A)	7170(40)	1960(40)	8480(30)	92(13)
H(3A)	6810(30)	2890(30)	7210(20)	62(9)
H(5A)	4200(30)	4660(30)	8440(20)	68(10)
H(6A)	4670(30)	3750(30)	9690(20)	64(10)
H(8A)	4680(50)	5200(50)	6930(40)	140(20)
H(9A)	3870(50)	4110(40)	5800(40)	120(18)
H(9B)	3650(50)	3530(50)	6620(40)	120(20)
H(9C)	4660(50)	3240(50)	6050(40)	110(20)
H(10A)	6020(50)	5070(50)	5820(40)	130(20)
H(10B)	6430(70)	3920(70)	6070(50)	190(40)
H(10C)	6790(50)	5110(50)	6590(40)	124(18)
H(11A)	8920(50)	6180(50)	8760(30)	117(17)
H(11B)	10110(50)	5850(40)	8340(30)	108(16)
H(11C)	9580(40)	5380(40)	9230(30)	98(16)
H(12A)	9560(30)	3190(30)	9180(30)	81(11)
H(12B)	9320(30)	2710(30)	8210(30)	80(12)
H(13A)	11200(50)	4310(50)	8450(40)	140(20)
H(13B)	10640(50)	3570(50)	7480(40)	140(20)
H(15A)	11750(50)	1900(50)	7240(40)	130(20)
H(16A)	13050(90)	400(80)	7190(70)	260(40)
H(17A)	13640(60)	380(60)	8660(50)	150(30)
H(18A)	13130(30)	1630(30)	9860(20)	49(9)
H(19A)	11960(40)	2840(40)	9710(30)	87(13)

8.2 Crystal data for $[(\eta^6\text{-p-cymene})\text{RuCl}_2(\text{MeSC}_3\text{H}_5)]$ (6)**Table 17:** Crystal data and structure refinement for $[(\eta^6\text{-p-cymene})\text{RuCl}_2(\text{MeSC}_3\text{H}_5)]$.

Empirical formula	C _{14.50} H ₂₃ Cl ₃ Ru S	
Formula weight	436.81	
Temperature	173(2) K	
Wavelength	71.073 pm	
Crystal system	monoclinic	
Space group	C2/c	
Unit cell dimensions	a = 2267.4(5) pm b = 1585.7(3) pm c = 1194.8(2) pm	$\alpha = 90^\circ$. $\beta = 120.58(3)^\circ$. $\gamma = 90^\circ$.
Volume	3.6983(13) nm ³	
Z	8	
Density (calculated)	1.569 Mg/m ³	
Absorption coefficient	1.382 mm ⁻¹	
F(000)	1768	
θ range for data collection	2.13 to 27.99°.	
Index ranges	-29 ≤ h ≤ 25, -20 ≤ k ≤ 7, -15 ≤ l ≤ 15	
Reflections collected	4660	

8. Appendix

Independent reflections	4450 [R(int) = 0.0337]
Completeness to $\theta = 27.99^\circ$	99.7 %
Absorption correction	Psi-scan
Refinement method	Full-matrix least-squares on F^2
Data / restraints / parameters	4450 / 2 / 183
Goodness-of-fit on F^2	1.853
Final R indices [$I > 2\sigma(I)$]	R1 = 0.0332, wR2 = 0.1044
R indices (all data)	R1 = 0.0350, wR2 = 0.1054
Largest diff. peak and hole	1.352 and -1.314 e. \AA^{-3}

Table 18: Atomic coordinates ($\times 10^4$) and equivalent isotropic displacement parameters ($\text{pm}^2 \times 10^{-1}$) for $[(\eta^6\text{-p-cymene})\text{RuCl}_2(\text{MeSC}_3\text{H}_5)]$. $U(\text{eq})$ is defined as one third of the trace of the orthogonalized U_{ij} tensor.

	x	y	z	U(eq)
Ru	2273(1)	4107(1)	678(1)	24(1)
Cl(1)	3261(1)	4291(1)	447(1)	33(1)
Cl(2)	1573(1)	4091(1)	-1661(1)	34(1)
S	2208(1)	5599(1)	303(1)	34(1)
C(1)	2908(1)	3701(2)	2705(2)	33(1)
C(2)	2367(1)	4210(2)	2568(2)	32(1)
C(3)	1671(1)	4016(2)	1634(3)	33(1)
C(4)	1508(1)	3316(2)	803(2)	34(1)
C(5)	2059(1)	2793(2)	946(2)	34(1)
C(6)	2740(1)	2984(2)	1876(2)	34(1)
C(11)	3642(2)	3929(2)	3648(3)	48(1)
C(21)	1384(2)	5964(2)	42(4)	52(1)
C(22)	1263(3)	6865(2)	-332(4)	75(1)
C(23)	860(4)	7208(5)	-1441(6)	83(2)
C(23A)	1336(8)	7309(8)	-1172(12)	76(3)
C(24)	2787(2)	6131(2)	1814(3)	54(1)
C(41)	782(1)	3090(2)	-248(3)	51(1)
C(42)	571(2)	2278(3)	152(4)	63(1)
C(43)	271(2)	3793(3)	-584(4)	75(1)
Cl(3)	219(1)	621(1)	1562(1)	82(1)
C(30)	0	-17(3)	2500	67(2)

Table 19: Bond lengths [pm] and angles [°] for $[(\eta^6\text{-p-cymene})\text{RuCl}_2(\text{MeSC}_3\text{H}_5)]$.

Ru-C(2)	216.5(2)	C(2)-Ru-C(5)	80.29(9)
Ru-C(3)	218.7(3)	C(3)-Ru-C(5)	67.58(10)
Ru-C(6)	219.0(2)	C(6)-Ru-C(5)	37.23(10)
Ru-C(1)	219.1(2)	C(1)-Ru-C(5)	68.31(9)
Ru-C(5)	220.0(2)	C(2)-Ru-C(4)	68.58(10)
Ru-C(4)	220.7(2)	C(3)-Ru-C(4)	37.35(10)
Ru-S	239.78(8)	C(6)-Ru-C(4)	68.21(10)
Ru-Cl(1)	241.04(7)	C(1)-Ru-C(4)	81.66(9)
Ru-Cl(2)	241.21(11)	C(5)-Ru-C(4)	38.06(10)
S-C(24)	181.1(3)	C(2)-Ru-S	94.85(7)
S-C(21)	182.4(4)	C(3)-Ru-S	99.62(7)
C(1)-C(2)	140.6(4)	C(6)-Ru-S	152.54(7)
C(1)-C(6)	142.6(4)	C(1)-Ru-S	116.08(7)
C(1)-C(11)	150.4(4)	C(5)-Ru-S	164.66(7)
C(2)-C(3)	142.8(4)	C(4)-Ru-S	126.65(8)
C(3)-C(4)	140.7(4)	C(2)-Ru-Cl(1)	120.50(8)
C(4)-C(5)	143.7(4)	C(3)-Ru-Cl(1)	158.79(8)
C(4)-C(41)	152.1(4)	C(6)-Ru-Cl(1)	90.29(7)
C(5)-C(6)	140.2(4)	C(1)-Ru-Cl(1)	92.09(7)
C(21)-C(22)	148.0(5)	C(5)-Ru-Cl(1)	114.67(7)
C(22)-C(23)	128.7(4)	C(4)-Ru-Cl(1)	152.25(8)
C(22)-C(23A)	130.4(5)	S-Ru-Cl(1)	80.37(2)
C(41)-C(43)	150.6(6)	C(2)-Ru-Cl(2)	150.12(8)
C(41)-C(42)	153.2(5)	C(3)-Ru-Cl(2)	112.76(8)
Cl(3)-C(30)	175.8(3)	C(6)-Ru-Cl(2)	124.28(7)
C(30)-Cl(3)#1	175.8(3)	C(1)-Ru-Cl(2)	162.25(7)
C(2)-Ru-C(3)	38.30(10)	C(5)-Ru-Cl(2)	95.43(7)
C(2)-Ru-C(6)	67.72(10)	C(4)-Ru-Cl(2)	89.76(7)
C(3)-Ru-C(6)	80.04(10)	S-Ru-Cl(2)	81.50(2)
C(2)-Ru-C(1)	37.67(10)	Cl(1)-Ru-Cl(2)	88.31(4)
C(3)-Ru-C(1)	68.68(10)	C(24)-S-C(21)	100.50(18)
C(6)-Ru-C(1)	37.99(10)	C(24)-S-Ru	109.18(12)

C(21)-S-Ru	107.82(12)
C(2)-C(1)-C(6)	117.9(2)
C(2)-C(1)-C(11)	121.1(3)
C(6)-C(1)-C(11)	120.9(3)
C(2)-C(1)-Ru	70.14(13)
C(6)-C(1)-Ru	70.97(13)
C(11)-C(1)-Ru	127.70(19)
C(1)-C(2)-C(3)	121.3(2)
C(1)-C(2)-Ru	72.19(13)
C(3)-C(2)-Ru	71.68(14)
C(4)-C(3)-C(2)	120.7(2)
C(4)-C(3)-Ru	72.10(14)
C(2)-C(3)-Ru	70.02(14)
C(3)-C(4)-C(5)	118.2(2)
C(3)-C(4)-C(41)	123.6(3)
C(5)-C(4)-C(41)	118.2(3)
C(3)-C(4)-Ru	70.55(15)
C(5)-C(4)-Ru	70.72(13)
C(41)-C(4)-Ru	129.53(18)
C(6)-C(5)-C(4)	120.6(2)
C(6)-C(5)-Ru	71.00(14)
C(4)-C(5)-Ru	71.22(14)
C(5)-C(6)-C(1)	121.4(2)
C(5)-C(6)-Ru	71.77(14)
C(1)-C(6)-Ru	71.05(14)
C(22)-C(21)-S	112.0(3)
C(23)-C(22)-C(23A)	44.0(7)
C(23)-C(22)-C(21)	130.1(5)
C(23A)-C(22)-C(21)	132.6(7)
C(43)-C(41)-C(4)	114.1(3)
C(43)-C(41)-C(42)	112.6(3)
C(4)-C(41)-C(42)	108.6(3)
Cl(3)#1-C(30)-Cl(3)	109.7(3)

8. Appendix

Table 20: Anisotropic displacement parameters ($\text{pm}^2 \times 10^{-1}$) for $[(\eta^6\text{-p-cymene})\text{RuCl}_2(\text{MeSC}_3\text{H}_5)]$. The anisotropic displacement factor exponent takes the form: $-2\pi^2[(ha^*)^2U_{11} + \dots + 2hka^*b^*U_{12}]$.

	U^{11}	U^{22}	U^{33}	U^{23}	U^{13}	U^{12}
Ru	29(1)	26(1)	18(1)	-1(1)	14(1)	0(1)
Cl(1)	33(1)	38(1)	32(1)	-1(1)	20(1)	-3(1)
Cl(2)	38(1)	43(1)	20(1)	0(1)	14(1)	-5(1)
S	52(1)	28(1)	29(1)	1(1)	26(1)	4(1)
C(1)	37(1)	38(1)	20(1)	6(1)	12(1)	-1(1)
C(2)	46(1)	37(1)	19(1)	-2(1)	20(1)	-2(1)
C(3)	38(1)	41(1)	30(1)	4(1)	24(1)	1(1)
C(4)	34(1)	45(1)	25(1)	2(1)	17(1)	-7(1)
C(5)	51(1)	27(1)	30(1)	-2(1)	25(1)	-8(1)
C(6)	42(1)	31(1)	34(1)	9(1)	23(1)	7(1)
C(11)	41(2)	60(2)	31(1)	7(1)	10(1)	-3(1)
C(21)	62(2)	50(2)	52(2)	13(1)	35(2)	22(2)
C(22)	113(3)	52(2)	65(2)	15(2)	49(2)	39(2)
C(24)	78(2)	38(2)	43(2)	-13(1)	28(2)	-11(2)
C(41)	38(1)	78(2)	33(1)	0(1)	16(1)	-18(1)
C(42)	56(2)	71(2)	71(2)	-11(2)	39(2)	-25(2)
C(43)	40(2)	95(3)	68(2)	18(2)	11(2)	-5(2)
Cl(3)	65(1)	115(1)	60(1)	13(1)	27(1)	24(1)
C(30)	38(2)	42(2)	87(4)	0	7(2)	0

8.3 Crystal data for $[(\eta^6\text{-p-cymene})\text{RuCl}(\text{SMe}_2)_2]^+ \text{SbF}_6^-$ (7)**Table 21:** Crystal data and structure refinement for $[(\eta^6\text{-p-cymene})\text{RuCl}(\text{SMe}_2)_2]^+ \text{SbF}_6^-$

Empirical formula	$\text{C}_{14}\text{H}_{26}\text{ClF}_6\text{RuS}_2\text{Sb}$
Formula weight	630.74 g/mol
Temperature	293(2) K
Wavelength	0.71073 Å
Crystal system, space group	monoclinic, $P2_1/c$
Unit cell dimensions	$a = 8.48280(10)$ Å $\alpha = 90^\circ$. $b = 17.2331(2)$ Å $\beta = 93.369(1)^\circ$. $c = 15.2935(2)$ Å $\gamma = 90^\circ$.
Volume	$2231.82(5)$ Å ³
Z, Calculated density	4, 1.877 g/cm ³
Absorption coefficient	2.238 mm ⁻¹
F(000)	1232
θ range for data collection	1.78 to 27.50 °
Limiting indices	$-11 < h < 11$, $-22 < k < 22$, $-17 < l < 19$
Reflections collected / unique ^{a)}	46487 / 5113 [R(int) = 0.0512]
Completeness to $\theta = 27.50$	99.8 %

8. Appendix

Refinement method	Full-matrix least-squares on F^2
Data / restraints / parameters	5113 / 0 / 331
Goodness-of-fit ^{d)} on F^2	1.221
Final R indices [$I > 2\sigma(I)$]	$R_1^{b)} = 0.0325$, $wR_2^{c)} = 0.0826$
R indices (all data)	$R_1^{b)} = 0.0362$, $wR_2^{c)} = 0.0902$
Extinction coefficient	0.0081(5)
Largest diff. peak and hole	1.242 and -0.808 e. \AA^{-3}

Table 22: Atomic coordinates ($\times 10^4$) and equivalent isotropic displacement parameters ($\text{\AA}^2 \times 10^3$) for $[(\eta^6\text{-p-cymene})\text{RuCl}(\text{SMe}_2)_2]^+ \text{SbF}_6^-$. U_{eq} is defined as one third of the trace of the orthogonalized U_{ij} tensor.

	x	y	z	U(eq)
S(1)	6067(1)	6273(1)	5428(1)	48(1)
S(2)	6754(1)	7994(1)	6316(1)	52(1)
Cl	5373(1)	7926(1)	4372(1)	57(1)
C(1)	3567(5)	6126(2)	7284(2)	61(1)
C(2)	3047(4)	6738(2)	6636(2)	47(1)
C(3)	2481(3)	6546(2)	5766(2)	46(1)
C(4)	2041(3)	7119(2)	5146(2)	47(1)
C(5)	2090(4)	7924(2)	5374(2)	51(1)
C(6)	2604(4)	8119(2)	6232(2)	53(1)
C(7)	3108(4)	7535(2)	6844(2)	51(1)
C(8)	1620(4)	8524(2)	4668(3)	65(1)
C(9)	-178(6)	8539(5)	4536(8)	118(3)

C(10)	2260(8)	9326(3)	4858(5)	91(2)
C(11)	5404(5)	5922(3)	4358(3)	70(1)
C(12)	8044(4)	6539(3)	5177(3)	62(1)
C(13)	7299(7)	7583(4)	7370(3)	79(1)
C(14)	6201(7)	8958(3)	6625(5)	91(2)

Table 23: Bond lengths (Å) and angles [°] for $[(\eta^6\text{-p-cymene})\text{RuCl}(\text{SMe}_2)_2]^+ \text{SbF}_6^-$.

Ru-C(4)	2.197(3)	C(4)-Ru-C(2)	68.11(11)
Ru-C(3)	2.200(3)	C(3)-Ru-C(2)	37.64(11)
Ru-C(2)	2.220(3)	C(7)-Ru-C(6)	37.60(14)
Ru-C(6)	2.229(3)	C(4)-Ru-C(6)	66.34(12)
Ru-C(5)	2.240(3)	C(3)-Ru-C(6)	78.53(12)
Ru-S(1)	2.3833(8)	C(2)-Ru-C(6)	67.82(13)
Ru-S(2)	2.3880(8)	C(7)-Ru-C(5)	67.37(13)
Ru-Cl	2.3946(7)	C(4)-Ru-C(5)	37.61(12)
S(1)-C(12)	1.801(4)	C(3)-Ru-C(5)	67.49(12)
S(1)-C(11)	1.803(4)	C(2)-Ru-C(5)	80.91(12)
S(2)-C(13)	1.797(5)	C(6)-Ru-C(5)	36.48(13)
S(2)-C(14)	1.798(5)	C(7)-Ru-S(1)	124.66(10)
C(1)-C(2)	1.496(5)	C(4)-Ru-S(1)	108.33(9)
C(2)-C(7)	1.412(5)	C(3)-Ru-S(1)	86.76(8)
C(2)-C(3)	1.426(4)	C(2)-Ru-S(1)	93.06(9)
C(3)-C(4)	1.403(5)	C(6)-Ru-S(1)	160.86(9)
C(4)-C(5)	1.431(5)	C(5)-Ru-S(1)	145.07(9)
C(5)-C(6)	1.399(5)	C(7)-Ru-S(2)	93.65(9)
C(5)-C(8)	1.531(5)	C(4)-Ru-S(2)	164.03(9)
C(6)-C(7)	1.423(5)	C(3)-Ru-S(2)	150.79(8)
C(8)-C(10)	1.507(7)	C(2)-Ru-S(2)	114.30(8)
C(8)-C(9)	1.527(6)	C(6)-Ru-S(2)	99.34(9)
C(7)-Ru-C(4)	79.25(12)	C(5)-Ru-S(2)	126.43(9)
C(7)-Ru-C(3)	66.71(12)	S(1)-Ru-S(2)	87.50(3)
C(4)-Ru-C(3)	37.23(12)	C(7)-Ru-Cl	147.27(10)
C(7)-Ru-C(2)	37.38(12)	C(4)-Ru-Cl	96.33(8)

8. Appendix

C(3)-Ru-Cl	126.45(8)	C(10)-C(8)-C(5)	114.0(4)
C(2)-Ru-Cl	163.84(8)	C(9)-C(8)-C(5)	108.8(4)
C(6)-Ru-Cl	110.88(9)		
C(5)-Ru-Cl	89.25(9)		
S(1)-Ru-Cl	87.69(3)		
S(2)-Ru-Cl	81.86(3)		
C(12)-S(1)-C(11)	97.9(2)		
C(12)-S(1)-Ru	112.70(14)		
C(11)-S(1)-Ru	105.22(16)		
C(13)-S(2)-C(14)	100.7(3)		
C(13)-S(2)-Ru	110.40(17)		
C(14)-S(2)-Ru	107.61(18)		
C(7)-C(2)-C(3)	116.3(3)		
C(7)-C(2)-C(1)	122.1(3)		
C(3)-C(2)-C(1)	121.7(3)		
C(7)-C(2)-Ru	69.90(17)		
C(3)-C(2)-Ru	70.43(15)		
C(1)-C(2)-Ru	129.3(3)		
C(4)-C(3)-C(2)	121.9(3)		
C(4)-C(3)-Ru	71.26(17)		
C(2)-C(3)-Ru	71.93(16)		
C(3)-C(4)-C(5)	121.0(3)		
C(3)-C(4)-Ru	71.51(16)		
C(5)-C(4)-Ru	72.81(17)		
C(6)-C(5)-C(4)	117.7(3)		
C(6)-C(5)-C(8)	123.6(3)		
C(4)-C(5)-C(8)	118.7(3)		
C(6)-C(5)-Ru	71.33(19)		
C(4)-C(5)-Ru	69.58(17)		
C(8)-C(5)-Ru	128.9(2)		
C(5)-C(6)-C(7)	120.8(3)		
C(5)-C(6)-Ru	72.18(18)		
C(7)-C(6)-Ru	69.46(18)		
C(2)-C(7)-C(6)	122.3(3)		
C(2)-C(7)-Ru	72.72(17)		
C(6)-C(7)-Ru	72.93(18)		
C(10)-C(8)-C(9)	110.8(5)		

Table 24: Anisotropic displacement parameters [$\text{\AA}^2 \times 10^3$] for $[(\eta^6\text{-p-cymene})\text{RuCl}(\text{SMe}_2)_2]^+ \text{SbF}_6^-$. The anisotropic displacement factor exponent takes the form $-2\pi^2 [(ha^*)^2U_{11} + \dots + 2 hka^*b^*U_{12}]$.

	U^{11}	U^{22}	U^{33}	U^{23}	U^{13}	U^{12}
S(1)	44(1)	45(1)	56(1)	3(1)	9(1)	1(1)
S(2)	50(1)	62(1)	46(1)	-4(1)	3(1)	-19(1)
Cl	58(1)	71(1)	43(1)	16(1)	14(1)	6(1)
C(1)	72(2)	64(2)	48(2)	7(2)	4(2)	-18(2)
C(2)	48(2)	57(2)	39(1)	-1(1)	11(1)	-15(1)
C(3)	42(1)	46(2)	49(2)	-5(1)	7(1)	-11(1)
C(4)	38(1)	56(2)	46(2)	-3(1)	1(1)	-5(1)
C(5)	43(2)	50(2)	60(2)	2(1)	9(1)	3(1)
C(6)	53(2)	48(2)	60(2)	-11(1)	19(1)	-2(1)
C(7)	52(2)	60(2)	42(2)	-10(1)	15(1)	-11(1)
C(8)	57(2)	62(2)	76(2)	14(2)	7(2)	7(2)
C(9)	58(3)	125(5)	170(7)	80(6)	-2(3)	9(3)
C(10)	94(4)	65(3)	113(4)	26(3)	7(3)	1(2)
C(11)	63(2)	69(2)	79(3)	-29(2)	13(2)	-3(2)
C(12)	45(2)	65(2)	76(2)	2(2)	12(2)	2(2)
C(13)	75(3)	101(4)	58(2)	4(2)	-14(2)	-21(3)
C(14)	85(3)	63(3)	123(5)	-19(3)	-14(3)	-26(2)

Table 25: Hydrogen coordinates ($\times 10^3$) and isotropic displacement parameters [$\text{\AA}^2 \times 10^3$] for $[(\eta^6\text{-p-cymene})\text{RuCl}(\text{SMe}_2)_2]^+ \text{SbF}_6^-$.

	x	y	z	U(eq)
H(1B)	4120(60)	5700(30)	7030(30)	84(15)
H(1C)	2680(60)	5950(30)	7520(30)	83(14)
H(3A)	2520(40)	6060(20)	5570(20)	47(9)
H(4A)	1740(40)	7000(20)	4540(20)	42(8)
H(6A)	2660(40)	8650(20)	6390(20)	52(9)
H(7A)	3500(50)	7690(20)	7360(30)	58(11)
H(8A)	2020(50)	8330(20)	4130(30)	65(11)
H(9A)	-450(70)	8930(40)	4110(40)	109(19)
H(9B)	160(110)	8130(60)	4050(60)	170(40)
H(9C)	-530(120)	8490(60)	5000(70)	180(40)
H(10A)	3340(100)	9320(50)	4940(50)	150(30)
H(10B)	1620(100)	9580(40)	5290(50)	140(30)
H(10C)	2100(70)	9680(30)	4300(40)	99(18)
H(11A)	5610(60)	6460(40)	4070(40)	95(16)
H(11B)	6090(80)	5600(40)	4140(40)	108(19)
H(11C)	4450(60)	5660(30)	4480(30)	74(13)
H(12A)	8110(60)	6970(30)	4800(30)	84(14)
H(12B)	8520(70)	6720(30)	5700(40)	98(17)
H(12C)	8520(50)	6080(30)	5020(30)	66(11)
H(13A)	8110(70)	7820(30)	7600(40)	97(17)
H(13B)	6440(60)	7610(30)	7740(30)	73(13)
H(13C)	7520(80)	7000(40)	7270(40)	120(20)
H(14A)	7020(70)	9220(30)	6770(30)	85(15)
H(14B)	5840(70)	9220(40)	6020(40)	109(19)
H(14C)	5360(80)	8890(40)	7040(50)	120(20)

8.4 Crystal data for $[\{(\eta^6\text{-p-cymene})\text{Ru}\}_2(\mu\text{-Cl})_3]^+ \text{SbF}_6^-$ (8)**Table 26:** Crystal data and structure refinement for $[\{(\eta^6\text{-p-cymene})\text{Ru}\}_2(\mu\text{-Cl})_3]^+ \text{SbF}_6^-$.

Empirical formula	$\text{C}_{20} \text{H}_{29} \text{Cl}_3 \text{F}_6 \text{Ru}_2 \text{Sb}$
Formula weight	813.67 g/mol
Temperature	293(2) K
Wavelength	0.71073 Å
Crystal system, space group	triclinic, P_{-1}
Unit cell dimensions	$a = 8.27860(10) \text{ \AA}$ $\alpha = 99.0940(10)^\circ$. $b = 10.6537(2) \text{ \AA}$ $\beta = 101.4800(10)^\circ$. $c = 16.6834(2) \text{ \AA}$ $\gamma = 108.5780(1)^\circ$.
Volume	$1327.45(3) \text{ \AA}^3$
Z, Calculated density	2, 2.036 g/cm ³
Absorption coefficient	2.485 mm^{-1}
F(000)	786
θ range for data collection	2.57 to 27.40°.
Limiting indices	$-10 < h < 10$, $-13 < k < 13$, $-21 < l < 21$
Reflections collected / unique ^{a)}	47238 / 6040 [R(int) = 0.0832]
Completeness to $\theta = 27.40$	99.9 %

8. Appendix

Refinement method	Full-matrix least-squares on F^2
Data / restraints / parameters	6040 / 0 / 325
Goodness-of-fit ^{d)} on F^2	1.068
Final R indices [$I > 2\sigma(I)$]	R1 = 0.0471, wR2c = 0.1225
R indices (all data)	R1 = 0.0702, wR2c = 0.1350
Extinction coefficient	0.0061(6)
Largest diff. peak and hole	1.051 and -0.691 eA ⁻³

Table 27: Atomic coordinates ($\times 10^4$) and equivalent isotropic displacement parameters ($\text{Å}^2 \times 10^3$) for $[(\eta^6\text{-p-cymene})\text{Ru}]_2(\mu\text{-Cl})_3^+ \text{SbF}_6^- \cdot \text{U}_{\text{eq}}$ is defined as one third of the trace of the orthogonalized U_{ij} -tensor.

	x	y	z	U(eq)
Ru(2)	-7057(1)	-6408(1)	2690(1)	48(1)
Cl(1)	-7804(2)	-5620(2)	1424(1)	74(1)
Cl(2)	-9362(2)	-5591(2)	2973(1)	81(1)
Cl(3)	-5392(2)	-3970(1)	3203(1)	86(1)
C(1)	-4691(12)	-714(7)	2926(6)	146(4)
C(2)	-6608(11)	-1523(6)	2569(5)	93(2)
C(3)	-7810(17)	-1767(9)	3068(5)	101(3)
C(4)	-9560(17)	-2593(10)	2717(6)	98(3)
C(5)	-10272(9)	-3217(6)	1854(4)	74(2)
C(6)	-9075(9)	-2968(6)	1353(4)	70(2)
C(7)	-7267(9)	-2126(6)	1704(5)	76(2)
C(8)	-12220(11)	-4163(11)	1485(8)	131(4)

C(9)	-13196(12)	-3215(11)	1195(9)	183(6)
C(10)	-12576(14)	-5408(11)	886(8)	158(5)
C(11)	-9389(11)	-9309(7)	1232(5)	112(3)
C(12)	-7992(10)	-8557(6)	2054(4)	76(2)
C(13)	-6190(10)	-7886(6)	2064(4)	69(2)
C(14)	-4897(8)	-7159(6)	2812(4)	58(1)
C(15)	-5323(7)	-7036(5)	3595(3)	57(1)
C(16)	-7100(9)	-7679(6)	3587(4)	65(2)
C(17)	-8413(9)	-8440(6)	2822(5)	73(2)
C(18)	-3958(8)	-6295(6)	4426(3)	67(1)
C(19)	-3331(12)	-7332(8)	4781(5)	108(3)
C(20)	-2384(10)	-5117(8)	4392(5)	102(2)

Table 28: Bond lengths (Å) and angles [°] for $[(\eta^6\text{-p-cymene})\text{Ru}]_2(\mu\text{-Cl})_3]^+ \text{SbF}_6^-$.

Ru(1)-C(6)	2.148(5)	C(2)-C(7)	1.402(10)
Ru(1)-C(3)	2.165(7)	C(2)-C(3)	1.409(13)
Ru(1)-C(7)	2.167(6)	C(3)-C(4)	1.380(14)
Ru(1)-C(5)	2.181(6)	C(4)-C(5)	1.404(12)
Ru(1)-C(2)	2.192(7)	C(5)-C(6)	1.408(9)
Ru(1)-Cl(1)	2.4322(15)	C(5)-C(8)	1.539(11)
Ru(1)-Cl(2)	2.4307(15)	C(6)-C(7)	1.420(9)
Ru(2)-C(13)	2.142(6)	C(8)-C(10)	1.435(14)
Ru(2)-C(17)	2.167(6)	C(8)-C(9)	1.557(11)
Ru(2)-C(14)	2.168(5)	C(11)-C(12)	1.514(9)
Ru(2)-C(16)	2.169(5)	C(12)-C(17)	1.390(9)
Ru(2)-C(12)	2.179(6)	C(12)-C(13)	1.429(10)
Ru(2)-C(15)	2.203(5)	C(13)-C(14)	1.391(9)
Ru(2)-Cl(2)	2.4303(14)	C(14)-C(15)	1.416(7)
Ru(2)-Cl(3)	2.4334(15)	C(15)-C(16)	1.408(8)
Ru(2)-Cl(1)	2.4336(13)	C(15)-C(18)	1.512(8)
C(1)-C(2)	1.485(11)	C(16)-C(17)	1.424(9)

8. Appendix

C(18)-C(20)	1.512(9)	Cl(3)-Ru(1)-Cl(2)	79.16(6)
C(18)-C(19)	1.513(8)	C(13)-Ru(2)-C(17)	68.0(3)
C(4)-Ru(1)-C(6)	67.6(3)	C(13)-Ru(2)-C(14)	37.7(2)
C(4)-Ru(1)-C(3)	37.4(4)	C(17)-Ru(2)-C(14)	80.4(2)
C(6)-Ru(1)-C(3)	80.2(3)	C(13)-Ru(2)-C(16)	80.5(2)
C(4)-Ru(1)-C(7)	80.0(3)	C(17)-Ru(2)-C(16)	38.3(2)
C(6)-Ru(1)-C(7)	38.4(3)	C(14)-Ru(2)-C(16)	67.6(2)
C(3)-Ru(1)-C(7)	67.4(3)	C(13)-Ru(2)-C(12)	38.6(3)
C(4)-Ru(1)-C(5)	38.0(3)	C(17)-Ru(2)-C(12)	37.3(2)
C(6)-Ru(1)-C(5)	38.0(2)	C(14)-Ru(2)-C(12)	69.0(2)
C(3)-Ru(1)-C(5)	68.7(3)	C(16)-Ru(2)-C(12)	68.7(2)
C(7)-Ru(1)-C(5)	69.2(2)	C(13)-Ru(2)-C(15)	68.5(2)
C(4)-Ru(1)-C(2)	68.2(4)	C(17)-Ru(2)-C(15)	68.7(2)
C(6)-Ru(1)-C(2)	68.8(2)	C(14)-Ru(2)-C(15)	37.80(19)
C(3)-Ru(1)-C(2)	37.7(3)	C(16)-Ru(2)-C(15)	37.6(2)
C(7)-Ru(1)-C(2)	37.5(3)	C(12)-Ru(2)-C(15)	82.0(2)
C(5)-Ru(1)-C(2)	82.3(3)	C(13)-Ru(2)-Cl(2)	151.9(2)
C(4)-Ru(1)-Cl(1)	147.8(3)	C(17)-Ru(2)-Cl(2)	93.55(17)
C(6)-Ru(1)-Cl(1)	93.05(17)	C(14)-Ru(2)-Cl(2)	163.63(15)
C(3)-Ru(1)-Cl(1)	167.7(3)	C(16)-Ru(2)-Cl(2)	98.22(16)
C(7)-Ru(1)-Cl(1)	101.0(2)	C(12)-Ru(2)-Cl(2)	114.7(2)
C(5)-Ru(1)-Cl(1)	111.9(2)	C(15)-Ru(2)-Cl(2)	125.83(15)
C(2)-Ru(1)-Cl(1)	130.2(3)	C(13)-Ru(2)-Cl(3)	126.4(2)
C(4)-Ru(1)-Cl(3)	130.5(3)	C(17)-Ru(2)-Cl(3)	154.8(2)
C(6)-Ru(1)-Cl(3)	147.5(2)	C(14)-Ru(2)-Cl(3)	99.86(16)
C(3)-Ru(1)-Cl(3)	100.7(3)	C(16)-Ru(2)-Cl(3)	118.27(18)
C(7)-Ru(1)-Cl(3)	111.54(19)	C(12)-Ru(2)-Cl(3)	164.4(2)
C(5)-Ru(1)-Cl(3)	168.5(2)	C(15)-Ru(2)-Cl(3)	95.89(14)
C(2)-Ru(1)-Cl(3)	91.83(18)	Cl(2)-Ru(2)-Cl(3)	79.15(6)
Cl(1)-Ru(1)-Cl(3)	79.47(6)	C(13)-Ru(2)-Cl(1)	93.01(17)
C(4)-Ru(1)-Cl(2)	93.7(3)	C(17)-Ru(2)-Cl(1)	123.49(19)
C(6)-Ru(1)-Cl(2)	131.0(2)	C(14)-Ru(2)-Cl(1)	116.55(15)
C(3)-Ru(1)-Cl(2)	112.6(3)	C(16)-Ru(2)-Cl(1)	161.79(19)
C(7)-Ru(1)-Cl(2)	169.26(19)	C(12)-Ru(2)-Cl(1)	95.66(17)
C(5)-Ru(1)-Cl(2)	100.47(17)	C(15)-Ru(2)-Cl(1)	153.22(15)
C(2)-Ru(1)-Cl(2)	147.1(3)	Cl(2)-Ru(2)-Cl(1)	79.49(5)
Cl(1)-Ru(1)-Cl(2)	79.60(5)	Cl(3)-Ru(2)-Cl(1)	79.27(5)

Ru(1)-Cl(1)-Ru(2)	85.06(4)	C(14)-C(13)-Ru(2)	72.2(3)
Ru(2)-Cl(2)-Ru(1)	84.99(5)	C(12)-C(13)-Ru(2)	72.1(3)
Ru(1)-Cl(3)-Ru(2)	84.96(5)	C(13)-C(14)-C(15)	121.1(6)
C(7)-C(2)-C(3)	117.5(8)	C(13)-C(14)-Ru(2)	70.2(3)
C(7)-C(2)-C(1)	119.5(9)	C(15)-C(14)-Ru(2)	72.4(3)
C(3)-C(2)-C(1)	122.9(9)	C(16)-C(15)-C(14)	117.5(5)
C(7)-C(2)-Ru(1)	70.3(4)	C(16)-C(15)-C(18)	119.3(5)
C(3)-C(2)-Ru(1)	70.1(4)	C(14)-C(15)-C(18)	123.1(5)
C(1)-C(2)-Ru(1)	128.5(4)	C(16)-C(15)-Ru(2)	69.9(3)
C(4)-C(3)-C(2)	120.9(8)	C(14)-C(15)-Ru(2)	69.8(3)
C(4)-C(3)-Ru(1)	70.1(4)	C(18)-C(15)-Ru(2)	133.4(3)
C(2)-C(3)-Ru(1)	72.2(4)	C(15)-C(16)-C(17)	121.1(5)
C(3)-C(4)-C(5)	123.4(9)	C(15)-C(16)-Ru(2)	72.5(3)
C(3)-C(4)-Ru(1)	72.5(5)	C(17)-C(16)-Ru(2)	70.8(3)
C(5)-C(4)-Ru(1)	72.8(4)	C(12)-C(17)-C(16)	121.2(6)
C(4)-C(5)-C(6)	115.8(7)	C(12)-C(17)-Ru(2)	71.8(3)
C(4)-C(5)-C(8)	122.1(8)	C(16)-C(17)-Ru(2)	70.9(3)
C(6)-C(5)-C(8)	122.1(7)	C(20)-C(18)-C(15)	115.6(5)
C(4)-C(5)-Ru(1)	69.2(4)	C(20)-C(18)-C(19)	109.6(6)
C(6)-C(5)-Ru(1)	69.8(3)	C(15)-C(18)-C(19)	107.7(5)
C(8)-C(5)-Ru(1)	129.0(5)		
C(5)-C(6)-C(7)	121.7(6)		
C(5)-C(6)-Ru(1)	72.3(3)		
C(7)-C(6)-Ru(1)	71.5(3)		
C(2)-C(7)-C(6)	120.7(7)		
C(2)-C(7)-Ru(1)	72.2(4)		
C(6)-C(7)-Ru(1)	70.1(3)		
C(10)-C(8)-C(5)	117.1(8)		
C(10)-C(8)-C(9)	116.5(10)		
C(5)-C(8)-C(9)	104.7(7)		
C(17)-C(12)-C(13)	117.3(6)		
C(17)-C(12)-C(11)	121.8(7)		
C(13)-C(12)-C(11)	120.9(7)		
C(17)-C(12)-Ru(2)	70.9(3)		
C(13)-C(12)-Ru(2)	69.3(3)		
C(11)-C(12)-Ru(2)	128.6(4)		
C(14)-C(13)-C(12)	121.6(6)		

Table 29: Anisotropic displacement parameters [$\text{\AA}^2 \times 10^3$] for $[(\eta^6\text{-p-cymene})\text{Ru}]_2(\mu\text{-Cl})_3]^+ \text{SbF}_6^-$. The anisotropic displacement factor exponent takes the form $-2\pi^2[(ha^*)^2U_{11} + \dots + 2hka^*b^*U_{12}]$.

Ru(1)	U^{11}	U^{22}	U^{33}	U^{23}	U^{13}	U^{12}
Ru(1)	76(1)	48(1)	49(1)	18(1)	14(1)	36(1)
Ru(2)	61(1)	45(1)	52(1)	20(1)	19(1)	30(1)
Cl(1)	126(1)	70(1)	53(1)	24(1)	32(1)	60(1)
Cl(2)	106(1)	87(1)	104(1)	57(1)	66(1)	67(1)
Cl(3)	89(1)	51(1)	105(1)	21(1)	-15(1)	30(1)
C(1)	141(8)	51(4)	183(9)	19(5)	-67(7)	23(4)
C(2)	120(6)	48(3)	95(5)	14(3)	-23(5)	42(4)
C(3)	182(10)	76(5)	65(5)	14(4)	13(6)	86(6)
C(4)	154(9)	98(6)	106(7)	54(6)	64(7)	100(7)
C(5)	80(4)	72(4)	94(5)	47(3)	28(3)	47(3)
C(6)	100(5)	60(3)	53(3)	21(3)	0(3)	43(3)
C(7)	83(4)	66(4)	99(5)	49(4)	28(4)	39(3)
C(8)	82(5)	135(8)	215(11)	113(8)	42(6)	56(5)
C(9)	86(6)	157(10)	349(18)	149(11)	43(8)	66(6)
C(10)	114(8)	90(7)	221(12)	15(7)	-26(8)	25(6)
C(11)	119(6)	70(4)	121(6)	3(4)	-14(5)	39(4)
C(12)	98(5)	52(3)	78(4)	16(3)	5(4)	40(3)
C(13)	104(5)	60(3)	71(4)	24(3)	33(4)	54(4)
C(14)	68(3)	58(3)	69(3)	27(3)	26(3)	41(3)
C(15)	71(3)	50(3)	66(3)	24(2)	16(3)	39(3)
C(16)	92(4)	61(3)	73(4)	41(3)	43(3)	44(3)
C(17)	71(4)	53(3)	107(5)	38(3)	28(4)	29(3)
C(18)	84(4)	67(3)	63(3)	19(3)	19(3)	43(3)
C(19)	146(7)	93(5)	87(5)	31(4)	-4(5)	63(5)
C(20)	94(5)	81(5)	118(6)	32(4)	2(4)	28(4)

Table 30: Hydrogen coordinates ($\times 10^3$) and isotropic displacement parameters [$\text{\AA}^2 \times 10^3$] for $[\{(\eta^6\text{-p-cymene})\text{Ru}\}_2(\mu\text{-Cl})_3]^+ \text{SbF}_6^-$.

	x	y	z	U(eq)
H(1C)	-4481	230	2941	175
H(1B)	-4037	-1034	2580	175
H(1A)	-4317	-816	3487	175
H(28)	-7520(100)	-1490(70)	3630(50)	100(20)
H(27)	-10060(110)	-2720(80)	3030(50)	100(30)
H(24)	-9490(80)	-3330(60)	820(40)	65(16)
H(26)	-6510(70)	-2060(50)	1340(30)	54(14)
H(8A)	-12638	-4435	1963	157
H(9C)	-14439	-3733	976	220
H(9B)	-12742	-2836	765	220
H(9A)	-13010	-2490	1667	220
H(11C)	-9522	-10254	1115	134
H(11B)	-9038	-8919	785	134
H(11A)	-10495	-9232	1275	134
H(22)	-5740(110)	-7930(80)	1610(50)	130(30)
H(23)	-3630(80)	-6700(60)	2840(30)	68(16)
H(21)	-7330(70)	-7460(50)	4110(30)	54(13)
H(25)	-9860(80)	-8760(60)	2830(30)	77(17)
H(18A)	-4545	-5940	4813	80
H(19C)	-2467	-6890	5313	130
H(19B)	-2812	-7735	4396	130
H(19A)	-4318	-8030	4858	130
H(20C)	-1602	-4710	4948	122
H(20B)	-2783	-4449	4181	122
H(20A)	-1770	-5443	4027	122

8.5 Crystal data for $[(\eta^6\text{-p-cymene})\text{RuCl}_2(4\text{-methylpyridine})]$ (11)**Table 31:** Crystal data and structure refinement for $[(\eta^6\text{-p-cymene})\text{RuCl}_2(4\text{-methylpyridine})]$.

Empirical formula	$\text{C}_{16} \text{H}_{21} \text{Cl}_2 \text{N Ru}$
Formula weight	399.31 g/mol
Temperature	293(2) K
Wavelength	0.71073 Å
Unit cell dimensions	$a = 16.3131(3) \text{ \AA}$ $\alpha = 90^\circ$ $b = 32.5700(7) \text{ \AA}$ $\beta = 90^\circ$ $c = 13.0671(3) \text{ \AA}$ $\gamma = 90^\circ$
Volume	$6942.8(3) \text{ \AA}^3$
Z, Calculated density	16, 1.528 g/cm ³
Absorption coefficient	1.201 mm^{-1}
F(000)	3232
θ range for data collection	2.74 to 27.47°
Limiting indices	$-21 < h < 21$, $-42 < k < 42$, $-14 < l < 16$
Reflections collected / unique ^{a)}	8594 / 3970 [R(int) = 0.0743]
Completeness to $\theta = 27.47$	99.7 %
Refinement method	Full-matrix least-squares on F^2

Data / restraints / parameters	3970 / 0 / 214
Goodness-of-fit ^{d)} on F ²	1.196
Final R indices [I>2σ (I)]	R ₁ ^{b)} = 0.0552, wR ₂ ^{c)} = 0.1608
R indices (all data)	R ₁ ^{b)} = 0.0645, wR ₂ ^{c)} = 0.1692
Extinction coefficient	0.00033(10)
Largest diff. peak and hole	1.783 and -0.852 e.Å ⁻³

Table 32: Atomic coordinates (x 10⁴) and equivalent isotropic displacement parameters (Å² x 10³) for [(η⁶-p-cymene)RuCl₂(4-methylpyridine)]. U_{eq} is defined as one third of the trace of the orthogonalized U_{ij} - tensor.

	x	y	z	U(eq)
Cl(1)	3619(1)	5501(1)	8551(1)	50(1)
Cl(2)	3554(1)	6532(1)	8762(1)	53(1)
N	2073(3)	6004(1)	8042(3)	41(1)
C(1)	3681(7)	5204(2)	6011(6)	99(3)
C(2)	2869(4)	5857(2)	5870(4)	57(1)
C(3)	2790(3)	6294(2)	5950(4)	51(1)
C(4)	3469(4)	6539(2)	6239(4)	50(1)
C(5)	4211(3)	6334(2)	6443(4)	53(1)
C(6)	4282(4)	5908(2)	6359(4)	55(1)
C(7)	3617(4)	5658(2)	6085(4)	55(1)
C(8)	3384(6)	7002(2)	6356(6)	77(2)
C(9)	3908(9)	7197(3)	5492(10)	148(5)
C(10)	2563(8)	7165(3)	6299(9)	130(4)
C(11)	1643(3)	6342(2)	8285(5)	51(1)

8. Appendix

C(12)	847(4)	6314(2)	8627(5)	57(2)
C(13)	444(3)	5950(2)	8734(4)	48(1)
C(14)	892(3)	5606(2)	8488(4)	51(1)
C(15)	1695(3)	5643(2)	8151(4)	46(1)
C(16)	-430(3)	5928(2)	9105(5)	64(2)

Table 33: Bond lengths (Å) and angles [°] for $[(\eta^6\text{-p-cymene})\text{RuCl}_2(4\text{-methylpyridine})]$.

Ru-C(5)	2.178(5)	N-Ru-C(5)	154.5(2)
Ru-C(6)	2.185(6)	N-Ru-C(6)	157.1(2)
Ru-C(3)	2.189(5)	C(5)-Ru-C(6)	37.4(3)
Ru-C(2)	2.189(5)	N-Ru-C(3)	92.41(18)
Ru-C(7)	2.211(5)	C(5)-Ru-C(3)	67.0(2)
Ru-C(4)	2.211(5)	C(6)-Ru-C(3)	79.3(2)
Ru-Cl(1)	2.4156(13)	N-Ru-C(2)	93.9(2)
Ru-Cl(2)	2.4202(13)	C(5)-Ru-C(2)	79.3(2)
N-C(15)	1.335(7)	C(6)-Ru-C(2)	66.5(2)
N-C(11)	1.343(7)	C(3)-Ru-C(2)	38.2(3)
C(1)-C(7)	1.487(9)	N-Ru-C(7)	120.0(2)
C(2)-C(7)	1.410(9)	C(5)-Ru-C(7)	67.9(2)
C(2)-C(3)	1.431(10)	C(6)-Ru-C(7)	37.2(2)
C(3)-C(4)	1.416(8)	C(3)-Ru-C(7)	68.5(2)
C(4)-C(5)	1.407(8)	C(2)-Ru-C(7)	37.4(2)
C(4)-C(8)	1.524(9)	N-Ru-C(4)	117.3(2)
C(5)-C(6)	1.398(10)	C(5)-Ru-C(4)	37.4(2)
C(6)-C(7)	1.401(9)	C(6)-Ru-C(4)	67.7(2)
C(8)-C(10)	1.441(14)	C(3)-Ru-C(4)	37.5(2)
C(8)-C(9)	1.552(13)	C(2)-Ru-C(4)	68.4(2)
C(11)-C(12)	1.377(8)	C(7)-Ru-C(4)	81.4(2)
C(12)-C(13)	1.364(9)	N-Ru-Cl(1)	84.96(12)
C(13)-C(14)	1.376(8)	C(5)-Ru-Cl(1)	120.29(17)
C(13)-C(16)	1.507(8)	C(6)-Ru-Cl(1)	92.84(17)
C(14)-C(15)	1.388(7)	C(3)-Ru-Cl(1)	153.05(17)
		C(2)-Ru-Cl(1)	115.12(19)

C(7)-Ru-Cl(1)	89.58(16)	C(1)-C(7)-Ru	130.3(5)
C(4)-Ru-Cl(1)	157.64(17)	C(10)-C(8)-C(4)	116.3(8)
N-Ru-Cl(2)	85.93(12)	C(10)-C(8)-C(9)	108.9(8)
C(5)-Ru-Cl(2)	90.75(17)	C(4)-C(8)-C(9)	106.4(7)
C(6)-Ru-Cl(2)	116.81(19)	N-C(11)-C(12)	121.0(6)
C(3)-Ru-Cl(2)	118.23(17)	C(13)-C(12)-C(11)	123.1(6)
C(2)-Ru-Cl(2)	156.41(19)	C(12)-C(13)-C(14)	115.4(5)
C(7)-Ru-Cl(2)	153.74(18)	C(12)-C(13)-C(16)	122.1(6)
C(4)-Ru-Cl(2)	90.74(16)	C(14)-C(13)-C(16)	122.6(5)
Cl(1)-Ru-Cl(2)	88.38(5)	C(13)-C(14)-C(15)	120.3(5)
C(15)-N-C(11)	117.0(5)		
N-C(15)-C(14)	123.2(5)		
C(15)-N-Ru	122.0(3)		
C(11)-N-Ru	120.8(4)		
C(7)-C(2)-C(3)	121.3(5)		
C(7)-C(2)-Ru	72.2(3)		
C(3)-C(2)-Ru	70.9(3)		
C(4)-C(3)-C(2)	120.5(5)		
C(4)-C(3)-Ru	72.1(3)		
C(2)-C(3)-Ru	70.9(3)		
C(5)-C(4)-C(3)	117.3(5)		
C(5)-C(4)-C(8)	121.9(6)		
C(3)-C(4)-C(8)	120.8(6)		
C(5)-C(4)-Ru	70.0(3)		
C(3)-C(4)-Ru	70.4(3)		
C(8)-C(4)-Ru	128.9(4)		
C(6)-C(5)-C(4)	121.7(5)		
C(6)-C(5)-Ru	71.6(3)		
C(4)-C(5)-Ru	72.6(3)		
C(5)-C(6)-C(7)	122.2(5)		
C(5)-C(6)-Ru	71.0(3)		
C(7)-C(6)-Ru	72.4(3)		
C(6)-C(7)-C(2)	117.0(6)		
C(6)-C(7)-C(1)	122.7(7)		
C(2)-C(7)-C(1)	120.3(7)		
C(6)-C(7)-Ru	70.4(3)		
C(2)-C(7)-Ru	70.5(3)		

Table 34: Anisotropic displacement parameters [$\text{\AA}^2 \times 10^3$] for $[(\eta^6\text{-p-cymene})\text{RuCl}_2(4\text{-methylpyridine})]$. The anisotropic displacement factor exponent takes the form $:-2\pi^2[(ha^*)^2U_{11}+\dots+2hka^*b^*U_{12}]$.

	U^{11}	U^{22}	U^{33}	U^{23}	U^{13}	U^{12}
Ru	32(1)	49(1)	29(1)	1(1)	1(1)	1(1)
Cl(1)	46(1)	61(1)	44(1)	13(1)	-4(1)	3(1)
Cl(2)	54(1)	66(1)	39(1)	-8(1)	-2(1)	-5(1)
N	39(2)	53(2)	32(2)	-2(2)	1(2)	3(2)
C(1)	167(9)	63(4)	66(5)	-3(4)	22(5)	19(5)
C(2)	64(4)	76(4)	29(2)	-8(2)	-2(2)	-19(3)
C(3)	45(3)	77(4)	31(2)	8(2)	-5(2)	6(2)
C(4)	61(3)	54(3)	36(3)	9(2)	-1(2)	-3(2)
C(5)	44(3)	83(4)	31(2)	8(2)	4(2)	-12(3)
C(6)	45(3)	83(4)	38(3)	8(3)	10(2)	19(3)
C(7)	70(4)	61(3)	34(2)	-6(2)	11(2)	12(3)
C(8)	118(6)	51(3)	62(4)	4(3)	1(4)	4(4)
C(9)	227(15)	71(6)	145(10)	27(6)	39(10)	-18(7)
C(10)	188(12)	73(5)	128(8)	19(6)	36(9)	41(7)
C(11)	43(3)	58(3)	52(3)	-2(3)	7(2)	3(2)
C(12)	48(3)	68(4)	54(3)	-10(3)	6(2)	11(3)
C(13)	41(3)	76(3)	28(2)	-2(2)	2(2)	-2(2)
C(14)	44(3)	66(3)	43(3)	1(2)	3(2)	-9(2)
C(15)	43(3)	53(3)	42(3)	-2(2)	1(2)	-2(2)
C(16)	41(3)	108(5)	43(3)	-9(3)	6(2)	-8(3)

Table 35: Hydrogen coordinates ($\times 10^3$) and isotropic displacement parameters [$\text{\AA}^2 \times 10^3$] for $[(\eta^6\text{-p-cymene})\text{RuCl}_2(4\text{-methylpyridine})]$.

	x	y	z	U(eq)
H(1C)	3620	5121	5309	119
H(1B)	3257	5079	6415	119
H(1A)	4207	5117	6259	119
H(2A)	2480(40)	5680(20)	5710(50)	62(18)
H(18)	2140(50)	6450(20)	5870(60)	90(20)
H(5A)	4670(60)	6570(20)	6800(70)	100(30)
H(6A)	4740(50)	5830(20)	6360(60)	70(20)
H(8A)	3620	7082	7015	92
H(9C)	3884	7491	5544	177
H(9B)	3698	7113	4838	177
H(9A)	4466	7108	5558	177
H(10C)	2570	7451	6473	155
H(10B)	2216	7019	6770	155
H(10A)	2356	7132	5616	155
H(11A)	1910(40)	6630(20)	8240(50)	62
H(12A)	610(50)	6440(20)	8830(60)	68
H(14A)	580(40)	5340(20)	8520(50)	61
H(15A)	1930(40)	5450(20)	7970(50)	55
H(16C)	-538	5658	9371	77
H(16B)	-796	5983	8547	77
H(16A)	-513	6127	9636	77

8.6 Crystal data for $[(\eta^6:\eta^1\text{-C}_6\text{H}_5(\text{CH}_2)_3\text{OH})\text{RuCl}_2]$ (13)**Table 36:** Crystal data and structure refinement for $[(\eta^6:\eta^1\text{-C}_6\text{H}_5(\text{CH}_2)_3\text{OH})\text{RuCl}_2]$.

Empirical formula	$\text{C}_9\text{H}_{12}\text{Cl}_2\text{O}_2\text{Ru}$
Formula weight	308.16
Temperature	293(2) K
Wavelength	0.71073 Å
Crystal system, space group	monoclinic, C2/c
Unit cell dimensions	$a = 13.6525(9)$ Å $\alpha = 90^\circ$. $b = 9.3455(8)$ Å $\beta = 90.47^\circ$. $c = 15.7922(11)$ Å $\gamma = 90^\circ$.
Volume	2014.8(3) Å ³
Z, Calculated density	4, 2.032 Mg/m ³
Absorption coefficient	2.041 mm ⁻¹
F(000)	1216
Θ range for data collection	3.68 to 28.29°.
Limiting indices	-18 ≤ h ≤ 18, -12 ≤ k ≤ 12, -20 ≤ l ≤ 20
Reflections collected / unique	11060 / 2483 [R(int) = 0.0835]
Completeness to $\theta =$	28.29 99.4 %

Absorption correction	Numerically
Refinement method	Full-matrix least-squares on F^2
Data / restraints / parameters	2483 / 0 / 167
Goodness-of-fit on F^2	1.086
Final R indices [$I > 2\sigma(I)$]	$R_1 = 0.0479$, $wR_2 = 0.0780$
R indices (all data)	$R_1 = 0.0678$, $wR_2 = 0.0843$
Extinction coefficient	0.00018(10)
Largest diff. peak and hole	0.793 and -0.889 e. \AA^{-3}

Table 37: Atomic coordinates ($\times 10^4$) and equivalent isotropic displacement parameters ($\text{\AA}^2 \times 10^3$) for $[(\eta^6\text{-}\eta^1\text{-C}_6\text{H}_5(\text{CH}_2)_3\text{OH})\text{RuCl}_2]$. U_{eq} is defined as one third of the trace of the orthogonalized U_{ij} -tensor.

	x	y	z	U(eq)
Ru(1)	3099(1)	890(1)	3481(1)	17(1)
Cl(1)	1413(1)	1648(1)	3425(1)	21(1)
Cl(2)	3010(1)	629(1)	1957(1)	21(1)
C(1)	3449(4)	837(6)	4828(3)	21(1)
C(2)	2771(4)	-260(6)	4621(3)	25(1)
C(3)	2969(4)	-1252(5)	3966(3)	24(1)
C(4)	3848(4)	-1149(5)	3527(3)	24(1)
C(5)	4538(4)	-65(6)	3717(3)	23(1)
C(6)	4329(3)	964(5)	4357(3)	20(1)
C(7)	4995(4)	2236(6)	4479(3)	25(1)

8. Appendix

C(8)	5063(4)	3205(6)	3707(4)	30(1)
C(9)	4145(4)	4018(6)	3498(3)	24(1)
O(1)	3391(3)	3085(4)	3155(2)	24(1)

Table 38: Bond lengths (Å) and angles [°] for $[(\eta^6\text{-}\eta^1\text{-C}_6\text{H}_5(\text{CH}_2)_3\text{OH})\text{RuCl}_2]$.

Ru(1)-C(2)	2.148(5)	C(4)-Ru(1)-C(6)	69.12(19)
Ru(1)-C(3)	2.152(5)	C(2)-Ru(1)-C(1)	38.25(19)
Ru(1)-O(1)	2.153(3)	C(3)-Ru(1)-C(1)	69.45(19)
Ru(1)-C(4)	2.163(5)	O(1)-Ru(1)-C(1)	102.45(17)
Ru(1)-C(6)	2.167(4)	C(4)-Ru(1)-C(1)	81.21(19)
Ru(1)-C(1)	2.177(4)	C(6)-Ru(1)-C(1)	38.24(17)
Ru(1)-C(5)	2.187(5)	C(2)-Ru(1)-C(5)	81.2(2)
Ru(1)-Cl(1)	2.4093(12)	C(3)-Ru(1)-C(5)	68.7(2)
Ru(1)-Cl(2)	2.4203(12)	O(1)-Ru(1)-C(5)	105.16(18)
C(1)-C(2)	1.417(7)	C(4)-Ru(1)-C(5)	37.9(2)
C(1)-C(6)	1.423(7)	C(6)-Ru(1)-C(5)	38.23(18)
C(2)-C(3)	1.418(7)	C(1)-Ru(1)-C(5)	68.58(19)
C(3)-C(4)	1.394(8)	C(2)-Ru(1)-Cl(1)	88.38(15)
C(4)-C(5)	1.414(7)	C(3)-Ru(1)-Cl(1)	101.81(15)
C(5)-C(6)	1.426(7)	O(1)-Ru(1)-Cl(1)	83.69(10)
C(6)-C(7)	1.508(7)	C(4)-Ru(1)-Cl(1)	135.32(15)
C(7)-C(8)	1.521(7)	C(6)-Ru(1)-Cl(1)	138.48(13)
C(8)-C(9)	1.499(7)	C(1)-Ru(1)-Cl(1)	104.15(13)
C(9)-O(1)	1.450(6)	C(5)-Ru(1)-Cl(1)	169.38(15)
C(2)-Ru(1)-C(3)	38.5(2)	C(2)-Ru(1)-Cl(2)	140.71(15)
C(2)-Ru(1)-O(1)	135.83(18)	C(3)-Ru(1)-Cl(2)	104.85(14)
C(3)-Ru(1)-O(1)	171.02(16)	O(1)-Ru(1)-Cl(2)	82.33(10)
C(2)-Ru(1)-C(4)	68.5(2)	C(4)-Ru(1)-Cl(2)	87.98(14)
C(3)-Ru(1)-C(4)	37.7(2)	C(6)-Ru(1)-Cl(2)	132.08(13)
O(1)-Ru(1)-C(4)	139.38(18)	C(1)-Ru(1)-Cl(2)	167.94(13)
C(2)-Ru(1)-C(6)	69.32(19)	C(5)-Ru(1)-Cl(2)	99.56(14)
C(3)-Ru(1)-C(6)	82.45(19)	Cl(1)-Ru(1)-Cl(2)	87.28(4)
O(1)-Ru(1)-C(6)	88.73(16)	C(2)-C(1)-C(6)	119.5(5)

C(2)-C(1)-Ru(1)	69.8(3)
C(6)-C(1)-Ru(1)	70.5(3)
C(1)-C(2)-C(3)	120.8(5)
C(1)-C(2)-Ru(1)	72.0(3)
C(3)-C(2)-Ru(1)	70.9(3)
C(4)-C(3)-C(2)	119.2(5)
C(4)-C(3)-Ru(1)	71.6(3)
C(2)-C(3)-Ru(1)	70.6(3)
C(3)-C(4)-C(5)	121.3(5)
C(3)-C(4)-Ru(1)	70.7(3)
C(5)-C(4)-Ru(1)	71.9(3)
C(4)-C(5)-C(6)	119.7(5)
C(4)-C(5)-Ru(1)	70.1(3)
C(6)-C(5)-Ru(1)	70.1(3)
C(1)-C(6)-C(5)	119.3(5)
C(1)-C(6)-C(7)	120.7(4)
C(5)-C(6)-C(7)	119.8(4)
C(1)-C(6)-Ru(1)	71.2(2)
C(5)-C(6)-Ru(1)	71.6(3)
C(7)-C(6)-Ru(1)	124.7(3)
C(6)-C(7)-C(8)	114.0(4)
C(9)-C(8)-C(7)	115.0(5)
O(1)-C(9)-C(8)	111.5(5)
C(9)-O(1)-Ru(1)	128.0(3)

8. Appendix

Table 39: Anisotropic displacement parameters ($\text{Å}^2 \times 10^3$) for $\{(\eta^6\text{-}\eta^1\text{-C}_6\text{H}_5(\text{CH}_2)_3\text{OH})\text{RuCl}_2\}$. The anisotropic displacement factor exponent takes the form: $-2\pi^2[(ha^*)^2U_{11} + \dots + 2hka^*b^*U_{12}]$.

	U^{11}	U^{22}	U^{33}	U^{23}	U^{13}	U^{12}
Ru(1)	20(1)	15(1)	16(1)	0(1)	-2(1)	-1(1)
Cl(1)	21(1)	21(1)	21(1)	-2(1)	-1(1)	0(1)
Cl(2)	24(1)	20(1)	18(1)	1(1)	-1(1)	-1(1)
C(1)	28(2)	20(2)	14(2)	-5(2)	-6(2)	2(2)
C(2)	32(3)	25(3)	19(2)	9(2)	3(2)	-1(2)
C(3)	29(3)	13(2)	28(3)	4(2)	-7(2)	-5(2)
C(4)	38(3)	14(2)	21(2)	-2(2)	-7(2)	8(2)
C(5)	18(2)	29(3)	21(2)	5(2)	-4(2)	9(2)
C(6)	19(2)	23(2)	17(2)	1(2)	-5(2)	2(2)
C(7)	29(3)	22(3)	24(3)	-2(2)	-4(2)	-3(2)
C(8)	28(3)	29(3)	33(3)	7(2)	-2(2)	-1(2)
C(9)	26(3)	19(2)	26(3)	1(2)	-1(2)	-7(2)
O(1)	22(2)	13(2)	37(2)	3(2)	-8(2)	1(1)

8.7 Crystal data for $[\{\eta^6\text{-C}_6\text{H}_5(\text{CH}_2)_3\text{OMe}\}\text{RuCl}_2]_2$ (14).**Table 40:** Crystal data and structure refinement for $[\{\eta^6\text{-C}_6\text{H}_5(\text{CH}_2)_3\text{OMe}\}\text{RuCl}_2]_2$.

Empirical formula	C ₁₀ H ₁₄ Cl ₂ O Ru	
Formula weight	322.18	
Temperature	293(2) K	
Wavelength	0.71073 Å	
Crystal system, space group	triclinic, P-1	
Unit cell dimensions	a = 7.4241(2) Å	$\alpha = 108.792(2)^\circ$.
	b = 7.7451(3) Å	$\beta = 92.177(2)^\circ$.
	c = 10.7216(3) Å	$\gamma = 103.886(2)^\circ$.
Volume	562.10(3) Å ³	
Z, Calculated density	2, 1.904 Mg/m ³	
Absorption coefficient	1.833 mm ⁻¹	
F(000)	320	
θ range for data collection	3.69 to 27.51°.	
Limiting indices	-8 ≤ h ≤ 9, -10 ≤ k ≤ 10, -13 ≤ l ≤ 13	
Reflections collected / unique	12912 / 2572 [R(int) = 0.0877]	
Completeness to $\theta =$	27.51	99.6 %

8. Appendix

Refinement method Full-matrix least-squares on F^2

Data / restraints / parameters 2572 / 0 / 128

Goodness-of-fit on F^2 1.052

Final R indices [$I > 2\sigma(I)$] $R_1 = 0.0444$, $wR_2 = 0.1095$

R indices (all data) $R_1 = 0.0495$, $wR_2 = 0.1128$

Extinction coefficient 0.014(3)

Largest diff. peak and hole 2.768 and -3.206 e. \AA^{-3}

Table 41: Atomic coordinates ($\times 10^4$) and equivalent isotropic displacement parameters ($\text{\AA}^2 \times 10^3$) for $[\{\eta^6\text{-C}_6\text{H}_5(\text{CH}_2)_3\text{OMe}\}\text{RuCl}_2]_2$. U_{eq} is defined as one third of the trace of the orthogonalized U_{ij} -tensor.

	x	y	z	U(eq)
Ru	6283(1)	8210(1)	9356(1)	13(1)
Cl(1)	3323(2)	8416(2)	10232(1)	16(1)
Cl(2)	7576(2)	9074(2)	11632(1)	21(1)
O(1)	-1041(8)	2795(16)	6067(12)	204(9)
C(1)	5620(7)	5155(7)	8381(5)	19(1)
C(2)	7562(8)	5876(7)	8789(5)	24(1)
C(3)	8636(7)	7371(8)	8418(5)	23(1)
C(4)	7711(7)	8145(7)	7641(5)	20(1)
C(5)	5738(7)	7422(7)	7210(5)	19(1)
C(6)	4695(7)	5936(7)	7589(5)	17(1)
C(7)	2607(7)	5209(8)	7211(5)	23(1)
C(8)	2130(8)	3512(8)	5911(5)	26(1)

C(9)	72(13)	2650(20)	5570(10)	124(7)
C(10)	-2950(9)	1954(12)	5805(9)	63(3)

Table 42: Bond lengths (Å) and angles [°] for $[[\{\eta^6\text{-C}_6\text{H}_5(\text{CH}_2)_3\text{OMe}\}\text{RuCl}_2]_2$.

Ru-C(4)	2.149(5)	C(5)-Ru-C(1)	68.6(2)
Ru-C(2)	2.167(5)	C(3)-Ru-C(1)	68.9(2)
Ru-C(5)	2.175(5)	C(4)-Ru-C(6)	69.07(19)
Ru-C(3)	2.177(5)	C(2)-Ru-C(6)	69.0(2)
Ru-C(1)	2.177(5)	C(5)-Ru-C(6)	37.73(19)
Ru-C(6)	2.183(5)	C(3)-Ru-C(6)	82.05(19)
Ru-Cl(2)	2.4055(12)	C(1)-Ru-C(6)	38.28(19)
Ru-Cl(1)	2.4424(12)	C(4)-Ru-Cl(2)	129.05(15)
Ru-Cl(1)#1	2.4477(12)	C(2)-Ru-Cl(2)	90.33(15)
Cl(1)-Ru#1	2.4477(11)	C(5)-Ru-Cl(2)	167.41(14)
O(1)-C(9)	1.010(11)	C(3)-Ru-Cl(2)	98.11(15)
O(1)-C(10)	1.386(9)	C(1)-Ru-Cl(2)	110.26(14)
C(1)-C(2)	1.411(7)	C(6)-Ru-Cl(2)	146.27(14)
C(1)-C(6)	1.429(7)	C(4)-Ru-Cl(1)	143.37(15)
C(2)-C(3)	1.418(8)	C(2)-Ru-Cl(1)	130.54(16)
C(3)-C(4)	1.415(8)	C(5)-Ru-Cl(1)	106.97(14)
C(4)-C(5)	1.435(7)	C(3)-Ru-Cl(1)	167.59(15)
C(5)-C(6)	1.409(7)	C(1)-Ru-Cl(1)	98.72(14)
C(6)-C(7)	1.507(7)	C(6)-Ru-Cl(1)	88.28(13)
C(7)-C(8)	1.534(7)	Cl(2)-Ru-Cl(1)	85.62(4)
C(8)-C(9)	1.491(10)	C(4)-Ru-Cl(1)#1	87.15(14)
C(4)-Ru-C(2)	68.7(2)	C(2)-Ru-Cl(1)#1	146.52(16)
C(4)-Ru-C(5)	38.75(19)	C(5)-Ru-Cl(1)#1	94.08(14)
C(2)-Ru-C(5)	81.5(2)	C(3)-Ru-Cl(1)#1	109.31(16)
C(4)-Ru-C(3)	38.2(2)	C(1)-Ru-Cl(1)#1	162.34(14)
C(2)-Ru-C(3)	38.1(2)	C(6)-Ru-Cl(1)#1	124.64(14)
C(5)-Ru-C(3)	69.6(2)	Cl(2)-Ru-Cl(1)#1	87.40(4)
C(4)-Ru-C(1)	81.4(2)	Cl(1)-Ru-Cl(1)#1	82.60(4)
C(2)-Ru-C(1)	37.9(2)	Ru-Cl(1)-Ru#1	97.40(4)

8. Appendix

C(9)-O(1)-C(10)	135.6(8)
C(2)-C(1)-C(6)	120.2(5)
C(2)-C(1)-Ru	70.7(3)
C(6)-C(1)-Ru	71.1(3)
C(1)-C(2)-C(3)	121.0(5)
C(1)-C(2)-Ru	71.4(3)
C(3)-C(2)-Ru	71.3(3)
C(4)-C(3)-C(2)	118.5(5)
C(4)-C(3)-Ru	69.8(3)
C(2)-C(3)-Ru	70.6(3)
C(3)-C(4)-C(5)	121.3(5)
C(3)-C(4)-Ru	72.0(3)
C(5)-C(4)-Ru	71.6(3)
C(6)-C(5)-C(4)	119.4(5)
C(6)-C(5)-Ru	71.4(3)
C(4)-C(5)-Ru	69.6(3)
C(5)-C(6)-C(1)	119.6(5)
C(5)-C(6)-C(7)	120.8(5)
C(1)-C(6)-C(7)	119.6(5)
C(5)-C(6)-Ru	70.9(3)
C(1)-C(6)-Ru	70.7(3)
C(7)-C(6)-Ru	129.0(3)
C(6)-C(7)-C(8)	110.4(4)
C(9)-C(8)-C(7)	111.8(5)
O(1)-C(9)-C(8)	134.1(8)

Table 43: Anisotropic displacement parameters ($\text{Å}^2 \times 10^3$) for $[\{\eta^6\text{-C}_6\text{H}_5(\text{CH}_2)_3\text{OMe}\}\text{RuCl}_2]_2$. The anisotropic displacement factor exponent takes the form: $-2\pi^2[(ha^*)^2U_{11} + \dots + 2hka^*b^*U_{12}]$.

	U^{11}	U^{22}	U^{33}	U^{23}	U^{13}	U^{12}
Ru	12(1)	12(1)	13(1)	3(1)	0(1)	2(1)
Cl(1)	15(1)	13(1)	17(1)	4(1)	3(1)	2(1)
Cl(2)	20(1)	21(1)	17(1)	7(1)	-5(1)	-2(1)
O(1)	15(3)	197(10)	196(10)	-173(9)	14(4)	-12(4)
C(1)	23(2)	11(2)	19(2)	1(2)	4(2)	3(2)
C(2)	27(3)	19(2)	24(3)	1(2)	0(2)	11(2)
C(3)	16(2)	23(3)	24(3)	-2(2)	4(2)	9(2)
C(4)	21(2)	17(2)	18(2)	2(2)	10(2)	2(2)
C(5)	25(2)	20(2)	11(2)	4(2)	6(2)	7(2)
C(6)	14(2)	15(2)	12(2)	-3(2)	0(2)	1(2)
C(7)	16(2)	26(3)	17(2)	-2(2)	-2(2)	2(2)
C(8)	20(3)	29(3)	20(3)	-2(2)	1(2)	2(2)
C(9)	39(5)	162(12)	52(6)	-73(7)	15(4)	-44(6)
C(10)	16(3)	52(5)	73(6)	-35(4)	-7(3)	0(3)

8. Appendix

Table 44: Hydrogen coordinates ($\times 10^4$) and isotropic displacement parameters ($\text{Å}^2 \times 10^3$) for $[\{\eta^6\text{-C}_6\text{H}_5(\text{CH}_2)_3\text{OMe}\}\text{RuCl}_2]_2$.

	x	y	z	U(eq)
H(1A)	4868	4328	8803	23
H(2A)	8118	5533	9488	29
H(3A)	9918	8028	8848	28
H(4A)	8372	9345	7547	24
H(5A)	5086	8135	6833	23
H(7B)	2109	6208	7104	27
H(7A)	2033	4831	7914	27
H(8B)	2617	3922	5197	31
H(8A)	2731	2567	5996	31
H(9B)	-226	2903	4769	149
H(9A)	-48	1299	5283	149
H(10C)	-3547	2515	6552	76
H(10B)	-3180	623	5648	76
H(10A)	-3447	2141	5033	76

8.8 Crystal data for $[(\eta^6\text{-p-cymene})(\eta^6\text{-C}_6\text{H}_3(\text{CMe}_2\text{OH})_{3,1,3,5})\text{Ru}]^{2+} (\text{Cl}^-)_2 \times 2 \text{H}_2\text{O}$ (16)**Table 45:** Crystal data and structure refinement for ($\text{Å}^2 \times 10^3$) for $[(\eta^6\text{-p-cymene})(\eta^6\text{-C}_6\text{H}_3(\text{CMe}_2\text{OH})_{3,1,3,5})\text{Ru}]^{2+} (\text{Cl}^-)_2 \times 2 \text{H}_2\text{O}$.

Empirical formula	$\text{C}_{25} \text{H}_{42} \text{Cl}_2 \text{O}_5 \text{Ru}$
Formula weight	594.56 g/ mol
Temperature	293(2) K
Wavelength	0.71073 Å
Crystal system, space group	monoclinic, $\text{P2}_1/\text{c}$
Unit cell dimensions	$a = 15.9661(3) \text{ Å}$ $\alpha = 90^\circ$. $b = 9.2832(2) \text{ Å}$ $\beta = 91.2690(10)^\circ$. $c = 18.3497(3) \text{ Å}$ $\gamma = 90^\circ$.
Volume	$2719.06(9) \text{ Å}^3$
Z, Calculated density	4, 1.452 g/cm^3
Absorption coefficient	0.805 mm^{-1}
F(000)	1240
θ range for data collection	1.28 to 27.49° .
Limiting indices	$-20 < h < 20$, $12 < k < 11$, $-23 < l < 23$
Reflections collected / unique ^{a)}	49249 / 6214 [R(int) = 0.1020]
Completeness to $\theta = 27.49$	99.8 %

8. Appendix

Refinement method	Full-matrix least-squares on F^2
Data / restraints / parameters	6214 / 0 / 435
Goodness-of-fit ^{d)} on F^2	1.111
Final R indices [$I > 2\sigma(I)$]	$R_1^{b)} = 0.0499$, $wR_2^{c)} = 0.1244$
R indices (all data)	$R_1^{b)} = 0.0608$, $wR_2^{c)} = 0.1313$
Extinction coefficient	0.0097(8)
Largest diff. peak and hole	0.908 and -1.017 e. \AA^{-3}

Table 46: Atomic coordinates ($\times 10^4$) and equivalent isotropic displacement parameters ($\text{Å}^2 \times 10^3$) for $[(\eta^6\text{-p-cymene})(\eta^6\text{-C}_6\text{H}_3(\text{CMe}_2\text{OH})_3\text{-1,3,5})\text{Ru}]^{2+} (\text{Cl})_2 \times 2 \text{H}_2\text{O}$. U_{eq} is defined as one third of the trace of the orthogonalized U_{ij} -tensor.

	x	y	z	U(eq)
Cl(2)	5631(1)	2962(2)	10046(1)	100(1)
C(1)	3139(2)	-366(4)	9117(2)	39(1)
C(2)	1631(2)	-134(4)	8982(2)	37(1)
C(3)	3277(2)	3746(4)	8962(2)	41(1)
C(4)	1774(2)	3798(4)	9053(2)	43(1)
C(5)	2525(2)	588(4)	7998(2)	40(1)
C(6)	3346(3)	3212(4)	9680(2)	44(1)
C(41)	1839(3)	3290(4)	9774(2)	45(1)
C(8)	2334(2)	-552(4)	9413(2)	38(1)
C(9)	1709(2)	427(4)	8263(2)	36(1)
C(10)	951(2)	780(4)	7776(2)	43(1)
C(11)	3243(2)	158(4)	8407(2)	40(1)
C(12)	2493(2)	4073(4)	8634(2)	39(1)
C(13)	2630(3)	3024(4)	10109(2)	46(1)
C(14)	2235(2)	-1276(4)	10159(2)	44(1)
C(15)	2404(3)	4734(4)	7881(2)	47(1)
O(17)	1185(2)	2014(3)	7371(2)	55(1)
O(18)	2955(2)	-1000(4)	10604(2)	55(1)
O(19)	4061(2)	1173(4)	7482(2)	70(1)
C(19)	1482(3)	-723(6)	10561(3)	60(1)
C(20)	2125(4)	-2890(5)	10010(3)	61(1)
C(21)	4110(2)	178(5)	8069(2)	51(1)
C(22)	168(3)	1083(6)	8204(3)	61(1)
C(23)	3201(4)	4660(6)	7443(3)	61(1)
C(24)	2732(5)	2557(7)	10889(3)	73(2)
C(25)	4258(4)	-1354(6)	7803(4)	73(2)
C(26)	2126(4)	6295(6)	7969(3)	66(1)

8. Appendix

C(27)	815(4)	-523(5)	7289(3)	66(1)
C(28)	4796(3)	641(8)	8604(4)	81(2)
O(1)	4786(3)	206(6)	6206(3)	98(2)
O(2)	172(5)	5932(9)	10581(4)	85(3)

Table 47: Bond lengths (Å) and angles [°] for $[(\eta^6\text{-C}_6\text{H}_3(\text{CMe}_2\text{OH})_3\text{-1,3,5})\text{Ru}]^{2+} (\text{Cl}^-)_2 \times 2 \text{H}_2\text{O}$.

Ru-C(4)	2.212(4)	C(10)-C(22)	1.517(6)
Ru-C(6)	2.227(4)	C(10)-C(27)	1.518(6)
Ru-C(3)	2.230(3)	C(11)-C(21)	1.530(5)
Ru-C(41)	2.231(3)	C(12)-C(15)	1.517(5)
Ru-C(1)	2.232(4)	C(13)-C(24)	1.502(6)
Ru-C(2)	2.239(3)	C(14)-O(18)	1.418(5)
Ru-C(11)	2.250(3)	C(14)-C(19)	1.514(6)
Ru-C(9)	2.252(3)	C(14)-C(20)	1.532(6)
Ru-C(12)	2.269(3)	C(15)-C(23)	1.520(7)
Ru-C(8)	2.273(3)	C(15)-C(26)	1.526(6)
Ru-C(13)	2.289(3)	O(19)-C(21)	1.420(5)
C(1)-C(11)	1.404(5)	C(21)-C(28)	1.516(7)
C(1)-C(8)	1.418(5)	C(21)-C(25)	1.524(7)
C(2)-C(8)	1.414(5)	C(5)-Ru-C(4)	116.95(15)
C(2)-C(9)	1.425(5)	C(5)-Ru-C(6)	137.04(15)
C(3)-C(12)	1.409(5)	C(4)-Ru-C(6)	77.91(16)
C(3)-C(6)	1.410(6)	C(5)-Ru-C(3)	109.25(14)
C(4)-C(41)	1.407(6)	C(4)-Ru-C(3)	65.67(15)
C(4)-C(12)	1.418(5)	C(6)-Ru-C(3)	36.90(14)
C(5)-C(9)	1.409(5)	C(5)-Ru-C(41)	149.07(16)
C(5)-C(11)	1.412(5)	C(4)-Ru-C(41)	36.92(15)
C(6)-C(13)	1.412(6)	C(6)-Ru-C(41)	65.65(16)
C(41)-C(13)	1.414(6)	C(3)-Ru-C(41)	77.64(14)
C(8)-C(14)	1.536(5)	C(5)-Ru-C(1)	66.22(14)
C(9)-C(10)	1.523(5)	C(4)-Ru-C(1)	174.24(14)
C(10)-O(17)	1.420(4)	C(6)-Ru-C(1)	103.11(15)

C(3)-Ru-C(1)	118.51(14)	C(1)-Ru-C(8)	36.67(13)
C(41)-Ru-C(1)	138.27(15)	C(2)-Ru-C(8)	36.53(12)
C(5)-Ru-C(2)	66.03(13)	C(11)-Ru-C(8)	66.02(13)
C(4)-Ru-C(2)	110.62(14)	C(9)-Ru-C(8)	66.67(12)
C(6)-Ru-C(2)	150.27(14)	C(12)-Ru-C(8)	173.30(12)
C(3)-Ru-C(2)	172.50(13)	C(5)-Ru-C(13)	173.24(14)
C(41)-Ru-C(2)	103.38(14)	C(4)-Ru-C(13)	66.05(15)
C(1)-Ru-C(2)	65.71(13)	C(6)-Ru-C(13)	36.40(15)
C(5)-Ru-C(11)	36.97(14)	C(3)-Ru-C(13)	65.87(14)
C(4)-Ru-C(11)	148.56(15)	C(41)-Ru-C(13)	36.42(16)
C(6)-Ru-C(11)	110.38(14)	C(1)-Ru-C(13)	111.37(14)
C(3)-Ru-C(11)	102.09(13)	C(2)-Ru-C(13)	119.32(14)
C(41)-Ru-C(11)	173.78(15)	C(11)-Ru-C(13)	137.76(15)
C(1)-Ru-C(11)	36.52(14)	C(9)-Ru-C(13)	149.85(14)
C(2)-Ru-C(11)	77.71(13)	C(12)-Ru-C(13)	78.33(13)
C(5)-Ru-C(9)	36.86(13)	C(8)-Ru-C(13)	103.58(13)
C(4)-Ru-C(9)	101.21(14)	C(11)-C(1)-C(8)	121.6(3)
C(6)-Ru-C(9)	172.53(14)	C(11)-C(1)-Ru	72.4(2)
C(3)-Ru-C(9)	135.97(13)	C(8)-C(1)-Ru	73.2(2)
C(41)-Ru-C(9)	118.00(14)	C(8)-C(2)-C(9)	122.3(3)
C(1)-Ru-C(9)	78.53(13)	C(8)-C(2)-Ru	73.03(19)
C(2)-Ru-C(9)	37.00(12)	C(9)-C(2)-Ru	71.99(18)
C(11)-Ru-C(9)	66.55(12)	C(12)-C(3)-C(6)	121.7(3)
C(5)-Ru-C(12)	100.54(14)	C(12)-C(3)-Ru	73.3(2)
C(4)-Ru-C(12)	36.87(13)	C(6)-C(3)-Ru	71.4(2)
C(6)-Ru-C(12)	66.37(14)	C(41)-C(4)-C(12)	121.8(4)
C(3)-Ru-C(12)	36.47(13)	C(41)-C(4)-Ru	72.3(2)
C(41)-Ru-C(12)	66.51(14)	C(12)-C(4)-Ru	73.8(2)
C(1)-Ru-C(12)	148.72(13)	C(9)-C(5)-C(11)	122.2(3)
C(2)-Ru-C(12)	136.99(13)	C(9)-C(5)-Ru	73.5(2)
C(11)-Ru-C(12)	116.94(13)	C(11)-C(5)-Ru	73.3(2)
C(9)-Ru-C(12)	108.44(12)	C(3)-C(6)-C(13)	121.1(4)
C(5)-Ru-C(8)	78.32(14)	C(3)-C(6)-Ru	71.7(2)
C(4)-Ru-C(8)	137.94(13)	C(13)-C(6)-Ru	74.2(2)
C(6)-Ru-C(8)	118.94(14)	C(4)-C(41)-C(13)	120.9(4)
C(3)-Ru-C(8)	150.15(13)	C(4)-C(41)-Ru	70.8(2)
C(41)-Ru-C(8)	111.16(13)	C(13)-C(41)-Ru	74.0(2)

8. Appendix

C(2)-C(8)-C(1)	117.9(3)	O(18)-C(14)-C(20)	111.6(4)
C(2)-C(8)-C(14)	121.6(3)	C(19)-C(14)-C(20)	109.2(4)
C(1)-C(8)-C(14)	120.5(3)	O(18)-C(14)-C(8)	109.6(3)
C(2)-C(8)-Ru	70.44(19)	C(19)-C(14)-C(8)	112.6(3)
C(1)-C(8)-Ru	70.1(2)	C(20)-C(14)-C(8)	106.4(3)
C(14)-C(8)-Ru	134.2(2)	C(12)-C(15)-C(23)	113.6(4)
C(5)-C(9)-C(2)	117.3(3)	C(12)-C(15)-C(26)	108.0(4)
C(5)-C(9)-C(10)	120.2(3)	C(23)-C(15)-C(26)	110.3(4)
C(2)-C(9)-C(10)	122.5(3)	O(19)-C(21)-C(28)	109.5(4)
C(5)-C(9)-Ru	69.69(19)	O(19)-C(21)-C(25)	111.7(4)
C(2)-C(9)-Ru	71.00(18)	C(28)-C(21)-C(25)	111.0(5)
C(10)-C(9)-Ru	132.6(2)	O(19)-C(21)-C(11)	106.2(3)
O(17)-C(10)-C(22)	110.5(3)	C(28)-C(21)-C(11)	112.9(4)
O(17)-C(10)-C(27)	111.7(4)	C(25)-C(21)-C(11)	105.4(4)
C(22)-C(10)-C(27)	110.1(4)		
O(17)-C(10)-C(9)	105.5(3)		
C(22)-C(10)-C(9)	112.9(3)		
C(27)-C(10)-C(9)	106.0(3)		
C(1)-C(11)-C(5)	118.7(3)		
C(1)-C(11)-C(21)	120.4(3)		
C(5)-C(11)-C(21)	120.9(3)		
C(1)-C(11)-Ru	71.1(2)		
C(5)-C(11)-Ru	69.73(19)		
C(21)-C(11)-Ru	134.2(3)		
C(3)-C(12)-C(4)	116.9(3)		
C(3)-C(12)-C(15)	122.7(3)		
C(4)-C(12)-C(15)	120.4(3)		
C(3)-C(12)-Ru	70.2(2)		
C(4)-C(12)-Ru	69.4(2)		
C(15)-C(12)-Ru	132.9(3)		
C(6)-C(13)-C(41)	117.6(4)		
C(6)-C(13)-C(24)	119.6(4)		
C(41)-C(13)-C(24)	122.8(4)		
C(6)-C(13)-Ru	69.4(2)		
C(41)-C(13)-Ru	69.6(2)		
C(24)-C(13)-Ru	132.5(3)		
O(18)-C(14)-C(19)	107.5(4)		

Table 48: Anisotropic displacement parameters [$\text{\AA}^2 \times 10^3$] for $[(\eta^6\text{-p-cymene})(\eta^6\text{-C}_6\text{H}_3(\text{CMe}_2\text{OH})_{3-1,3,5})\text{Ru}]^{2+} (\text{Cl}^-)_2 \times 2 \text{H}_2\text{O}$. The anisotropic displacement factor exponent takes the form $-2\pi^2[(ha^*)^2U_{11} + \dots + 2hka^*b^*U_{12}]$.

	U^{11}	U^{22}	U^{33}	U^{23}	U^{13}	U^{12}
Ru	31(1)	30(1)	35(1)	-2(1)	1(1)	-1(1)
Cl(1)	67(1)	71(1)	60(1)	14(1)	-15(1)	-23(1)
Cl(2)	88(1)	106(1)	105(1)	-4(1)	-7(1)	41(1)
C(1)	39(2)	34(2)	45(2)	0(2)	-7(1)	8(1)
C(2)	38(2)	25(2)	47(2)	0(1)	-1(1)	-4(1)
C(3)	39(2)	37(2)	46(2)	-2(2)	2(2)	-12(1)
C(4)	42(2)	29(2)	58(2)	-3(2)	4(2)	3(1)
C(5)	45(2)	39(2)	35(2)	-4(2)	3(1)	-2(1)
C(6)	46(2)	42(2)	45(2)	-6(2)	-7(2)	-8(2)
C(41)	51(2)	32(2)	53(2)	-7(2)	21(2)	0(2)
C(8)	45(2)	27(2)	41(2)	0(1)	-3(1)	1(1)
C(9)	39(2)	28(2)	40(2)	-3(1)	-5(1)	-3(1)
C(10)	46(2)	34(2)	50(2)	9(2)	-14(2)	-6(1)
C(11)	37(2)	33(2)	50(2)	-10(2)	7(1)	2(1)
C(12)	43(2)	25(2)	49(2)	-3(1)	0(2)	-4(1)
C(13)	67(2)	37(2)	34(2)	-8(1)	4(2)	-5(2)
C(14)	52(2)	40(2)	41(2)	4(2)	-3(2)	1(2)
C(15)	54(2)	36(2)	49(2)	3(2)	-8(2)	-8(2)
O(17)	60(2)	44(2)	59(2)	18(1)	-22(2)	-15(1)
O(18)	57(2)	62(2)	44(2)	-6(1)	-8(1)	6(2)
O(19)	78(2)	59(2)	74(2)	14(2)	33(2)	6(2)
C(19)	60(3)	66(3)	55(3)	9(2)	11(2)	4(2)
C(20)	80(3)	43(2)	59(3)	13(2)	-4(2)	-7(2)
C(21)	47(2)	52(2)	55(2)	1(2)	19(2)	5(2)
C(22)	40(2)	57(3)	86(3)	21(3)	-6(2)	0(2)
C(23)	91(3)	50(3)	42(2)	5(2)	12(2)	2(2)

8. Appendix

C(24)	105(4)	74(4)	39(2)	-6(2)	5(2)	-14(3)
C(25)	73(3)	53(3)	94(4)	-3(3)	36(3)	14(2)
C(26)	78(3)	48(2)	73(3)	12(2)	10(3)	14(2)
C(27)	77(3)	44(2)	77(3)	-1(2)	-30(3)	-9(2)
C(28)	42(2)	112(5)	88(4)	-19(4)	12(2)	-7(3)
O(1)	109(4)	115(4)	71(3)	-4(3)	25(3)	12(3)
O(2)	101(6)	82(6)	74(5)	22(4)	13(4)	9(4)

Table 49: Hydrogen coordinates ($\times 10^3$) and isotropic displacement parameters [$\text{\AA}^2 \times 10^3$] for $[(\eta^6\text{-p-cymene})(\eta^6\text{-C}_6\text{H}_3(\text{CMe}_2\text{OH})_{3-1,3,5})\text{Ru}]^{2+} (\text{Cl}^-)_2 \times 2 \text{H}_2\text{O}$.

	x	y	z	U(eq)
H(36)	3500(20)	-760(40)	9350(20)	35(10)
H(39)	1080(30)	-330(40)	9160(20)	43(10)
H(38)	3770(30)	3830(50)	8620(20)	45(11)
H(4A)	1260(30)	3930(50)	8850(20)	52
H(35)	2570(20)	1010(40)	7620(20)	25(9)
H(37)	3790(40)	2980(60)	9860(30)	69(17)
H(42)	1330(30)	3110(50)	9980(30)	57(13)
H(15A)	2040(30)	4310(50)	7640(30)	56
H(32)	840(40)	2090(70)	7070(40)	90(20)
H(30)	3250(40)	-1490(70)	10410(30)	80(20)
H(19D)	4297	835	7128	105
H(19C)	1500(30)	-1150(60)	11090(30)	72
H(19B)	1000(40)	-940(60)	10350(30)	72
H(19A)	1460(30)	270(70)	10560(30)	72
H(20C)	2040(30)	-3380(60)	10510(30)	73
H(20B)	2670(40)	-3150(60)	9830(30)	73
H(20A)	1580(40)	-3150(50)	9650(30)	73
H(22C)	-300(30)	1100(60)	7840(30)	73

H(22B)	300(40)	1820(60)	8630(30)	73
H(22A)	10(30)	380(70)	8440(30)	73
H(23C)	3120(30)	5050(60)	7030(30)	73
H(23B)	3400(30)	3680(70)	7290(30)	73
H(23A)	3610(30)	5140(60)	7690(30)	73
H(24C)	3050(40)	3310(70)	11150(40)	87
H(24B)	3450(40)	1990(60)	10940(30)	87
H(24A)	2260(40)	2650(80)	11020(30)	87
H(25C)	4760(40)	-1370(70)	7510(30)	87
H(25B)	3750(40)	-1500(70)	7480(30)	87
H(25A)	4350(40)	-1950(70)	8290(40)	87
H(26C)	2060(40)	6590(60)	7420(30)	79
H(26B)	2700(40)	6840(60)	8200(30)	79
H(26A)	1730(40)	6300(70)	8240(30)	79
H(27C)	280(30)	-60(60)	6890(30)	80
H(27B)	760(40)	-1320(70)	7520(30)	80
H(27A)	1300(40)	-670(60)	7050(30)	80
H(28C)	5470(40)	440(70)	8430(30)	97
H(28B)	4970(40)	-490(70)	9040(30)	97
H(28A)	4770(40)	1020(80)	9020(40)	97
H(29)	4490(30)	450(50)	6510(30)	50(13)
H(99)	350(60)	4620(110)	10480(50)	160(30)
H(98)	850(90)	6430(150)	10110(80)	260(60)
H(1)	5041(16)	980(30)	6033(15)	0(6)

9 List of Abbreviations

δ	Chemical shift (NMR)
η	Shows hapticity of π -bonding ligands
ν	Frequency
μl	Microlitre
2D NMR	Two dimensional NMR spectra
ADMET	Acyclic diene metathesis
ATRA	Atom transfer radical additions
br	Broad
Bu	Butyl
Bz	Benzyl
calcd.	Calculated
CM	Cross metathesis
COD	Cyclooctadiene
Cosy	Correlation spectroscopy (NMR)
C_p, C_p^*	η^5 -Cyclopentadienyl, Pentamethylcyclopentadienyl
CV	cyclic voltammetry
d	Doublet
d	Doublet (NMR)
dd	Doublet of doublets (NMR)
DFT	Density function theory
DMSO	Dimethylsulfoxide
dt	Doublet of triplets (NMR)
eq.	equivalent
Et	Ethyl group
GOF	Goodness of fit
h	Hour(s)
hept	Heptet (NMR)
HMBC	Heteronuclear multiple bond correlation (NMR)

HMQC	Heteronuclear multiple quantum bond correlation (NMR)
HSQC	Heteronuclear single quantum correlation (NMR)
IR	Infrared
<i>J</i>	Coupling constant in Hertz
L	Ligand
<i>m</i>	Meta position
m	Multiplet (NMR spectroscopy)
M	Molar mass
m.p.	Melting point
Me	Methyl group
MHz	Megahertz
min	Minute(s)
ml	Millilitre
NMR	Nuclear magnetic resonance
NOE	Nuclear Overhauser effect (NMR)
<i>o</i>	Ortho position
<i>p</i>	Para position
Ph	Phenyl
ppm	Parts per milion
Pr	Propyl
py	Pyridine
q	Quartet (NMR)
RCM	Ring closing metathesis polymerisation reaction
ROMP	Ring opening metathesis polymerisation reaction
s	Singlet (NMR)
sept	Septet (NMR)
t	Triplet
T	Temperature
Tf	Triflate, Trifluoromethanesulfonate

9. List of Abbreviations

THF	Tetrahydrofuran
tt	Triplet of triplets (NMT)
UV	Ultraviolet
V	Crystal cell volume
VIS	Visible part of spectrum
Z	Molecules per elementary cell
ZPE	Zero point energy

10 References

1. M. A. Bennett; A. K. Smith, *J. Chem. Soc., Dalton Trans.* **1974**, 233.
2. R. A. Zelonka; M. C. Baird, *Can. J. Chem.* **1972**, (50), 3063.
3. J. Cubrilo; R. F. Winter; D. Gudat, *Chem. Commun.* **2005**, 510.
4. S. H. Yang; S. Chang, *Org. Lett.* **2001**, (3), 4209.
5. S. Chang; Y. Na; E. Choi; S. Kim, *Org. Lett.* **2001**, (3), 2089.
6. M. Lee; S. Ko; S. Chang, *J. Am. Chem. Soc.* **2000**, (122), 12011.
7. Y. Na; S. Chang, *Org. Lett.* **2000**, (2), 1887.
8. E. G. Fidalgo; L. Plasseraud; G. Süss-Fink, *J. Mol. Catal. A* **1998**, (132), 5.
9. M. Lee, S. C., *Tetrahedron Lett.* **2000**, (41), 7507.
10. D. Carmona; M. P. Lamata; L. A. Oro, *Eur. J. Inorg. Chem.* **2002**, (9), 2239.
11. F. Simal; A. Demonceau; A. F. Noels, *Tetrahedron Lett.* **1998**, (39), 3493.
12. D. L. Davies; J. Fawcett; S. A. Garatt; D. R. Russell, *Organometallics*, **2001**, (20), 3029.
13. C. J. Boxwell; P. J. Dyson; D. J. Ellis; T. Welton, *J. Am. Chem. Soc.*, **2002**, (124), 9334.
14. Handbook of Methathesis; Vol.1-3 (Ed.: R. H. Grubbs), *Wiley-VCH, Weinheim*, **2003**.
15. U. Frenzel; O. Nuyken, *J. Polym. Sci. Part A*, **2002**, (40), 2895.
16. C. W. Bielawski; D. Benitez; R. H. Grubbs, *Science*, **2002**, (297), 2041.
17. Fürstner, A., *Angew. Chem.* **2000**, (112), 3140.
18. A. Fürstner, *Angew. Chem., Int. Ed.* **2000**, (39), 3012.
19. T. E. Hopkins; K. B. Wagener, *Adv. Mater.* **2002**, (114), 1703.
20. S.J. Connon; S. Blechert, *Angew. Chem.* **2003**, (115), 1944.
21. A. K. Chatterjee; T. L. Choi; D. P. Sanders; R. H. Gubbs, *J. Am. Chem. Soc.* **2003**, (125), 11360.
22. J. Louie; C. W. Bielawski; R. H. Grubbs, *J. Am. Chem. Soc.* **2001**, (123), 11312.
23. S. D. Drouin; F. Zamainian; D. E. Fogg, *Organometallics*, **2001**, (20), 5495.
24. R. R. Schrock; J. S. Murdzek; G. C. Bazan; J. Robbins; M. Dimare; M. O' Regan, *J. Am. Chem. Soc.* **1990**, (112), 3875.
25. G. C. Bazan; E. Khosravi; R. R. Schrock; W. J. Feast; V. C. Gibson; M. B. O' Regan; J. K. Thomas; W. M. Davis, *J. Am. Chem. Soc.* **1990**, (112), 8378.

10. References

26. R. R. Schrock; A. H. Hoveyda, *Angew. Chem.* **2003**, (115), 4740.
27. S. T. Nguyen; R. H. Grubbs; J. W. Ziller, *J. Am. Chem. Soc.* **1993**, (115), 9858.
28. S. T. Nguyen; L. K. Johnson; R. H. Grubbs; J. W. Ziller, *J. Am. Chem. Soc.* **1992**, (114), 3974.
29. E. L. Dias; S. T. Nguyen; R. H. Grubbs, *J. Am. Chem. Soc.* **1997**, (119), 3887.
30. C. Adlhart; P. Chen, *J. Am. Chem. Soc.* **2004**, (126), 3496.
31. J. A. Love; M. S. Sanford; M. W. Day; R. H. Grubbs, *J. Am. Chem. Soc.* **2003**, (122), 8204.
32. M. S. Sanford; J. A. Love; R. H. Grubbs, *J. Am. Chem. Soc.* **2001**, (123), 6543.
33. J. S. Kingsbury; J. P. A. Harrity; P. J. Bonitatebus; A. H. Hoveyda, *J. Am. Chem. Soc.* **1999**, 121, 791.
34. S. B. Garber; J. S. Kingsbury; B. L. Gray; A. H. Hoveyda, *J. Am. Chem. Soc.* **2000**, (122), 8168.
35. L. J. Gooseen; J. Paetzold; K. Debasis, *Chem. Commun.* **2003**, 706.
36. A.W. Stumpf; E. Saive; A. Demonceau; A. F. Noels, *J. Chem. Soc., Chem. Commun.* **1995**, 1127.
37. A. Hafner, A. M., P.A. van der Schaaf, *Angew. Chem., Int. Ed. Engl.* **1997**, (36), 2121.
38. A. Fürstner; M. Picquet; C. Bruneau; P. H. Dixneuf, *Chem. Commun.* **1998**, 1315.
39. F. Simal; A. Demonceau; A. F. Noels, *Angew. Chem., Int. Ed.* **1999**, (38), 538.
40. M. A. Bennett; A. K. Smith, *J. Chem. Soc., Dalton Trans.* **1974**, 233.
41. A. Serron; S. P. Nolan, *Organometallics*, **1995**, (14), 4611.
42. G. Helmchen; J. Dibo; D. Flubacher; B. Wiese, *Organic Synthesis via Organometallics, OSM 5. Proceedings of the Fifth Symposium in Heidelberg, September 26 to 28 1996*.
43. J. Baran; I. Bogdanska; D. Jan; L. Delaude; A. Demonceau; A. F. Noels, *J. Mol. Catal. A*, **2002**, (190), 109.
44. A. Fürstner; T. Müller, *J. Am. Chem. Soc.* **1999**, (121), 7814.
45. F. Simal; D. Jan; L. Delaude; A. Demonceau; M.-R. Spirlet; A. F. Noels, *Can. J. Chem.* **2001**, (79), 529.
46. L. Quebatte; M. Haas; E. Solari; R. Scopelliti; Q. T. Nguyen; K. Severin, *Angew. Chem.* **2005**, (117), 1108.

47. A. Demonceau; A. W. Stumpf; E. Saive; A. F. Noels, *Macromolecules*, **1997**, (30), 3127.
48. A. Hafner, A. M., P.A. van der Schaaf, *Angew. Chem.* **1997**, (109), 2213.
49. M. J. Bloemink; J. Reedijk, *Met. Ions. Biol. Syst.* **1996**, (32), 641.
50. H. Z. Sun; H. Y. Li; P. J. Sadler, *Chem. Rev.* **1999**, (99), 2817.
51. Y. K. Yan; M. Melchart; A. Habtemariam; Sadler, P. J., *Chem. Commun.* **2005**, 4764.
52. C. S. Allardyce; P. J. Dyson; D. J. Ellis; P. A. Salter; R. Scopeliti, *J. Organomet. Chem.* **2003**, (668), 35.
53. M. Picquet; C. Bruneau; P. H. Dixneuf, *Chem. Commun.* **1998**, 2249.
54. M. Picquet; D. Touchard; C. Bruneau; P. H. Dixneuf, *New. J. Chem.* **1999**, (23), 141.
55. I. Alaoui-Abdallaoui, D. S., P. H. Dixneuf, *J. Mol. Cat. A: Chem* **2002**, (182/183), 577.
56. R. Castarlenas, D. S., A. F. Noels, A. Demonceau, P. H. Dixneuf, *J. Organomet. Chem.* **2002**, (663), 235.
57. B. Cetinkaya; S. Demir; I. Özdemir; I. Toupet; D. Semeril; C. Bruneau; P. H. Dixneuf, *Chem. Eur. J.* **2003**, (9), 2323.
58. R. Akiyama; S. Kobayashi, *Angew. Chem. int. Ed.* **2002**, (41), 2602.
59. M. Picquet; C. Bruneau; P. H. Dixneuf, *Chem. Commun.* **1998**, 2249.
60. A. Fürstner, L. A., *Chem. Commun.* **1999**, 95.
61. A. Fürstner, M. L., C. W. Lehmann, M. Picquet, R. Kunz, C. Bruneau, D. Touchard, P. H. Dixneuf, *Chem. Eur. J.* **2000**, (6), 1847.
62. Y. Nishibayashi; I. Wakiji; M. Hidai, *J. Am. Chem. Soc.* **2000**, (122), 11019.
63. Y. Nishibayashi; Y. Inada; M. Hidai; S. Uemura, **2002**, (124), 7900.
64. Y. Nishibayashi; Y. Inada; M. Hidai; S. Uemura, **2003**, (125), 6060.
65. G. Marconi; H. Baier; F. W. Heinemann; P. Pinto; H. Pritzkow; U. Zenneck, *Inorg. Chim. Acta.*, **2003**, (352), 188.
66. Y. Miyaki; T. Onishi; H. Kurosawa, *Inorg. Chim. Acta.* **2000**, (300-302), 369.
67. P. D. Smith; A. D. Wright, *J. Organomet. Chem.* **1998**, (559), 141.
68. K. Y. Ghebreyessus; J. F. Nelson, *Organometallics*, **2002**, (19), 3387.
69. M. A. Bennett; A. J. Edwards; J. R. Harper; T. Khimyak; A. C. Willis, *J. Organomet. Chem.* **2001**, (629), 7.
70. P. D. Smith; T. Gelbrich; M. B. Hursthouse, *J. Organomet. Chem.* **2002**, (659), 1.

10. References

71. J. F. Nelson; K. G. Ghebreyessus; V. C. Cook; A. J. Edwards; W. Wielandt; S. B. Wild; A. C. Willis, *Organometallics*, **2002**, 1727.
72. J. W. Faller; D. G. D. Alles, *Organometallics*, **2003**, 22.
73. K. Umezawa-Vizzini; I. K. Guzman-Jimenez; K. H. Whitmire; T. R. Lee, *Organometallics*, **2003**, (22), 3059.
74. P. Pinto; G. Marconi; F. W. Heinemann; U. Zenneck, *Organometallics*, **2004**, (23), 374.
75. K. Umezawa-Vizzini; T. R. Lee, *Organometallics*, **2003**, (22), 3066.
76. K. Umezawa-Vizzini; T. R. Lee, *Organometallics*, **2004**, (23), 1448.
77. H. Brintzinger; D. Fischer; R. Mulhaupt; B. Rieger; R. Waymouth, *Angew. Chem. Int. Ed. Engl.* **1995**, (34), 1143.
78. S. B. Windicke; E. Burri; R. Scopelliti; K. Severin, *Organometallics*, **2003**, (22), 1894.
79. J. Soleimannejad; C. White, *Organometallics*, **2005**, (24), 2538.
80. M. Gaye; B. Demerseman; P. H. Dixneuf, *J. Organomet. Chem.* **1991**, (411), 263.
81. R.S. Glass, L. B. J., M. E. Jatcko, *Tetrahedron* **1989**, 45, (5), 1263.
82. T. Ohnishi; Y. Miyaki; H. Asano; H. Kurosawa, *Chem. Lett.* **1999**, 810.
83. Y. Miyaki; T. Onishi; S. Ogoshi; H. Kurosawa, *J. Organomet. Chem.* **2000**, (616), 135.
84. W. Reppe; O. Schlichting; K. Klager; T. Toepel, *Liebigs Ann. Chem.* **1948**, (560), 3.
85. S. W. Benson, *Thermochemical Kynetics*, Wiley: New York, **1968**.
86. R. H. Grubbs, *C&EN*, **2003**, (81), 112.
87. N. E. Shore; B. M. Trost; I. Fleming, In *Comprehensive Organic Synthesis*, Eds.; Pergamon: Oxford, **1991**, Vol.5, 1129-1162.
88. J. Li; H. Jiang; M. Chen, *J. Org. Chem.* **2001**, (66), 3627.
89. E. Negishi; M. Ay; T. Sugihara, *Tetrahedron*, **1993**, (49), 5471.
90. I. Ojima; A. T. Vu; J. V. McCullagh; A. Kinoshita, *J. Am. Chem. Soc.* **1999**, (121), 3230.
91. G. B. Hoven; J. Efskind; C. Romming; K. Undheim, *J. Org. Chem.* **2002**, (67), 2459.
92. J. H. Hardesty; J. B. Koerner; A. Albright; G.-Y. Lee, *J. Am. Chem. Soc.* **1999**, (121), 6055.
93. K. Kirchner; M. J. Calhorda; R. Schmid; L. F. Veiros, *J. Am. Chem. Soc.* **2003**, (125), 11721.

94. Y. Yamamoto; H. Takagishi; R. Ogawa; K. Itoh, *J. Am. Chem. Soc.* **2003**, (125), 143.
95. M. O. Albers; D. J. A. de Waal; D. C. Lilles; D. J. Robinson; E. Singleton; M. B. Wiege, *J. Chem. Soc., Chem. Commun.* **1986**, 1680.
96. B. M. Trost; M. T. Rudd, *J. Am. Chem. Soc.* **2001**, (123), 8862.
97. J. Le. Paih; S. Derien; C. Bruneau; B. Demerseman; L. Toupet; P. H. Dixneuf, *Angew. Chem.* **2001**, (113), 2996.
98. E. Becker; K. Mereiter; M. Puchberger; R. Schmid; K. Kirchner, *Organometallics*, **2003**, (22), 2124.
99. M. V. Russo; A. Furlani, *Tetrahedron Lett.* **1976**, (30), 2655.
100. P. Bicev; A. Furlani; G. Sartori, *Gazz. Chim. Ital.* **1973**, (103), 849.
101. M. S. Sigman; A. W. Fatland; B. E. Eaton, *J. Am. Chem. Soc.* **1998**, (120), 5130.
102. T. B. Rauchfuss, *Inorg. Chem.* **2004**, (43), 14-26.
103. M. A. Bennett; L. Y. Goh; A. C. Willis, *J. Am. Chem. Soc.* **1996**, (118), 4984.
104. R. Yee Cheong Shin; Goh, L. Y., *Acc. Chem. Res.* **2006**, (39), 301.
105. Y. Yamamoto; S. Sakamoto; Y. Ohki; A. Usuzawa; M. Fujita; T. Mochida, *Dalton Trans.* **2003**, 3534.
106. B. C. Ranu; S. Banerjee, *Org. Lett.* **2005**, (7), 3049.
107. R. S. Glass; L. B. Jeffrey; M. E. Jatcko, *Tetrahedron*, **1989**, 5, (45), 1263.
108. G. Tresoldi; L. Baradello; S. Lanza; P. Cardiano, *Eur. J. Inorg. Chem.* **2005**, (12), 2423.
109. R. Y. C. Shin; M. A. Bennett; A. J. Edwards; J. R. Harper; T. Khimyak; A. C. Willis; S. Y. Ng; G. K. Tan; L. L. Goh, *Inorg. Chem.* **2003**, (42), 96.
110. L. Carter; D. L. Davies; J. Fawcett; D. R. Russell, *Polyhedron*, **1993**, (10), 1123.
111. R. Aronson; M. R. J. Elsegood; J. W. Steed; D. A. Tocher, *Polyhedron*, **1991**, (10), 1727.
112. C. S. Allardyce; P. J. Dyson; D. J. Ellis; S. L. Heath, *Chem. Commun.* **2001**, 1396.
113. F. Grepioni; D. Braga, *Organometallics* **1995**, (14), 121.
114. Greponi, F.; Braga, D.; Dyson, P. J.; Johnson, B. F. G.; Sanderson, F. M.; Calhorda, M. J.; Veiros, L. F., *Organometallics* **1995**, 14, (1), 121-130.
115. Pandey, D. S.; Sahay, A. N.; Sisoida, O. S.; Jha, N. K.; Sharma, P.; Klaus, H. E.; Caberra, A., Synthesis, characterization and crystal structure of $[(h^6-C_6Me_6)Ru(\mu-Cl)_3Ru(h^6-C_6Me_6)]^+ PF_6^-$. *J. Organomet. Chem.* **1999**, 592, 278-282.

10. References

116. M. S. Sanford; J. A. Love; R. H. Grubbs, *Organometallics* **2001**, (20), 5314.
117. E. Anders; A. Opitz; K. Wermann; B. Wiedel; M. Walther; W. Imhof; H. Görls, *J. Org. Chem.* **1999**, (64), 3113.
118. E. Anders; J. G. Tropsch; A. R. Katritzky; D. Rasala; J.-J. Vanden Eynde, *J. Org. Chem.* **1989**, (54), 4808.
119. Steedman, J. A.; Burrell, A. K., *Acta Cryst.* **1997**, (C53), 864.
120. Fürstner, A.; Liebl, M.; Lehmann, C. W.; Picquet, M.; Kunz, R.; Bruneau, C.; Touchard, D.; Dixneuf, P. H., *Chem. Eur. J.* **2000**, 6, (10), 1847-1857.
121. Umezawa-Vizzini, K.; Guzman-Jimenez, I. Y.; Whitmire, K. H.; Lee, T. R. *Organometallics* **2003**, 22, (15), 3059-3065.
122. P. Pertici; G. Vitulli; M. Paci; L. J. Porri, *Chem. Soc., Dalton Trans.* **1989**, 1961.
123. A. Fürstner; M. Liebl; C. W. Lehmann; M. Picquet; R. Kunz; C. Bruneau; D. Touchard; P. H. Dixneuf, *Chem. Eur. J.* **2000**, (6), 1847.
124. D. Pillete; L. Ouzzine; L. H. Bozec; P.H. Dixneuf; C.E.F. Rickard; W.R. Roper, *Organometallics* **1992**, (11), 809.
125. T. J. Geldbach; P. S. Pregosin, *Organometallics* **2003**, 22, (7), 1443.
126. J. Zhang; T. B. Gunnoe, *Organometallics*, **2003**, (11), 2293.
127. B. Therrien; L. Vieille-Petit; J. Jeanette-Gris; P. Stepnicka; G. Süß-Fink, *J. Organomet. Chem.* **2004**, (689), 2456.
128. P. Lahuerta; J. Latorre; J. Soto; Y. Mugnier, *Polyhedron*, **1989**, (8), 2803.
129. R. Kitaura *et al.*, *Inorg.Chim. Acta* **2002**, (334), 142.
130. M. A. Bennett; T. - N. Huang; T. W. Matheson; A. K. Smith; S. Ittel; W. Nickerson, *Inorg. Synth.* **1980**, (21), 75.
131. Fujimoto, R. A.; *al., e.*, *J. Med. Chem.* **1989**, (32), 1259.
132. D. R. Robertson; T. A. Stephenson; T. Arthur, *J. Organomet. Chem.* **1978**, (162), 121.
133. F. B. McCormick; D. C. Cox; W. B. Gleason, *Organometallics*, **1993**, (12), 610.
134. F. B. McCormick; W. B. Gleason, *Acta Crystallogr.* **1988**, (C44), 603.
135. T. Steiner, *Angew. Chem.* **2002**, (114), 50.
136. N. Pinault; D. W. Bruce, *Coord. Chem. Rev.* **2003**, (241), 1.
137. D. Sinou, *Adv. Synth. Catal.* **2002**, (344), 221.
138. M. A. Bennett, *Coord. Chem. Rev.* **1997**, (166), 225.
139. L. J. Higham; M. K. Whittlesey; P. T. Wood, *Dalton Trans.* **2004**, 4204.

140. V. Cadierno; P. Crochet; S. E. Garcia-Garrido; J. Gimeno, *Dalton Trans.* **2004**, 3635.
141. U. Kölle; R. Görissen; A. Hörnig, *Inorg. Chim. Acta* **1994**, (218), 33.
142. D. Devanne; P. H. Dixneuf, *J. Organomet. Chem.* **1990**, (390), 371.
143. R. Bhalla; C. J. Boxwell; S. B. Duckett; P.J. Dyson; D. G. Humphrey; J. W. Steed; P. Suman, *Organometallics* **2002**, (21), 924.
144. N. K. Szymczak; F. Han; D. R. Tyler, *Dalton Trans.* **2004**, 3941.
145. W. S. Sheldrick; S. Heeb, *Inorg. Chim. Acta* **1990**, (168), 93.
146. P. Annen; S. Schildberg; W. S. Sheldrick, *Inorg. Chim. Acta*, **2000**, (307), 115.
147. K. P. C. Vollhardt, *Angew. Chem. Int. Ed. Engl.* **1984**, (23), 539.
148. J. P. Collman; L. S. Hegedus; J. R. Norton; R. G. Finke, Principles and Applications of Organotransition Metal Chemistry, University Science Books, Mill Valley **1987**.
149. Y. Wakatsuki; H. Yamazaki, *J. Organomet. Chem.* **1977**, (139), 169.
150. S. Saito; Y. Yamamoto, *Chem. Rev.*, **2000**, 2901.
151. Y. Yamamoto; A. Nagata; H. Nagata; Y. Ando; Y. Arikawa; K. Tatsumi; K. Itoh, *Chem. Eur. J.*, **2003**, (9), 2469.
152. V. Gevorgyan; A. Takeda; M. Homma; N. Sadayori; U. Radhakrishnan; Y. Yamamoto, *J. Am. Chem. Soc.*, **1999**, (121), 6391.
153. J. J. Eisch; X. Ma; K. I. Han; J. N. Gitua; C. Krüger, *Eur. J. Inorg. Chem.* **2001**, 77.
154. C. S. Yi; N. Liu, *Synlett.*, **1999**, 281.
155. Y. Yamamoto; T. Arakawa; R. Ogawa; K. Itoh, *J. Am. Chem. Soc.*, **2003**, (125), 12143.
156. A. Furlani; K. H. Hornemann; Russo, M. V., *Gazz. Chim. Ital.* **1987**, 117.
157. P. Vest; J. Anhaus; C. H. Bajaj; R. van Eldrik, *Organometallics* **1991**, (10), 818.
158. R. Hoffmann, *Science*, **1981**, (211), 959.
159. C. Ernst; O. Walter; E. Dinjus, *J. Prakt. Chem.* **1999**, 8, (341), 801.
160. P. Leigh; S. Bodige; H. E. Selnau, *Organometallics* **1995**, (14), 4222.
161. Holleman-Wiberg, *Lehrbuch der Anorganischen Chemie*, , (101), ed., 1709.
162. M. I. Rybinskaya; A. R. Kudinov; V. S. Kaganovich, *J. Organomet. Chem.*, **1983**, (246), 279.
163. M. I. Rybinskaya; A. R. Kudinov; Kaganovich, V. S., *J. Organomet. Chem.* **1982**, (235), 215.
164. M. A. Bennett; T. W. Matheson, *J. Organomet. Chem.*, **1979**, (175), 87-93.

10. References

165. E. O. Fischer; C. Elschenbroich, *Chem. Ber.*, **1970**, (103), 162.
166. M. S. W. Chan; K. Vanka; C. C. Pye; Ziegler, T., *Organometallics* **1999**, (18), 4624.
167. R. J. Haines; Preez, A. L. d., *J. Am. Chem. Soc.* **1971**, (93), 2820.
168. Sheldrick, G. M. *SHELX-97, Program for Crystal Structure Solution and Refinement*, Institut für Anorganische Chemie der Universität, Tammanstraße 4: Göttingen, 1997.
169. Herrendorf, W.; Bärnighausen, H. *Program HABITUS*, Karlsruhe, Germany, 1993.
170. M. A. Bennett; T. - N. Huang; T. W. Matheson; A. K. Smith; S. Ittel; W. Nickerson, *Inorg. Synth.* **1974**, (21), 75.
171. J. D. Wilkey; G. B. Schuster, *J. Org. Chem.* **1987**, (52), 2117.
172. R. A. Fujimoto; J. Boxer; R. H. Jackson; J. P. Simke; R. F. Neale; E. W. Snowhill; B. J. Barbaz; M. Williams; Sillis, M. A., *J. Med. Chem.* **1989**, (32), 1259.

11 Curriculum Vitae for Jadranka Čubrilo

PERSONAL DETAILS:

Date of Birth: 21.10.1976

Nationality: Serbian

EDUCATION:

2003-2007 Ph.D studies in the field of Inorganic Chemistry at the **University of Stuttgart**

2003 Diplomarbeit at the **University of Stuttgart**, titled "Novel Half-Sandwich Complexes of Ruthenium: Synthesis and Their Reactions with Alkynols"

1995-2000 Graduate studies in Chemistry,
Faculty of Natural Sciences, Institute of Chemistry, **Novi Sad University**,
Final exam "Intermediates in the synthesis of analogues of tiazofurane"

1991-1995 Grammar School in Sombor, Serbia

WORK HISTORY:

2007 **Technical Business Development Executive**
lavera Organic Skin Care, Hong Kong

2003-2007 **Teaching Assistant**
University of Stuttgart and University of Regensburg, Germany

2002-2003 **Technical support**
Kao Chemicals Corporation, Novi Sad, Serbia

INTERNSHIP AND SCHOLARSHIPS

- 2001 **University of Illinois Chicago-Urbana, USA,**
- 10/2003- **Württemberg Landesstiftung Scholarship, Germany**
03/2004

ACHIEVEMENT:

- 2003 6th International Symposium of the **Volkswagen-Stiftung** on Intra-and Intermolecular Electron Transfer-Waldeberg, Germany
- 2004 14th International Symposium **on Homogeneous Catalysis ISHC- München** presented poster "The coupling of alkynols and Phenylate on a Ruthenium Template"
- 2005 Coordinating chemistry meeting, **Kaiserslautern, Germany**, oral presentation "Synthesis of novel naphthalenide Ru complexes from disubstituted propargylic alcohols and tetraphenylborate- unusual coupling of alkynols"
- 2005 **Publication: Chemical Communication**, 2005,510-512
"Coupling of alkynols and a phenyl group to novel η^5 -dihydronaphthalenide ligand on a Ruthenium template"
- 2006 Coordination chemistry meeting **Göttingen, Germany**, oral presentation "Reactivity and crystals structures of novel half sandwich Ru complexes containing non-tethered thioether ligands"
- 2006 **Publication Zeitschrift für Anorganische und Allgemeine Chemie (ZAAC)**,2006,632,400-408
"Tethering versus Non-Coordination of Hydroxy and Methoxy Side Chains in Arene Half Sandwich Dichloro Ruthenium Complexes"
- 2006 **Publication: J. Organomet. Chem.**
"p-Cymene Thioether Complexes"